

FEDERAL UNIVERSITY OF PARÁ  
INSTITUTE OF TECHNOLOGY  
POST GRADUATE PROGRAM IN ELECTRICAL ENGINEERING

Ph.D. Thesis

EXPERIMENTAL EVALUATION, DIAGNOSIS, AND PREDICTION OF THE IMPACTS OF POWER  
QUALITY DISTURBANCES IN IE2, IE3, AND IE4 CLASS EFFICIENCY MOTORS.

JONATHAN MUÑOZ TABORA

DM: TD03 / 2024

UFPA / ITEC / PPGEE  
Guama University Campus  
Belem-Para-Brazil

**2024**

FEDERAL UNIVERSITY OF PARÁ  
INSTITUTE OF TECHNOLOGY  
POST GRADUATE PROGRAM IN ELECTRICAL ENGINEERING

Ph.D. Thesis

EXPERIMENTAL EVALUATION, DIAGNOSIS, AND PREDICTION OF THE IMPACTS OF  
POWER QUALITY DISTURBANCES IN IE2, IE3, AND IE4 CLASS EFFICIENCY MOTORS.

Ph.D, Thesis submitted to the  
Examining Committee of the  
Post graduate Program in  
Electrical Engineering from the  
Federal University of Para to  
obtain the Ph.D. Degree in  
Electrical Engineering, Area of  
Concentration in Electrical  
Energy Systems.

UFPA / ITEC / PPGEE  
Guama University Campus  
Belém-Para-Brazil

**2024**

**Dados Internacionais de Catalogação na Publicação (CIP) de acordo com ISBD**  
**Sistema de Bibliotecas da Universidade Federal do Pará**  
**Gerada automaticamente pelo módulo Ficat, mediante os dados fornecidos pelo(a) autor(a)**

---

- M967e Munoz Tabora, Jonathan.  
EXPERIMENTAL EVALUATION, DIAGNOSIS, AND  
PREDICTION OF THE IMPACTS OF POWER QUALITY  
DISTURBANCES IN IE2, IE3, AND IE4 CLASS EFFICIENCY  
MOTORS / Jonathan Munoz Tabora. — 2024.  
188 f. : il. color.
- Orientador(a): Profª. Dra. Maria Emília de Lima Tostes  
Coorientador(a): Prof. Dr. Edson Ortiz de Matos  
Tese (Doutorado) - Universidade Federal do Pará, Instituto de  
Tecnologia, Programa de Pós-Graduação em Engenharia Elétrica,  
Belém, 2024.
1. power quality. 2. energy efficiency. 3. electric motors.  
4. temperature. 5. efficiency motors. I. Título.

CDD 621.3

---

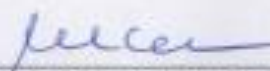
**"EVALUATION, DIAGNOSIS AND PREDICTION OF THE IMPACTS OF POWER  
QUALITY DISTURBANCES IN IE2, IE3 AND IE4 CLASS EFFICIENCY MOTORS"**

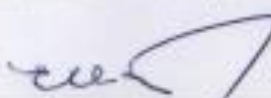
AUTOR: **JONATHAN MUNOZ TABORA**

TESE DE DOUTORADO SUBMETIDA À BANCA EXAMINADORA APROVADA PELO  
COLEGIADO DO PROGRAMA DE PÓS-GRADUAÇÃO EM ENGENHARIA ELÉTRICA, SENDO  
JULGADA ADEQUADA PARA A OBTENÇÃO DO GRAU DE DOUTOR EM ENGENHARIA  
ELÉTRICA NA ÁREA DE SISTEMAS DE ENERGIA ELÉTRICA.

APROVADA EM: 20/03/2024

**BANCA EXAMINADORA:**

  
\_\_\_\_\_  
**Prof.ª Dr.ª Maria Emília de Lima Tostes**  
(Orientadora - PPGE/UFPA)

  
\_\_\_\_\_  
**Prof. Dr. Edson Ortiz de Matos**  
(Coorientador - FEEB/UFPA)

  
\_\_\_\_\_  
**Prof. Dr. Thiago Mota Soares**  
(Avaliador Interno - PPGE/UFPA)

  
\_\_\_\_\_  
**Prof. Dr. Ubiratan Holanda Bezerra**  
(Avaliador Interno - PPGE/UFPA)

\_\_\_\_\_  
**Prof. Dr. Carlos Aparecido Ferreira**  
(Avaliador Externo - UERJ)

\_\_\_\_\_  
**Prof. Dr. Fernando José Teixeira Estêvão Ferreira**  
(Avaliador Externo - UC)

**VISTO:**

\_\_\_\_\_  
**Prof. Dr. Diego Lisboa Cardoso**  
(Coordenador do PPGE/ITEC/UFPA)

## DEDICATORY

*Dedico este trabajo a mis padres: Manuel Muñoz y Enma Tabora, que con amor y sacrificio me ayudaron a ser quien soy hoy, a Henry y Darwin por también cuidar de mi a lo largo de mi vida, a mi hija Lunita y su madre Verena.*

# AKNOWLEDGEMENTS

Deseo agradecer a Dios y la intercesión de la Virgen María, por haber escuchado mi oración y la de todos por la salud de mi padre, teniendo misericordia de él y salvándolo de la muerte. No permitió la muerte mientras estuve fuera de mi querido país, Honduras. También por ir delante de mí y acompañarme en todo este recorrido, fortaleciendo mis debilidades y ayudándome a vencer mis miedos. Por regalarme seis de los mejores años de mi vida llenos de personas, conocimiento, viajes y experiencias que sin duda recordaré durante toda mi vida.

A mi hija Lunita, mi princesa, por motivarme a ser mejor y buscar lo mejor para ella., a su madre Verena por cuidar siempre bien de ella. A mi familia en Honduras, que sin saber lo que hacía, siempre me apoyaron en la realización de cada uno de mis sueños, siempre acompañándome y ayudándome a lograr éste, mi objetivo.

À professora Maria Emilia Tostes, por ter gentilmente me orientado e principalmente por sempre demonstrar disposição no desenvolvimento deste trabalho, com ela aprendi a humildade, e a importância da gestão no sucesso. Ao professor Edson Ortiz, pela colaboração na montagem da bancada utilizada, orientação, revisão e conselhos para a melhoria dos experimentos e do trabalho em geral, ao Thiago Soares, por sempre me orientar e apoiar desde a minha chegada ao Brasil. E ao Professor Ubiratan H. Bezerra, pelos conselhos e orientações para o aprimoramento de cada um dos trabalhos realizados, que tomei como exemplo para minha vida acadêmica e profissional e por sua humildade.

A todos os colegas do CEAMAZON, que sempre estiveram dispostos a me ajudar de todas as formas possíveis, incluindo-me nessa linda família que eles têm e da qual sempre me sentirei parte onde quer que esteja. Ao meu amigo Luiz Sales, por me apoiar e me ensinar muitas coisas sobre o Brasil quando cheguei. Ao meu amigo Carlos Rodrigues, com quem tenho uma amizade sincera e de coração no Brasil. Ao meu amigo Ulisses, por confiar em mim e em minhas habilidades e ao meu amigo Josivan por ser um grande amigo e apoio no CEAMAZON.

Aos professores Fernando Ferreira e Aníbal T. de Almeida pela recepção, conhecimento e apoio durante minha estada em Portugal, bem como a João Lourenço por sua amizade e ajuda durante minha estada em Portugal. Também à CAPES, por meio do programa PDSE, pelo apoio financeiro para minha estada em Portugal. Ao Conselho Nacional de Desenvolvimento Científico e Tecnológico (CNPq), pelo apoio no desenvolvimento do presente trabalho.

A la Organización de Estados Iberoamericanos (OEI), por su importante apoyo para la realización de este trabajo, a partir del Programa Paulo Freire +, y las becas 20/20 en Honduras.

## RESUMO

Os motores elétricos continuam a ser a maior carga de maior uso final de energia elétrica do mundo. Com os avanços tecnológicos, suas aplicações se expandiram para abranger novas categorias como ser os veículos elétricos, transporte, navegação, entre outros. A Europa iniciou o processo de transição para as classes de motores de eficiência IE4, diante disso, espera-se que outras regiões sigam a transição para classes de motores de maior eficiência. Em algumas regiões, a tensão operacional pode ser diferente da nominal, de acordo com a norma IEC 60038-2009, isto somado a outros distúrbios como ser o desequilíbrio e harmônicos de tensão pode resultar em impactos no desempenho dessas novas tecnologias. Nesse contexto, esforços significativos têm sido dedicados à manutenção preditiva, com o objetivo de aprimorar as técnicas existentes com novas propostas que aumentem sua eficácia no diagnóstico da saúde das máquinas rotativas na presença de diferentes distúrbios presentes nos SEP. Este trabalho avalia o impacto da variação de tensão, harmônicos de tensão e diferentes porcentagens de desequilíbrios com sub e sobretensão na temperatura e desempenho de motores elétricos de indução de baixa potência classes IE2, IE3 e IE4. O estudo incorpora uma análise técnica, econômica, estatística e térmica para obter indicadores importantes relacionados ao consumo de energia, à eficiência, ao fator de potência e à temperatura. Na busca por técnicas inovadoras e complementares, este estudo também apresenta um novo Indicador de Degradação de Motor Elétrico (EMDI) baseado na análise no domínio da frequência das formas de onda da corrente do motor elétrico para diagnosticar a integridade das máquinas rotativas. Os resultados mostram que em condições ideais de operação o motor de ímãs permanentes classe IE4 apresenta melhor desempenho em termos de consumo e temperatura, porém apresentando características não lineares. Logo na presença dos diferentes distúrbios o cenário muda ao apresentar um menor desempenho quando comparado com os motores de indução gaiola de esquilo nas mesmas condições de operação. A análise realizada permitirá estabelecer e quantificar os impactos dos diferentes distúrbios presentes nos sistemas elétricos de potência no desempenho das novas tecnologias de motores elétricos a serem introduzidos posteriormente. Com relação ao indicador de diagnóstico de saúde do motor proposto, os resultados apresentados apoiam fortemente a eficácia da abordagem proposta para facilitar a implementação de práticas de manutenção preditiva. Outra importante contribuição da presente tese, é que seus resultados serão base para a implementação de uma nova regulação para a introdução de requisitos mínimos de eficiência dos motores elétricos em Honduras

**Palavras-chaves:** Variação de tensão, desequilíbrio de tensão, harmônicos, temperatura, classes de eficiência, motor de ímãs permanentes, manutenção preditiva.

# ABSTRACT

Electric motors remain the largest end-use of electricity in the world and a fundamental part of the industrial sector. In addition, with technological advances, their applications have expanded into new categories such as electric vehicles, transportation, and navigation, among others. Europe has started to upgrade to IE4 efficiency motor classes, and it is expected that other regions will follow the transition to higher efficiency motor classes. In some regions, the operating voltage may differ from the nominal voltage according to IEC 60038-2009. This, together with other disturbances such as unbalance and voltage harmonics, can affect the performance of these new technologies. In this context, significant efforts have been made in predictive maintenance to improve existing techniques with new proposals that increase their effectiveness in diagnosing the health of rotating machines in the presence of different disturbances present in SEPs. This work evaluates the impact of voltage variations, voltage harmonics, and different percentages of under and over-voltage unbalances on the temperature and performance of low-power induction motors of IE2, IE3, and IE4 classes. The study includes technical, economic, statistical, and thermal analysis to obtain important indicators related to energy consumption, efficiency, power factor, and temperature. In the search for innovative and complementary techniques, this study also presents a new Electric Motor Degradation Indicator (EMDI) based on frequency domain analysis of electric motor current waveforms for the diagnosis of rotating machinery integrity. The results show that under ideal operating conditions, the permanent magnet motor of the IE4 class has a better performance in terms of power consumption and temperature, but it has a non-linear characteristic. Then, in the presence of certain disturbances, the scenario changes, with lower performance compared to squirrel-cage induction motors under the same operating conditions. The analysis performed will allow to identify and quantify the impact of the different perturbations present in the electrical power systems on the performance of the new electric motor technologies to be introduced. Regarding the proposed motor health diagnostic indicator, the results presented strongly support the effectiveness of the proposed approach in facilitating the implementation of predictive maintenance practices. Another important contribution of this thesis is that its results will form the basis for the implementation of a new regulation for the introduction of minimum efficiency requirements for electric motors in Honduras.

**Keywords: Voltage variation, voltage unbalance, harmonics, temperature, efficiency classes, permanent magnet motors, predictive maintenance.**



## ACRONYMS AND ABBREVIATIONS.

SCIM: Squirrel cage induction motor;

IM: Induction Motor;

LSPMM: Line-start Permanent magnet motor;

VU: Voltage unbalance;

VH: Voltage Harmonics;

VV: Voltage Variation;

MEPS: Minimum Energy Performance Standards;

IEC: International Electrotechnical Commission;

IE: International Efficiency;

IR: Efficiency index (*Índice de rendimiento*)

EMDI: Electric Motor Degradation Index;

THD: Total Harmonic Distortion rate%

AC: Alternating Current;

NEMA: National Electrical Manufacturers Association;

ANEEL: National Electric Energy Agency

THDI: Total Harmonic Distortion of Current;

FEMM software: Finite Element Method Magnetics

# SUMMARY

<b>Chapter 1 .....</b>	<b>23</b>
<b>1.1. General Considerations .....</b>	<b>23</b>
<b>1.2. Minimum Energy Performance Standards .....</b>	<b>24</b>
<b>1.3. Brazilian Induction Motor Regulation .....</b>	<b>26</b>
<b>1.4. Methodology for the Literature Review.....</b>	<b>27</b>
<b>1.5. Bibliometric Analysis .....</b>	<b>28</b>
<b>1.6. Systematic Review .....</b>	<b>31</b>
1.6.1. Efficient Electric Motors .....	31
1.6.2. Voltage Unbalance State of art .....	31
1.6.3. Voltage Harmonics State of the Art .....	32
1.6.4. Voltage Magnitude Variation in Induction Motors.....	34
1.6.5. Diagnosis of Electric Motors .....	35
<b>1.7. Test Bench Description .....</b>	<b>37</b>
<b>1.8. Research Goals .....</b>	<b>39</b>
<b>1.9. Thesis Contributions .....</b>	<b>40</b>
<b>1.10. Thesis Structure .....</b>	<b>42</b>
<b>1.11. Chapter Bibliography .....</b>	<b>43</b>
<b>Chapter 2 .....</b>	<b>52</b>
<b>2.1. The Induction Machine.....</b>	<b>52</b>
<b>2.2. Improvements in Induction Motors .....</b>	<b>54</b>
2.2.1. Active Materials .....	55
2.2.2. Windage and Friction Losses.....	56
<b>2.3. Permanent Magnet Motors .....</b>	<b>57</b>
<b>2.4. Line Start Permanent Magnet Motor LSPMM .....</b>	<b>58</b>
2.4.1. LSPMM Starting .....	59
<b>2.5. Comparison of IE2, IE3 &amp; IE4 Motor Efficiency Classes .....</b>	<b>61</b>
2.5.1. Input Current Distortion .....	61
2.5.2. Total Power and Power Factor .....	62
2.5.3. Electric Motor Temperature.....	63

2.6. Chapter Conclusion.....	64
2.7. Chapter Bibliography .....	65
<b>Chapter 3 .....</b>	<b>69</b>
3.1. Harmonic Distortion .....	69
3.2. Harmonics Limits .....	70
3.3. Losses due to Harmonics in Induction Motors .....	70
3.4. Voltage Harmonics Impacts on IE2, IE3 and IE4 IMs classes.....	73
3.4.1. Methodology .....	73
3.5. Technical Assessment .....	74
3.5.1. Current Increase due to Harmonics .....	74
3.5.2. Total Current Harmonic Distortion .....	74
3.5.3. Reactive Power and Power Factor with Voltage Harmonics .....	76
3.5.4. Temperature Increase due to Harmonics .....	77
3.6. Statistical Assessment .....	80
3.6.1. Correlation Matrix for Temperature.....	80
3.6.2. Temperature Models for Voltage Harmonics Impacts on Temperature .....	84
3.7. Finite Element Thermal Validation of the LSPMM in VH presence .....	88
3.8. Final Considerations.....	91
3.9. Chapter Bibliography .....	92
<b>Chapter 4 .....</b>	<b>94</b>
4.1. General Considerations .....	94
4.2. Voltage Unbalance Definitions .....	95
4.2.1. Complex Voltage Unbalance Factor (CVUF).....	97
4.2.2. Complex Voltage Unbalance Factor (CVUF) Diagram .....	98
4.3. Voltage Variation (VV) and Voltage Unbalance (VU) Basics.....	99
4.3.1. Voltage Unbalance Analysis .....	100
4.4. Assessing Voltage Unbalance Conditions in IE2, IE3 & IE4 classes IMs. ....	105
4.4.1. Methodology .....	105
4.5. Technical Analysis.....	105
4.5.1. Current Behaviour.....	105

4.5.2. Power Factor .....	107
4.5.3. Total Power .....	108
4.5.4. Current Total Harmonic Distortion .....	108
4.5.5. Temperature Variation due to Voltage Unbalance.....	109
<b>4.6. Statistic Assessment .....</b>	<b>112</b>
4.6.1. Correlation Matrix for harmonic content .....	112
4.6.2. Temperature models for VU in IE2, IE3 and IE4 class motors .....	113
<b>4.7. Final Considerations.....</b>	<b>117</b>
<b>4.8. Chapter Bibliography .....</b>	<b>118</b>
<b>Chapter 5 .....</b>	<b>120</b>
<b>5.1. Introduction .....</b>	<b>120</b>
5.1.1. General Considerations .....	120
5.1.2. Chapter Motivation and Contribution.....	121
<b>5.2. Theoretical Foundation .....</b>	<b>122</b>
5.2.1. Energy Efficiency Policies in Induction Motors.....	122
5.2.2. Process toward More Efficient Motors.....	123
<b>5.3. Energy Efficiency and Power Quality Assessment.....</b>	<b>124</b>
5.3.1. Methodology .....	124
<b>5.4. Results and Discussion.....</b>	<b>126</b>
5.4.1. Voltage Harmonics Impacts on Power Quality.....	126
5.4.2. Voltage Unbalance Impacts on Power Quality .....	129
<b>5.5. Final Considerations.....</b>	<b>135</b>
<b>5.6. Chapter Bibliography .....</b>	<b>136</b>
<b>Chapter 6 .....</b>	<b>138</b>
<b>6.1. General Considerations .....</b>	<b>138</b>
<b>6.2. Theoretical Foundation .....</b>	<b>139</b>
6.2.1. Standard IEC 60038-2009 .....	139
6.2.2. Permanent-Magnet Motors.....	140
<b>6.3. Assessing Voltage Magnitude Variation in IE2, IE3 &amp; IE4 classes IMs.....</b>	<b>142</b>
6.3.1. Standard IEC 60038-2009 .....	142
<b>6.4. Technical Assessment .....</b>	<b>143</b>

6.4.1. Load Curve in VV Conditions .....	143
6.4.2. Active Power and Current Total Harmonic Distortion .....	144
6.4.3. Power Factor .....	144
6.4.4. Efficiency .....	146
6.4.5. Temperature Assessment .....	147
<b>6.5. Statistical Assessment .....</b>	<b>149</b>
6.5.1. Correlation Matrix for Voltage Variation Conditions .....	149
<b>6.6. Economic Analysis .....</b>	<b>151</b>
<b>6.7. Final Considerations.....</b>	<b>155</b>
<b>6.8. Chapter Bibliography .....</b>	<b>156</b>
<b>Chapter 7 .....</b>	<b>157</b>
<b>7.1. Introduction .....</b>	<b>157</b>
7.1.1. General Considerations .....	157
7.1.2. Chapter Motivation and Contribution.....	158
<b>7.2. Theoretical Foundation.....</b>	<b>158</b>
7.2.1. Time-domain and Frequency-domain Analysis.....	158
7.2.2. Metric for Electric Motor Degradation Measurement.....	160
<b>7.3. Electric Motor Degradation Index .....</b>	<b>161</b>
7.3.1. Methodology .....	161
<b>7.4. Results and Discussion.....</b>	<b>164</b>
7.4.1. Nominal Condition.....	164
7.4.2. Single Phasing .....	165
7.4.3. Voltage Variation .....	166
<b>7.5. On-site Validation.....</b>	<b>168</b>
7.5.1. Measurement Campaigns .....	168
<b>7.6. Final Considerations.....</b>	<b>171</b>
<b>7.7. Chapter Bibliography.....</b>	<b>171</b>
<b>Chapter 8 .....</b>	<b>172</b>
<b>8.1. Journal Conferences Publications .....</b>	<b>172</b>
8.1.1. Papers published in International Journals with Qualis A1-A3 (Brazil) /Q1 (International).....	172

8.1.2. Papers published in other Journals. ....	173
8.1.3. Scientific papers submitted/ready to be submitted to journals in 2024. ....	173
<b>8.2. International Conferences .....</b>	<b>174</b>
8.2.1. Papers published in International Conferences .....	174
8.2.2. Scientific papers submitted/ready to be submitted to journals in 2024. ....	178
<b>8.3. Publications in Book Chapters .....</b>	<b>178</b>
<b>8.4. Participation as a speaker at international events .....</b>	<b>179</b>
<b>8.5. Application of Standards and Regulations for electric induction motors in Honduras</b>	<b>179</b>
<b>Chapter 9 .....</b>	<b>180</b>
9.1. General Considerations .....	180
9.2. Comparison of Motor Efficiency Classes in Good Power Quality Conditions .....	180
9.3. Impacts of Voltage Harmonics on IE2, IE3 and IE4 Class motors.....	181
9.4. Impacts of Voltage Unbalance on IE2, IE3, and IE4 Class motors .....	182
9.5. Impacts of Voltage Magnitude Variation on IE2, IE3 and IE4 Class motors .....	183
9.6. Electric Motor Degradation Indicator .....	183
9.7. Final Considerations and Future Works .....	184
IE2 Class Motor.....	186
IE3 Class Motor.....	187
IE4 Class LSPMM.....	188

## SUMMARY OF FIGURES

Figure 1-1 – Energy efficiency classes classification and consumption : (a) IEC 60034-30 nominal efficiency class limits, for four-pole motors (0.12-1000-kW power range) [6]; (b) Energy consumption of electric motor systems by efficiency level, 2000-2017 [7]. .....	25
Figure 1-2 - Countries with MEPS for electric motors in 2024. ....	26
Figure 1-3 - Methodology for literature review based on the PRISMA statement. ....	27
Figure 1-4 - Publications related to electric motors in recent years. ....	29
Figure 1-5 - Distribution of publications related to energy forecasting worldwide. ....	29
Figure 1-6 - Distribution of studies by subject area. ....	30
Figure 1-7 - Thematic map of keywords separated by relevant categories.....	30
Figure 1-8 - Publications related to electric motors diagnosis in the last 20 years. ....	35
Figure 1-9 - General test setup for the power quality disturbances tests.....	38
Figure 1-10 - General test setup for the electric motor degradation index tests.....	38
Figure 1-11 – Thermographic images of the LSPMM with: (a) 25% of 5th harmonic voltage distortion; (b) 10% of 5th harmonic voltage distortion. ....	39
Figure 2-1 - Induction Motor components [2].....	52
Figure 2-2 - Distribution of motor losses and percentage of losses for 0.75 kW – 160 kW IM's. ....	53
Figure 2-3 - Typical fraction of losses in 50-Hz, four-pole squirrel cage induction motors for (a) Losses variation as a function of output power [8]; (b) Losses variation as a function of load [9]. ....	54
Figure 2-4 - Impact of possible areas of improvement for induction motor performance [11].....	55
Figure 2-5 – Permanent magnet motors: (a) Surface mounted permanent magnet motor (SPM)[22] [23]; (b) Interior permanent magnet motor (IPM) [22] [24].....	57
Figure 2-6 - Structure of a four-pole LSPMM [28].....	58
Figure 2-7 - Typical rotor configurations for LSPMM's :(a) Spoke rotor; (b) W Type magnetic circuit structure; (c) Swastika magnetic circuit structure; (d) V-type magnetic circuit structure; (e) U-type magnetic circuit structure; (f) Series-type magnetic circuit structure [29], [30]. ....	59
Figure 2-8 – Starting torque in LSPMM and SCIM: (a) Starting behavior of torque components for LSPMM 's [31]; (b) Torque behavior for IM and LSPMM during starting [26].....	60
Figure 2-9 - Comparison between IE2, IE3 and IE4 efficiency class motors (a)Stator currents; (b) Total Harmonic Distortion of Current. ....	61
Figure 2-10 - Consumption in IE2, IE3 and IE4 class motors (a) Total Power; (b) Power F. ....	62
Figure 2-11 - Temperature rise for IE2, IE3 & IE4 IM 's classes: (a) Graphics from measurements and (b) LSPMM captured angle. ....	63
Figure 3-1 – Additional Negative and zero sequence losses in induction motors. ....	72

Figure 3-2 - Flowchart of methodology used to obtain the results from the measurements. .....	73
Figure 3-3 - Current increase for 2nd, 3rd, 5th, 7th and all harmonic order combined for induction motors (a) IE2 SCIM; (b) IE3 SCIM; (c) IE4 LSPMM. ....	74
Figure 3-4 - Total current harmonic distortion (THDI) variation for 2nd, 3rd, 5th, 7th and all harmonic order combined for induction motors (a) IE2 SCIM; (b) IE3 SCIM; (c) IE4 LSPMM. ....	75
Figure 3-5 - Reactive power increase for 2nd, 3rd, 5th, 7th and all harmonic order combined for induction motors (a) IE2 SCIM; (b) IE3 SCIM; (c) IE4 LSPMM. ....	76
Figure 3-6 - Power factor decrease for 2nd, 3rd, 5th, 7th and all harmonic order combined for induction motors (a) IE2 SCIM; (b) IE3 SCIM; (c) IE4 LSPMM. ....	77
Figure 3-7 - Temperature rise in the presence of voltage harmonics of 2nd, 3rd, 5th, 7th and all harmonic order combined for induction motors (a) IE2 SCIM; (b) IE3 SCIM; (c) IE4 LSPMM. ....	78
Figure 3-8 - Thermographic images of the LSPMM in presence of 2 <sup>nd</sup> voltage harmonics in frontal and lateral view (a) Thermal equilibrium frontal view; (b) 25% of 2 <sup>nd</sup> voltage harmonic in frontal view; (c) Thermal equilibrium lateral view; (d) 25% of 2 <sup>nd</sup> voltage harmonic in lateral view .....	79
Figure 3-9 - Thermographic images of the LSPMM in presence of 5 <sup>th</sup> voltage harmonics in frontal and lateral view (a) Thermal equilibrium frontal view; (b) 25% of 5 <sup>th</sup> voltage harmonic in frontal view; (c) Thermal equilibrium lateral view; (d) 25% of 5 <sup>th</sup> voltage harmonic in lateral view .....	79
Figure 3-10 - Correlation matrix between temperature and input parameters in IE2 class SCIM for (a) second harmonic voltage distortion; (b) third harmonic voltage distortion. ....	81
Figure 3-11 - Temperature regression versus motor input parameters for IE2 class SCIM with voltage distortion of (a) 2nd harmonic voltage distortion; (b) 3rd harmonic voltage distortion.....	81
Figure 3-12 - Correlation matrix between temperature and input parameters in IE3 class SCIM for (a) second harmonic voltage distortion; (b) third harmonic voltage distortion. ....	82
Figure 3-13 - Temperature regression versus motor input parameters for IE3 class SCIM with voltage distortion of (a) 2nd harmonic voltage distortion; (b) 3rd harmonic voltage distortion.....	82
Figure 3-14 - Correlation matrix between temperature and input parameters in IE4 class LSPMM for (a) second harmonic voltage distortion; (b) third harmonic voltage distortion.....	83
Figure 3-15 - Temperature regression versus motor input parameters for IE4 class LSPMM with voltage distortion of (a) 2nd harmonic voltage distortion; (b) 3rd harmonic voltage distortion.....	83
Figure 3-16 Incremental Impact of Voltage distortion on Temperature: (a) Long bars represents a predictor that contribute the newest information to the model; (b) Predictors used in the model (a gray background represents an X variable not in the model).....	85



Figure 3-17 – Temperature as a function of 2 <sup>nd</sup> voltage harmonic: (a) Prediction plot for Temperature model with 95% of prediction interval; (b) Prediction plot with large residual versus the fitted values. ....	86
Figure 3-18 - Adjusted coefficient of determination (adjusted R2) for generated models presented in Table 2. ....	86
Figure 3-19 - Line-start permanent magnet motor simulation on FEMM:(a) LSPMM geometry and materials and (b) LSPMM mesh.....	88
Figure 3-20 - Density flux plot for (a) Nominal conditions; (b) 2nd voltage harmonics and (c) 5th voltage harmonics.....	89
Figure 3-21 - Quarter section of motor illustrating the areas with convection boundary conditions. ....	90
Figure 3-22 - Temperature distribution (in Kelvin) in the motor from the FEMM thermal simulation for: (a) Second Voltage Harmonic and (b) Fifth Voltage Harmonic. ....	90
Figure 3-23 - Comparison between the model and measured temperature for 25% voltage harmonic distortion of 2nd and 5th order harmonics. ....	91
Figure 4-1 - Power derating curve for Induction Motors .....	95
Figure 4-2 - The Complex Voltage Unbalance Factor Diagram [13]. ....	98
Figure 4-3 - Induction motor subjected to voltage unbalance: (a) Induction motor with a low maintenance program, (b) Input voltage magnitudes in induction motor terminals. ....	99
Figure 4-4 - Voltage Unbalance supply on a delta-connected IM and the resulting positive (a) and negative (b) sequence components. ....	100
Figure 4-5 - Induction motor voltages when subjected to voltage unbalance (a) Balanced voltage phasors; (b) Unbalanced voltage phasors. ....	101
Figure 4-6 – Positive and negative sequences for impedances for IE2 , IE3 and IE4 Class motors(a) Positive sequence and (b) Negative sequence. ....	104
Figure 4-7 - Flowchart of methodology used to obtain the results from the measurements. ....	105
Figure 4-8 - Line and average current for VU in IE4 LSPMM with: (a) 1% Under Voltage;(b) 3% Under Voltage; (c) 4% Under Voltage;(d) 1% Over Voltage; (e) 3% Over Voltage;(f) 4 % Over Voltage.....	106
Figure 4-9 - Average Current for under and over voltage unbalance conditions for: (a) IE2 SCIM; (B) IE3 SCIM; (c) IE4 LSPMM .....	107
Figure 4-10 - Power Factor (a-c) and Positive-Phase sequence voltage variation (d-e) with Under and Over Voltage Unbalance for IE2 Class SCIM, IE3 Class SCIM and IE4 Class LSPMM. ....	107
Figure 4-11 - Total power variation with Under and Over Voltage Unbalance for: (a) IE2 Class SCIM; (b) IE3 Class SCIM; (c) IE4 Class LSPMM. ....	108
Figure 4-12 - Current Total Harmonic Distortion for under and over voltage unbalance conditions for: (a) IE2 SCIM; (b) IE3 SCIM; (c) IE4 LSPMM. ....	109
Figure 4-13 - Frame Temperature with 1% under voltage (a & b); 3% under voltage (c & d); 4% under voltage. ....	110
Figure 4-14 - Frame Temperature with 1% over voltage (a & b); 3% over voltage (c & d); 4% over voltage (e & f). ....	110

Figure 4-15 - Temperature increase in IE2, IE3 and IE4 class IM's with: (a) 1% under voltage; (b) 3% under voltage; (c) 4% under voltage; (d) 1% over voltage; (e) 3% over voltage; (f) 4% over voltage. ....	111
Figure 4-16 - Correlation matrix for IE3 Class SCIM motor parameters in the presence of VU with: (a) 4% Under voltage; (b) 4% Over voltage. ....	112
Figure 4-17 - Correlation matrix for IE4 Class LSPMM motor parameters in the presence of VU with: (a) 4% Under voltage; (b) 4% Over voltage. ....	112
Figure 4-18 - Temperature for the IE4 Class LSPMM: (a) Prediction plot for Temperature model with 95% of prediction interval; (b) Highlighting initial motors temperature measurements before applying unbalanced voltage supply. ....	114
Figure 4-19 - Residuals versus fitted or predicted temperature values. ....	114
Figure 4-20 - Adjusted coefficient (Adjusted R <sup>2</sup> ) for generated models presented in Table 7 .....	115
Figure 5-1 - Steps toward the implementation of energy efficiency actions on induction motor policies.....	122
Figure 5-2 – Methodology flowchart. ....	125
Figure 5-3 - Speed variation for IE2, IE3 & IE4 Class motors in presence of 2nd, and combined 2nd, 3rd, 5th and 7th voltage harmonics.....	126
Figure 5-4 - Speed variation for IE2, IE3 & IE4 Class motors in presence of 5th and 7th voltage harmonics. ....	127
Figure 5-5 - Harmonic currents present in IM 's with harmonic voltage distortion of (a) 2nd harmonic order; (b) 5th harmonic order; (c) 7th harmonic order (d) 2nd, 3rd, 5th and 7th harmonic order combined. ....	128
Figure 5-6 - Speed variation for IE2, IE3 & IE4 Class motors in presence of 0%-4% Voltage Unbalance Conditions with under and over voltages; .....	129
Figure 5-7 - - Fifth harmonic currents variations for phases a-b-c for the IE3 Class motor for (a) 1% VU with Under Voltage; (b) 4% VU with Under Voltage; (c) 1% VU with Over Voltage; (d) 4% VU with Over Voltage .....	130
Figure 5-8 – Fifth harmonic currents variations for phases a-b-c for the IE4 Class motor for (a) 1% VU with Under Voltage; (b) 4% VU with Under Voltage; (c) 1% VU with Over Voltage; (d) 4% VU with Over Voltage .....	131
Figure 5-9 - Seventh harmonic currents variations for phases a-b-c for the IE3 Class motor for (a) 1% VU with Under Voltage; (b) 4% VU with Under Voltage; (c) 1% VU with Over Voltage; (d) 4% VU with Over Voltage .....	132
Figure 5-10 - Seventh harmonic currents variations for phases a-b-c for the IE4 Class motor for (a) 1% VU with Under Voltage; (b) 4% VU with Under Voltage; (c) 1% VU with Over Voltage; (d) 4% VU with Over Voltage .....	133
Figure 5-11 - Phase “a” harmonic current variation for 4% Voltage unbalance with undervoltage for (a) IE3 and (b) IE4 Class motors .....	134
Figure 5-12 - Phase “a” harmonic current variation for 4% Voltage unbalance with overvoltage for IE3 (a) and IE4 (b) Class motors .....	134
Figure 6-1 - Image of Table 1 of the IEC 60038-2009 standard in relation to allowable voltages in power systems worldwide [5, p. 2009]. ....	139

Figure 6-2 - Three-phase nominal voltage by region for a nominal 220 V LSPMM in a delta connection. ....	140
Figure 6-3 - Line-start permanent magnet: (a) Component description in the first panel and (b) magnetic flux lines. ....	141
Figure 6-4 - Experimental input current as a function of load for 0.75 kW: (a) IE4 Class LSPMM and (b) IE3 Class SCIM motor at nominal voltage and frequency conditions. ....	141
Figure 6-5 - Methodology flowchart.....	142
Figure 6-6 - Experimental input current as a function of load at different voltage magnitudes. ....	143
Figure 6-7 - LSPMM under VV conditions. (a) Active power and (b) current total harmonic distortion.....	144
Figure 6-8 - Experimental power factor as a function of load under VV conditions.....	145
Figure 6-9 - Ridgeline plot of power factor under VV conditions for the LSPMM. ....	145
Figure 6-10 - Contour plots for power factor variation with power and load for IE4 Class motor with (a) 0.90 p.u., (b) 1.00 p.u., and (c) 1.05 p.u. ....	146
Figure 6-11 - Experimental efficiency as a function of load under VV conditions. ....	147
Figure 6-12 - Frame temperature variation in the LSPMM under VV conditions. Frontal temperature with (a) 0.90 p.u., (b) 1.00 p.u., and (c) 1.10 p.u. ....	148
Figure 6-13 - Frame temperature variation in the LSPMM under VV conditions. Lateral temperature with (a) 0.90 p.u., (b) 1.00 p.u., and (c) 1.10 p.u. ....	148
Figure 6-14 - Measured absolute temperature under VV conditions: (a) lateral view; (b) frontal view.....	148
Figure 6-15 - Correlation matrix between voltage magnitude and input parameters in the LSPMM for (a) output load between 0% and 30%, (b) output load between 40% and 70%, and (c) output load between 80% and 125%.....	150
Figure 6-16 - Consumption as a function of voltage magnitude under different load conditions. ....	151
Figure 6-17 - Representation of the time-of-use tariff pricing scheme considered in the economic analysis. ....	152
Figure 6-18 - Payback for the initial cost of a new motor by changing the LSPMM voltage supply level: (a) without considering the TOU; (b) considering the TOU. ....	154
Figure 7-1 - Graphical representation of the Electric Motor Degradation Index (EMDI) methodology.....	159
Figure 7-2 – General test setup. ....	162
Figure 7-3 – Methodology Flowchart. ....	163
Figure 7-4 – EMDI calculation in dB for the nominal voltage operation condition and loading varying from 30% to 125% of nominal for: (a) IE2 Class motor and (b) IE3 Class motor. ....	164
Figure 7-5 – Single phasing triggered in IE3 Class motor to evaluate the EMDI. ....	165
Figure 7-6 – EMDI calculation in dB for a single phase-loss in the IE3 Class motor. ....	166
Figure 7-7 – Input current variation as a function of load in VV conditions.....	167
Figure 7-8 – EMDI calculation in VV conditions for nominal load condition. ....	167

Figure 7-9 – Pumping System at the Federal University of Pará: (a) 15 kW SCIM and (b) Power quality analyzer for electric motors consumption measurement. ....	168
Figure 7-10 – Voltage magnitude variation for the electric motor input. ....	169
Figure 7-11 – Measured input line currents as a function of time. ....	169
Figure 7-12 – Electric motor diagnosis indicator comparison in VV conditions. ....	170
Figure 10-1 - IE2 Class induction motor nameplate. ....	186
Figure 10-2 - IE2 Class induction motor parameters. ....	186
Figure 10-3 – IE3 Class induction motor nameplate. ....	187
Figure 10-4 - IE2 Class induction motor parameters. ....	187
Figure 10-5 – IE4 Class line-start permanent magnet motor nameplate. ....	188

## SUMMARY OF TABLES

Table 1-1. Review of literature regarding induction motors and voltage unbalance .....	32
Table 1-2. Review of literature regarding induction motors and harmonics.....	34
Table 1-3. Induction motor parameters. ....	38
Table 3-1 Harmonic order sequences .....	71
Table 3-2 - Summary of temperature models for voltage harmonics in IMs classes IE2, IE3 and IE4. ....	87
Table 4-1 Phase-voltage magnitudes IM with under and overvoltage.....	103
Table 4-2 Voltage Unbalance Parameters for IE2 Class IM with under and overvoltage .	103
Table 4-3. Voltage Unbalance Parameters for IE3 Class IM with under and overvoltage	104
Table 4-4 Voltage Unbalance Parameters for IE4 Class IM with under and overvoltage .	104
Table 4-5 Summary of temperature models for voltage unbalance in IM ´s classes IE2, IE3 and IE4. ....	116
Table 5-1. Induction Motors parameters .....	124
Table 5-2. Voltage Unbalance magnitudes .....	125
Table 7-1. Electric Motor Degradation Indicator in Nominal Conditions for IE2 Class motor. .....	164
Table 7-2. Squirrel Cage Induction Motor in Pump System parameters .....	168

## Chapter 1

# Global Overview of Electric Motors

Europe has started the transition process towards IE4 motor class. By setting a precedent, it is expected that other regions will follow these implementations toward higher efficiency motor classes. This chapter presents a national (Brazil) and global overview related to energy efficiency in electric motors. Then, a review of the literature related to the impact of different power quality disturbances in electric motors is presented. The objectives and contributions of this thesis are also presented.

### 1.1. General Considerations

In 2015, the Paris Agreement represented a significant global step in addressing climate change. Since then, it has driven the implementation of policies and regulations focused on energy efficiency, playing a key role in achieving environmental goals and promoting sustainable practices internationally. In this context, Induction motors (IMs) represent an important category for energy savings with about 53% of the world's final electrical energy consumption [1].

In Brazil, according to the Ministry of Mines and Energy in the document “National Energy Efficiency Plan” [2], the industry consumes 36% of the total national electricity and the driving systems in operation consume 68% of this electricity. Therefore, it is reported that approximately 35% of the country's total electrical energy is consumed by electric motors.

The three-phase squirrel-cage induction motors were the first and only equipment to be regulated by presidential decree in Brazil, with the publication of Presidential Decree No. 4.508 of December 11, 2002. This led to a major transformation of the electric motor market in Brazil. First, the regulations established the minimum power ratings for classes IR1 (standard motors)<sup>1</sup> and IR2 (high-efficiency motors). Motors (with the characterization shown in Appendix 1 of the decree) with powers lower than those of class IR1 could not be manufactured, marketed, or imported. This decree was backed up by Law No. 10,295 of October 17, 2001, which establishes the National Policy for the Conservation and Rational Use of Energy, known as the "Energy Efficiency Law", enacted following the energy crisis that occurred at the time, popularly known as the "Blackout".

---

<sup>1</sup> IR is equivalent to IE, in BRAZIL, IR= Índice de rendimento

Later, the Interministerial Decree No. 553 of December 8, 2005, was published, which established IR2 as the new efficiency class but also set a deadline for the market to adapt to it. According to this decree, as of 2010, the manufacture, import, and sale of squirrel-cage induction motors in Brazil had to meet the minimum efficiency requirements of class IR2.

In June 2017, following the evolution of the regulation based on the Impact Study of the Premium Motor Regulation prepared by Eletrobras (2015), Interministerial Decree No. 1 of June 29, 2017, was published. This decree established that three-phase squirrel-cage induction motors sold in Brazil, as well as imported motors, must have an efficiency equal to or greater than the minimum efficiency for the premium class (IE3), with a deadline for the market to adapt 2 years after its publication. In addition to raising the minimum efficiency from IR2 to IR3, the scope of electric motors covered has been expanded to include motors with a fractional commercial power rating of less than 500 hp [3], [4]. The next section presents the minimum energy performance standards and their relationship to IEC 60034-30-1 for electric motor efficiency.

## **1.2. Minimum Energy Performance Standards**

Each year, approximately 30 million new electric motors are sold worldwide for industrial use, and approximately 300 million motors are in use in industry, infrastructure, and large buildings [5]. To help realize the huge potential for cost-effective energy savings, many countries around the world have established local regulations known as MEPS (Minimum Energy Performance Standards). MEPS are regulations that set a floor for the efficiency class of motors and motor-driven equipment that can be sold in a market, whether domestically manufactured or imported, and currently exist in more than 80 countries around the world. Substitution between efficiency classes can lead to great savings in economic and energy terms. However, the efficiency and performance of IMs depend not only on their design and technology but also on the operating conditions. Since the power quality in real electrical systems is far from ideal, the efficiencies of electric motors also deviate from their ideal value depending on the operating conditions.

The super-premium efficiency IE4 class motor was introduced in 2008 by the IEC standard 60034-30-1. This fact encouraged the transformation of a competitive market for even more efficient motors and made manufacturers go beyond AC induction motor technologies to achieve the required minimum full-load efficiency values. Figure 1-1a shows the efficiency classes according to the IEC standard [3] for four-pole 50/60 Hz motors [6]. The IE5 class technologies

are not yet defined in detail but are planned for a future edition of the standard. The goal is to reduce IE5 losses by about 20% compared to IE4 efficiency class.

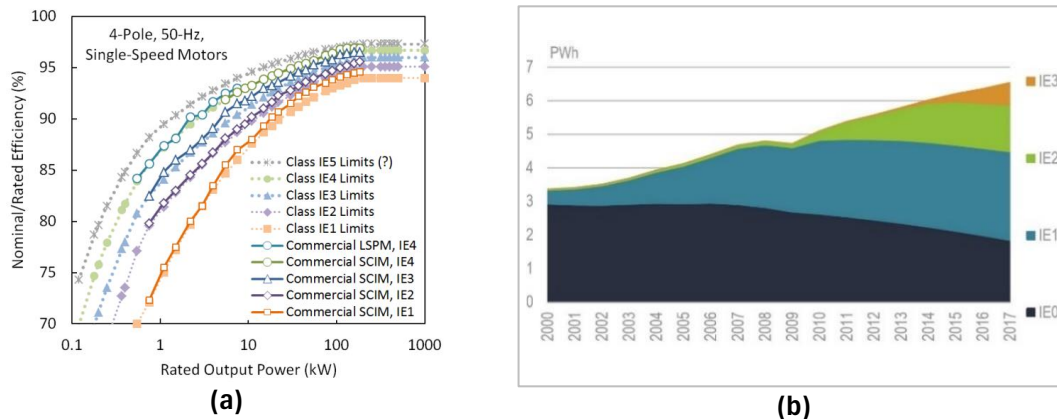


**Figure 1-1** – Energy efficiency classes classification and consumption : (a) IEC 60034-30 nominal efficiency class limits, for four-pole motors (0.12-1000-kW power range) [6]; (b) Energy consumption of electric motor systems by efficiency level, 2000-2017 [7].

The average life of three-phase electric motors varies from 12 to 20 years, depending on the rated power, operating conditions, and power supply. In industry, many motors do not even meet the IE1 efficiency class. In 2017, approximately 30% of the world's electricity consumption was associated with unregulated electric motors classified as IE0. IE1 class induction motors cover about 40% of global electricity consumption, with IE2 and IE3 motors taking an increasing share, as shown in Figure 1.1 (b) [7]. It is estimated that almost three-quarters of the world's electricity demand for all motors is consumed by medium-sized induction motors (0.75-375 kW) [8]. Thus, there is still a huge energy savings potential that can be increased by adopting energy-efficient motor policies and programs.

Establishing a legal and institutional framework for MEPS, adopting international standards, and collecting information on the baseline data of the motor market, including information on tariffs and carbon emission factors, current, historical, and projected. Hypothetical scenarios should then be developed for the energy, economic, and environmental impacts. Typically, IE2 with a timetable for graduation to IE3 is recommended for countries with a domestic motor manufacturing industry, and IE3 is recommended for countries without a domestic motor manufacturing industry. Finally, monitoring, verification, and enforcement must be established to ensure the success of MEPS. Figure 1-2 shows countries around the world that have adopted MEPS. In the EU, all electric motors with a rated power between 0.75kW and equal to or less than 1000kW must meet the IE3 level from July 2021 and motors between 75kW and 200kW must meet the IE4 level from July 2023 [9], [10].



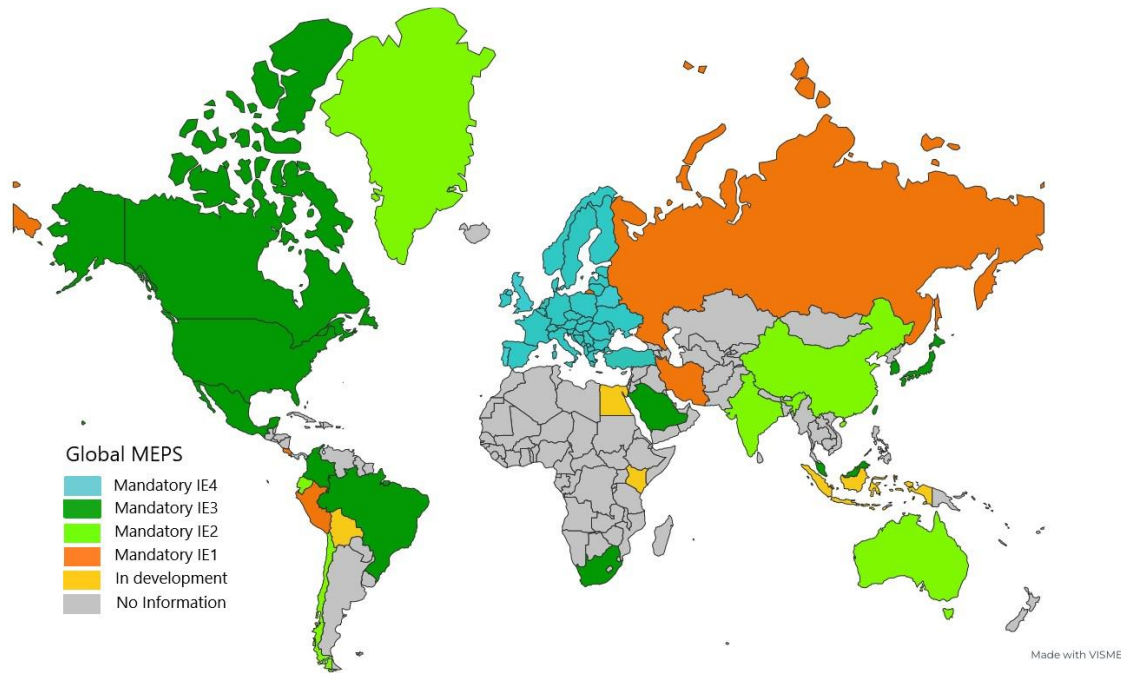


**Figure 1-2** - Countries with MEPS for electric motors in 2024.

### 1.3. Brazilian Induction Motor Regulation

In August 2019, the new Energy Efficiency Law for Electric Motors came into force, which establishes the minimum level of performance in IE3, according to Interministerial Regulation No. 1 [4]. With the implementation of high-efficiency motors, it is expected to save more than 11 TWh of electricity between 2019 and 2030, in addition to \$4.7 million in energy costs by 2020 and \$172 million by 2050 [7]. Although the new law is positive, the requirements published in the regulation do not include the electric motors already installed. On average, 20.1 million three-phase motors are installed in Brazil [11]. A study carried out in Switzerland showed that in industries there are a large number of motors operating beyond their life expectancy [12], this is because they have probably been repaired more than once, studies show that the efficiency losses can vary from 3 to 7.5 percentage points with each rewinding if the proper procedure is not used [11], however, with the correct winding process, there is evidence of increases in motor efficiencies, as shown in [13], [14].

To maintain or even increase productivity in the industrial sector by consuming less electricity, Public Call No. 002/2015 [15] promotes the replacement of old or reconditioned electric motors with more modern and efficient motors, through a limited bonus system for the replacement of three-phase induction electric motors manufactured until 2009 and with a power between 0.75 kW and 250 kW, and single-phase electric motors with a power equal to or greater than 0.75 kW.

It is important to note that the bonus percentage is defined by the concessionaire, who must submit the amounts for approval by ANEEL [16].

The initial cost of the electric motor represents approximately 5% of the cost of operation throughout its useful life, efficiency improvements come with increases in the initial value of electric motors, especially when new technologies are implemented, as is the case of the IE4 class permanent magnet motor, although initially the value of these motors was up to 2 times the value of the IE3 SCIM [17], which increase the payback of the investment, over the years its value has been decreasing until reaching values of 1.3 times the cost of the SCIM [18], being more profitable for replacement in the industry.

### 1.4. Methodology for the Literature Review

For the development of the literature review, the work in [19], based on the PRISMA (Preferred Reporting Items for Systematic Reviews and Meta-Analyses) statement, was used as a reference [20]. The methodology, shown in Figure 1-3, includes a bibliometric analysis that aims to map the scientific production, identify the research patterns, and evaluate the influence of the journals and the institutions in the field of electric motors.

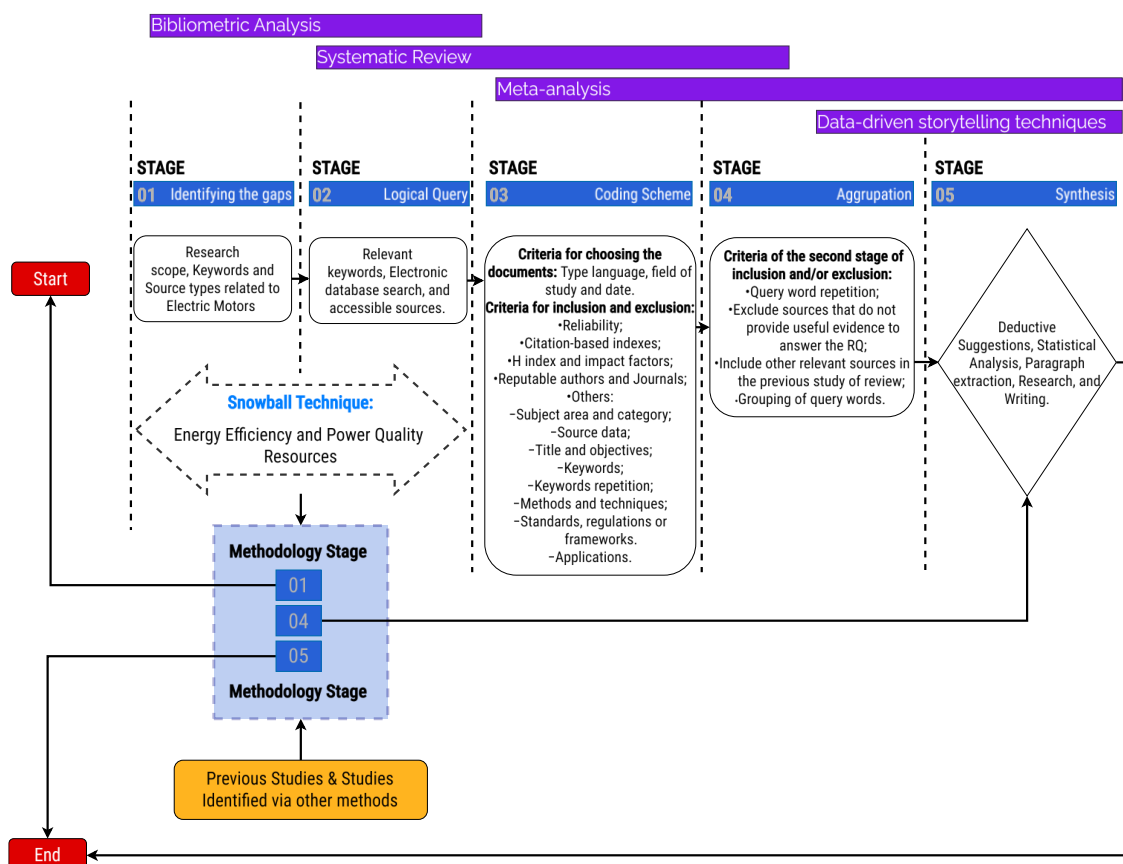


Figure 1-3 - Methodology for literature review based on the PRISMA statement.

For the study, the most relevant keywords defined on the basis of the subject of this thesis and used for the search were: "induction motors" AND "permanent magnet motors" OR "asynchronous motors" OR "synchronous motors" AND "energy" AND "efficiency" AND "power quality" AND "diagnostics" AND NOT "electrical" AND "vehicles" AND NOT "traction motor". Searches were conducted using the academic platform Scopus. Inclusion and exclusion criteria were used to filter and exclude the documents related to other fields of knowledge. After analyzing the data, a systematic analysis was carried out, separating, and grouping them according to the approach used. Finally, techniques for visualizing the synthesized data are used to graphically present the results of the proposed previous study.

Considering that the authors have previously conducted literature reviews on medium and long-term forecasting, a section of previous studies and studies identified through other methods was considered to complement the methodology applied according to the first (1st), fourth (4th), or fifth (5th) methodological step. The snowball method, which consists of using the reference list of an article or its citations to identify other articles on the analyzed topic, was also used in this previous study. The selected papers are also classified according to the methodological stage to complement the systematic review [5].

### **1.5. Bibliometric Analysis**

A survey of publications related to energy forecasting was conducted over the last 24 years, as shown in Figure 1-4. The figure shows that the highest peak of publications for the defined string was reached in 2009. However, the values were almost reached in 2023. In 2024 it will be possible to observe if there is a repetitive pattern or if the trends continue to increase, surpassing the 2009 values with more than 139 publications.

Research on electric motors is led by China, the United States, and Japan, as shown in Figure 1-5. India, Canada, Italy, the United Kingdom, the Russian Federation, Germany and South Korea are the top 10 countries with the most publications on this topic. Brazil, where this study was carried out, is in 15th place, according to the survey.

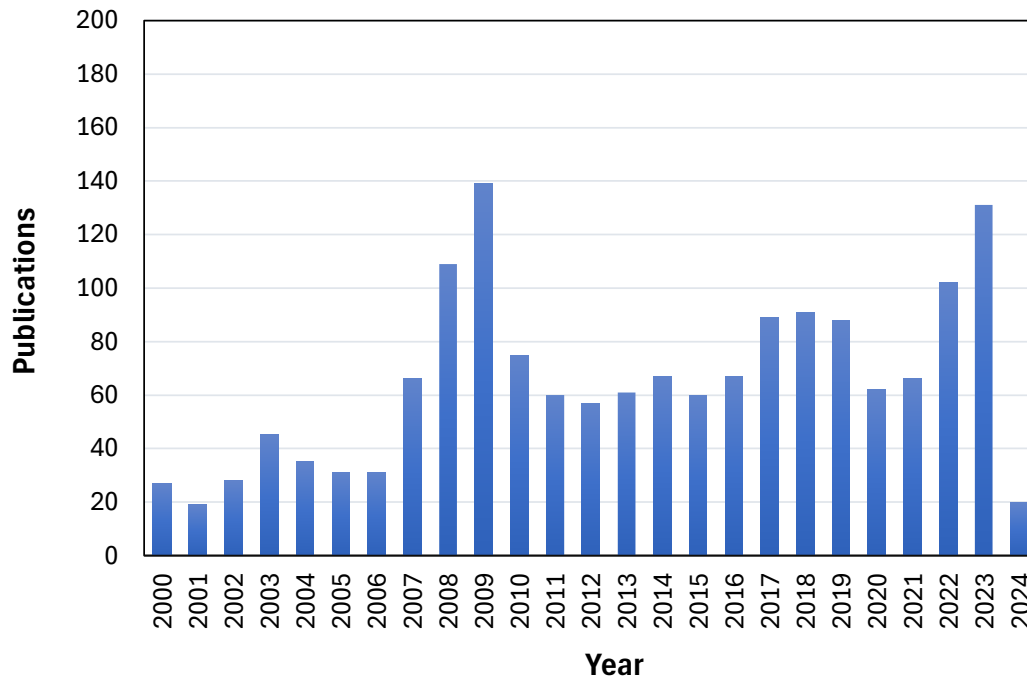


Figure 1-4 - Publications related to electric motors in recent years.

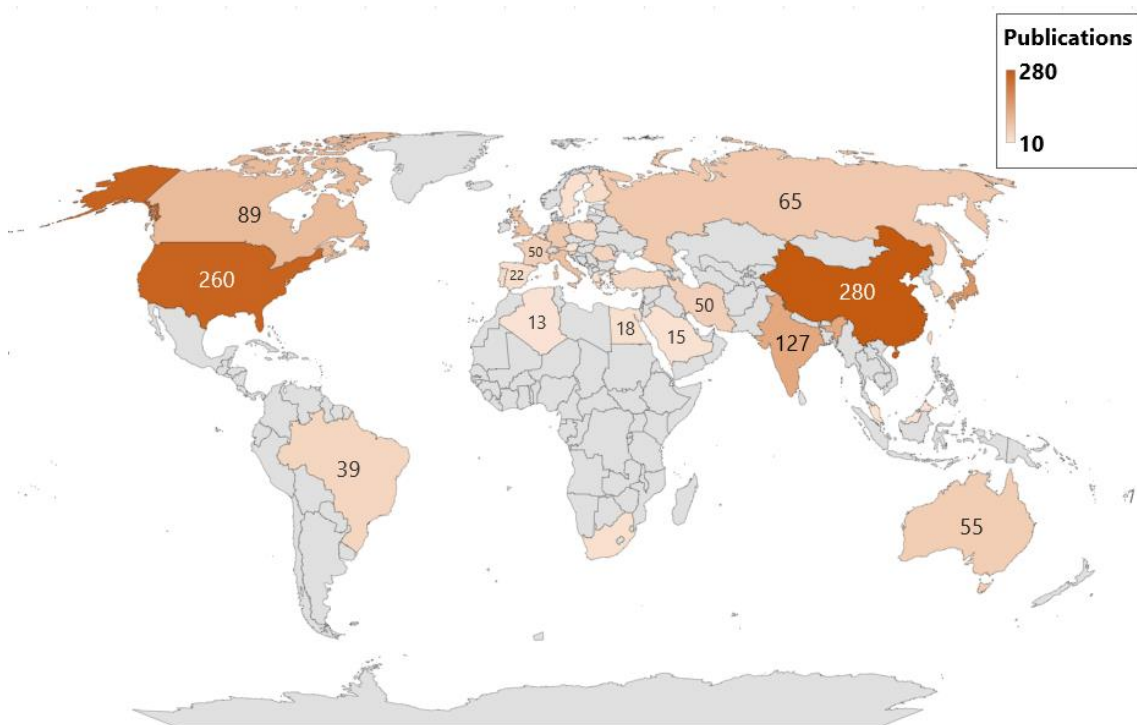
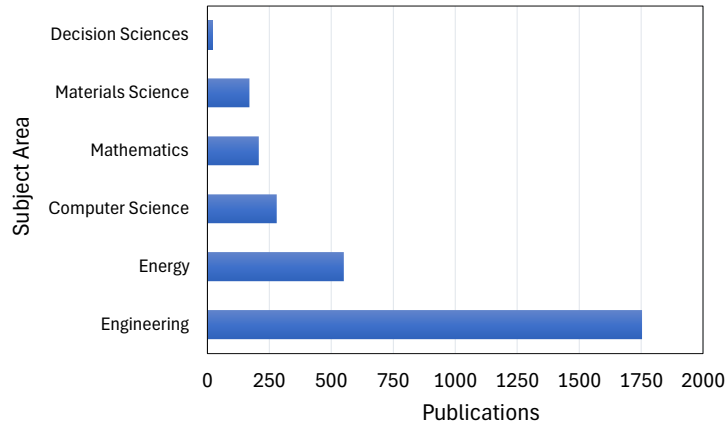


Figure 1-5 - Distribution of publications related to energy forecasting worldwide.

Figure 1-6 shows the fields of study related to electric motors. It can be seen that engineering and energy are the dominant fields, with a significant proportion of the research undertaken in the field of computer science, but also including other categories such as mathematic, materials science and decision sciences.



**Figure 1-6** - Distribution of studies by subject area.

An important analysis based on the collected information is the relevant keywords within the analyzed studies. For this purpose, the VOSViewer software was used to generate a thematic map of the keywords according to the number of times they were cited in the studies, as well as the connections with other studies and keywords, as shown in Figure 1-7.

To define and classify the universe of keywords, a clustering process was performed in the software, which resulted in three main areas: Induction Motors, Fault Diagnosis, Synchronous Motors, Permanent Magnet Motors, Power Quality and Energy Efficiency, all of which will be discussed in the systematic review in the following subsections.

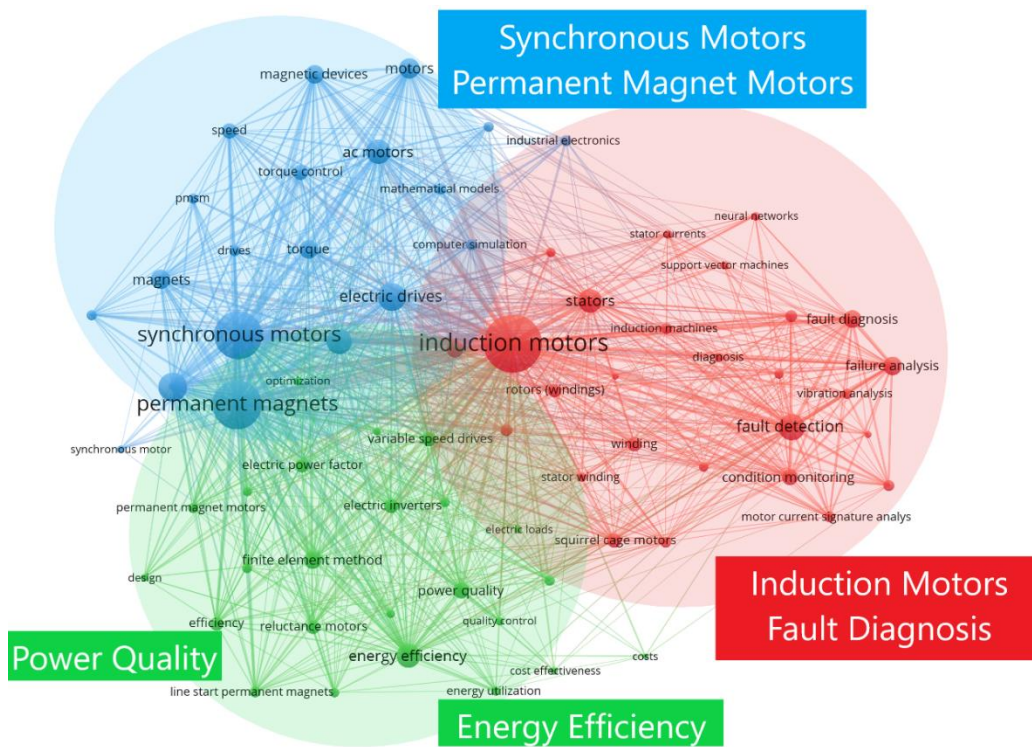


**Figure 1-7** - Thematic map of keywords separated by relevant categories.

## **1.6. Systematic Review**

### **1.6.1. Efficient Electric Motors**

The introduction of different efficiency classes has come as a consequence of studies and tests carried out by researchers and manufacturers in order to identify the losses in induction motors and the ways to reduce them. An analysis of the technical and economic benefits of substitution between these technologies has been presented in [17], [21], [22], [23], [24], [25], [26], [27], [28], [29]. In addition, the studies in [23], [24], [27], [28], [30], [31], [32], [33], [34], [35], [36], [37], [38] include the main design features, weaknesses and strengths related to the LSPMM. Then, from a regulatory and policy point of view, different analyses comparing the challenges and projections related to efficient motors have also been presented in [5], [39], [40], [41], [42]. In [17], an example of field replacement of a squirrel cage induction motor by a line start permanent magnet motor (LSPMM) is presented. A good performance and lower consumption are obtained with these technologies; however, the harmonic losses seem to be higher in the LSPMMs at no-load conditions.

New higher efficiency motors are built according to the IEC 60034-7 standard [43]. This standard specifies the requirements concerning the classification of construction types, mounting arrangements, and terminal box position, which contribute to the substitution between technologies. Studies have shown that the higher initial cost of higher efficiency motors can be amortized in a short period due to energy savings and initial financial incentive programs; higher efficiency, power factor, and thermal behavior are also some of the benefits obtained with these technologies. However, a cost-benefit analysis, taking into account the type of application and supply conditions, must be developed before substitution.

### **1.6.2. Voltage Unbalance state of art**

The effect of voltage unbalance on the performance of IMs has been studied extensively. Its negative effects on torque, power factor, and efficiency have been documented in [6], [44], [45], [46], [47], [48], also voltage unbalance results in higher current unbalance, increased losses, and consequently temperature rise.

Given the multiple damages that this disturbance represents in the IMs, different standards have defined the maximum limits allowed for this phenomenon. Currently, there are four definitions of voltage unbalance, defined by NEMA, IEEE, CIGRÉ and [49], [50], [51], each with

different considerations and interpretations, mainly because the same percentage of unbalance can be obtained for different voltage magnitudes, with undervoltage and overvoltage. In [52], a complete analysis of the effect of voltage unbalance is developed. This includes under- and overvoltage. According to the experimental results, an undervoltage unbalance will usually cause the worst temperature rise, and a higher positive sequence voltage will also lead to a higher motor efficiency and a lower power factor.

Concerning temperature, voltage unbalance (VU) induces an uneven increase in current, amplifying joule losses and consequently elevating operating temperatures [6], [44], [46], [47], [49], [53], [54]. Additionally, various voltage unbalance configurations can coexist within electrical systems. Experimental findings in [55], experimental results show that unbalance with undervoltage results in the greatest temperature increases. In general, for every 10°C increase in winding temperature, the life of the motor is reduced by half [55].

According to Yaw-Juen Wang [56], in addition to the magnitude of the voltages, the angle of the unbalance is also necessary to fully analyze the effects of unbalance in electric motors. Related studies considering the complex voltage unbalance factor are presented in [56], [57], [58], [59]. A summary of the literature review related to VU and electric motors, classified according to the approaches analyzed in this work, is presented in Table 1-1.

**Table 1-1. Review of literature regarding induction motors and voltage unbalance**

Paper Main Subject	Relevant Literature
Induction motors comparison	[17], [21], [22], [24], [25], [26], [28], [31], [55], [60], [61], [62]
Voltage Unbalance impacts on induction motors	[6], [44], [45], [46], [47], [48]
Standards related to Voltage Unbalance	[49], [50], [51]
Economic substitution studies	[17], [29]
Line-start permanent magnet motor (LSPMM)	[5,17,18,21, 22, 24–28,31,32,43,45–51]
Temperature increases due to voltage unbalance	[6], [44], [72], [47], [46], [49], [53], [54]

### 1.6.3. Voltage Harmonics State of the Art

The effects of poor power quality caused by voltage harmonics in industry have been studied to analyze their main effects on the performance of induction motors. Continuous operation of motors on a polluted harmonic system results in higher temperatures in the stator and rotor windings and in the core due to additional harmonic losses, torque reduction, noise, and mechanical vibrations, according to the literature [22], [63], [73], [74], [75]. The close interaction

between current harmonics, saturation and mechanical problems such as bearing failure and static eccentricity can lead to premature failure and consequently reduced service life as presented in [76], [77], [78].

The presence of nonlinear loads in electrical systems results in current and voltage distortions that can have detrimental effects depending on the type of load and its interaction with other system components. According to [79], harmonic distortion is commonly found in disturbed power distribution systems and in most cases includes 3rd, 5th, 7th, 9th and 11th order harmonics.

Due to the synchronous speed, no currents are induced inside the LSPMM rotor (neglecting spatial and time harmonics), so the rotor temperature of these motors is about 30% lower than that of the induction motors with the same output power [31]. In [83], the rated load winding temperature rise of IE4 IMs is lower when compared with IE3 class and that of IE3 class is lower than the IE2 class IMs. Fifth and seventh voltage harmonics are analyzed in [60], [61], showing that fifth harmonic results in higher temperature increases when compared with the seventh harmonic, mainly due to the counter-rotating field with respect to fundamental frequency produced by the fifth negative sequence harmonic.

Concerning temperature, thermography has been one of the most used methods in the industry for the identification of faults in electric motors, as well as predictive maintenance. The works presented in [7,14–18], show theoretical and practical studies of electric motor monitoring techniques including statistical and computational intelligence analysis with useful results for the identification of faults of different natures such as electrical, mechanical, thermal, and environmental. According to [84], temperature rise of IMs due to harmonics is approximately between 4–6 °C.

In the literature, many works have focused on evaluating motors' performances and losses using techniques based on numerical-computation-based models. The works presented in [19,20] use the same LSPMM technology used in this work to model and validate the LSPMM model through experimental tests. The studies use the parameters of the LSPMM equivalent circuit calculated empirically, as well as numerical methods that are later validated by means of experimental measurements, however without considering harmonics in the motor supply.

A summary of the literature review related to harmonics and electric motors, classified according to the approaches analyzed in this work, is presented in Table 1-2.



**Table 1-2. Review of literature regarding induction motors and harmonics.**

Paper Main Subject	Relevant Literature
Harmonics impacts on induction motors	[5,6,22,34,35,36,39–44]
Harmonics presence and diagnosis in power systems	[11,12,44]
Fault diagnosis in induction motors	[78], [80], [81], [91]
Temperature increases due to harmonics	[3,5,34–36,52]

#### 1.6.4. Voltage Magnitude Variation in Induction Motors

The literature on voltage-variation (VV) conditions disturbances and permanent-magnet synchronous motors is limited. Early studies assessing the effects of VV were documented in the late 1920s when the authors of [93] conducted a detailed evaluation of a 5-hp motor under VV conditions, revealing the detrimental effects of this disturbance on efficiency, power factor, and torque. The study [93] also found that core losses are directly proportional to voltage magnitude when assessing torque, efficiency, and power factor. However, Joule losses considerably increase under undervoltage conditions compared with those under overvoltage conditions, although both cases result in losses higher than those obtained under nominal conditions. Similar results regarding efficiency and losses were found in [94] using an SCIM model.

In [95], VV was analyzed based on a dynamic motor model constructed in Simulink. In this model, core losses varied with voltage magnitude and, to a lesser extent, with load variations. However, Joule losses decreased with the decreasing voltage magnitude. In [96], the efficiency in an SCIM model varied proportionally with the voltage magnitude up to values of 1.05 p.u., after which it began to decrease.

Other studies analyzing this disturbance, including temperature assessment, have also been presented [96], [97], [98], [99], [100], [101], [102], [103], [104]. Furthermore, techniques for reducing losses and increasing efficiency in brushless DC (BLDC) motors have been reported in [17,18].

Electric motors play a crucial role in the global consumption matrix [107]. To minimize carbon emissions, considerable efforts have been devoted to increasing the efficiency of electric motors, with numerous studies and analyses exploring innovative technologies [10], [108]. Despite the thermal evolution of magnets in recent years, different disturbances present in power electrical systems still affect the performance of LSPMMs by increasing losses and temperature [109], [110]. When combined with magnitude variation, voltage imbalance intensifies its effects on electric motors in terms of efficiency and temperature. Furthermore, it even more adversely

affects emerging technologies such as permanent-magnet synchronous motors [111], [112]. These findings reveal that a voltage imbalance combined with overvoltage considerably increases power consumption, reduces the power factor, and elevates temperatures.

### 1.6.5. Diagnosis of Electric Motors

Predictive maintenance continues to be a subject of study to put an end to unintentional stops in production processes and their economic consequences. Studies on electric motor diagnosis have increased in the last 20 years, as shown in Figure 1-8, obtained from a bibliometric analysis on electric motor diagnosis and predictive maintenance. Fault Diagnosis, IMs and condition monitoring stand out as the most used words in the literature. The main techniques currently used in fault detection for induction motors are thermal monitoring [113], [114], [115], [116], [117], [118], [119], vibration analysis (mechanical monitoring) [120], [121], acoustical analysis [122], [123], speed and torque oscillations [124], [125], partial discharges [126], [127], [128], flux monitoring [129], optical monitoring, electrical monitoring, and computational intelligence techniques [130], [131]. The primary failures in electric motors predominantly occur in the bearings, accounting for over 40% of the total faults. This is followed by the stator with 37% and the rotor with 12%.

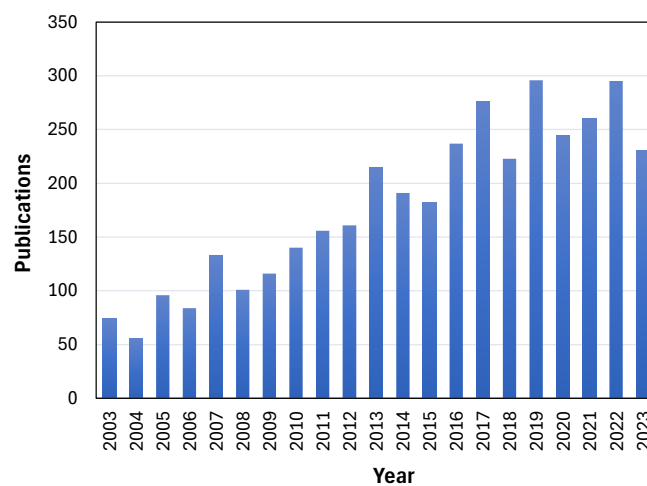


**Figure 1-8** - Publications related to electric motors diagnosis in the last 20 years.

The leading causes of these failures include insufficient maintenance, improper installation, misalignment, overloads, and damage to the rotor bars or rings [130], [132]. Given the significant proportion of mechanical issues contributing to these faults, many techniques have traditionally relied on mechanical concepts. However, in recent years, new approaches have emerged and can be broadly classified into three main categories [133]:

- Model-based methods: These techniques are grounded in mathematical models that generate predictions for comparison with experimental measurements.
- Signal-based models: These methods utilize various analyses such as time-domain analysis, frequency-domain analysis, enhanced frequency analysis, and time-frequency analysis to extract relevant information from the signals.
- Knowledge-based techniques: This category encompasses both supervised and unsupervised learning systems that leverage accumulated knowledge to detect and diagnose faults in electric motors.

A bibliographic review on fault diagnosis using signal processing techniques in induction motors is presented in [78]. The review indicates that current signature acquisition and processing can be used to characterize the failure nature in electrical machines. The review also shows that mechanical and electrical failures of induction motors exhibit explicit harmonic component in stator current. Work in [76] also presents a methodology to detect harmonics in power systems using wavelet transform.

However, in real applications, a preprocessing step is necessary before applying the proposed harmonics wavelet method due to the high noise levels. In [77], a systematic literature review of recent failure prognosis systems is provided, including the main approaches and some of the most prominent application domains for failure diagnosis. The works in [75,79] also show alternatives for the fault diagnosis in electric motors. The presence of harmonics in fault conditions are also mentioned in these studies.

Real-time detection studies have been presented in [133], [134], [135], [136], using statistical and machine learning techniques to predict faults in electric motors. The data used are normally obtained from sensors and cloud-based motor condition monitoring systems, and then, processed for further analysis using different techniques such as artificial neural networks (ANN), fuzzy logic, and support vector machines (SVM's) among others. The study in [133] presented a novel motor condition monitoring system using 1-D convolutional neural networks, the learning of the motor data characteristics allows one to classify the variability of the current signatures for different types of faults, with the data obtained from the current signals reducing the iteration time considerably and with efficiencies greater than 97% based on experimental results. Thermography continues to be a highly reliable technique for detecting motor faults, including misalignment, cooling problems, bearing damage, connection problems, and others. Works

using thermography have been presented in [113], [114], [115], [116], [117], [118], [119], the study in [113] presents the compilation of some industrial cases obtained in a petrochemical plant, and the authors show how infrared thermography can provide useful information about the presence of faults in IM's, but also the authors highlight the importance of the thermographer's experience when interpreting the results. Despite the diversity of existing techniques for fault prediction, their effectiveness has also been questioned according to the technique used and the type of fault in question [131].

### 1.7. Test Bench Description

The effects of voltage harmonics, voltage unbalance, and voltage magnitude variations were evaluated using the test benches shown in Figure 1-9 and Figure 1-10. The bench comprises a three-phase alternating current (AC) programmable source (1), in which different voltages applied to the IE2, IE3 and IE4 Class Induction motors (4) were configured. The induction motors input parameters were measured using a class "A" power-quality analyzer (2), and an electromagnetic brake (3) was used as the electric load. The rated data for each motor is presented in Table 1-3 and photographs of the nameplates of each motor are presented in the Appendix. The tests were conducted at the Amazon Energy Efficiency Center (CEAMAZON) of the Federal University of Pará (UFPA). At first, the induction motors were subjected to a perfect three-phase sine voltage of 220 V for 1 h and 10 min so that they reached their thermal equilibrium<sup>2</sup>, and, in a second moment:

- The value of each voltage harmonic (2nd, 3rd, 5th, and 7th) increased by 2% every 10 minutes until it reached 25%;
- Each motor was individually subjected to 1 hour and 10 minutes of 1%, 3%, and 4% NEMA voltage unbalance until thermal equilibrium was restored;
- The LSPMM was supplied with a nominal voltage of 220V (1.00 p.u.), which was used as the base voltage to define the undervoltage and overvoltage values per unit. The LSPMM was then subjected to VV conditions of 0.90, 0.95, 1.0, 1.05 and 1.10 p.u. with loads ranging from 0% to 125%.

---

<sup>2</sup> Thermal equilibrium is defined by the Standard IEC 60034-1:2010 as the state where the several parts of the machine do not vary by more than a gradient of 2 K per hour.

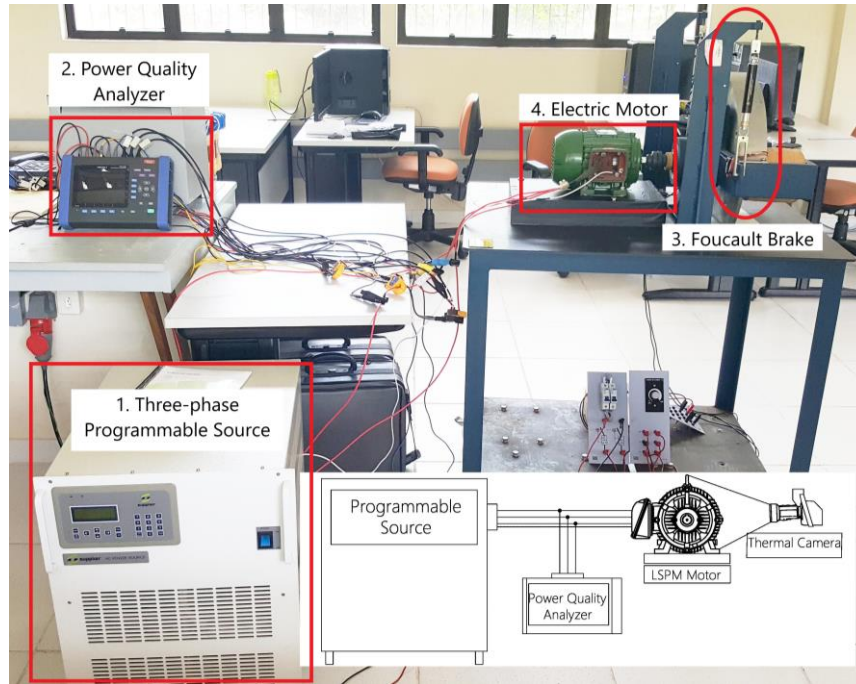


Figure 1-9 - General test setup for the power quality disturbances tests.

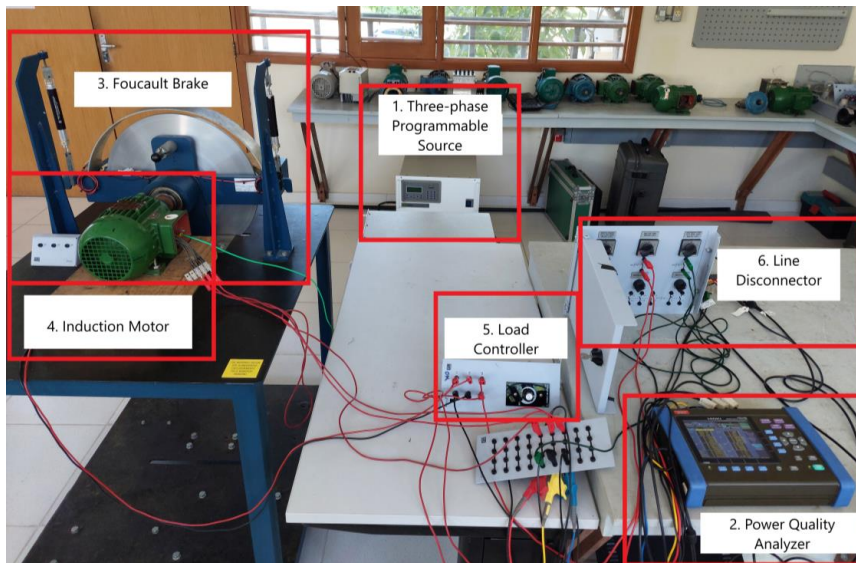
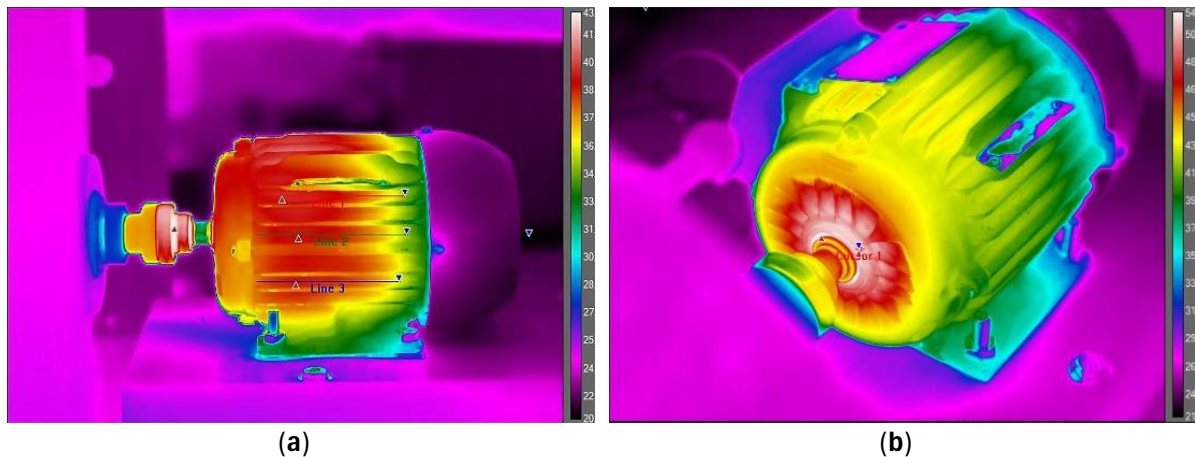


Figure 1-10 - General test setup for the electric motor degradation index tests.

Table 1-3. Induction motor parameters.

IM Class	IE2	IE3	IE4
Technology	SCIM	SCIM	LSPMM
Power (kW)	0.75 kW	0.75 kW	0.75 kW
Voltage (Volts)	220/380 V	220/380 V	220/380 V
Speed (rpm)	1730	1725	1800
Torque (Nm)	4.12	4.13	3.96
Current (A)	2.98/1.73	2.91/1.68	3.08/1.78
Efficiency (%)	82.6	82.6	87.4
Power Factor	0.80	0.82	0.73

A FLIRTM model T620 infrared camera with a calculated emissivity of 0.94 was used to measure the induction motor frame temperature. The thermographic images of the motor were taken at two angles every 2 minutes from thermal equilibrium to the end of the experiment for each disturbance analyzed in order to analyze the temperature variation in each motor class. Figure 1-11a and Figure 1-11b shows the angles taken during the experiments.



**Figure 1-11** – Thermographic images of the LSPMM with: (a) 25% of 5th harmonic voltage distortion; (b) 10% of 5th harmonic voltage distortion.

## 1.8. Research Goals

Based on a literature review, this study contributes considerably to the field by analyzing the impact of power quality disturbances on IE2, IE3 and IE4 class motors. Therefore, the general purpose of this work is to present a technical, thermal, and economic evaluation of the impact of voltage magnitude variation, voltage harmonics and voltage unbalance on the behavior of IE2, IE3 and IE4 efficiency class induction motors. Then, by means of a degradation indicator proposed in this work, the impact of these disturbances on the motor health is analyzed. In the light of this general goal, the following specific goals have been outlined:

- Determination of the orders and magnitudes of the harmonic voltages to be evaluated in accordance with current literature and electrical standards.
- Determination of the voltage unbalance percentages as well as the magnitudes with under and over voltage according to the current literature and electrical standards.
- From the literature and standards, define the voltage magnitudes to be evaluated on electric motors.

- Analysis of the individual impact of each voltage harmonic, voltage magnitude, and voltage unbalance in the performance and temperature for the 0.75 kW output power of the IE2, IE3 and IE4 efficiency motor classes.
- Statistical analysis using multiple regression and least squares to generate temperature models for low power electric motors from the thermographic captures.
- Technical-economic analysis considering the current costs of each technology and the paybacks as well as the technical considerations derived from the experiments carried out.
- Search for methodologies that can be applied to the predictive maintenance of electric motors subjected to conditions of low power quality.

### **1.9. Thesis Contributions**

This work presents a series of methodologies aimed at analyzing the performance of 0.75 kW output power electric motors in the presence of different disturbances present in current electrical systems, such as voltage variation, voltage harmonics and voltage unbalance, in order to establish conclusions and guidelines to be considered by specialists in the substitution between technologies. In this sense, the main contributions of this work are detailed below:

1. Analysis of the main improvements in relation to savings and performance in the IE2, IE3 and IE4 class technologies at a 0.75 kW output power, under ideal operating conditions, to analyze the main operational characteristics of each technology, with a special focus on the line-start permanent magnet motor (LSPMM), to obtain key factors and conclusions to be considered for the substitution between technologies.
2. A comparison of the responses of electric motors classes IE2, IE3 and IE4, the latter being a hybrid motor with squirrel cage and permanent magnets, when subjected to voltage harmonics of second, third, fifth, seventh order and a combination of all in the supply voltage. In addition, a statistical study using correlation matrices between the temperature and the input parameters of each motor is presented to analyze behavioral patterns for the temperature increase for each harmonic in the study. The thermal modeling and validation of the LSPMM in the FEM software when subjected to negative sequence voltage harmonics is also presented.

3. *Technical, thermal, and economic evaluation of voltage unbalance (VU) impacts:* A comprehensive evaluation of the effects of VU under different load conditions is conducted. This study identifies the voltage magnitudes that exert the most substantial influence on motor behavior depending on the type of application and load conditions by assessing different non-nominal voltages. This analysis provides valuable insights into decision-making processes and offers guidance to specialists in optimizing motor performance;
4. A comparison between energy efficiency gain and power quality degradation related to electric motors, with special attention to the harmonics generated by each disturbance, in order to verify the hypothesis: Are the most efficient motors less efficient in terms of power quality?
5. *Technical, thermal, and economic evaluation of voltage variation (VV) impacts:* A comprehensive evaluation of the effects of VV under different load conditions is conducted. This study identifies the voltage magnitudes that exert the most substantial influence on motor behavior depending on the type of application and load conditions by assessing different non-nominal voltages. This analysis provides valuable insights into decision-making processes and offers guidance to specialists in optimizing motor performance;
6. In the search for innovative and complementary techniques, this study introduces a novel methodology based on the frequency-domain analysis of electric motor current waveforms. The approach utilizes spectral analysis of the motor's load current during online operation. To accomplish this, the Contact Degradation Indicator (CDI), originally developed for predictive diagnosis of failures in electric power substation bays [4], will be adapted to create the Electric Motor Degradation Indicator (EMDI). By utilizing a degradation coefficient, this methodology aims to provide a reliable reference for assessing the health state of electric motors.



## 1.10. Thesis Structure

This work is structured as follows:

- ✓ **Chapter 1 - Introduction:** This chapter presents the initial considerations of the work, the contextualization of induction motors in the world and in Brazil. A bibliometric and systematic review on the topic of study proposed in this doctoral thesis. The motivations and the goals to be achieved with this research, a bibliographic survey of the related works found in the literature, and, finally, the original contributions of the thesis.
- ✓ **Chapter 2 – Evolution of Electric Motors:** This chapter reviews the evolution of electric induction motors, the constructive improvements they have undergone over the years, up to the introduction of new technologies such as Line Start. Permanent Magnet Motor (LSPMM), finally, a comparison between the IE2, IE3 and IE4 class motors is presented.
- ✓ **Chapter 3 –Voltage Harmonics:** This chapter will present the main effects of voltage harmonics on the performance and temperature of induction electric motors classes IE2, IE3 and IE4. Statistical correlation and temperature models will be also presented.
- ✓ **Chapter 4 – Voltage Unbalance:** This chapter presents through experimental tests, the temperature and performance response of IE2, IE3 and IE4 electric motors classes in the presence of different unbalanced voltages.
- ✓ **Chapter 5 – Power Quality and Energy Efficiency:** In this chapter a discussion on the relationship between power quality and energy efficiency applied on electric motors in the presence of harmonics and voltage unbalance will be presented.
- ✓ **Chapter 6 – Voltage Magnitude Variation:** The impacts of voltage variation on the response of synchronous motors will be discussed in this chapter, a discussion of the impacts on temperature and an economic and statistical analysis will also be presented.
- ✓ **Chapter 7 – Electric Motor Degradation Index:** In this chapter a methodology for the predictive diagnosis of the motor is proposed from the analysis in the frequency domain. The methodology is validated in the field in a pumping system.
- ✓ **Chapter 8– Author Publications:** The publications made during the doctoral period are listed as well as other achievements.
- ✓ **Chapter 9 – Final Considerations:** This chapter discusses the overall conclusions and future work.

## 1.11. Chapter Bibliography

- [1] International Energy Agency (IEA), “Publications.” Accessed: Aug. 15, 2019. [Online]. Available: <https://www.iea-4e.org/publications>
- [2] “Plano Nacional de Eficiência Energética - Plano Nacional de Eficiência Energética - Ministério de Minas e Energia.” Accessed: Mar. 08, 2020. [Online]. Available: <http://www.mme.gov.br/web/guest/secretarias/planejamento-e-desenvolvimento-energetico/publicacoes/plano-nacional-de-eficiencia-energetica>
- [3] IEC 60034-30-1:2014, “Rotating electrical machines - Part 30-1: Efficiency classes of line operated AC motors (IE code).” Accessed: Aug. 15, 2019. [Online]. Available: <https://webstore.iec.ch/publication/136>
- [4] OFFICIAL DIARY OF THE UNION, “INTERMINISTERIAL ORDINANCE N° 1, OF 29 JUNE 2017 - National Press.” Accessed: Mar. 08, 2020. [Online]. Available: <http://www.in.gov.br/materia>
- [5] A. Anibal, B. Rob, B. Conrad U., D. Martin, and H. William, “Motor MEPS Guide, 1st Edition Zurich Switzerland, February.” 1st Edition Zurich Switzerland, Feb. 2009. Accessed: May 27, 2020. [Online]. Available: [https://www.motorsystems.org/files/otherfiles/0000/0100/meps\\_guide\\_feb2009.pdf](https://www.motorsystems.org/files/otherfiles/0000/0100/meps_guide_feb2009.pdf)
- [6] F. J. T. E. Ferreira, B. Leprettre, and A. T. de Almeida, “Comparison of Protection Requirements in IE2-, IE3-, and IE4-Class Motors,” *IEEE Transactions on Industry Applications*, vol. 52, no. 4, pp. 3603–3610, Jul. 2016, doi: 10.1109/TIA.2016.2545647.
- [7] International Energy Agency (IEA), “Energy Efficiency 2018 - Analysis and outlooks to 2040 - en - OECD.” Accessed: Aug. 15, 2019. [Online]. Available: <http://www.oecd.org/publications/energy-efficiency-2018-9789264024304-en.htm>
- [8] P. Waide and C. Brunner, “Energy-Efficiency Policy Opportunities for Electric Motor-Driven Systems,” Jan. 2011.
- [9] J. Fong, F. J. T. E. Ferreira, A. M. Silva, and A. T. de Almeida, “IEC61800-9 System Standards as a Tool to Boost the Efficiency of Electric Motor Driven Systems Worldwide,” *Inventions*, vol. 5, no. 2, Art. no. 2, Jun. 2020, doi: 10.3390/inventions5020020.
- [10] A. T. de Almeida, F. J. T. E. Ferreira, and J. Fong, “Perspectives on Electric Motor Market Transformation for a Net Zero Carbon Economy,” *Energies*, vol. 16, no. 3, Art. no. 3, Jan. 2023, doi: 10.3390/en16031248.
- [11] “WEG - Uso Eficiente da Energia Elétrica.” Accessed: Mar. 08, 2020. [Online]. Available: [https://d335luupugsy2.cloudfront.net/cms/files/92176/1580492002Cartilha\\_Weg\\_versaoWE3\\_INTERATIVA.pdf](https://d335luupugsy2.cloudfront.net/cms/files/92176/1580492002Cartilha_Weg_versaoWE3_INTERATIVA.pdf)
- [12] R. Werle, C. U. Brunner, and R. Tieben, “Swiss motor efficiency program EASY: results 2010 - 2014,” p. 14.
- [13] F. J. T. E. Ferreira and A. T. de Almeida, “Induction motor downsizing as a low-cost strategy to save energy,” *Journal of Cleaner Production*, vol. 24, pp. 117–131, Mar. 2012, doi: 10.1016/j.jclepro.2011.11.014.
- [14] “Optimized Rewinding of Oversized Induction Motors | IEEE Conference Publication | IEEE Xplore.” Accessed: Feb. 10, 2024. [Online]. Available: <https://ieeexplore.ieee.org/document/10238885>
- [15] ANEEL, “CALL N°. 002/2015 PRIORITY ENERGY EFFICIENCY PROJECT: ‘ENCOURAGING THE REPLACEMENT OF ELECTRIC MOTORS: PROMOTING ENERGY EFFICIENCY IN THE DRIVING POWER SEGMENT.’” Accessed: Mar. 08, 2020. [Online]. Available: [https://www.aneel.gov.br/sala-de-imprensa-exibicao/-/asset\\_publisher/XGPXSqdmFHrE/content/chamada-de-projeto-para-incentivar-substituicao-de-motores-eletricos-e-prorrogada/656877?inheritRedirect=false](https://www.aneel.gov.br/sala-de-imprensa-exibicao/-/asset_publisher/XGPXSqdmFHrE/content/chamada-de-projeto-para-incentivar-substituicao-de-motores-eletricos-e-prorrogada/656877?inheritRedirect=false)
- [16] “National Electric Energy Agency - ANEEL.” Accessed: Apr. 04, 2020. [Online]. Available: <https://www.aneel.gov.br/>

- [17] A. T. D. Almeida, F. J. T. E. Ferreira, and A. Quintino, “Technical and economical considerations on super high-efficiency three-phase motors,” in *48th IEEE Industrial Commercial Power Systems Conference*, May 2012, pp. 1–13. doi: 10.1109/ICPS.2012.6229618.
- [18] WEG, “See+.” Accessed: Mar. 08, 2020. [Online]. Available: <https://www.weg.net/see+/pages/regua.jsp>
- [19] H. Abusaada and A. Elshater, “Notes on Developing Research Review in Urban Planning and Urban Design Based on PRISMA Statement,” *Social Sciences*, vol. 11, no. 9, Art. no. 9, Sep. 2022, doi: 10.3390/socsci11090391.
- [20] D. Moher, A. Liberati, J. Tetzlaff, and D. G. Altman, “Preferred reporting items for systematic reviews and meta-analyses: the PRISMA statement,” *BMJ*, vol. 339, p. b2535, Jul. 2009, doi: 10.1136/bmj.b2535.
- [21] U.S. Department of Energy, Energy Efficiency & Renewable Energy, “Premium Efficiency Motor Selection and Application Guide – A Handbook for Industry,” Energy.gov. Accessed: Aug. 15, 2019. [Online]. Available: <https://www.energy.gov/eere/amo/downloads/premium-efficiency-motor-selection-and-application-guide-handbook-industry>
- [22] F. J. T. E. Ferreira, G. Baoming, and A. T. de Almeida, “Reliability and Operation of High-Efficiency Induction Motors,” *IEEE Transactions on Industry Applications*, vol. 52, no. 6, pp. 4628–4637, Nov. 2016, doi: 10.1109/TIA.2016.2600677.
- [23] A. Hassanpour Isfahani and S. Vaez-Zadeh, “Line start permanent magnet synchronous motors: Challenges and opportunities,” *Energy*, vol. 34, no. 11, pp. 1755–1763, Nov. 2009, doi: 10.1016/j.energy.2009.04.022.
- [24] M. G. Kahrisangi, A. H. Isfahani, S. Vaez-Zadeh, and M. R. Sebdani, “Line-start permanent magnet synchronous motors versus induction motors: A comparative study,” *Front. Electr. Electron. Eng.*, vol. 7, no. 4, pp. 459–466, Dec. 2012, doi: 10.1007/s11460-012-0217-8.
- [25] A. T. de Almeida, F. J. T. E. Ferreira, and G. Baoming, “Beyond Induction Motors—Technology Trends to Move Up Efficiency,” *IEEE Transactions on Industry Applications*, vol. 50, no. 3, pp. 2103–2114, May 2014, doi: 10.1109/TIA.2013.2288425.
- [26] F. J. T. E. Ferreira, A. M. Silva, V. P. B. Aguiar, R. S. T. Pontes, E. C. Quispe, and A. T. de Almeida, “Overview of Retrofitting Options in Induction Motors to Improve Their Efficiency and Reliability,” in *2018 IEEE International Conference on Environment and Electrical Engineering and 2018 IEEE Industrial and Commercial Power Systems Europe (EEEIC / I CPS Europe)*, Jun. 2018, pp. 1–12. doi: 10.1109/EEEIC.2018.8493887.
- [27] M. GWOŹDZIEWICZ and L. ANTAL, “INVESTIGATION OF LINE START PERMANENT MAGNET SYNCHRONOUS MOTOR AND INDUCTION MOTOR PROPERTIES, Prace Naukowe Instytutu Maszyn, Napędów i Pomiarów Elektrycznych, Politechniki Wrocławskiej.” Prace Naukowe Instytutu Maszyn, Napędów i Pomiarów Elektrycznych, Politechniki Wrocławskiej., 2010. [Online]. Available: <https://pdfs.semanticscholar.org/e9ce/18be7c97cf70342b3135d9cd8364e14538bb.pdf>
- [28] C. Debruyne, S. Derammelaere, J. Desmet, and L. Vandeveldde, “Comparative study of the influence of harmonic voltage distortion on the efficiency of induction machines versus line start permanent magnet machines,” in *2012 IEEE 15th International Conference on Harmonics and Quality of Power*, Hong Kong, China: IEEE, Jun. 2012, pp. 342–349. doi: 10.1109/ICHQP.2012.6381217.
- [29] V. P. B. Aguiar, R. S. T. Pontes, and F. J. T. E. Ferreira, “Technical and Economic Evaluation of Efficiency Improvement after Rewinding in Low-Power Induction Motors: A Brazilian Case,” *Energies*, vol. 11, no. 7, Art. no. 7, Jul. 2018, doi: 10.3390/en11071701.
- [30] H. Kim, Y. Park, H.-C. Liu, P.-W. Han, and J. Lee, “Study on Line-Start Permanent Magnet Assistance Synchronous Reluctance Motor for Improving Efficiency and Power Factor,” *Energies*, vol. 13, no. 2, Art. no. 2, Jan. 2020, doi: 10.3390/en13020384.
- [31] C. Debruyne, “Impact of voltage distortion on energy efficiency of induction machines and line start permanent magnet machines,” dissertation, Ghent University, 2014. Accessed: Aug. 15, 2019. [Online]. Available: <http://hdl.handle.net/1854/LU-4383637>

- [32] İ. Tarimer, “Investigation of the Effects of Rotor Pole Geometry and Permanent,” 1, vol. 90, no. 2, pp. 67–72, 2009, doi: 10.5755/j01.eee.90.2.10512.
- [33] T. J. E. Miller, “Synchronization of Line-Start Permanent-Magnet AC Motors,” *IEEE Transactions on Power Apparatus and Systems*, vol. PAS-103, no. 7, pp. 1822–1828, Jul. 1984, doi: 10.1109/TPAS.1984.318630.
- [34] A. Chama, A. Sorgdrager, and R.-J. Wang, “Analytical synchronization analysis of line-start permanent magnet synchronous motors,” *Progress In Electromagnetics Research M*, vol. 48, pp. 183–193, Jun. 2016, doi: 10.2528/PIERM16050311.
- [35] “Design and Analysis of a Hybrid Permanent Magnet Assisted Synchronous Reluctance Motor Considering Magnetic Saliency and PM Usage - IEEE Journals & Magazine.” Accessed: May 16, 2020. [Online]. Available: <https://ieeexplore.ieee.org/document/8115172>
- [36] M. J. Melfi, S. D. Rogers, S. Evon, and B. Martin, “Permanent Magnet Motors for Energy Savings in Industrial Applications,” in *2006 Record of Conference Papers - IEEE Industry Applications Society 53rd Annual Petroleum and Chemical Industry Conference*, Sep. 2006, pp. 1–8. doi: 10.1109/PCICON.2006.359695.
- [37] A. Takahashi, S. Kikuchi, K. Miyata, and A. Binder, “Asynchronous Torque of Line-Starting Permanent-Magnet Synchronous Motors,” *IEEE Transactions on Energy Conversion*, vol. 30, no. 2, pp. 498–506, Jun. 2015, doi: 10.1109/TEC.2014.2361836.
- [38] C. Vavra, “Understanding permanent magnet motors,” *Control Engineering*. Accessed: May 17, 2020. [Online]. Available: <https://www.controleng.com/articles/understanding-permanent-magnet-motors/>
- [39] A. T. de Almeida, J. Fong, H. Falkner, and P. Bertoldi, “Policy options to promote energy efficient electric motors and drives in the EU,” *Renewable and Sustainable Energy Reviews*, vol. 74, pp. 1275–1286, Jul. 2017, doi: 10.1016/j.rser.2017.01.112.
- [40] A. De Almeida, J. Fong, C. U. Brunner, R. Werle, and M. Van Werkhoven, “New technology trends and policy needs in energy efficient motor systems - A major opportunity for energy and carbon savings,” *Renewable and Sustainable Energy Reviews*, vol. 115, p. 109384, Nov. 2019, doi: 10.1016/j.rser.2019.109384.
- [41] F. J. T. E. Ferreira and A. T. de Almeida, “Induction motor downsizing as a low-cost strategy to save energy,” *Journal of Cleaner Production*, vol. 24, pp. 117–131, Mar. 2012, doi: 10.1016/j.jclepro.2011.11.014.
- [42] “Minimum Energy Performance Standards (MEPS) – Policies,” IEA. Accessed: Jul. 26, 2020. [Online]. Available: <https://www.iea.org/policies/333-minimum-energy-performance-standards-meps>
- [43] “IEC 60034-7:2020 | IEC Webstore.” Accessed: Feb. 11, 2024. [Online]. Available: <https://webstore.iec.ch/publication/64225>
- [44] S. Singh and A. Singh, “Steady-state Performance Assessment of Induction Motor under Unbalanced Voltage Condition,” *Electric Power Components and Systems*, vol. 41, Oct. 2013, doi: 10.1080/15325008.2013.817492.
- [45] D. Zhang, R. An, and T. Wu, “Effect of Voltage Unbalance and Distortion on the Loss Characteristics of Three Phase Cage Induction Motor,” *IET Electric Power Applications*, vol. 12, Oct. 2017, doi: 10.1049/iet-epa.2017.0464.
- [46] A. B. F. Neves, M. V. B. de Mendonça, A. de L. Ferreira Filho, and G. Z. Rosa, “Effects of voltage unbalance and harmonic distortion on the torque and efficiency of a Three-Phase Induction Motor,” in *2016 17th International Conference on Harmonics and Quality of Power (ICHQP)*, Oct. 2016, pp. 943–948. doi: 10.1109/ICHQP.2016.7783350.
- [47] W. Abu-Elhaija and A. Muetze, “A voltage unbalance factor coding technique for three-phase induction motors,” *International Transactions on Electrical Energy Systems*, vol. 28, no. 6, p. e2554, 2018, doi: 10.1002/etep.2554.

- [48] E. Quispe, “Efectos del desequilibrio de tensiones sobre la operación del motor de inducción trifásico. Énfasis en la caracterización del desequilibrio de tensiones y el efecto sobre la potencia nominal,” 2012. doi: 10.13140/RG.2.1.3406.7287.
- [49] NEMA MG1-2016, “Motors and Generators.” Accessed: Aug. 15, 2019. [Online]. Available: <https://www.nema.org/Standards/Pages/Motors-and-Generators.aspx>
- [50] “IEEE Recommended Practice for Monitoring Electric Power Quality,” *IEEE Std 1159-2019 (Revision of IEEE Std 1159-2009)*, pp. 1–98, Aug. 2019, doi: 10.1109/IEEESTD.2019.8796486.
- [51] “Power Quality Indices and Objectives,” e-cigre. Accessed: Apr. 04, 2020. [Online]. Available: <https://e-cigre.org/publication/261-power-quality-indices-and-objectives>
- [52] Ching-Yin Lee, “Effects of unbalanced voltage on the operation performance of a three-phase induction motor,” *IEEE Transactions on Energy Conversion*, vol. 14, no. 2, pp. 202–208, Jun. 1999, doi: 10.1109/60.766984.
- [53] M. Kostic, “Effects of Voltage Quality on Induction Motors’ Efficient Energy Usage,” *Induction Motors - Modelling and Control*, Nov. 2012, doi: 10.5772/51223.
- [54] P. Gnaciński, “Gnacinski P. Thermal loss of life and load-carrying capacity of marine induction motors. Energy Conversion and Management, vol. 78: 574-583, Febr. 2014,” *Energy Conversion and Management*, vol. 78, pp. 574–583, Feb. 2014, doi: 10.1016/j.enconman.2013.11.023.
- [55] A. H. Bonnett, “The impact that voltage and frequency variations have on AC induction motor performance and life in accordance with NEMA MG-1 standards,” in *Conference Record of 1999 Annual Pulp and Paper Industry Technical Conference (Cat. No.99CH36338)*, Seattle, WA, USA: IEEE, 1999, pp. 16–26. doi: 10.1109/PAPCON.1999.779341.
- [56] Yaw-Juen Wang, “Analysis of effects of three-phase voltage unbalance on induction motors with emphasis on the angle of the complex voltage unbalance factor,” *IEEE Transactions on Energy Conversion*, vol. 16, no. 3, pp. 270–275, Sep. 2001, doi: 10.1109/60.937207.
- [57] E. El-Kharashi, M. El-Dessouki, J. G. Massoud, A. W. Farid, and M. A. Al-Ahmar, “The use of the current complex factor to determine the precise output energy of the induction motor,” *Electric Power Systems Research*, vol. 154, pp. 23–36, Jan. 2018, doi: 10.1016/j.epsr.2017.08.008.
- [58] A. L. Ferreira Filho, J. A. A. Cormane, D. C. Garcia, M. V. C. Costa, M. A. G. Oliveira, and F. A. do Nascimento, “Analysis of the complex voltage unbalance factor behavior resulting from the variation of voltage magnitudes and angles,” in *Proceedings of 14th International Conference on Harmonics and Quality of Power - ICHQP 2010*, Sep. 2010, pp. 1–7. doi: 10.1109/ICHQP.2010.5625315.
- [59] A. I. Adekitan, “A New Definition of Voltage Unbalance Using Supply Phase Shift,” *J Control Autom Electr Syst*, vol. 31, no. 3, pp. 718–725, Jun. 2020, doi: 10.1007/s40313-020-00579-8.
- [60] M. T. Jonathan, E. Ortiz de Matos, T. M. Soares, M. E. de L. Tostes, and J. C. Paye, “Fifth & Seventh Harmonic Effects on the Performance of IE2, IE3 & IE4 Induction Motor Classes,” in *Proceedings of the 13th Latin-American Congress on Electricity Generation and Transmission - CLAGTEE 2019*, Santiago, Chile, Oct. 2019, p. 6. [Online]. Available: <http://www.clagtee2019.pucv.cl/2019/book.html>
- [61] M. T. Jonathan, T. M. Soares, M. E. de L. Tostes, E. Ortiz de Matos, and C. E. Moreira, “Impactos do 5o Harmônico na Temperatura de Motores Elétricos Classes IE2, IE3 e IE4.,” in *Conferência Brasileira sobre Qualidade da Energia Elétrica (CBQEE)*, São Paulo, Brazil, Sep. 2019, p. 6. [Online]. Available: <http://sbqee.org.br/cbqee/>
- [62] A. T. de Almeida, F. J. T. E. Ferreira, and J. A. C. Fong, “Standards for Super-Premium Efficiency class for electric motors,” in *Conference Record 2009 IEEE Industrial Commercial Power Systems Technical Conference*, May 2009, pp. 1–8. doi: 10.1109/ICPS.2009.5463983.
- [63] C. Debruyne, L. Vandeveld, and J. Desmet, “Harmonic effects on Induction and Line Start Permanent Magnet Machines,” in *International Conference on Energy Efficiency in Motor Driven Systems (EEMODS 2013)*, Rio de Janeiro, RJ, Brazil, Oct. 2013.
- [64] T. Zawilak and J. Zawilak, “MINIMIZATION OF HIGHER HARMONICS IN LINE-START PERMANENT MAGNET SYNCHRONOUS MOTOR,” *Przegląd Elektrotechniczny*, vol. 84, Jan. 2008.

- [65] E. Vera, “Optimal design of line-start permanent magnet synchronous motors of high efficiency. Electric power. Ecole Centrale de Lille, 2015. English. NNT: 2015ECLI0022. tel-01308575,” 2015.
- [66] F. Ferreira, M. V. Cistelegan, and A. de Almeida, “Voltage Unbalance Impact on the Performance of Line-Start Permanent-Magnet Synchronous Motors.,” Nantes, France, 2009.
- [67] F. Kalluf, C. Pompermaier, M. V. F. da Luz, and N. Sadowski, “Braking torque analysis of the single phase line-start permanent magnet synchronous motor,” *The XIX International Conference on Electrical Machines - ICEM 2010*, 2010, doi: 10.1109/ICELMACH.2010.5608211.
- [68] A. Kumar and A. Srivastava, “Performance Comparison of Two Different Rotor Topologies of Line Start Permanent Magnet Synchronous Motors,” *Engineering Technology*, vol. 5, p. 8.
- [69] Mingji Liu, Zhi Han, Yawei Pei, and Pengfei Shi, “Optimization of permanent magnet motor air-gap flux density based on the non-uniform air gap,” in *Proceedings 2013 International Conference on Mechatronic Sciences, Electric Engineering and Computer (MEC)*, Dec. 2013, pp. 3422–3426. doi: 10.1109/MEC.2013.6885604.
- [70] A. Sorgdrager, R.-J. Wang, and A. J. Grobler, “Transient performance optimisation of line-start permanent magnet synchronous motors using Taguchi regression rate method,” Jan. 2017.
- [71] X. Zeng, L. Quan, X. Zhu, L. Xu, and F. Liu, “Investigation of an Asymmetrical Rotor Hybrid Permanent Magnet Motor for Approaching Maximum Output Torque,” *IEEE Transactions on Applied Superconductivity*, vol. 29, no. 2, pp. 1–4, Mar. 2019, doi: 10.1109/TASC.2019.2893708.
- [72] F. J. T. E. Ferreira, J. Alberto, and A. T. de Almeida, “Voltage Unbalance Impact on Coil-Side Temperature Rise in a Delta-Connected, Dual-Winding Induction Motor,” in *2020 IEEE International Conference on Industrial Technology (ICIT)*, Feb. 2020, pp. 925–930. doi: 10.1109/ICIT45562.2020.9067201.
- [73] “IEEE Recommended Practice for Monitoring Electric Power Quality,” *IEEE Std 1159-1995*, pp. i-, 1995, doi: 10.1109/IEEESTD.1995.79050.
- [74] E. C. de Lima, J. M. de C. Filho, and J. S. de Sá, “Diagnosis of induction motors operating under distorted and unbalanced voltages,” in *2016 17th International Conference on Harmonics and Quality of Power (ICHQP)*, Oct. 2016, pp. 786–791. doi: 10.1109/ICHQP.2016.7783368.
- [75] E. F. Fuchs, D. J. Roesler, and M. A. S. Masoum, “Are harmonic recommendations according to IEEE and IEC too restrictive?,” *IEEE Transactions on Power Delivery*, vol. 19, no. 4, pp. 1775–1786, Oct. 2004, doi: 10.1109/TPWRD.2003.822538.
- [76] A. Munoz R. and G. Nahmias C., “Mechanical vibration of three-phase induction motors fed by nonsinusoidal currents,” in *3rd International Power Electronic Congress. Technical Proceedings. CIEP '94*, Aug. 1994, pp. 166–172. doi: 10.1109/CIEP.1994.494416.
- [77] X. Song, J. Hu, H. Zhu, and J. Zhang, “Effects of the Slot Harmonics on the Stator Current in an Induction Motor with Bearing Fault,” *Mathematical Problems in Engineering*. Accessed: Jun. 16, 2020. [Online]. Available: <https://www.hindawi.com/journals/mpe/2017/2640796/>
- [78] “Static air-gap eccentricity fault diagnosis using rotor slot harmonics in line neutral voltage of three-phase squirrel cage induction motor,” ResearchGate. Accessed: Jun. 15, 2020. [Online]. Available: [https://www.researchgate.net/publication/306417959\\_Static\\_air-gap\\_eccentricity\\_fault\\_diagnosis\\_using\\_rotor\\_slot\\_harmonics\\_in\\_line\\_neutral\\_voltage\\_of\\_three-phase\\_squirrel\\_cage\\_induction\\_motor](https://www.researchgate.net/publication/306417959_Static_air-gap_eccentricity_fault_diagnosis_using_rotor_slot_harmonics_in_line_neutral_voltage_of_three-phase_squirrel_cage_induction_motor)
- [79] M. Kordestani, A. A. Safavi, and M. Saif, “Harmonic Fault Diagnosis in Power Quality System Using Harmonic Wavelet,” Jul. 2017. doi: 10.1016/j.ifacol.2017.08.2370.
- [80] “Fault diagnosis and condition monitoring of electrical machines - A Review | Request PDF,” ResearchGate. Accessed: Jun. 16, 2020. [Online]. Available: [https://www.researchgate.net/publication/224713187\\_Fault\\_diagnosis\\_and\\_condition\\_monitoring\\_of\\_electrical\\_machines\\_-\\_A\\_Review](https://www.researchgate.net/publication/224713187_Fault_diagnosis_and_condition_monitoring_of_electrical_machines_-_A_Review)
- [81] W. Li and C. Mechefske, “Induction motor fault detection using vibration and stator current methods,” *Insight - Non-Destructive Testing and Condition Monitoring*, vol. 46, pp. 473–478, Aug. 2004, doi: 10.1784/insi.46.8.473.39379.

- [82] IEC 60034-7:1992, “Classification of types of constructions and mounting arrangements (IM Code).” Accessed: Aug. 15, 2019. [Online]. Available: <https://webstore.iec.ch/publication/145>
- [83] L. Aarniovuori, M. Niemelä, J. Pyrhönen, W. Cao, and E. B. Agamloh, “Loss Components and Performance of Modern Induction Motors,” in *2018 XIII International Conference on Electrical Machines (ICEM)*, Sep. 2018, pp. 1253–1259. doi: 10.1109/ICELMACH.2018.8507189.
- [84] H. O. Mirzamani and A. L. Choobari, “Study of harmonics effects on performance of induction motors,” in *Proceedings of the 4th WSEAS international conference on Applications of electrical engineering*, in AEE’05. Prague, Czech Republic: World Scientific and Engineering Academy and Society (WSEAS), Mar. 2005, pp. 389–394.
- [85] H. G. Beleiu, V. Maier, S. G. Pavel, I. Birou, C. S. Pică, and P. C. Dărab, “Harmonics Consequences on Drive Systems with Induction Motor,” *Applied Sciences*, vol. 10, no. 4, Art. no. 4, Jan. 2020, doi: 10.3390/app10041528.
- [86] C. Debruyne, J. Desmet, S. Derammelaere, and L. Vandeveldel, “Derating factors for direct online induction machines when supplied with voltage harmonics: A critical view,” in *2011 IEEE International Electric Machines Drives Conference (IEMDC)*, May 2011, pp. 1048–1052. doi: 10.1109/IEMDC.2011.5994745.
- [87] S. X. Duarte and N. Kagan, “A Power-Quality Index to Assess the Impact of Voltage Harmonic Distortions and Unbalance to Three-Phase Induction Motors,” *IEEE Transactions on Power Delivery*, vol. 25, no. 3, pp. 1846–1854, Jul. 2010, doi: 10.1109/TPWRD.2010.2044665.
- [88] H. O. Mirzamani and A. L. Choobari, “Study of harmonics effects on performance of induction motors,” 2005.
- [89] “519-2014 - IEEE Recommended Practice and Requirements for Harmonic Control in Electric Power Systems.” Accessed: May 15, 2020. [Online]. Available: <https://standards.ieee.org/standard/519-2014.html>
- [90] M. Kordestani, M. Saif, M. E. Orchard, R. Razavi-Far, and K. Khorasani, “Failure Prognosis and Applications—A Survey of Recent Literature,” *IEEE Transactions on Reliability*, pp. 1–21, 2019, doi: 10.1109/TR.2019.2930195.
- [91] S. M. K. Zaman and X. Liang, “An Effective Induction Motor Fault Diagnosis Approach Using Graph-Based Semi-Supervised Learning,” *IEEE Access*, vol. 9, pp. 7471–7482, 2021, doi: 10.1109/ACCESS.2021.3049193.
- [92] F. J. T. E. Ferreira, A. T. de Almeida, J. F. S. Carvalho, and M. V. Cistelecan, “Experiments to observe the impact of power quality and voltage-source inverters on the temperature of three-phase cage induction motors using an infra-red camera,” in *2009 IEEE International Electric Machines and Drives Conference*, May 2009, pp. 1311–1318. doi: 10.1109/IEMDC.2009.5075373.
- [93] J. T. Allan, “The effect of voltage variation on the operation of induction motors,” *Transactions of the South African Institute of Electrical Engineers*, vol. 20, no. 6, pp. 137–155, Jun. 1929.
- [94] “Power savings obtained from supply voltage variation on squirrel cage induction motors | IEEE Conference Publication | IEEE Xplore.” Accessed: Apr. 19, 2023. [Online]. Available: <https://ieeexplore.ieee.org/document/4763392>
- [95] “Investigation of voltage and frequency variation on induction motor core and copper losses | IEEE Conference Publication | IEEE Xplore.” Accessed: Apr. 19, 2023. [Online]. Available: <https://ieeexplore.ieee.org/document/7934894>
- [96] E. B. Agamloh, S. Peele, and J. Grappe, “A comparative analysis of voltage magnitude deviation and unbalance on standard and premium efficient induction motors,” in *Conference Record of 2012 Annual IEEE Pulp and Paper Industry Technical Conference (PPIC)*, Jun. 2012, pp. 1–8. doi: 10.1109/PPIC.2012.6293004.
- [97] “The impact that voltage and frequency variations have on AC induction motor performance and life in accordance with NEMA MG-1 standards.” Accessed: Sep. 15, 2022. [Online]. Available: <https://ieeexplore.ieee.org/document/779341>
- [98] A. H. Bonnett, “The impact that voltage and frequency variations have on AC induction motor performance and life in accordance with NEMA MG-1 standards,” in *Conference Record of 1999*

- Annual Pulp and Paper Industry Technical Conference (Cat. No.99CH36338)*, Jun. 1999, pp. 16–26. doi: 10.1109/PAPCON.1999.779341.
- [99] N. Mendes *et al.*, “ANN for Motor Loading Diagnosis under Voltage Variation Conditions,” in *2023 IEEE Kansas Power and Energy Conference (KPEC)*, Apr. 2023, pp. 1–6. doi: 10.1109/KPEC58008.2023.10215414.
- [100] J. M. Tabora, L. C. D. S. Júnior, M. E. de L. Tostes, E. O. de Matos, and U. H. Bezerra, “Efficient Electric Motors Performance Under Voltage Variation Conditions,” in *2023 IEEE Kansas Power and Energy Conference (KPEC)*, Apr. 2023, pp. 1–6. doi: 10.1109/KPEC58008.2023.10215475.
- [101] M. Kostic, M. Ivanovic, and S. Minic, “Reduction of electric energy consumption in induction motor drives by setting supply voltage,” in *2012 2nd International Symposium On Environment Friendly Energies And Applications*, Jun. 2012, pp. 128–133. doi: 10.1109/EFEA.2012.6294073.
- [102] K. Zhao, L. Cheng, C. Zhang, D. Nie, and W. Cai, “Induction motors lifetime expectancy analysis subject to regular voltage fluctuations,” in *2017 IEEE Electrical Power and Energy Conference (EPEC)*, Oct. 2017, pp. 1–6. doi: 10.1109/EPEC.2017.8286230.
- [103] W. Wang and Z. Lu, “Analysis of Model Predictive Current-Controlled Permanent Magnet Synchronous Motor Drives with Inaccurate DC Bus Voltage Measurement,” *Energies*, vol. 13, no. 2, Art. no. 2, Jan. 2020, doi: 10.3390/en13020353.
- [104] H.-J. Lee and J.-G. Shon, “Improved Voltage Flux-Weakening Strategy of Permanent Magnet Synchronous Motor in High-Speed Operation,” *Energies*, vol. 14, no. 22, Art. no. 22, Jan. 2021, doi: 10.3390/en14227464.
- [105] A. Sikora, A. Zielonka, and M. Woźniak, “Minimization of Energy Losses in the BLDC Motor for Improved Control and Power Supply of the System under Static Load,” *Sensors*, vol. 22, no. 3, Art. no. 3, Jan. 2022, doi: 10.3390/s22031058.
- [106] A. Sikora and M. Woźniak, “Impact of Current Pulsation on BLDC Motor Parameters,” *Sensors*, vol. 21, no. 2, Art. no. 2, Jan. 2021, doi: 10.3390/s21020587.
- [107] “World Energy Outlook 2019 – Analysis,” IEA. Accessed: Jun. 10, 2022. [Online]. Available: <https://www.iea.org/reports/world-energy-outlook-2019>
- [108] D. F. de Souza, F. A. M. Salotti, I. L. Sauer, H. Tatzizawa, A. T. de Almeida, and A. G. Kanashiro, “An assessment of the impact of Brazilian energy efficiency policies for electric motors,” *Energy Nexus*, vol. 5, p. 100033, Mar. 2022, doi: 10.1016/j.nexus.2021.100033.
- [109] J. M. Tabora *et al.*, “Virtual Modeling and Experimental Validation of the Line-Start Permanent Magnet Motor in the Presence of Harmonics,” *Energies*, vol. 15, no. 22, Art. no. 22, Jan. 2022, doi: 10.3390/en15228603.
- [110] F. J. T. E. Ferreira, G. Baoming, and A. T. de Almeida, “Stator Winding Connection-Mode Management in Line-Start Permanent Magnet Motors to Improve Their Efficiency and Power Factor,” *IEEE Transactions on Energy Conversion*, vol. 28, no. 3, pp. 523–534, Sep. 2013, doi: 10.1109/TEC.2013.2270084.
- [111] J. M. Tabora, M. E. de Lima Tostes, E. O. de Matos, and U. H. Bezerra, “Voltage Unbalance and Variations Impacts on IE4 Class LSPMM,” in *2021 14th IEEE International Conference on Industry Applications (INDUSCON)*, Aug. 2021, pp. 940–946. doi: 10.1109/INDUSCON51756.2021.9529505.
- [112] J. M. Tabora, F. V. Vieira Bezerra, T. M. Soares, E. Ortiz de Matos, M. E. de Lima Tostes, and U. Holanda Bezerra, “Electric Motor Degradation Indicator in Non-Ideal Supply Conditions,” in *2023 IEEE Workshop on Power Electronics and Power Quality Applications (PEPQA)*, Oct. 2023, pp. 1–5. doi: 10.1109/PEPQA59611.2023.10325777.
- [113] D. López-Pérez and J. Antonino-Daviu, “Application of Infrared Thermography to Failure Detection in Industrial Induction Motors: Case Stories,” *IEEE Transactions on Industry Applications*, vol. 53, no. 3, pp. 1901–1908, May 2017, doi: 10.1109/TIA.2017.2655008.
- [114] A. Mahami, C. Rahmoune, T. Bettahar, and D. Benazzouz, “Induction motor condition monitoring using infrared thermography imaging and ensemble learning techniques,” *Advances in Mechanical*



- Engineering*, vol. 13, no. 11, p. 16878140211060956, Nov. 2021, doi: 10.1177/16878140211060956.
- [115] M. Manana, A. Arroyo, A. Ortiz, C. J. Renedo, S. Perez, and F. Delgado, “Field winding fault diagnosis in DC motors during manufacturing using thermal monitoring,” *Applied Thermal Engineering*, vol. 31, no. 5, pp. 978–983, Apr. 2011, doi: 10.1016/j.applthermaleng.2010.11.023.
- [116] G. Singh, T. C. Anil Kumar, and V. N. A. Naikan, “Fault diagnosis of induction motor cooling system using infrared thermography,” in *2016 IEEE 6th International Conference on Power Systems (ICPS)*, Mar. 2016, pp. 1–4. doi: 10.1109/ICPES.2016.7584040.
- [117] M. Ghods, J. Faiz, A. A. Pourmoosa, and S. Khosrogorji, “Analytical Evaluation of Core Losses, Thermal Modelling and Insulation Lifespan Prediction for Induction Motor in Presence of Harmonic and Voltage Unbalance,” *International Journal of Engineering*, vol. 34, no. 5, pp. 1213–1224, May 2021, doi: 10.5829/ije.2021.34.05b.14.
- [118] J. M. Tabora, M. E. De Lima Tostes, E. O. De Matos, U. H. Bezerra, T. M. Soares, and B. S. De Albuquerque, “Assessing Voltage Unbalance Conditions in IE2, IE3 and IE4 Classes Induction Motors,” *IEEE Access*, vol. 8, pp. 186725–186739, 2020, doi: 10.1109/ACCESS.2020.3029794.
- [119] J. Muñoz Tabora, M. E. de Lima Tostes, E. Ortiz de Matos, T. Mota Soares, and U. H. Bezerra, “Voltage Harmonic Impacts on Electric Motors: A Comparison between IE2, IE3 and IE4 Induction Motor Classes,” *Energies*, vol. 13, no. 13, Art. no. 13, Jan. 2020, doi: 10.3390/en13133333.
- [120] W. R. Finley, M. M. Howdowanec, and W. G. Holter, “Diagnosing motor vibration problems,” in *Conference Record of 2000 Annual Pulp and Paper Industry Technical Conference (Cat. No.00CH37111)*, Jun. 2000, pp. 165–180. doi: 10.1109/PAPCON.2000.854217.
- [121] V. Climente-Alarcon, J. A. Antonino-Daviu, F. Vedreño-Santos, and R. Puche-Panadero, “Vibration Transient Detection of Broken Rotor Bars by PSH Sidebands,” *IEEE Transactions on Industry Applications*, vol. 49, no. 6, pp. 2576–2582, Nov. 2013, doi: 10.1109/TIA.2013.2265872.
- [122] I. Ibrahim, R. Silva, M. H. Mohammadi, V. Ghorbanian, and D. A. Lowther, “Surrogate-Based Acoustic Noise Prediction of Electric Motors,” *IEEE Transactions on Magnetics*, vol. 56, no. 2, pp. 1–4, Feb. 2020, doi: 10.1109/TMAG.2019.2945407.
- [123] S. Sathyan, U. Aydin, and A. Belahcen, “Acoustic Noise Computation of Electrical Motors Using the Boundary Element Method,” *Energies*, vol. 13, no. 1, Art. no. 1, Jan. 2020, doi: 10.3390/en13010245.
- [124] M. Liu, K. W. Chan, J. Hu, W. Xu, and J. Rodriguez, “Model Predictive Direct Speed Control With Torque Oscillation Reduction for PMSM Drives,” *IEEE Transactions on Industrial Informatics*, vol. 15, no. 9, pp. 4944–4956, Sep. 2019, doi: 10.1109/TII.2019.2898004.
- [125] A. Saito, M. Kuroishi, and H. Nakai, “Vibration Prediction Method of Electric Machines by using Experimental Transfer Function and Magnetostatic Finite Element Analysis,” *J. Phys.: Conf. Ser.*, vol. 744, p. 012088, Sep. 2016, doi: 10.1088/1742-6596/744/1/012088.
- [126] G. C. Stone, M. K. W. Stranges, and D. G. Dunn, “Common Questions on Partial Discharge Testing: A Review of Recent Developments in IEEE and IEC Standards for Offline and Online Testing of Motor and Generator Stator Windings,” *IEEE Industry Applications Magazine*, vol. 22, no. 1, pp. 14–19, Jan. 2016, doi: 10.1109/MIAS.2015.2458337.
- [127] G. C. Stone, H. G. Sedding, and C. Chan, “Experience With Online Partial-Discharge Measurement in High-Voltage Inverter-Fed Motors,” *IEEE Transactions on Industry Applications*, vol. 54, no. 1, pp. 866–872, Jan. 2018, doi: 10.1109/TIA.2017.2740280.
- [128] B. Hu *et al.*, “A Partial Discharge Study of Medium-Voltage Motor Winding Insulation Under Two-Level Voltage Pulses With High  $Dv/Dt$ ,” *IEEE Open Journal of Power Electronics*, vol. 2, pp. 225–235, 2021, doi: 10.1109/OJPEL.2021.3069780.
- [129] I. Zamudio-Ramirez, R. A. Osornio-Rios, J. A. Antonino-Daviu, H. Razik, and R. de J. Romero-Troncoso, “Magnetic Flux Analysis for the Condition Monitoring of Electric Machines: A Review,” *IEEE Transactions on Industrial Informatics*, vol. 18, no. 5, pp. 2895–2908, May 2022, doi: 10.1109/TII.2021.3070581.

- [130] E. L. Bonaldi, L. E. de L. de Oliveira, J. G. B. da Silva, G. Lambert-Torres, and L. E. B. da Silva, *Predictive Maintenance by Electrical Signature Analysis to Induction Motors*. IntechOpen, 2012. doi: 10.5772/48045.
- [131] J. Antonino-Daviu, “Electrical Monitoring under Transient Conditions: A New Paradigm in Electric Motors Predictive Maintenance,” *Applied Sciences*, vol. 10, no. 17, Art. no. 17, Jan. 2020, doi: 10.3390/app10176137.
- [132] A. Choudhary, D. Goyal, S. L. Shimi, and A. Akula, “Condition Monitoring and Fault Diagnosis of Induction Motors: A Review,” *Arch Computat Methods Eng*, vol. 26, no. 4, pp. 1221–1238, Sep. 2019, doi: 10.1007/s11831-018-9286-z.
- [133] T. Ince, S. Kiranyaz, L. Eren, M. Askar, and M. Gabbouj, “Real-Time Motor Fault Detection by 1-D Convolutional Neural Networks,” *IEEE Transactions on Industrial Electronics*, vol. 63, no. 11, pp. 7067–7075, Nov. 2016, doi: 10.1109/TIE.2016.2582729.
- [134] B. G. Joung, W. J. Lee, A. Huang, and J. W. Sutherland, “Development and Application of a Method for Real Time Motor Fault Detection,” *Procedia Manufacturing*, vol. 49, pp. 94–98, Jan. 2020, doi: 10.1016/j.promfg.2020.07.002.
- [135] M. Şimşir, R. Bayır, and Y. Uyaroğlu, “Real-Time Monitoring and Fault Diagnosis of a Low Power Hub Motor Using Feedforward Neural Network,” *Computational Intelligence and Neuroscience*, vol. 2016, p. e7129376, Dec. 2015, doi: 10.1155/2016/7129376.
- [136] H. Zhang, B. Ge, and B. Han, “Real-Time Motor Fault Diagnosis Based on TCN and Attention,” *Machines*, vol. 10, no. 4, Art. no. 4, Apr. 2022, doi: 10.3390/machines10040249.

## Chapter 2

### Evolution of Electric Motors

This chapter presents the basics of electric induction motors, the main losses that occur during power conversion, and the design improvements made over the years up to the introduction of new technologies such as line-start permanent magnet motors (LSPMMs). Finally, to analyze the main improvements achieved at the power levels analyzed, a comparison is made between IE2, IE3, and IE4 class motors under the same operating conditions, with a view to future substitution.

#### 2.1. The Induction Machine

Nowadays, the induction machine is by far the most widely used electrical machine in electrical drives, its several advantages in line starting capability, and simple and robust construction have led to the widespread use of IMs as the main end users of electrical energy, with more than 50% of the world's electrical energy and almost 70% of the industrial related electrical power consumption according to the International Energy Agency [1]. Figure 2-1 presents the components of an induction motor.

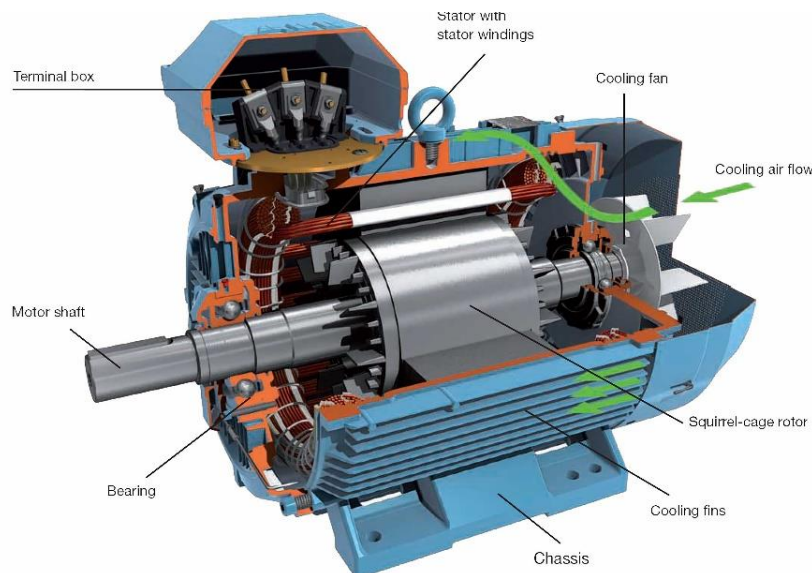


**Figure 2-1** - Induction Motor components [2].

The function of a motor is to convert electrical energy into mechanical energy to perform useful work [3]. Most of the electrical input power is converted into mechanical energy with inevitably a certain amount of losses that depend on the motor technology, materials, design, environmental conditions, Operations and Maintenance (O&M), etc.

Induction motors have been the subject of numerous studies to evaluate the components of losses and the technical and economic means to reduce them. Due to their importance in industry, many improvements have been made in their design and construction over the last 20 years to achieve greater operating efficiency. Two types of losses occur in induction motors: fixed losses, which occur whenever the motor is energized and remains constant for a given voltage and speed, and variable losses, which increase with the motor load [4]. Figure 2-2 presents the distribution of IM losses.

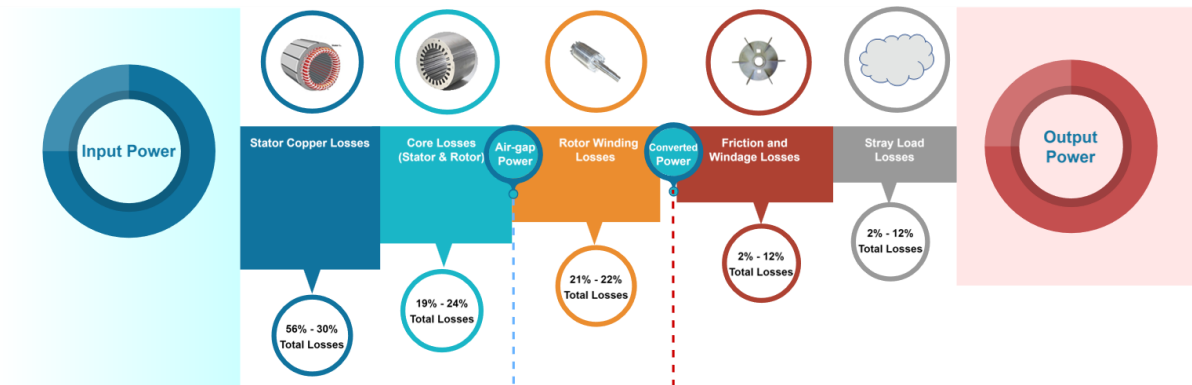


**Figure 2-2** - Distribution of motor losses and percentage of losses for 0.75 kW – 160 kW IM's.

Core, friction, and wind losses are the constant losses. The core is the most expensive part of an induction motor, providing the flux with a low reluctance magnetic path. Core losses represent the energy required to overcome the resistance to changing magnetic fields within the core material of the stator and rotor (hysteresis) and Foucault currents. Friction and wind losses are zero at startup and increase with speed due to bearing friction and air resistance. Since the motor speed is usually constant, these losses are nearly constant.

Variable losses are also known as copper losses. They consist of resistance losses in the stator and rotor and miscellaneous stray load losses. Copper losses in the stator and rotor windings are proportional to the square of the current and directly proportional to the rotor and stator resistances (conductor and bar cross sections). Stray load losses, on the other hand, result from various sources such as leakage fluxes induced by load currents, surface, slot conditions, etc. For years, they have been associated with harmonics as well as practical limitations in the machine [5]. As the load changes, so does the current flowing in the rotor and stator windings, and so both the stray load losses and the stator and rotor losses change.

Both constant and copper losses can be obtained by performing no-load and blocked rotor tests on the three-phase induction motor. The standards in [6], [7] can be used. Losses in IMs

depend on motor load and power, for low power induction motors, ohmic losses represent about 80% of the total losses, while for large machines they are reduced to about 50%, as shown in Figure 2-3a [8]. Variations in losses due to motor load are shown in Figure 2-3b [9].

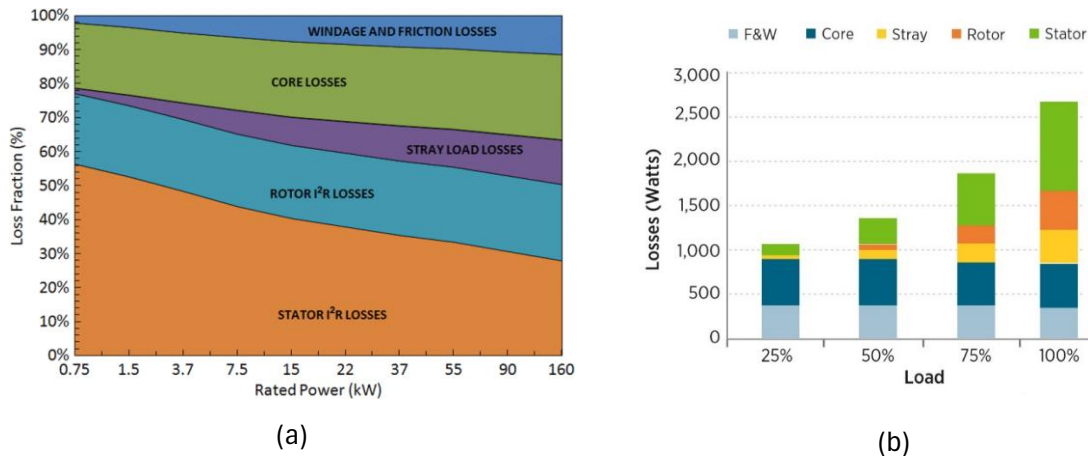


**Figure 2-3** - Typical fraction of losses in 50-Hz, four-pole squirrel cage induction motors for (a) Losses variation as a function of output power [8]; (b) Losses variation as a function of load [9].

The authors in [10], presented an updated, more realistic distribution of modern induction motor loss components as a function of rated power and efficiency class classification. The results show that IE4-classified motors had the largest share of stator copper losses and the rotor copper losses decreased with increasing efficiency. Core losses increased with efficiency, while friction, windings, and auxiliary load losses remained relatively constant.

## 2.2. Improvements in Induction Motors

Due to the various sources of losses in induction motors, several classifications have been developed in terms of their origin and impact, resulting in a ranking of the main efficiency improvement factors. These are shown in Figure 2.4 [11], where each level represents the impact of that area on efficiency. In the next section, we will review the major improvements that have been made to induction motors over the past 20 years in each of the areas shown in Figure 2.4.

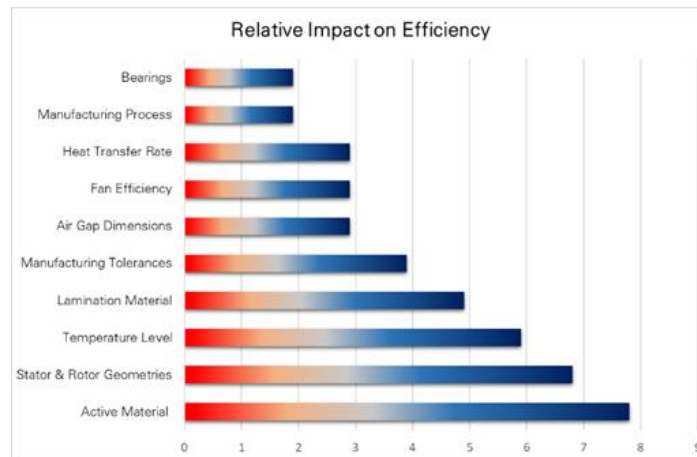


Figure 2-4 - Impact of possible areas of improvement for induction motor performance [11].

### 2.2.1. Active Materials

The materials involved in the conversion of electrical energy are called active materials. They are the core, rotor, and stator assembly (stator windings and rotor cage) [11]. Improving the active materials has the greatest impact on reducing losses and thus increasing the efficiency of IMs. By increasing the use of active material (i.e. more copper wiring in the stator and higher slot fill), the efficiency of standard motors can be increased, e.g. by about 8 percentage points in the case of 1 kW and 1.5 percentage points in the case of 100 kW [12]. To reduce the main losses in the stator windings, the manufacturer in [13] replaced the winding diagram with concentric coils by a winding diagram with equal, offset coils, which resulted in a reduction of almost 8% of the initial resistance.

New developments to reduce rotor winding losses are the emerging technologies of LSPMM, IM using die-cast copper rotors, switched reluctance (SR), and synchronous reluctance (SynRM) motors. These technologies are commercially available in many countries and can achieve efficiencies significantly higher than premium efficiency induction motors (IE3 classes).

Copper rotor motors significantly reduce rotor losses due to the volumetric conductivity, which is approximately 66% higher than aluminum [14]. Constructed with prefabricated copper bars that are typically driven into the rotor slot and soldered to the shading rings at both ends of the rotor, copper-rotor induction motors have reduced  $RI^2$  losses, resulting in a lower operating temperature. A lower temperature means that a smaller cooling fan can be used, resulting in reduced friction and wind losses [9].

A definition of LSPMMs is presented in the next sections. In induction motors, rotor losses include two components, i.e. core losses and rotor cage losses (end rings and rotor bars). In LSPMMs, due to the synchronous speed, no currents are induced inside the rotor (neglecting spatial and time harmonics), so the rotor temperature of these motors is about 30% lower than that of induction motors with the same output power [15].

To reduce core losses, high-quality magnetic materials can be used. Generally, two types of commercial magnetic steel are used in electric machines, M400-50A and M800-50A [15]. The first number indicates the specific iron loss in W/kg at a peak induction of 1.5 T. For M400-50A the specific iron loss is 4W/kg. The second number indicates the thickness of the lamination, for M400-50A the thickness is 0.5mm. In [13], it is presented that the use of the electromagnetic steel sheet M270-50 with specific losses (2.7 W/kg) results in a reduction of 70% and 35% compared to M800-50A and M400-65 losses for a 7.5 kW IM.

Amorphous metals (AM) are a promising material for high-efficiency motors; when AM are used for the iron core, losses are reduced by up to a tenth of the losses of normal iron [16]. However, amorphous metals are hard and brittle, making them difficult to machine and process, increasing their cost.

### **2.2.2. Windage and Friction Losses**

Windage and friction losses can be reduced by properly designing the fan and reducing bearing/seal friction. In [17], two cooling fans of different sizes are tested for a 3.7 kW IM. In order to reduce mechanical losses, the size of the cooling fan must be reduced, but reducing the size of the cooling fan results in higher efficiencies but also higher temperatures. The use of low-friction bearings can also reduce friction losses in IMs. The authors in [18] present a comparison between six bearings from five different manufacturers, where it is observed that a reduction of 40-70% in friction losses can be achieved thanks to several design features, such as the internal geometry of the raceways, the type of grease as well as the polymer material of the cage, which features a lower coefficient of friction than the conventional steel cage [19].

Higher-efficiency motors also present a decrease in line currents, which results in a decrease in the operating temperature. Experimental tests performed on a 7.5 kW four-pole motor show that at full load, an IE3 class SCIM and an IE4 class SCIM have an end shield temperature near

the shaft/bearing housing that is 10 and 15 °C (approximately) lower, respectively, than that of an IE2 class SCIM. For insulation, the National Electrical Manufacturers Association (NEMA) [20] provides acceptable temperature rise for fully loaded motors. Three classes of insulation are commonly used in IMs, these are Class B (maximum temperature of 130°C), Class F (maximum temperature of 155°C), and Class H (maximum temperature of 180°C). Manufacturers use F/H class insulation in most motors, as this offers a clear advantage in terms of heat dissipation and temperature rise [21].

### 2.3. Permanent Magnet Motors

In addition to the induction motors shown in Section 2.1, there are permanent magnet motors which, unlike SCIM, have magnets attached to the surface (Surface Permanent Motor, SPM) or inside the rotor (Internal Permanent Magnet Motor, IPM) to create a permanent magnetic field. This design replaces the IM squirrel cage and significantly reduces rotor I<sup>2</sup>R losses. Figure 2-5 shows the two common categories of permanent magnet motors [9], [22]. In SPM motors, the magnets are attached to the outside of the rotor surface. Because of this mechanical attachment, their mechanical strength is weaker than that of IPM motors. IPM motors have a permanent magnet embedded in the rotor itself.

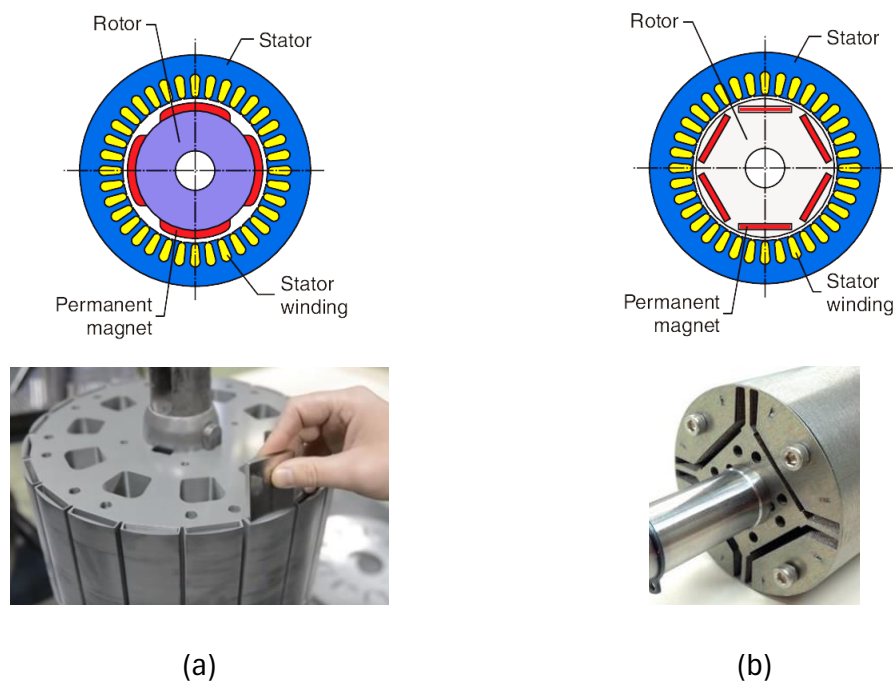


**Figure 2-5** – Permanent magnet motors: (a) Surface mounted permanent magnet motor (SPM)[22] [23]; (b) Interior permanent magnet motor (IPM) [22] [24].



Despite the reduction in losses and consumption, the PM motor is designed for variable speed operation and must be controlled by a specially designed inverter or variable speed drive (VSD) to properly start and synchronize the PM motor. Although a VSD can provide great savings and benefits when operating an IM, there are many other applications where the need for greater operating efficiency does not justify the additional investment in a VSD, such as fixed-speed applications. Given this scenario, the Line Starts Permanent Magnet Motor (LSPMM) becomes one of the best candidates, being present in this study, the following sections describe the main design and operational characteristics.

#### 2.4. Line Start Permanent Magnet Motor LSPMM

The line-start permanent magnet motor (LSPMM) combines the advantages of induction and synchronous machines, using a stator as one of the IMs and a hybrid rotor with a squirrel cage and pairs of permanent magnet poles. Due to the bar-shaped conductors in the rotor, LSPMMs have self-starting capability, and no additional devices are required, but there are still difficulties with the high starting torque [25]. The LSPMM offers many advantages over the IM: higher efficiency and power factor at different load levels, synchronous constant speed, and lower operating temperatures. In terms of reactive power ( $Q$ ) due to the magnetic field generated by permanent magnets, the LSPMM absorbs significantly less reactive power [26]. Also, as standard IMs, LSPMMs are built according to IEC 60034-7 [27, pp. 60034–7], which facilitates substitution between these technologies. Figure 2-6 shows the main components and configuration of a four-pole LSPMM.

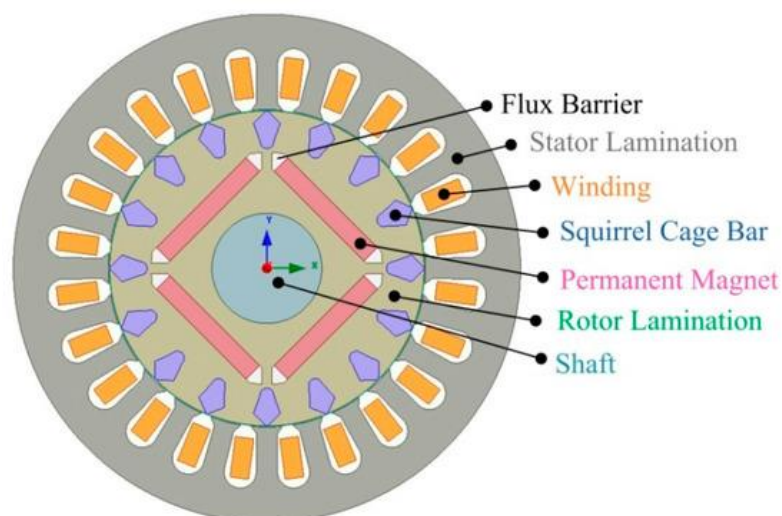


**Figure 2-6** - Structure of a four-pole LSPMM [28]

Manufacturers have used different combinations of magnets in the rotor, some of which are shown in Figure 2-7. The type of configuration depends on the manufacturer as well as on the characteristics of the magnets used. In [29], different permanent magnet types and configurations are analyzed; the authors conclude that rotors with internal magnet types provide higher efficiency and that V-type rotors (Figure 2-7d) and magnet material type NdFe35 provide better efficiencies and power density in LSPMMs.

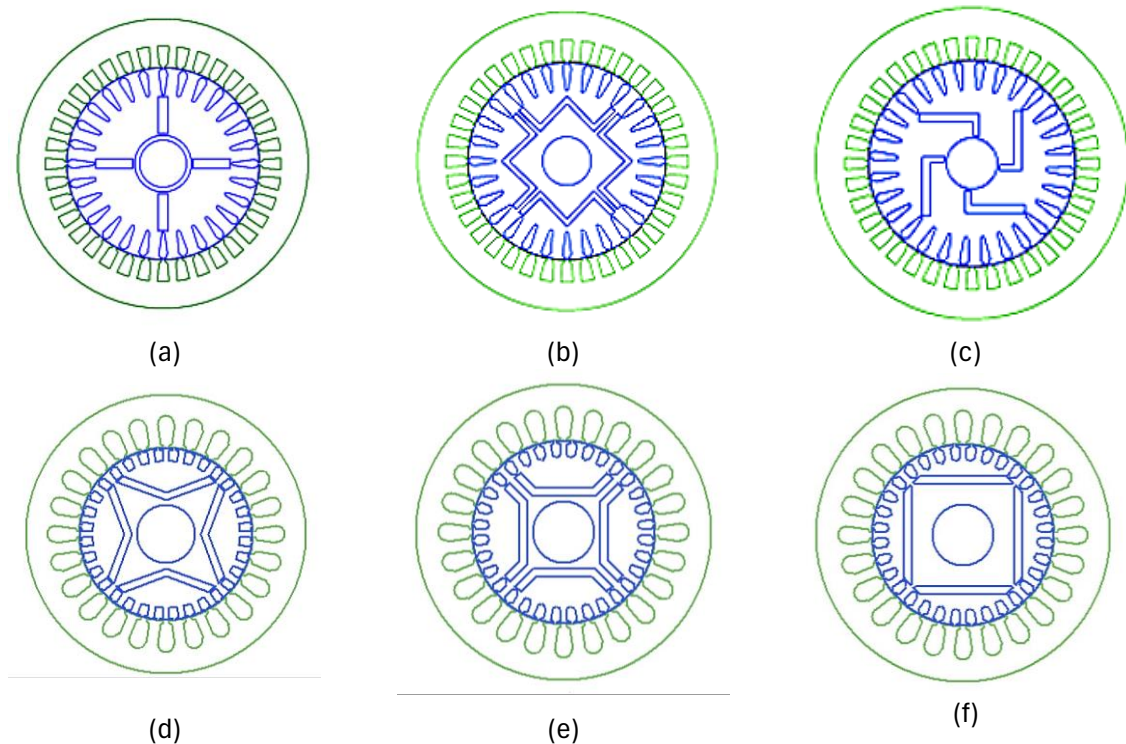


**Figure 2-7** - Typical rotor configurations for LSPMM's :(a) Spoke rotor; (b) W Type magnetic circuit structure; (c) Swastika magnetic circuit structure; (d) V-type magnetic circuit structure; (e) U-type magnetic circuit structure; (f) Series-type magnetic circuit structure [29], [30].

#### 2.4.1. LSPMM Starting

The LSPMM starts as an induction motor by the interaction between the fundamental fields generated by the stator winding and the rotor winding, which generates an asynchronous electromagnetic torque used to start the motor. However, a braking torque occurs due to the interaction between the fundamental fields generated by the stator winding and the permanent magnets (PM) in the rotor. The behavior of torque vs. speed during startup for an LSPMM is shown in Figure 2-8a.

The top curve represents the cage torque, which is the torque that would be obtained without the PM. The lower curve represents the average net torque, which is the sum of the cage torque and the magnetic braking torque. It can be observed that the presence of the magnets results in a decrease of the cage torque, this is due to the generating action of the magnets, which gives rise to a component of the stator current that produces resistive losses in the stator circuit resistance [31]. The torque-speed curves also vary according to the PM configuration inside the rotor [32]. Figure 2-8b shows a comparison between the starting torque of an IM and an LSPMM.

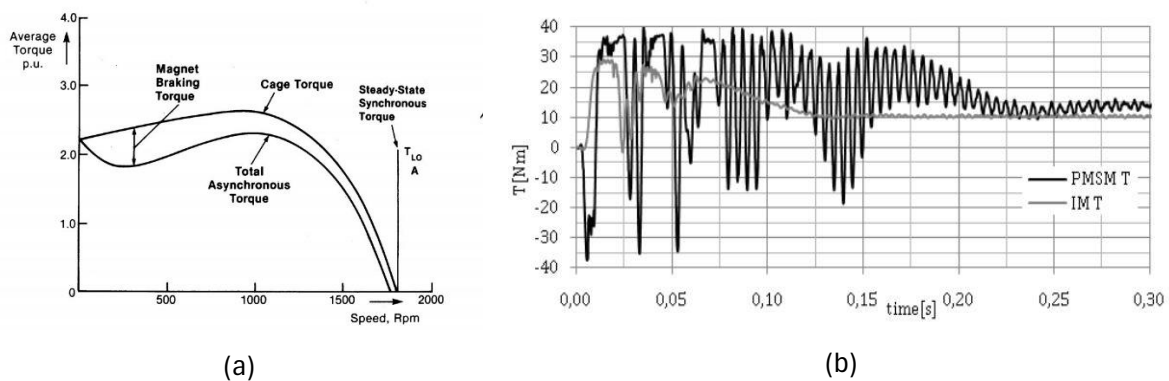


**Figure 2-8** – Starting torque in LSPMM and SCIM: (a) Starting behavior of torque components for LSPMM 's [31]; (b) Torque behavior for IM and LSPMM during starting [26].

Figure 2-8b shows the torque response for IM and LSPMM, and it can be seen that the LSPMM exhibits significant oscillations during start-up compared to the IM. This oscillation behavior is due to two principal components, one with the double slip frequency due to reluctance variation with rotation, and the other with the slip frequency due to magnetic saturation [33]. In [34] different curves during start-up of different permanent magnet motors are presented, as well as solutions to reduce oscillations and braking torque in these technologies. This fact should be considered when changing between IM's and LSPMM's, especially in applications with frequent start/stop cycles.

## 2.5. Comparison of IE2, IE3 & IE4 Motor Efficiency Classes

In order to analyze the main strengths and weaknesses of the new technologies, this section shows a comparison of the performance of three 0.75 kW motors, IE2, IE3 and IE4, under ideal power conditions and the same load conditions, with a view to future substitutions.

### 2.5.1. Input Current Distortion

With respect to the input current, it can be seen in Figure 2-9a that the LSPMM current is significantly reduced compared to the IE2 and IE3 classes of IMs. The stator current in IMs is the sum of two components: the magnetizing current, which is necessary to create the magnetic field in the air gap, and the current due to the load connected to the motor output. The magnetizing current is present at all times during motor operation and, in some 4-pole motors, can reach 50% of the nominal motor current [35]. In the LSPMM, the amplitude of the input current shows a decrease in its value with respect to the IE2 and IE3 technologies for the same percentage of load, due to the presence of permanent magnets in the rotor, which contribute significantly to the reduction of the magnetizing current of the machine.

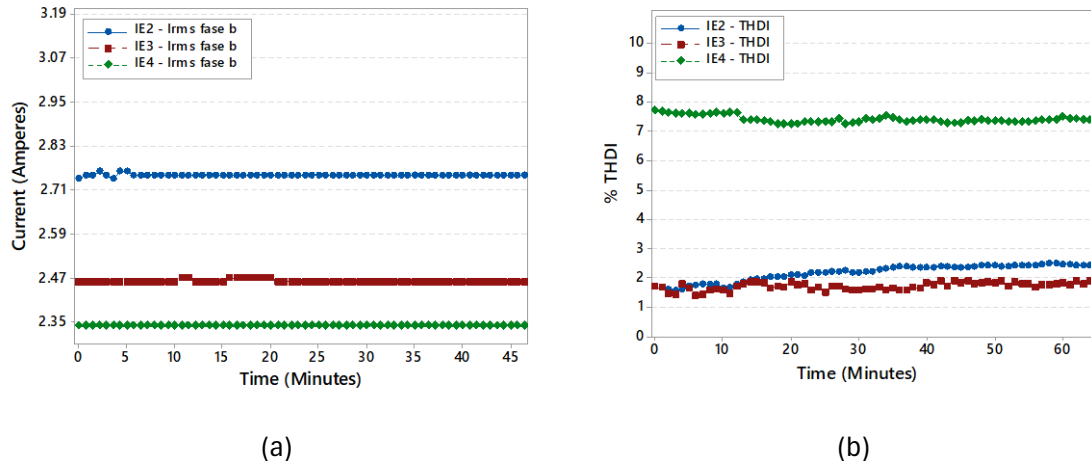


**Figure 2-9** - Comparison between IE2, IE3 and IE4 efficiency class motors (a) Stator currents; (b) Total Harmonic Distortion of Current.

Although the IE4 LSPMM presents lower currents, it also presents a distorted sinusoidal waveform compared to the IE2 and IE3 classes of IM, this is [36]. To quantify the percentage of distortion present in each current sinusoid, the Total Harmonic Distortion of Current (THDI) was obtained for each of the motors. Figure 2-9b shows that the percentage THDI of the IE4 class permanent magnet motor is almost four times higher than that of the IE2 and IE3 motor classes. The current waveform of the LSPMM has 5th and 7th order harmonics, as well as higher order

harmonics (17th and 23rd). This distortion in LSPMMs has been previously documented in [26] [37] [38].

Harmonics, depending on their order and percentage, have different effects on electrical system components and loads. While both motors have even, odd and intermediate harmonics, the LSPMM has higher proportions and more harmonics, including high-frequency harmonics up to order 50. Researchers and manufacturers see the LSPMM as a possible replacement for the SCIM in the future, but studies should be carried out first and foremost for large-scale applications.

### 2.5.2. Total Power and Power Factor

In terms of total consumption, the IE3 and IE4 motors show a reduction in active and reactive power compared to the IE2 motor class, resulting in a significant reduction in total power, as shown in Figure 2-10a. The observed reduction leads to a lower consumption, which can lead to great savings in the energy bill and a lower payback time according to the operating hours. The power factor of the IE3 class motor also shows a considerable increase with respect to the IE2 class, as shown in Figure 2-10b, going from 0.64 to 0.72, with which considerable benefits can be obtained in the industrial sector in terms of losses, delay in investments in capacitor banks and general efficiency of the system. Regarding the IE4 class motor, although it shows an improvement compared to the IE2 class motor, it presents a lower power factor compared to the IE3 class motor.

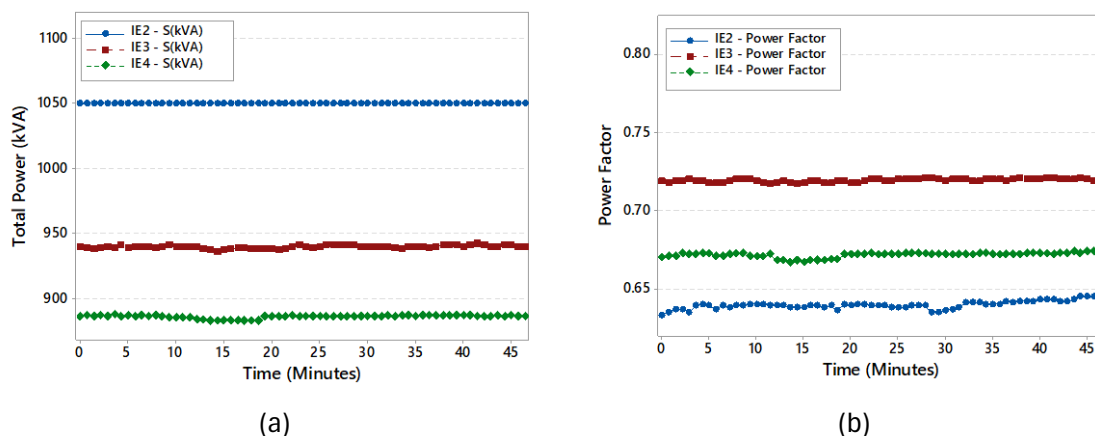
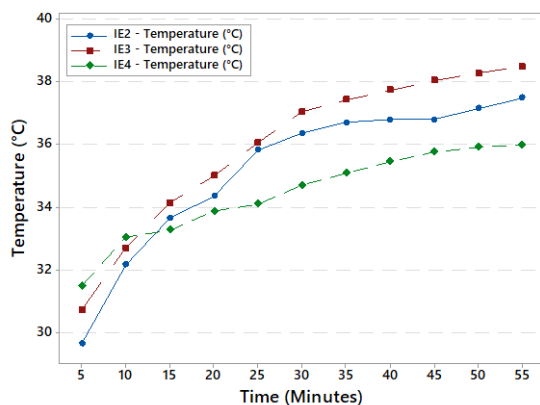


**Figure 2-10** - Consumption in IE2, IE3 and IE4 class motors (a) Total Power; (b) Power F.

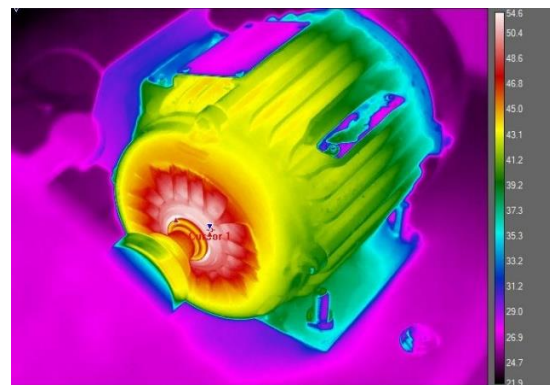
The low power factor in synchronous motors has already been discussed in [30], [39], [40] and is related to the rotor magnetic saliency ratio ( $\varepsilon = L_d/L_q$ ) which describes the ratio between the main rotor flux inductance (d axis,  $L_d$ ) and the main torque producing inductance (q axis,  $L_q$ ), [22], [41]. Due to the permanent magnet motor, having the magnets inside the rotor result in a larger magnetic saliency, for which manufacturers still need to analyze ways to reduce this ratio.

### 2.5.3. Electric Motor Temperature

The synchronous speed of the LSPMMs allows a quieter operation and a reduction in the current, active, and reactive power consumption, thanks to the permanent magnets, when compared to the IE2 and IE3 classes of IMs. In addition, these motors have lower operating temperatures due to the reduction of the current in the windings and the practically zero rotor current (neglecting the harmonic currents). Figure 2-11a shows the front temperature rise of each IM in one hour interval, it is observed how the hybrid motor presents a higher initial temperature, but with smaller increments until reaching 36°C, below the other motors.



(a)



(b)

**Figure 2-11** - Temperature rise for IE2, IE3 & IE4 IM 's classes: (a) Graphics from measurements and (b) LSPMM captured angle.

The temperature reduction can be explained by the design and operating characteristics of the LSPMM. When the rotor reaches synchronous speed, resulting in zero slip, there is no electromagnetic field generated in the rotor bars to produce rotor current, except for harmonic currents.

This significantly reduces the temperature of the shaft and consequently other components [15], [35]. In [42] it is reported that this temperature reduction is approximately 30% lower. In addition, these emerging technologies exhibit an increase in active materials [43], which contributes to reduced temperature variations due to the increase in area for the flux path in these technologies.

## 2.6. Chapter Conclusion

The aim of this chapter was to provide a brief description of the electric motor, its main losses and the means used by manufacturers and researchers to reduce them, as well as the evolution of these machines until the introduction of new technologies such as the LSPMM. Finally, a technical comparison was made between the IE2, IE3 and IE4 classes of IM with 0.75 kW output power, considering the new law on the energy efficiency of electric motors, which increases the minimum efficiency values for the IE4 class motor. Then, based on experimental measurements, the three technologies were compared under the same operating conditions with the aim of substituting between efficiency classes. The results show that the IE3 class motor achieves lower currents and power factor, but with a higher operating temperature compared to the IE2 class motor. The IE4 class permanent magnet motor shows the lowest currents, consumption, and operating temperature, as well as quieter operation, but with a higher percentage of harmonic distortion and a lower power factor compared to the IE3 class motor at the same load.

In general, the results observed show that the transition to the IE3 efficiency class will result in great benefits in terms of energy, economy, and environment, both for Brazil and for the neighboring countries, since it is a major exporter within the region.

The following chapter will show the main effects of voltage harmonics on electric motors classes IE2, IE3 and IE4.

## 2.7. Chapter Bibliography

- [1] International Energy Agency (IEA), “Publications.” Accessed: Aug. 15, 2019. [Online]. Available: <https://www.iea-4e.org/publications>
- [2] Unknown, “Induction Motor components.” Accessed: Jun. 03, 2020. [Online]. Available: [http://www.trielectricinternational.com/Home/Spare\\_Parts\\_for\\_Motors](http://www.trielectricinternational.com/Home/Spare_Parts_for_Motors)
- [3] S. Chapman, *Electric Machinery Fundamentals*. McGraw-Hill Companies, Incorporated, 2005.
- [4] A. Sumper and A. Baghini, *Electrical Energy Efficiency: Technologies and Applications*. 2012. doi: 10.1002/9781119990048.
- [5] H. Köfler, “Stray Load Losses in Induction Machines, a Review of experimental measuring Methods and a critical Performance Evaluation,” in *International Conference on Renewable Energy and Power Quality (ICREPQ)*, ., 2003. Accessed: Aug. 15, 2019. [Online]. Available: <https://graz.pure.elsevier.com/en/publications/stray-load-losses-in-induction-machines-a-review-of-experimental->
- [6] IEC 60034-30-1:2014, “Rotating electrical machines - Part 30-1: Efficiency classes of line operated AC motors (IE code).” Accessed: Aug. 15, 2019. [Online]. Available: <https://webstore.iec.ch/publication/136>
- [7] “IEEE 112-2017 - IEEE Standard Test Procedure for Polyphase Induction Motors and Generators.” Accessed: Aug. 15, 2019. [Online]. Available: <https://standards.ieee.org/standard/112-2017.html>
- [8] A. T. de Almeida, F. J. T. E. Ferreira, and G. Baoming, “Beyond Induction Motors—Technology Trends to Move Up Efficiency,” *IEEE Transactions on Industry Applications*, vol. 50, no. 3, pp. 2103–2114, May 2014, doi: 10.1109/TIA.2013.2288425.
- [9] U.S. Department of Energy, Energy Efficiency & Renewable Energy, “Premium Efficiency Motor Selection and Application Guide – A Handbook for Industry,” Energy.gov. Accessed: Aug. 15, 2019. [Online]. Available: <https://www.energy.gov/eere/amo/downloads/premium-efficiency-motor-selection-and-application-guide-handbook-industry>
- [10] L. Aarniovuori, M. Niemelä, J. Pyrhönen, W. Cao, and E. B. Agamloh, “Loss Components and Performance of Modern Induction Motors,” in *2018 XIII International Conference on Electrical Machines (ICEM)*, Sep. 2018, pp. 1253–1259. doi: 10.1109/ICELMACH.2018.8507189.
- [11] J. F. Fuchsloch, W. R. Finley, and R. W. Walter, “The Next Generation Motor,” *IEEE Industry Applications Magazine*, vol. 14, no. 1, pp. 37–43, Jan. 2008, doi: 10.1109/MIA.2007.909803.
- [12] F. Parasiliti and P. Bertoldi, Eds., *Energy Efficiency in Motor Driven Systems*. Berlin Heidelberg: Springer-Verlag, 2003. Accessed: Aug. 15, 2019. [Online]. Available: <https://www.springer.com/gp/book/9783540006664>
- [13] I. Peter, G. Scutaru, and C. G. Nistor, “Manufacturing of asynchronous motors with squirrel cage rotor, included in the premium efficiency category IE3, at S.C. Electroprecizia Electrical-Motors S.R.L. Săcele,” in *2014 International Conference on Optimization of Electrical and Electronic Equipment (OPTIM)*, May 2014, pp. 421–425. doi: 10.1109/OPTIM.2014.6850971.
- [14] Copper Development Association, “Mineral Producer Installing 150 Copper-Rotor Motors Rising Energy Costs Drive Upgrades, Rapid Payback Expected.” Accessed: Aug. 15, 2019.



- [Online]. Available: [https://www.copper.org/environment/sustainable-energy/electric-motors/case-studies/nyco\\_a6118.html](https://www.copper.org/environment/sustainable-energy/electric-motors/case-studies/nyco_a6118.html)
- [15] C. Debruyne, “Impact of voltage distortion on energy efficiency of induction machines and line start permanent magnet machines,” dissertation, Ghent University, 2014. Accessed: Aug. 15, 2019. [Online]. Available: <http://hdl.handle.net/1854/LU-4383637>
- [16] HITACHI, “Development of Motor with Amorphous Metal : Research & Development : Hitachi.” Accessed: Aug. 15, 2019. [Online]. Available: <https://www.hitachi.com/rd/portal/contents/story/amorphous/index.html>
- [17] D.-J. Kim, J.-H. Choi, Y.-D. Chun, D.-H. Koo, and P.-W. Han, “The Study of the Stray Load Loss and Mechanical Loss of Three Phase Induction Motor considering Experimental Results,” *Journal of Electrical Engineering and Technology*, vol. 9, Jan. 2014, doi: 10.5370/JEET.2014.9.1.121.
- [18] F. J. T. E. Ferreira, A. M. Silva, V. P. B. Aguiar, R. S. T. Pontes, E. C. Quispe, and A. T. de Almeida, “Overview of Retrofitting Options in Induction Motors to Improve Their Efficiency and Reliability,” in *2018 IEEE International Conference on Environment and Electrical Engineering and 2018 IEEE Industrial and Commercial Power Systems Europe (EEEIC / I CPS Europe)*, Jun. 2018, pp. 1–12. doi: 10.1109/EEEIC.2018.8493887.
- [19] “SKF Energy Efficient deep groove ball bearings.” Accessed: Aug. 15, 2019. [Online]. Available: <https://www.skf.com/br/industry-solutions/electric-motors/electric-motors-for-consumer-goods/applications/brush-motors/skf-energy-efficient-deep-groove-ball-bearing/index.html>
- [20] NEMA MG1-2016, “Motors and Generators.” Accessed: Aug. 15, 2019. [Online]. Available: <https://www.nema.org/Standards/Pages/Motors-and-Generators.aspx>
- [21] F. J. T. E. Ferreira, G. Baoming, and A. T. de Almeida, “Reliability and Operation of High-Efficiency Induction Motors,” *IEEE Transactions on Industry Applications*, vol. 52, no. 6, pp. 4628–4637, Nov. 2016, doi: 10.1109/TIA.2016.2600677.
- [22] C. Vavra, “Understanding permanent magnet motors,” *Control Engineering*. Accessed: May 17, 2020. [Online]. Available: <https://www.controleng.com/articles/understanding-permanent-magnet-motors/>
- [23] *Así se fabrican los motores eléctricos*. Accessed: May 20, 2020. [Online Video]. Available: <https://www.youtube.com/watch?v=QfNrEBODs3s>
- [24] T. Ishikawa and N. Igarashi, “Failure Diagnosis of Demagnetization in Interior Permanent Magnet Synchronous Motors Using Vibration Characteristics,” *Applied Sciences*, vol. 9, no. 15, Art. no. 15, Jan. 2019, doi: 10.3390/app9153111.
- [25] J. Lee, S. Rhyu, I. Jung, and Y. Kim, “Design of high efficiency line start permanent magnet motor for submersible pumps,” in *2016 IEEE 16th International Conference on Environment and Electrical Engineering (EEEIC)*, Jun. 2016, pp. 1–4. doi: 10.1109/EEEIC.2016.7555600.
- [26] M. GWOŹDZIEWICZ and L. ANTAL, “INVESTIGATION OF LINE START PERMANENT MAGNET SYNCHRONOUS MOTOR AND INDUCTION MOTOR PROPERTIES, Prace Naukowe Instytutu Maszyn, Napędów i Pomiarów Elektrycznych, Politechniki Wrocławskiej.” *Prace Naukowe Instytutu Maszyn, Napędów i Pomiarów Elektrycznych, Politechniki Wrocławskiej.*, 2010. [Online]. Available: <https://pdfs.semanticscholar.org/e9ce/18be7c97cf70342b3135d9cd8364e14538bb.pdf>
- [27] IEC 60034-7:1992, “Classification of types of constructions and mounting arrangements (IM Code).” Accessed: Aug. 15, 2019. [Online]. Available: <https://webstore.iec.ch/publication/145>

- [28] M. Rezazadeh Mehrjou, N. Mariun, N. Misron, M. A. M. Radzi, and S. Musa, “Broken Rotor Bar Detection in LS-PMSM Based on Startup Current Analysis Using Wavelet Entropy Features,” *Applied Sciences*, vol. 7, no. 8, Art. no. 8, Aug. 2017, doi: 10.3390/app7080845.
- [29] İ. Tarımer, “Investigation of the Effects of Rotor Pole Geometry and Permanent,” *1*, vol. 90, no. 2, pp. 67–72, 2009, doi: 10.5755/j01.eee.90.2.10512.
- [30] E. Vera, “Optimal design of line-start permanent magnet synchronous motors of high efficiency. Electric power. Ecole Centrale de Lille, 2015. English. NNT: 2015ECLI0022. tel-01308575,” 2015.
- [31] T. J. E. Miller, “Synchronization of Line-Start Permanent-Magnet AC Motors,” *IEEE Transactions on Power Apparatus and Systems*, vol. PAS-103, no. 7, pp. 1822–1828, Jul. 1984, doi: 10.1109/TPAS.1984.318630.
- [32] A. Kumar and A. Srivastava, “Performance Comparison of Two Different Rotor Topologies of Line Start Permanent Magnet Synchronous Motors,” *Engineering Technology*, vol. 5, p. 8.
- [33] A. Takahashi, S. Kikuchi, K. Miyata, and A. Binder, “Asynchronous Torque of Line-Starting Permanent-Magnet Synchronous Motors,” *IEEE Transactions on Energy Conversion*, vol. 30, no. 2, pp. 498–506, Jun. 2015, doi: 10.1109/TEC.2014.2361836.
- [34] M. Popescu, T. J. E. Miller, M. I. McGilp, G. Strappazzon, N. Trivillin, and R. Santarossa, “Line-start permanent-magnet motor: single-phase starting performance analysis,” *IEEE Transactions on Industry Applications*, vol. 39, no. 4, pp. 1021–1030, Jul. 2003, doi: 10.1109/TIA.2003.813745.
- [35] A. Hughes and B. Drury, *Electric Motors and Drives - 4th Edition*, 4th ed. United Kingdom: Elsevier Ltd., 2013. Accessed: Aug. 15, 2019. [Online]. Available: <https://www.elsevier.com/books/electric-motors-and-drives/hughes/978-0-08-098332-5>
- [36] J. M. Tabora, T. M.S., E. Ortiz de Matos, M. E. de Lima Tostes, and J. C. Paye, “Fifth & Seventh Harmonic Effects on the Performance of IE2, IE3 & IE4 Induction Motor Classes,” Santiago de Chile, 2019.
- [37] F. team, “Proceedings of the 6th International Conference eemods ’09 - Energy Efficiency in Motor Driven Systems, Nantes, FRANCE, 14-17 September 2009,” EU Science Hub - European Commission. Accessed: Aug. 15, 2019. [Online]. Available: <https://ec.europa.eu/jrc/en/publication/books/proceedings-6th-international-conference-eemods-09-energy-efficiency-motor-driven-systems-nantes>
- [38] T. Zawilak and J. Zawilak, “MINIMIZATION OF HIGHER HARMONICS IN LINE-START PERMANENT MAGNET SYNCHRONOUS MOTOR,” *Przegląd Elektrotechniczny*, vol. 84, Jan. 2008.
- [39] H. Kim, Y. Park, H.-C. Liu, P.-W. Han, and J. Lee, “Study on Line-Start Permanent Magnet Assistance Synchronous Reluctance Motor for Improving Efficiency and Power Factor,” *Energies*, vol. 13, no. 2, Art. no. 2, Jan. 2020, doi: 10.3390/en13020384.
- [40] P. Zhang, D. M. Ionel, and N. A. O. Demerdash, “Saliency ratio and power factor of IPM motors optimally designed for high efficiency and low cost objectives,” in *2014 IEEE Energy Conversion Congress and Exposition (ECCE)*, Sep. 2014, pp. 3541–3547. doi: 10.1109/ECCE.2014.6953882.
- [41] S. Tahı, R. Ibtıouen, and M. Bounekhla, “Design Optimization of Two Synchronous Reluctance Machine Structures with Maximized Torque and Power Factor,” *Progress In Electromagnetics Research B*, vol. 35, pp. 369–387, Jan. 2011, doi: 10.2528/PIERB11091101.
- [42] A. Fasquelle, “Contribution à la modélisation multi-physique : électro-vibro-acoustique et aérothermique de machines de traction,” Jan. 2007.

- [43] A. T. de Almeida, F. J. T. E. Ferreira, and J. A. C. Fong, “Standards for Super-Premium Efficiency class for electric motors,” in *Conference Record 2009 IEEE Industrial Commercial Power Systems Technical Conference*, May 2009, pp. 1–8. doi: 10.1109/ICPS.2009.5463983.

## Chapter 3

### Voltage Harmonics Impacts on Efficient Electric Motors

Currently all electrical systems present waveforms with the presence of harmonic distortions, the distribution companies supply the loads with currents at the fundamental frequency and inevitably with currents at higher frequencies. However, only fundamental frequency current can provide real power. The main effects of voltage and current harmonics on the performance and temperature of low-power class IE2, IE3, and IE4 induction motors are presented in this chapter.

#### 3.1. Harmonic Distortion

The introduction of new types of electronic power sources has increased distortions in the waveforms of power systems over the last few decades. These power sources act as non-linear loads. Harmonic distortion exists due to the presence of these non-linear loads and devices in the power system. Currently, all electrical systems present waveforms with the presence of harmonic distortion, the distribution companies supply the loads with currents at the fundamental frequency and inevitably currents at higher frequencies. However, only the fundamental frequency current can deliver real power [1]. All harmonics present in a waveform are known as total harmonic distortion (THD), which is one of the most commonly used parameters to evaluate voltage or current quality. The mathematical expression is given by:

$$THD\% = \frac{\sqrt{\sum_{h=2}^{h_{max}} V_h^2}}{V_1} * 100 \quad (1)$$

Where  $V_h$  is the harmonic voltage of the order  $h$ ,  $V_1$  is the fundamental measured voltage and  $h_{max}$  is the order of the maximum harmonic considered.

Since a perfectly sinusoidal voltage is practically impossible due to technical limitations, many studies have been developed to analyze the impact of distorted voltages and currents on electric motors, but with the introduction of new technologies, it is necessary to know their response to the presence of these disturbances in electrical systems.

### 3.2. Harmonics Limits

Harmonics have been present in power systems since the first generators. The first AC sources were highly distorted until AC generator designers succeeded in building units that delivered near sinusoidal voltages [1], [2]. In 1893, only eight years after the first AC power plant was built, engineers conducted a harmonic analysis to identify and solve a motor heating problem. A year later, one of the first documents in which the word "harmonic" was printed and used in the context of the Fourier series applied to electrical systems is an 1894 paper by Edwin J. Houston and Arthur E. Kennelly [2], [3].

However, the harmonic components were so small that their effects on the systems were negligible and became widespread especially after power electronic devices significantly penetrated the power systems and resulted in an increase in the harmonic and interharmonics content in the sinusoidal wave, prompting the need to pay more attention to them.

To ensure a supply with acceptable power quality limits and losses, voltage distortions must be limited to certain values defined by international standards. Standard IEEE 519-2014 [4], sets limits of 5% and 8% for individual and total harmonic distortion at the point of common coupling (PCC) for voltages below 1 kV. The IEC 61000 [5] series includes harmonics and interharmonics as one of the conducted low-frequency electromagnetic phenomena. The IEC 61000-2-4 series [6] provides harmonic and inter-harmonic compatibility levels for industrial plants and it defines values ranging from 0.2% to 6% for individual harmonics and 8% for the THD.

In Brazil, the National Electric Energy Agency (ANEEL) [7] is responsible for the regulation and supervision of the generation, transmission, distribution, and sale of electric energy, by the law and the guidelines and policies of the federal government. The PRODIST module 8 [8], establishes the limits or reference values applicable to the total and individual harmonic distortions. For voltages of less than 1 kV, it sets 10% for the THD, while for the individual components, it sets 2.5% for even components not multiples of three, 7.5% for odd components not multiples of three, and 6.5% for components multiples of three.

### 3.3. Losses due to Harmonics in Induction Motors

The presence of harmonic voltage distortion in the motor supply leads to additional harmonic losses in the rotor and stator, torque reduction, noise, slippage, and mechanical vibrations, all

of which contribute to an increase in the internal temperature of the motor, particularly in the windings and stator core [9], [10] [11], [12], [13].

The harmonics are divided into positive sequence harmonics, negative sequence harmonics, and zero sequence harmonics as shown in Table 3-1. According to the literature, negative sequence harmonics result in greater negative effects due to their opposite rotating magnetic field, unlike positive sequence harmonics which result in positive torque, while zero sequence harmonics do not result in significant effects because most motors are connected in a delta or ungrounded star connection.

**Table 3-1 Harmonic order sequences**

Harmonic Sequence		
Sequence	Sequence	Sequence
Positive (+)	Negative (-)	Zero (0)
Harmonic order	Harmonic order	Harmonic order
1	2	3
4	5	6
7	8	9
10	11	12
13	14	15

Harmonics are also divided into time harmonics and space harmonics, the latter being more related to motor geometry and mainly considered by design engineers. Losses caused by space harmonics result in additional losses that are usually grouped with stray load losses. Although they cannot be eliminated due to the magnetic interaction of the conductors in the slots, they can be reduced by good motor design.

The presence of positive, negative, and zero-sequence harmonics results in additional losses in each of the components, as shown in Figure 3-1. A similar scenario occurs with unbalanced voltages, as discussed in Chapter 4. The following subsections show the effects of each component.

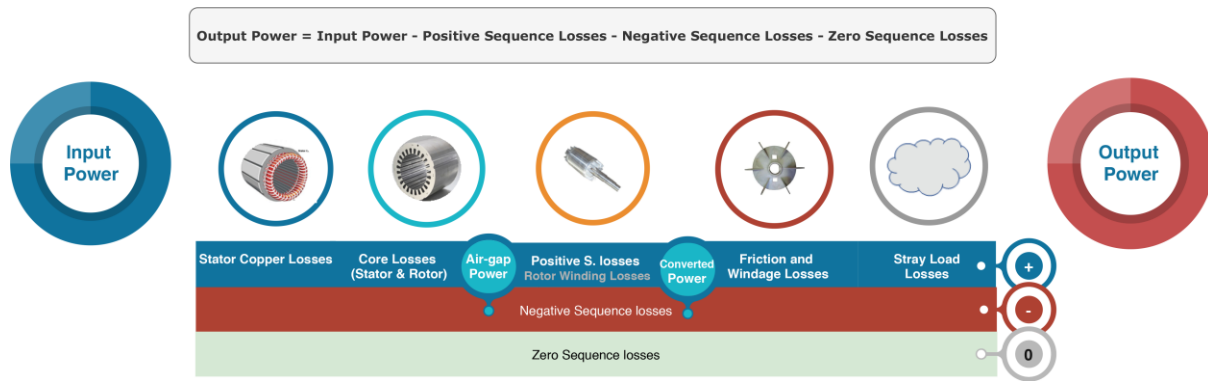


**Figure 3-1** – Additional Negative and zero sequence losses in induction motors.

As shown in Figure 3.1, the harmonic orders cause additional losses, depending on the harmonic order, the percentage present in the waveform, and the induction motor technology, as will be discussed later. Core losses will be influenced by harmonics, harmonic stresses will result in a higher induced voltage and consequently a higher magnetizing current. In [14] it is shown that for IM the magnetizing losses are a function of the magnitude of the harmonic, the order, and the phase angle of the peak induction. In [15] the authors conclude that the influence of the harmonic phase angle is similar for LSPMM and IM in terms of magnetization losses.

The increase in voltage and current due to harmonics causes additional losses in the stator and rotor windings, resulting in higher temperatures, especially in lower-power motors where copper losses account for nearly 80% of the total losses. In terms of the effect on motor torque, negative sequence harmonics produce a reverse field concerning the fundamental, resulting in reduced torque. Positive sequence components produce a forward rotating field that adds to the torque. The positive and negative sequence torque components cause vibration and reduce motor life. Zero sequence harmonics (3, 6, 9, 12) produce a stationary field, but because the harmonic field frequencies are higher, magnetic losses are increased and the harmonic energy is dissipated as heat.

### 3.4. Voltage Harmonics Impacts on IE2, IE3 and IE4 IMs classes.

#### 3.4.1. Methodology

This section analyzes the main improvements in terms of savings and performance of electric motors, presenting through experimental tests a comparison of the responses of IE2, IE3 and IE4 induction motors classes of 0.75 kW output power when subjected to harmonics present in current electrical systems, of second, third, fifth, seventh order and a combination of all in the supply voltage. Furthermore, a statistical study is presented, using correlation coefficients between the temperature and the input parameters of each motor, to analyze the behavioral patterns for the temperature increase for each of the harmonics studied. With regard to the methodology used for the treatment of the measured data and obtaining the results, Figure 3-2 presents the steps carried out during this work.

In the first step, the induction motors were subjected to nominal voltages until achieve the motors thermal equilibrium. In a second moment, the value of each voltage harmonic (2nd, 3rd, 5th, and 7th) was increased by 2% every 10 minutes until it reached 25% of voltage distortion. The motor input measurements were made with the power quality analyzer equipment as well as the thermographic images taken with the infrared camera. The input data were recorded for further processing and analysis.

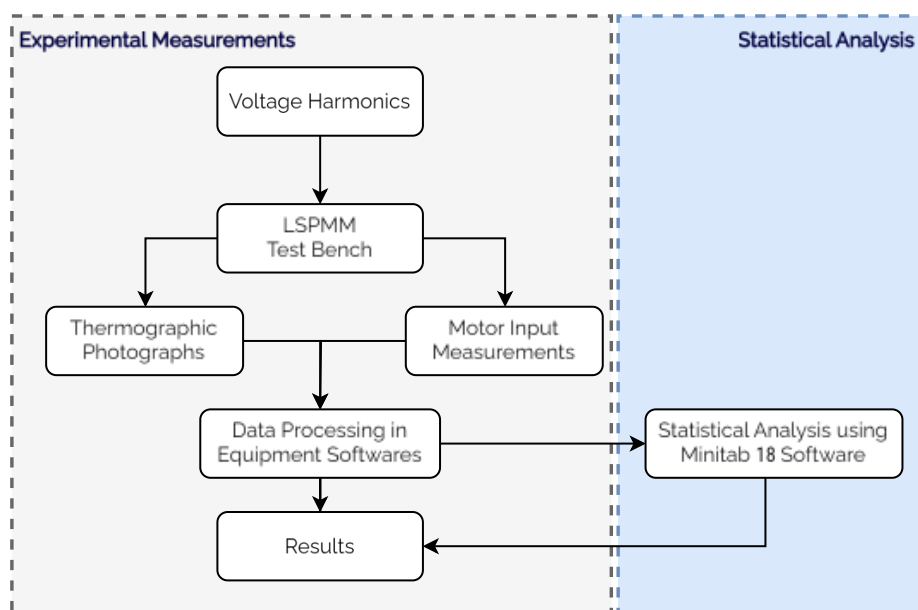


Figure 3-2 - Flowchart of methodology used to obtain the results from the measurements.



### 3.5. Technical Assessment

#### 3.5.1. Current Increase due to Harmonics

Of the three analyzed technologies, the LSPMM class IE4 had the lowest input current consumption for the same load percentage. However, the presence of voltage harmonics makes this scenario change. In Figure 3-3a–c, the increase in input current of each motor is presented in the presence of voltage harmonics. In general, it can be seen how the second voltage harmonic turns out to be the most critical of the individual harmonics, resulting in the greatest increases in the line current, then, the combination of all harmonics results in the highest current demanded, which affects strongly the IE4 class LSPMM, which reaches currents up to two times its initial value. The fifth negative sequence harmonic results in a greater increase when compared to the seventh positive sequence harmonic for the three technologies. Third voltage harmonic did not result in any impact for the IE2 and IE3 class motors, however for the IE4 class motor it showed a slight increase, showing similar values with seventh voltage harmonic.

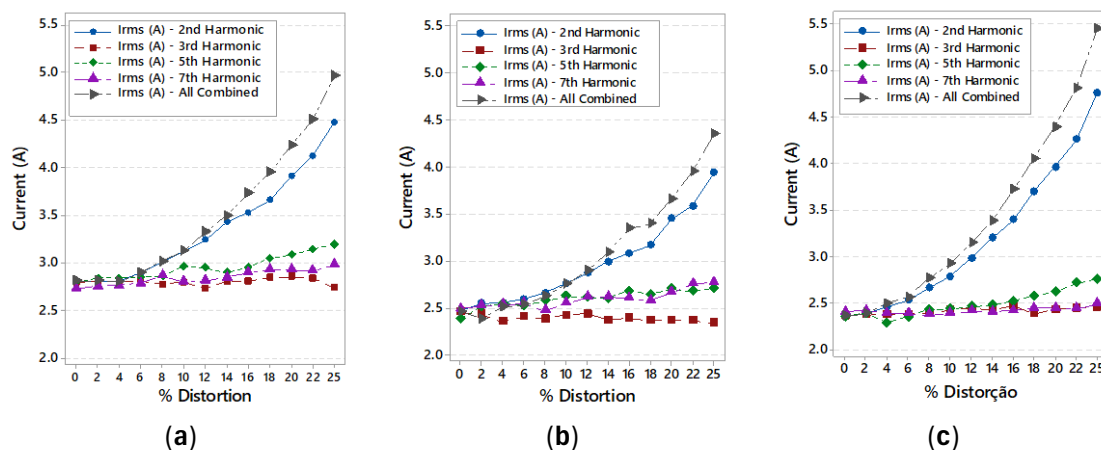


**Figure 3-3** - Current increase for 2nd, 3rd, 5th, 7th and all harmonic order combined for induction motors (a) IE2 SCIM; (b) IE3 SCIM; (c) IE4 LSPMM.

#### 3.5.2. Total Current Harmonic Distortion

Harmonic voltages produce harmonic currents, which, according to the order, percentage, and motor technology, can result in negative impacts on the operation, as well as a reduction in its useful life. In addition to the electric current, it was commented that the LSPMM total current harmonic distortion (THDI) presented values of up to four times the THDI of the other technologies.

To analyze the variation of this parameter, Figure 3-4a–c presents THDI for the IE2, IE3 and IE4 class motors. It can be seen that the fifth harmonic does not produce a considerable variation of THDI in relation to its initial value, fifth and seventh harmonics result in uniform increases for the three technologies, reaching values around 50% and 40% for 25% distortion, respectively. The second voltage harmonic turns out to be much more damaging to the LSPMM, where THDI reaches over 150% and the combination of all results in values close to 175%, well above the IE2 and IE3 class motors, which show similar increases and do not exceed 150% of THDI.

This increase is mainly due to the increase in voltage distortion for each motor, but also to the appearance of new harmonics within the waveform. It was observed that with harmonic voltage distortion percentages higher than 8%, new harmonic currents appeared. It was observed that from percentages higher than 8% of voltage distortion, new harmonic currents appeared, this will be presented in 5.4.1. In this way, with the presence of the fifth harmonic voltage, a seventh order harmonic current component appeared; while with the presence of seventh harmonic voltage, a fifth order harmonic current component appeared. With the presence of second harmonic voltage, a 4th order harmonic current component also appeared. All this contributes to the increase in THDI, occurring for all motors under study and being higher in the LSPMM due to the presence of permanent magnets.

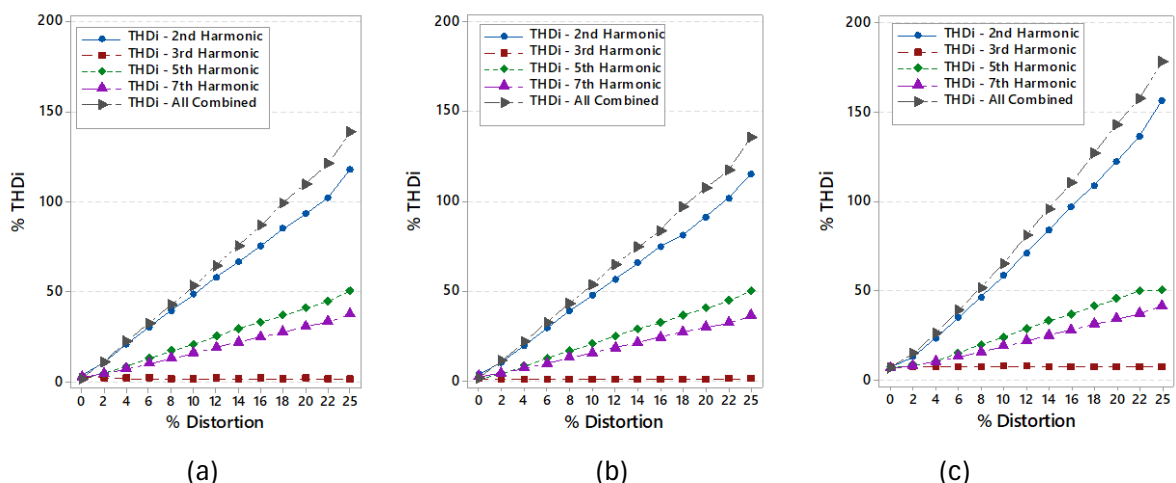


**Figure 3-4** - Total current harmonic distortion (THDI) variation for 2nd, 3rd, 5th, 7th and all harmonic order combined for induction motors (a) IE2 SCIM; (b) IE3 SCIM; (c) IE4 LSPMM.

### 3.5.3. Reactive Power and Power Factor with Voltage Harmonics

The presence of permanent magnets contributes to the reduction of the magnetization current due to the magnetic fields generated in the air gap, with which a lower reactive power consumption is expected for the LSPMM. This can be observed in Figure 3-5c, where for 0% harmonic distortion this motor has lower consumption than the IE2 and IE3 class motors (Figure 3-5a,b). The presence of voltage harmonics results in a greater reactive power consumed, which varies according to the harmonic content. It can be seen that the fifth harmonic does not represent any considerable increase in this variable then the seventh harmonic, that despite being of positive sequence results in a slight increase of reactive power, while the fifth harmonic being negative sequence results in a higher consumption. Within these harmonics the hybrid motor has lower reactive consumption, followed by the IE3 class motor, being the high efficiency motor (IE2 class) the one that consume the most reactive power from the network.

The reactive power consumption is considerably increased with the presence of a second voltage harmonic, resulting in increases of up to 10 times that experienced with the aforementioned harmonics, the LSPMM being the most affected with this voltage harmonic.

The combination of all harmonics turns out to be the most damaging, reaching 2 kvar values for the LSPMM, which will result in a low power factor for this technology, as will be presented in the following figure.

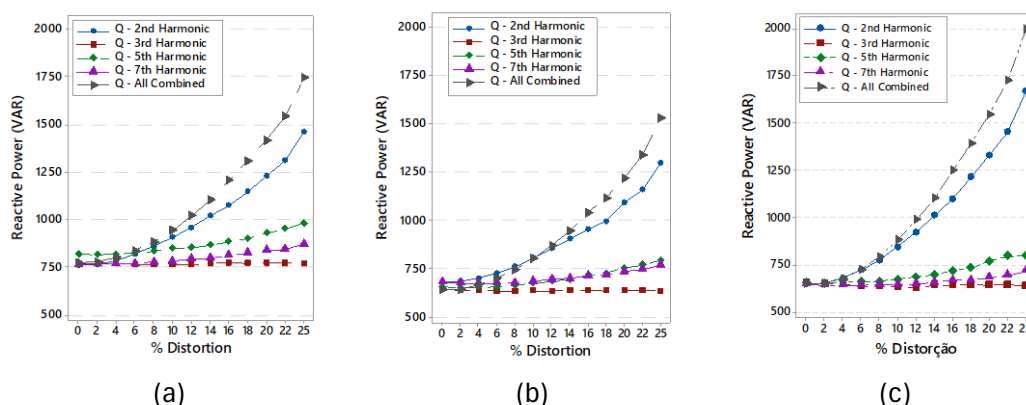


**Figure 3-5** - Reactive power increase for 2nd, 3rd, 5th, 7th and all harmonic order combined for induction motors (a) IE2 SCIM; (b) IE3 SCIM; (c) IE4 LSPMM.

Because the active power did not increase at the same rate as the reactive power, the motors suffered a decrease in their power factor. It can be seen in Figure 3-6a–c how fifth and seventh harmonics result in slight decreases in the power factor, the fifth harmonic being more

damaging, while the fifth harmonic remains varying over its initial value, except for the IE4 class hybrid motor, where it experiences a slight increase. For the second harmonic, it was already observed it produced large increases in current and reactive power, the power factor was also impacted with the presence of this harmonic, falling to values of down to 0.45 for the LSPMM, while the motor classes IE2 and IE3 have similar decreases with values close to 0.54, as presented. The presence of different combined harmonics in the supply voltage results in greatest decreases in power factor, it is observed based on the results that the presence of the second harmonic with negative sequence produces the greatest contribution in relation to the other harmonics present.

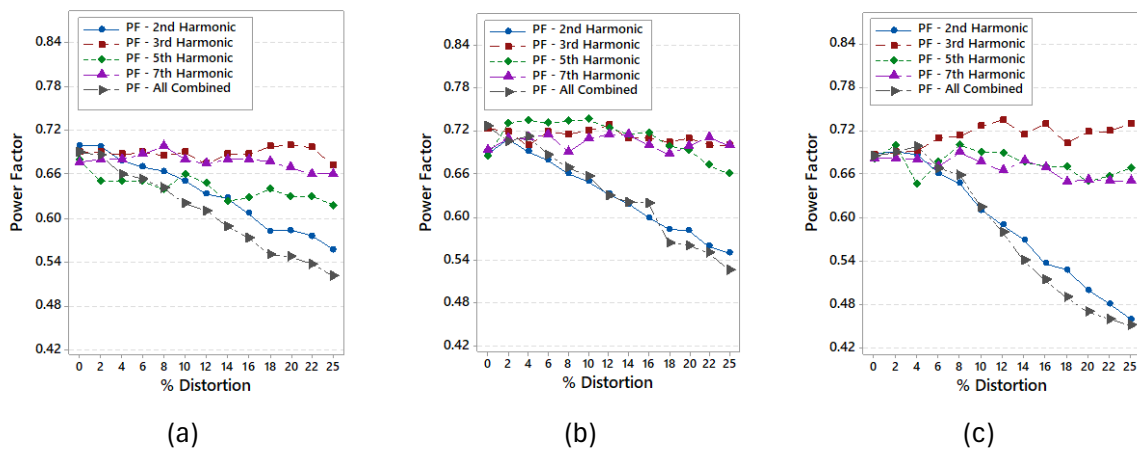


**Figure 3-6** - Power factor decrease for 2nd, 3rd, 5th, 7th and all harmonic order combined for induction motors (a) IE2 SCIM; (b) IE3 SCIM; (c) IE4 LSPMM.

### 3.5.4. Temperature Increase due to Harmonics

Harmonics result in increases in the losses experienced by each motor and these losses vary according to the percentage of load, the level and type of harmonic content in the waveform, as well as the present technology. Because these losses are manifested primarily in the form of heat, the temperature is an indication of their increase with each harmonic analyzed. This increase is presented in Figure 3-7a–c.

Initially, the motors have different operating temperatures with sinusoidal voltage without distortion, the IE3 class motor being the one with the highest operating temperature and the IE4 class motor having the lowest due to the lower operational current. The third zero sequence harmonic does not produce considerable increases in the temperature of the three IMs. Fifth and seventh harmonics result in similar increases for the three motors, however due to the higher

initial temperature, the IE3 class motor reaches values close to 48 °C. With the second voltage harmonic, the hybrid motor experiments the greatest temperature increase, reaching values of 60 °C, while the IE3 class motor has the lowest temperature increase with this harmonic. In general, the IE4 class hybrid motor is the one that is most affected by the presence of harmonics in the supply voltage, while the IE3 class motor shows a greater tolerance for this type of disturbance.

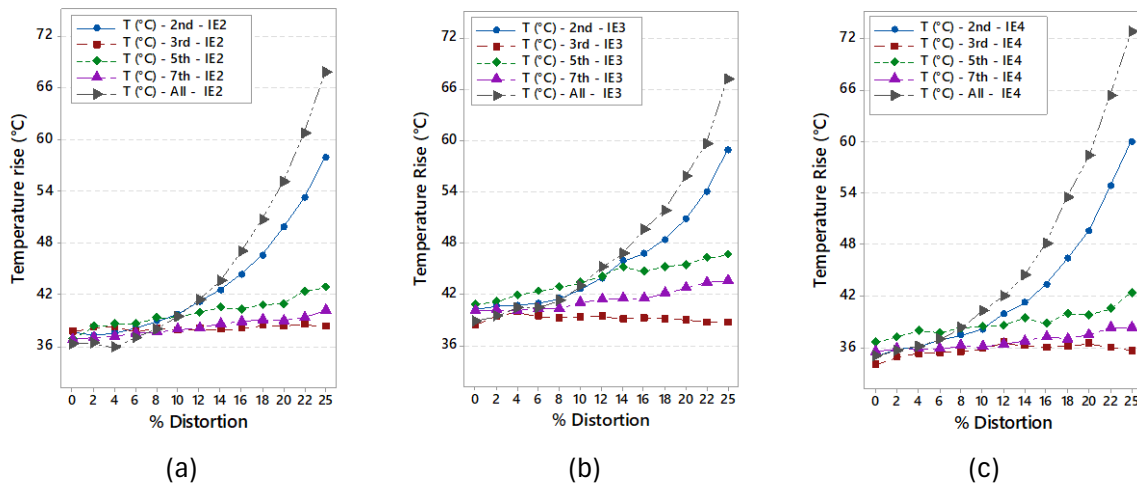


**Figure 3-7** - Temperature rise in the presence of voltage harmonics of 2nd, 3rd, 5th, 7th and all harmonic order combined for induction motors (a) IE2 SCIM; (b) IE3 SCIM; (c) IE4 LSPMM.

As it was observed in Figure 3-7, harmonics result in increases in the LSPMM input power, and this increase translates into losses due to overloads that can reduce the motor’s useful life, as well as reduce efficiency and increase consumption, which translate into higher operating costs for users. Figure 3-8 and Figure 3-9 present these losses observed in the LSPMM thermography images, for the thermal equilibrium condition without the presence of harmonics [thermograms (a) and (c)], and the same angles in the presence of 25% of 2nd and 5th order voltage harmonic distortions. The deviation produced by the negative sequence voltage harmonic disturbance is considerable and not recommended since it can degrade the insulation in the motor windings and produce internal short circuits.

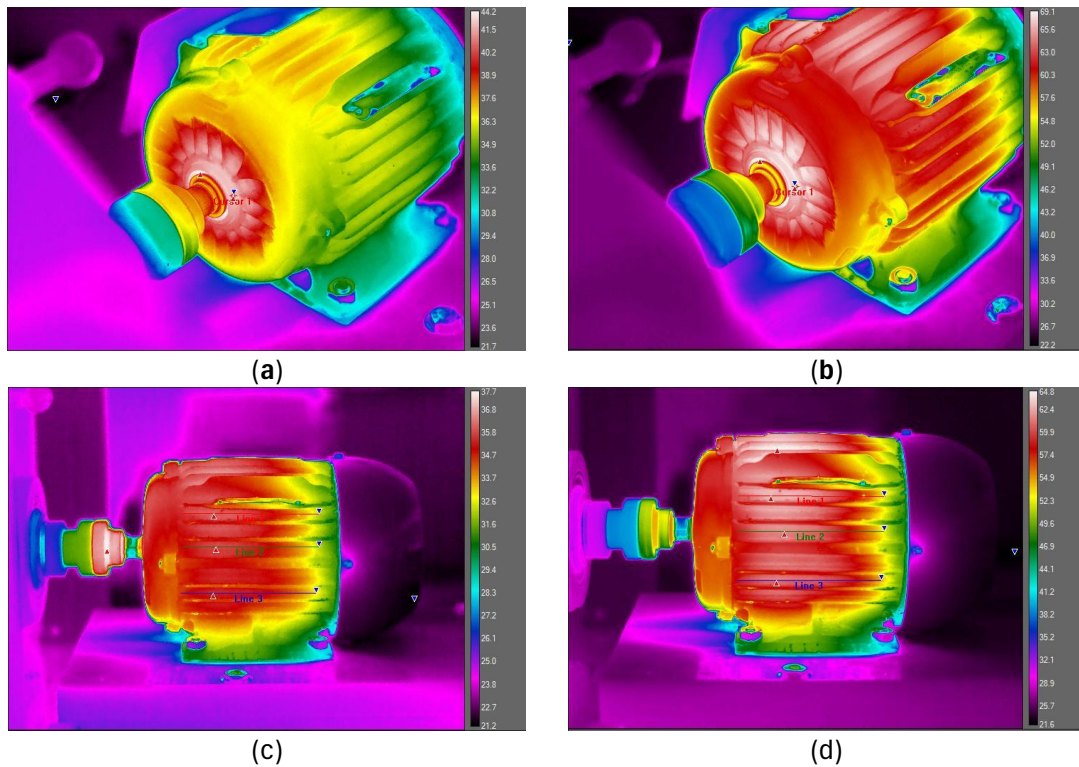


**Figure 3-8** - Thermographic images of the LSPMM in presence of 2<sup>nd</sup> voltage harmonics in frontal and lateral view (a) Thermal equilibrium frontal view; (b) 25% of 2<sup>nd</sup> voltage harmonic in frontal view; (c) Thermal equilibrium lateral view; (d) 25% of 2<sup>nd</sup> voltage harmonic in lateral view

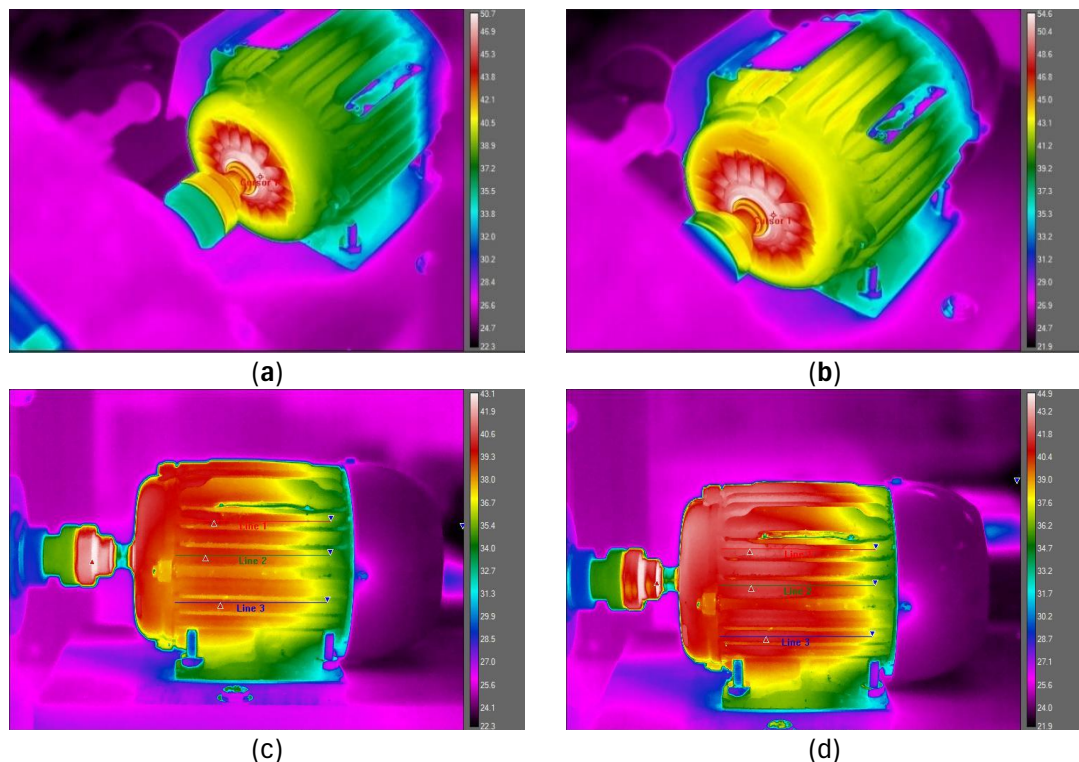


**Figure 3-9** - Thermographic images of the LSPMM in presence of 5<sup>th</sup> voltage harmonics in frontal and lateral view (a) Thermal equilibrium frontal view; (b) 25% of 5<sup>th</sup> voltage harmonic in frontal view; (c) Thermal equilibrium lateral view; (d) 25% of 5<sup>th</sup> voltage harmonic in lateral view

### 3.6. Statistical Assessment

#### 3.6.1. Correlation Matrix for Temperature

Harmonic voltages cause an increase in the line current, which results in an increase in losses and, consequently, in the motor temperature. To analyze the harmonic influence in the motor temperature, a Spearman's correlation analysis was developed in Minitab 18 [63], between the thermographic images data and the motor input parameters, in order to verify the relationship between these variables. Spearman's correlation assesses the monotonic relationship between two variables. This correlation coefficient uses only the ranks of the values and not the values themselves. Thus, this measure is suitable for both ordinal and continuous variables. It is a useful test when Pearson's correlation cannot be performed due to violations of normality, a non-linear relationship or when ordinal variables are being used [64–66]. For this case and after finding a non-linear relationship between some variables, Spearman's correlation method was used [67]. The development of the Spearman's rank correlation coefficient is presented in (2):

$$r_s = 1 - \frac{6 \sum_{i=1}^n D_i^2}{n(n^2 - 1)} \quad (2)$$

where  $n$  is the number of value pairs and  $D_i = X_i - Y_i$  is the difference between each corresponding  $X_i$  and  $Y_i$  value rank.

In general, correlation analysis results in a number between  $-1$  and  $+1$ , called the correlation coefficient. The higher the coefficient, the closer the relationship between the variables. The analysis was performed for each harmonic considered in this study. Figure 3-10-Figure 3-15 show the correlation matrices and the graphical representation between these variables for the second and third harmonic voltage in the IE2, IE3 and IE4 class motors, respectively. In the correlation matrix, the upper cell shows the Spearman coefficient while the lower cell shows the  $p$ -value, useful for rejecting the null hypothesis when compared to the significance level (0.05 assumed). In the graphical representation, the temperature variation (Y axis) versus the second and third order harmonic voltages, line current, THDI, power factor and active power (X axis) is presented.

Regression (red) and smoother lowess (green) lines are also included within the graphics to better see and explore the potential relationships between the analyzed variables.

In this way, where high correlation coefficients are obtained, the variables show similar variation patterns, while where the coefficients have values close to zero, no similar variation patterns are observed, as in the case of the third harmonic voltage. For the IE2 class motor, the second harmonic voltage is presented in Figure 3-10a and Figure 3-11a, Spearman coefficients are observed quite close to  $\pm 1$ , which indicates a high correlation between the variables present in the matrix. In addition, the  $p$ -value is zero for each second harmonic correlation in the motors, presenting lower values, compared with the level of significance ( $\alpha = 0.05$ ). This behavior is also observed for the IE3 and IE4 class motors, for which a non-linear initial growth is also observed.

A different scenario is observed for the third harmonic voltage, for which the electric motor delta-connected is an open circuit and not considerable effects are expected. In Figure 3-10b, it is observed that all parameters have low correlation values between them, especially in relation to temperature. There is practically no solid relationship between the variables, and it occurs when the relationship is random or non-existent, showing low correlation coefficients. This behavior is observed in Figure 3-11b.

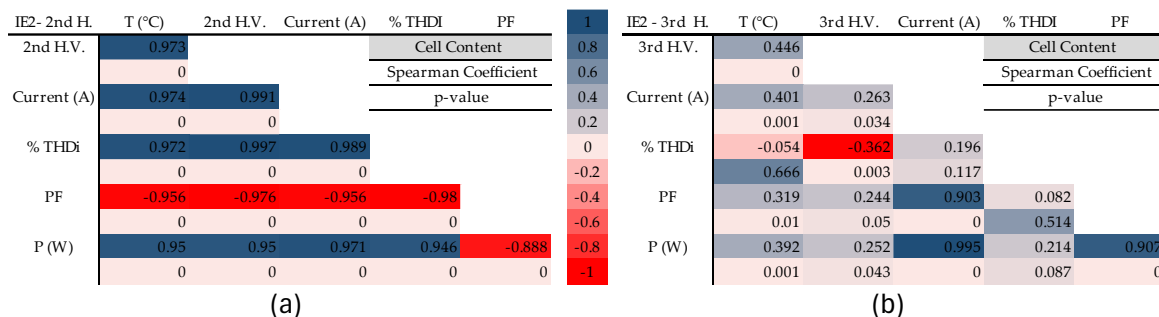


Figure 3-10 - Correlation matrix between temperature and input parameters in IE2 class SCIM for (a) second harmonic voltage distortion; (b) third harmonic voltage distortion.

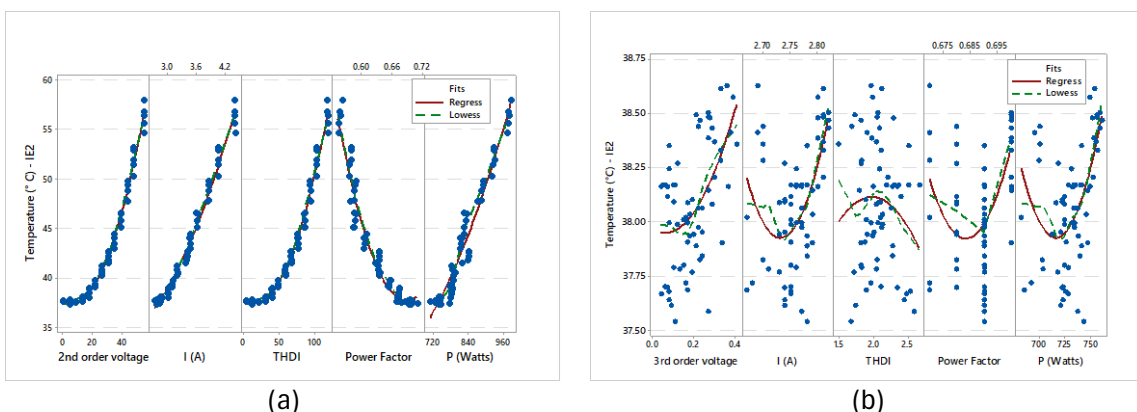


Figure 3-11 - Temperature regression versus motor input parameters for IE2 class SCIM with voltage distortion of (a) 2nd harmonic voltage distortion; (b) 3rd harmonic voltage distortion.



It is observed for the second harmonic voltage that, in relation to the temperature, all variables have high correlation values, which indicates that when one of them increases, the temperature also does. Among the other variables analyzed, it is observed that high correlation values are also observed, with which the co-linearity must be analyzed when creating models involving these variables. The only variable that varied during the experiment was the voltage distortion, which as mentioned increased in percentages of two until reaching 25%.

For the IE3 class motor, Figure 3-12b and Figure 3-13b, the third harmonic has similar results compared to the IE2 class motor, presenting low correlation values, and in this case the  $p$ -value is greater than the significance value for some correlations, with which it is not possible to reject the null hypothesis, so it is not possible to state that there is a relationship between the variables in question.

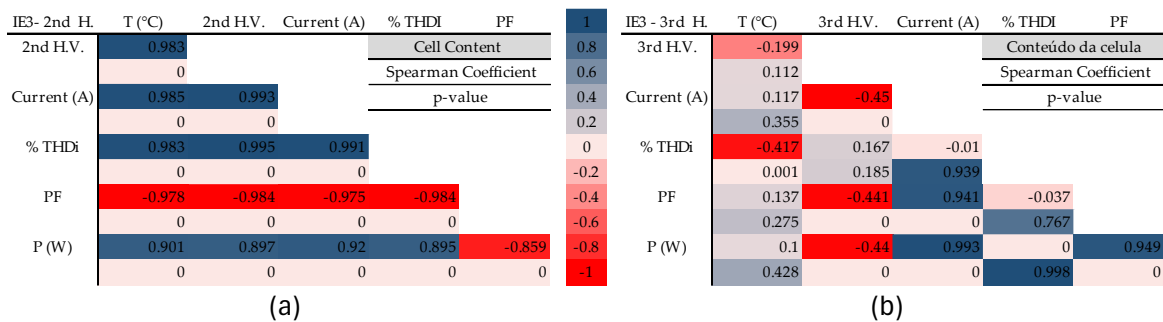


Figure 3-12 - Correlation matrix between temperature and input parameters in IE3 class SCIM for (a) second harmonic voltage distortion; (b) third harmonic voltage distortion.

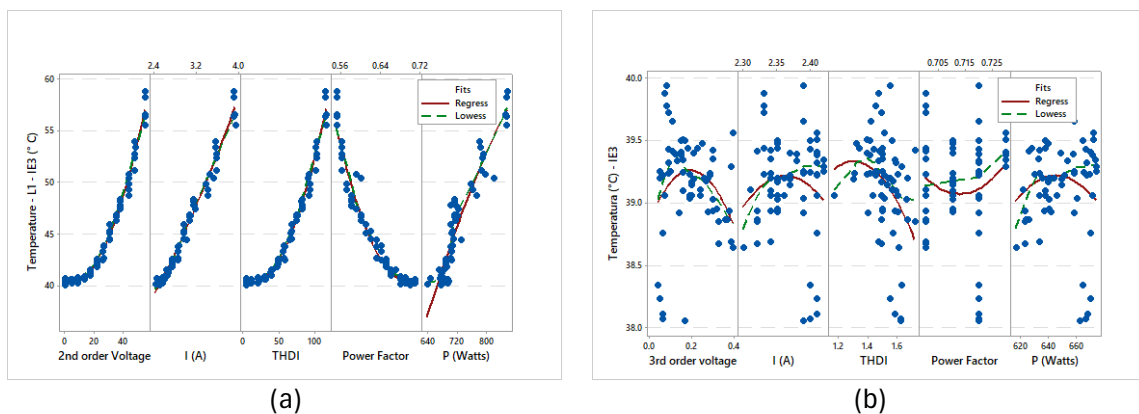


Figure 3-13 - Temperature regression versus motor input parameters for IE3 class SCIM with voltage distortion of (a) 2nd harmonic voltage distortion; (b) 3rd harmonic voltage distortion.

Third harmonic voltage shows different results for the IE4 LSPMM, shown in Figure 3-14b and Figure 3-15b. Higher correlation coefficients can be observed for the LSPMM, but not as strong as those obtained for the second harmonic voltage. The  $p$ -value also remains below 0.05 among most of the variables, as shown. In general, with the second negative sequence

harmonic, the temperature has a defined growth pattern from its initial temperature for the three analyzed induction motors, being lower for the LSPMM, to a temperature close to 60 °C for the three technologies. For the third zero sequence harmonic, the temperature varies around its initial value for the entire experiment. This scenario is different for the LSPMM where, despite showing a lower correlation, a growth pattern is observed in Figure b.

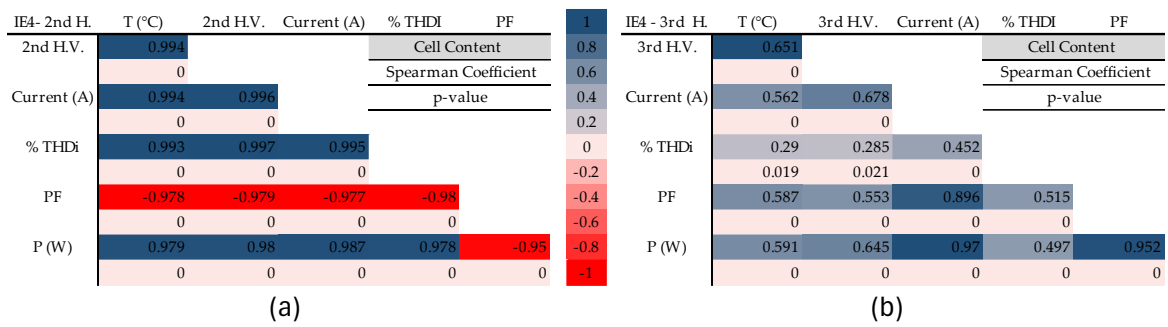


Figure 3-14 - Correlation matrix between temperature and input parameters in IE4 class LSPMM for (a) second harmonic voltage distortion; (b) third harmonic voltage distortion.

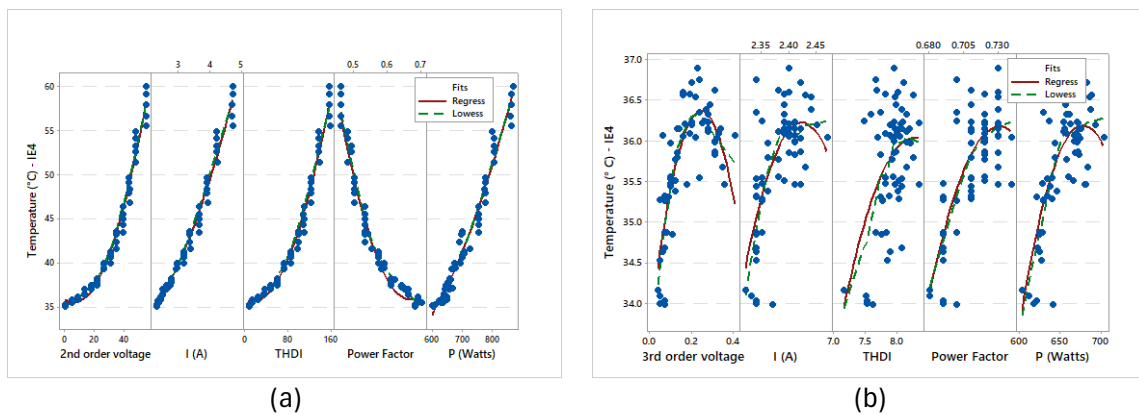


Figure 3-15 - Temperature regression versus motor input parameters for IE4 class LSPMM with voltage distortion of (a) 2nd harmonic voltage distortion; (b) 3rd harmonic voltage distortion.

### 3.6.2. Temperature Models for Voltage Harmonics Impacts on Temperature

In the results presented above, it is possible to observe how the parameters present certain patterns of behavior that vary according to the harmonic analyzed. Based on this, an analysis of the data was developed in order to create models that represent the behavior of the temperature in relation to the harmonics present in the supply voltage for the three low powers analyzed in this study. To analyze the influence of these additional harmonics on the temperature of each technology, the multiple regression of the Minitab software [16] was used, which fits linear and quadratic models with up to five predictor variables and one continuous variable using least squares estimation in a step-by-step procedure.

To perform the analysis, the LSPMM IE4 class is considered with the presence of 2nd order voltage distortions. The side temperature of the motor presented in Figure 1.5a is used as a predictive variable and its increase is presented in Figure 3-7c and as predictive variables, the voltage distortions of 1st  $U_1(1)$ , 2nd  $U_1(2)$ , 4th  $U_1(4)$ , 5th  $U_1(5)$  and 7th  $U_1(7)$  order were considered due to the presence of harmonic current in the sinusoidal wave analyzed in the last section. Equation (3) presents the model to represent the temperature rise for the IE4 LSPMM in the presence of 2nd order voltage distortion.

$$T(^{\circ}C) = 32.32 - 0.092U_2 + 2.06U_2 + 7.8U_5 + 0.0093U_2^2 - 0.1036U_2U_4 - 32.6U_3U_5 \quad (3)$$

where  $U_2$ ,  $U_3$ ,  $U_4$  and  $U_5$  are the 2nd, 4th, 5th and 7th order voltage distortion, respectively.

The adjusted coefficient of determination (adjusted R<sup>2</sup>), which indicates what proportion of the total variation of the Y response is explained by the adjusted model, can be used to check the model's adequacy. With the model presented in (3), an adjusted R<sup>2</sup> = 0.9859 is obtained, also the p-value is less than 0.05, which makes it possible to reject the null hypothesis and confirm that there is a relationship between these variables. To analyze the incremental impact that each harmonic voltage brings to the model, the increase in the adjusted R<sup>2</sup> with each predictor variable is presented in Figure 3-16a. Although the 4th, 5th and 7th order voltage distortions are present in the waveform and equation model, they do not contribute significantly to the fit of the model, with the 2nd harmonic distortion being the one that best represents the temperature increase for each distortion percentage, as shown in Figure 3.14b.

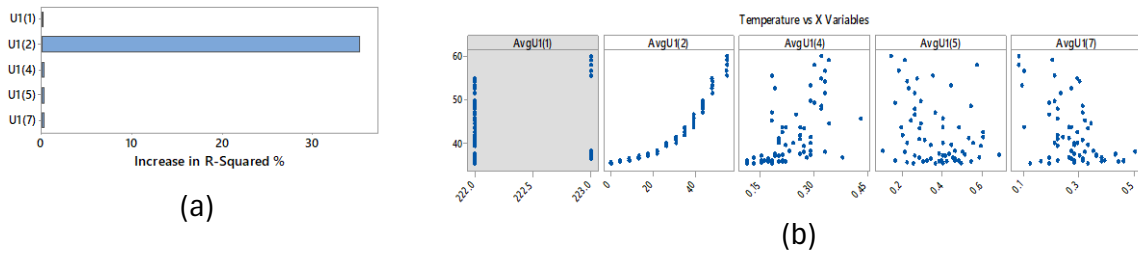


**Figure 3-16** Incremental Impact of Voltage distortion on Temperature: (a) Long bars represents a predictor that contribute the newest information to the model; (b) Predictors used in the model (a gray background represents an X variable not in the model).

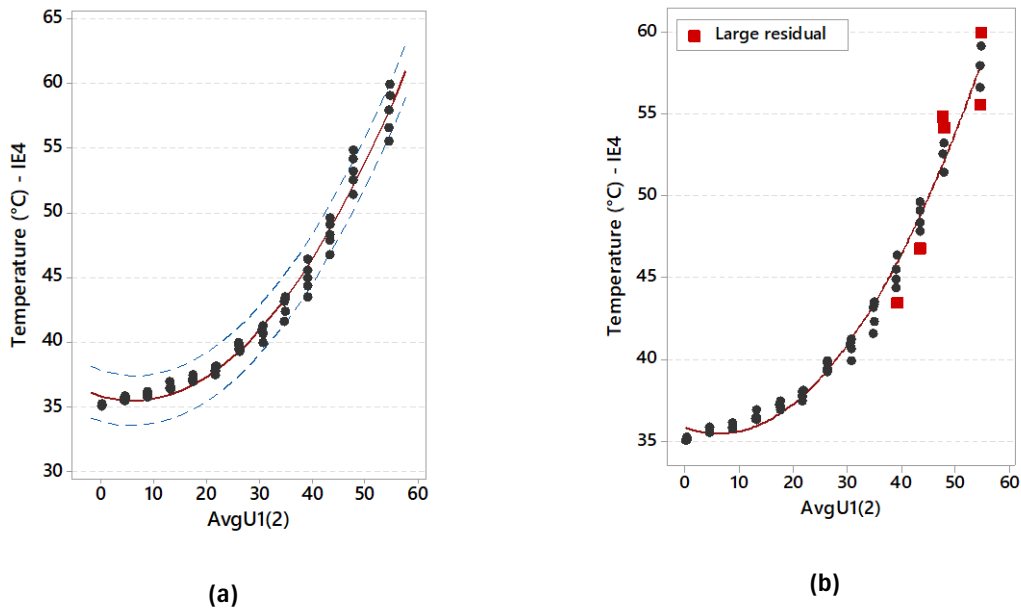
Based on the above, it is possible to reduce the equation of the generated model for temperature by considering only the second harmonic voltage distortion without a significant reduction in the value of the adjusted  $R^2$ . The equation of the resulting model when considering only the 2nd harmonic voltage as a predictor variable for temperature is shown in (3).

$$T (^{\circ}C) = 35.84 - 0.1199U_2 + 0.009547U_2^2 \quad (3)$$

Where  $U_2$  is the 2nd order voltage distortion.

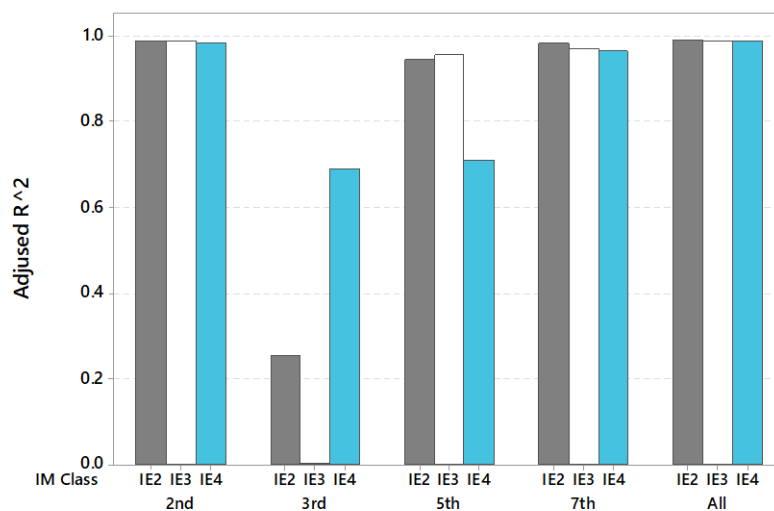
For the model presented in (3), an adjusted  $R^2 = 0.9822$  is obtained, also with a p-value less than 0.05. The reduction of the predictor variables causes a reduction of the terms of the equation for the temperature model, but also a reduction of the adjusted value of  $R^2$ , but the model represents in a perfectly acceptable way the increase of the temperature for each increase of the second harmonic voltage distortion.

Figure 3-17a shows the prediction curve of the IE4 LSPMM for the 2nd order voltage distortion, where the red fitted line shows the predicted temperature for each 2nd order voltage distortion and the blue dashed lines show the 95% prediction interval. In Figure 3-17b, the same curve is shown with large residuals in red, these points are not well fitted by the model, this is due to the fact that the temperature experienced higher  $\Delta T$ 's mainly for the larger percentages of distortion, with the sample points suffering large deviations with respect to the regression line as the actual distortion increases.



**Figure 3-17** – Temperature as a function of 2<sup>nd</sup> voltage harmonic: (a) Prediction plot for Temperature model with 95% of prediction interval; (b) Prediction plot with large residual versus the fitted values.

This analysis was performed to create the temperature vs. voltage distortion models for each harmonic analyzed as long as it did not imply a reduction in the model fit. Figure 3-18 shows the adjusted R<sup>2</sup> values for each of the models that were created, and Table 3-2 shows the results of the models that were created. It can be seen that the LSPMM presents quadratic models for all the harmonics analyzed except for the 5th order harmonic voltage, for which an adjusted R<sup>2</sup> of 0.71 and a Spearman correlation coefficient of 0.84 are obtained. In addition, among the three efficiency classes, the LSPMM is the only one that has an incremental pattern for the 3rd harmonic, for which the model reaches an R<sup>2</sup>=0.6893.



**Figure 3-18** - Adjusted coefficient of determination (adjusted R<sup>2</sup>) for generated models presented in Table 2.

**Table 3-2** - Summary of temperature models for voltage harmonics in IMs classes IE2, IE3 and IE4.

Harmonic order	IM Class	Equation Model	Adjusted R <sup>2</sup>
2 <sup>nd</sup>	IE2	$T(^{\circ}C) = 37.77 - 0.1052 X_2 + 0.008128 X_2^2$	98.94%
	IE3	$T(^{\circ}C) = 40.38 - 0.05692 X_2 + 0.006554 X_2^2$	98.69%
	IE4	$T(^{\circ}C) = 35.84 - 0.1199 X_2 + 0.009547 X_2^2$	98.27%
3 <sup>rd</sup>	IE2	$T(^{\circ}C) = 37.81 + 1.424 X_3$	25.54%
	IE3	$T(^{\circ}C) = 38.9 + 0.5120 X_3$	0.48%
	IE4	$T(^{\circ}C) = 33.60 + 22.21 X_3 - 44.58 X_3^2$	68.93%
5 <sup>th</sup>	IE2	$T(^{\circ}C) = 37.43 + 0.0965 X_5$	94.55%
	IE3	$T(^{\circ}C) = 41.11 + 0.1105 X_5$	95.57%
	IE4	$T(^{\circ}C) = 37.12 + 0.07724 X_5$	71%
7 <sup>th</sup>	IE2	$T(^{\circ}C) = 38.94 + 0.06673 X_7$	98.23%
	IE3	$T(^{\circ}C) = 42.40 + 0.02418 X_7 + 0.001114 X_7^2$	97.21%
	IE4	$T(^{\circ}C) = 39.74 + 0.02029 X_7 + 0.000862 X_7^2$	96.49%
All Combined	IE2	$T(^{\circ}C) = 38.55 + 1.88 X_2 - 8.2 X_4 - 2.24 X_5 - 0.038 X_2^2 + 0.056 X_5^2 + 0.35 X_4 X_5$	99.15%
	IE3	$T(^{\circ}C) = 39.147 - 0.0654 X_2 + 0.009538 X_2^2$	98.79%
	IE4	$T(^{\circ}C) = 36.361 + 2.65 X_2 - 3.03 X_5 + 0.1077 * X_5^2 - 0.0861 X_2 X_5$	98.83%

\* Where  $X_2, X_3, X_4, X_5$  and  $X_7$  represent the 2<sup>nd</sup>, 3<sup>rd</sup>, 4<sup>th</sup>, 5<sup>th</sup> and 7<sup>th</sup> order voltage harmonics.

Also, it has been shown that the third voltage harmonic does not have a significant effect on the electric motors, which is also observed in the models obtained, where values lower than 0.26 were obtained for the IE2 and IE3 class motors, from which it can be concluded that these models do not represent the temperature variation in an acceptable way for this specific harmonic.

For the combination of all harmonics, a multiple regression was performed with all harmonics present in the waveform. For the IE3 IM class, it is observed that only the 2nd order voltage harmonic is present, which means that it has the greatest impact on the temperature variation for this combination of harmonics. In the presence of harmonics in the supply voltage, new current harmonics appeared in the wave form of the input current. Therefore, for this combination of harmonics, the 4th positive sequence harmonic, which is part of the predictive variables for IE2 and IE4 class motors as shown, has been considered for the three efficiency classes.

### 3.7. Finite Element Thermal Validation of the LSPMM in VH presence

For the LSPMM modelling and simulation, initially the problem was defined in the software FEMM, with information such as frequency and depth, since the software presents a 2D visualization, however the problem solution is based on the 3D dimension. After defining the problem, the geometry is inserted, created from the physical dimensions of the motor (rotor diameter, number of slots, air gap distance, etc.). For this study, the complete motor was considered, to better visualize the paths of flux lines in each harmonic distortion condition. The materials were inserted based on the materials obtained from manufacturer information for the motor analyzed (Figure 3-19a).

The boundary conditions, useful to help direct the motor response in the simulation (magnetic flux response, current response, etc.) are also defined during the motor modelling step, then the mesh is created and refined until a constant response is obtained (Figure 3-19b), finally the simulation is performed, and from which the results presented in this section are obtained.

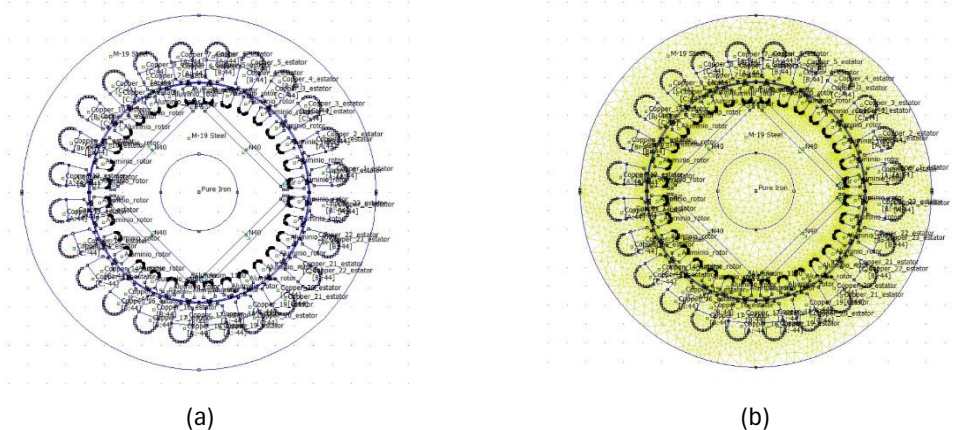


**Figure 3-19** - Line-start permanent magnet motor simulation on FEMM:(a) LSPMM geometry and materials and (b) LSPMM mesh.

The presence of voltage harmonics results in additional harmonic currents, which induce harmonic voltages in the rotor bars that produce harmonic currents circulating in the rotor squirrel cage. These additional harmonic components produce additional magnetic fields that result in opposite torques, which are translated into a reduction in speed for asynchronous electric motors. Figure 3-20 presents the magnetic field lines in the LSPMM in nominal conditions (Figure 3-20a), 2nd voltage harmonic (Figure 3-20b), and 5th voltage harmonic (Figure 3-20c) created using the FEMM software and the data obtained from the experiments

performed. It can be seen how the harmonics result in a larger number of flux lines, observed through the magnetic field density, but also, it is important to note how the trajectory of the flux lines changes with the presence of harmonics, with special focus on the 2nd harmonic flux lines that present longer trajectories, which in turn translates into higher reluctance and consequently higher magnetic losses. However, the LSPMM speed does not vary for any of the analyzed harmonics, which does not mean that the harmonics do not impact other variables such as consumption, temperature, and power factor.

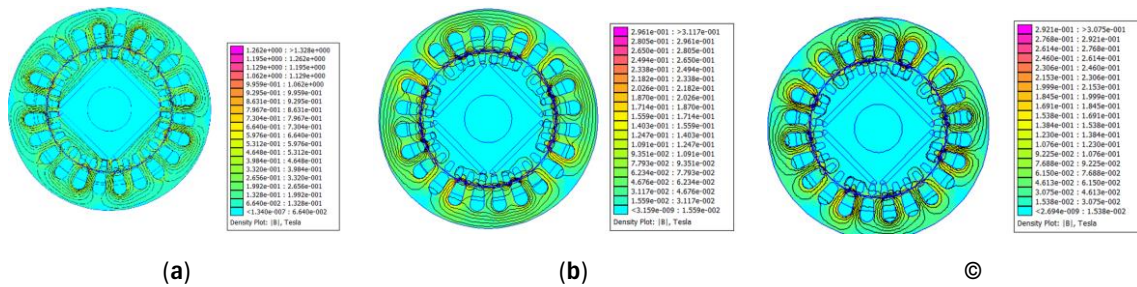


**Figure 3-20** - Density flux plot for (a) Nominal conditions; (b) 2nd voltage harmonics and (c) 5th voltage harmonics.

The objective of using the finite element analysis is to make a thorough diagnosis of the motor electromagnetic behavior using a method that is non-invasive and has no interference with the operation of the motor being analyzed. Using this method, it was possible to extract the resistive losses in the stator armature as well as the torque via the Weighted Stress Tensor method [21]. These simulations are done, considering the motor is operating at no-load, with only the fault brakes which in this case are neglected. To perform the thermal analysis, FEMM solves the problem around the transient temperature model. From that, it is possible to obtain the temperature and gradient values of the temperature model.).

In order to account for temperature exchange with the air, we apply the convection boundary condition. Here we define the thermal transfer coefficient for the inner parts as well as the exterior part of the motor from the parameters used in reference [22], and adjusted based on the motor output power, given that the one considered in this study presented a lower power (0.75 kW). For the exterior part of the frame, the coefficient was 30 W/m<sup>2</sup> °C. As for the inner parts of the motor, the air gap and cooling air vents the coefficient is higher at 65 W/m<sup>2</sup> °C in this case, the gaps between the stator/rotor armature and coil ends were not considered as their value is negligible. Figure 3-21 illustrates the areas where these boundary conditions were applied.



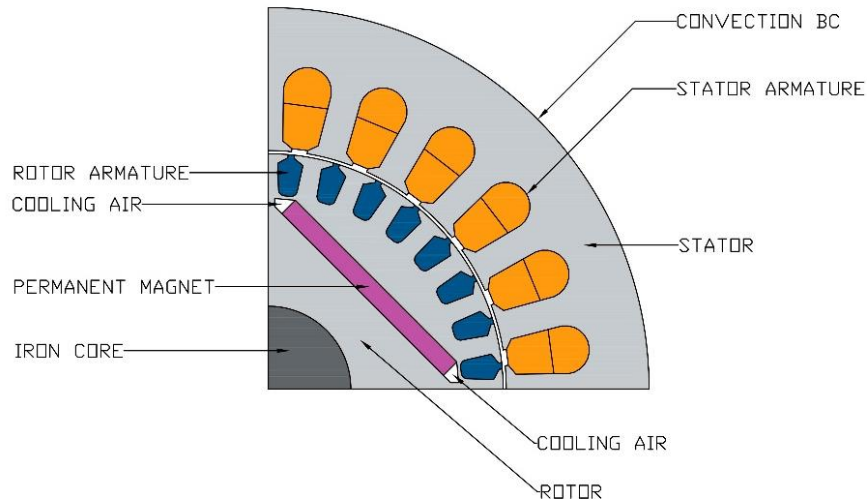


**Figure 3-21** - Quarter section of motor illustrating the areas with convection boundary conditions.

The temperature distribution in the motor at full load for each voltage harmonic is presented in Figure 3-22. For the second voltage harmonic (Figure 3-22a) it is observed how the rotor presents the higher temperatures, which, despite the synchronism (zero slip), can be justified by the second harmonic component configured at the motor input, as well as the new harmonics that appear as a result of the saturation in the ferromagnetic core. Regarding the 5th harmonic, (Figure 3-22b) a similar pattern is observed, however with lower temperatures, which shows that this harmonic is less detrimental to the LSPMM.

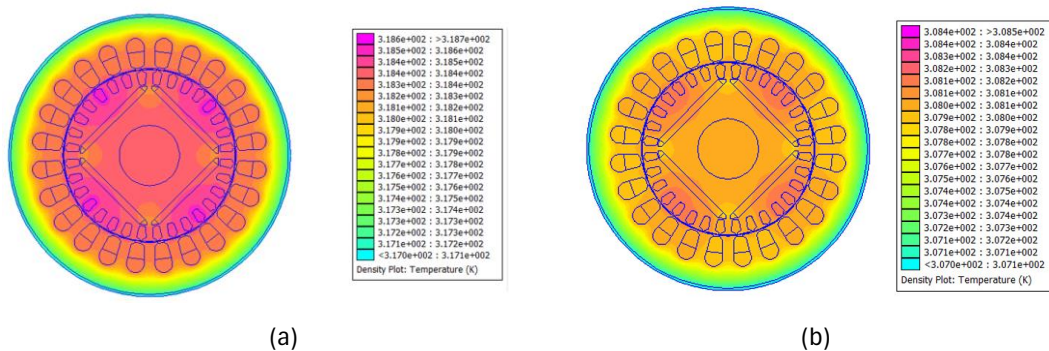


**Figure 3-22** - Temperature distribution (in Kelvin) in the motor from the FEMM thermal simulation for: (a) Second Voltage Harmonic and (b) Fifth Voltage Harmonic.

Analogous to the experiment results, the harmonic analysis was carried out for the simulation. Figure 3-23 shows the LSPMM lateral temperature as simulated in FEMM with 25% of voltage harmonic and its comparison with the experimentally measured temperature in the lateral view of Figure 1.5a. It should however be noted that there is a big discrepancy due to the number of elements in the mesh, as well as not having considered the influence of the permanent magnets-magnetization being affected.

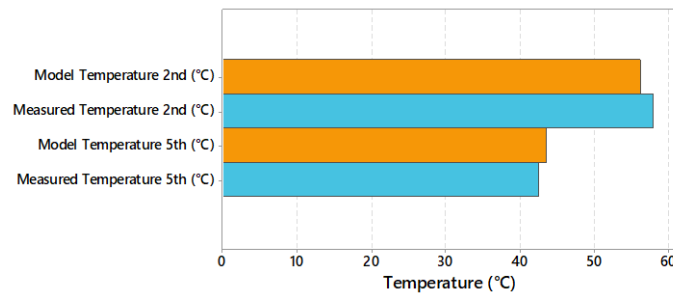


**Figure 3-23** - Comparison between the model and measured temperature for 25% voltage harmonic distortion of 2nd and 5th order harmonics.

Based on the results obtained from the computational simulation, as well as from the experimental measurements, errors of 6.3% and 2.8% for the 2nd and 5th harmonics, respectively, were found, which validates the model proposed in this work on the Line-start permanent magnet motor.

### 3.8. Final Considerations

This chapter has evaluated the main effects of the harmonic voltage on low power electric motors of IE2, IE3 and IE4 classes. In general, it has been observed that negative sequence harmonics (2nd and 5th order) have a greater negative impact on each of the motors analyzed, followed by positive sequence harmonics (7th order). The zero-sequence harmonics of the 3rd order did not have a significant negative effect on the IMs, mainly due to the motor connection (delta connection). This behavior was validated by Spearman correlation matrices of the temperature with respect to the input parameters of the motors.

A statistical analysis was also carried out with the aim of creating models representing the variation of temperature as a function of the current harmonic, first with multiple regression and later using only the current harmonic voltage. Good approximations were obtained through the R2 parameter for the harmonics analyzed, with the exception of the zero-sequence 3rd harmonic, mainly due to the delta connection of the electric motors. Based on the above, the models can be used to estimate the temperature increase based on the harmonic present for the analyzed power. The line-start permanent magnet motor has also been analyzed experimentally and through computational simulations using FEMM. The computational simulation showed that the developed model reliably represents the performance of the motor under non-ideal conditions, such as in the presence of the negative sequence voltage harmonic. The analysis of another detrimental disturbance present in electrical systems, such as voltage unbalance in more efficient motors, will be discussed in Chapter 4, below.

### 3.9. Chapter Bibliography

- [1] L. A. Kumar and S. A. Alexander, *Computational Paradigm Techniques for Enhancing Electric Power Quality*. CRC Press, 2018.
- [2] A. Eigeles Emanuel, “Harmonics in the early years of electrical engineering: a brief review of events, people and documents,” in *Ninth International Conference on Harmonics and Quality of Power. Proceedings (Cat. No.00EX441)*, Oct. 2000, pp. 1–7 vol.1. doi: 10.1109/ICHQP.2000.896990.
- [3] “Gaiser, Terry. ‘Understanding Harmonics’, Western Energy Institute, 2018.” Accessed: May 15, 2020. [Online]. Available: [https://uploads.westernenergy.org/2019/08/16075249/Tab-17-Harmonics-Demonstration-Fluke\\_Gaiser.pdf](https://uploads.westernenergy.org/2019/08/16075249/Tab-17-Harmonics-Demonstration-Fluke_Gaiser.pdf)
- [4] “519-2014 - IEEE Recommended Practice and Requirements for Harmonic Control in Electric Power Systems.” Accessed: May 15, 2020. [Online]. Available: <https://standards.ieee.org/standard/519-2014.html>
- [5] “IEC 61000-3:2020 SER | IEC Webstore.” Accessed: May 15, 2020. [Online]. Available: <https://webstore.iec.ch/publication/62426>
- [6] “IEC 61000-2-4:2002 | IEC Webstore | electromagnetic compatibility, EMC, smart city.” Accessed: May 15, 2020. [Online]. Available: <https://webstore.iec.ch/publication/4135>
- [7] “National Electric Energy Agency - ANEEL.” Accessed: Apr. 04, 2020. [Online]. Available: <https://www.aneel.gov.br/>
- [8] “PRODIST – Módulo 8 – Qualidade da Energia Elétrica - ANEEL.” Accessed: May 15, 2020. [Online]. Available: <http://app.aneel.gov.br/modulo-8>
- [9] F. J. T. E. Ferreira, G. Baoming, and A. T. de Almeida, “Reliability and Operation of High-Efficiency Induction Motors,” *IEEE Transactions on Industry Applications*, vol. 52, no. 6, pp. 4628–4637, Nov. 2016, doi: 10.1109/TIA.2016.2600677.
- [10] “IEEE Recommended Practice for Monitoring Electric Power Quality,” *IEEE Std 1159-1995*, pp. i-, 1995, doi: 10.1109/IEEESTD.1995.79050.
- [11] C. Debruyne, L. Vandeveld, and J. Desmet, “Harmonic effects on Induction and Line Start Permanent Magnet Machines,” in *International Conference on Energy Efficiency in Motor Driven Systems (EEMODS 2013)*, Rio de Janeiro, RJ, Brazil, Oct. 2013.
- [12] E. C. de Lima, J. M. de C. Filho, and J. S. de Sá, “Diagnosis of induction motors operating under distorted and unbalanced voltages,” in *2016 17th International Conference on Harmonics and Quality of Power (ICHQP)*, Oct. 2016, pp. 786–791. doi: 10.1109/ICHQP.2016.7783368.
- [13] E. F. Fuchs, D. J. Roesler, and M. A. S. Masoum, “Are harmonic recommendations according to IEEE and IEC too restrictive?,” *IEEE Transactions on Power Delivery*, vol. 19, no. 4, pp. 1775–1786, Oct. 2004, doi: 10.1109/TPWRD.2003.822538.
- [14] C. Debruyne, J. Desmet, S. Derammelaere, and L. Vandeveld, “Derating factors for direct online induction machines when supplied with voltage harmonics: A critical view,” in *2011 IEEE International Electric Machines Drives Conference (IEMDC)*, May 2011, pp. 1048–1052. doi: 10.1109/IEMDC.2011.5994745.
- [15] C. Debruyne, J. Desmet, B. Vervish, S. Derammelaere, and L. Vandeveld, “Influence of harmonic voltage distortion on asynchronous generators,” in *8th IEEE Symposium on Diagnostics for Electrical Machines, Power Electronics Drives*, Sep. 2011, pp. 159–164. doi: 10.1109/DEMPED.2011.6063618.
- [16] “Minitab 18 Statistical Software (2010). [Computer software]. State College, PA: Minitab, Inc. (www.minitab.com).” Accessed: Aug. 15, 2019. [Online]. Available: <https://www.minitab.com/es-mx/>
- [17] C. Heumann and Shalabh, Michael Schomaker, *Introduction to Statistics and Data Analysis With Exercises, Solutions and Applications in R /*, 1st ed. Gewerbestrasse 11, 6330 Cham, Switzerland: Springer International Publishing AG, 2016. [Online]. Available: 10.1007/978-3-319-46162-5
- [18] G. G. de O. Costa, *Probabilidades e Estatísticas Inferencial: Teoria e Prática*, 2nd Edition. Brazil: EDITORA ATLAS S.A., 2018. Accessed: Jun. 16, 2020. [Online]. Available:

- <https://www.institutodeengenharia.org.br/site/2018/07/25/livro-curso-de-probabilidades-e-estatisticas-inferencial-teoria-e-pratica/>
- [19] “Spearman’s Rank-Order Correlation - A guide to when to use it, what it does and what the assumptions are.” Accessed: Jun. 16, 2020. [Online]. Available: <https://statistics.laerd.com/statistical-guides/spearmans-rank-order-correlation-statistical-guide.php>
- [20] Minitab, 2018, “A comparison of the Pearson and Spearman correlation methods,” Minitab 18, Support. [Online]. Available: <https://support.minitab.com/en-us/minitab/18/help-and-how-to/statistics/basic-statistics/supporting-topics/correlation-and-covariance/a-comparison-of-the-pearson-and-spearman-correlation-methods/#comparison-of-pearson-and-spearman-coefficients>
- [21] S. Saha and Y. Cho, “Starting Characteristic Analysis of LSPM for Pumping System Considering Demagnetization,” *undefined*, 2015, Accessed: Mar. 16, 2022. [Online]. Available: <https://www.semanticscholar.org/paper/Starting-Characteristic-Analysis-of-LSPM-for-System-Saha-Cho/26294607254e76bf172d45825973f83ac4b7cbb9>
- [22] M. F. Palangar, “Design, analysis and optimization of line-start permanent-magnet synchronous motors: simultaneous electromagnetic and thermal analysis.” Accessed: Nov. 01, 2022. [Online]. Available: <https://theses.flinders.edu.au/view/8616886a-3b6f-4c97-a9d0-95452aa86a65/1>

## Chapter 4

# Voltage Unbalance Impacts on Efficient Electric Motors

Voltage unbalance (VU) is a phenomenon present in all electrical systems. The National Electrical Manufacturers Association (NEMA) [32] recommends derating motors above this percentage because of the numerous negative effects that are visible at unbalances greater than 1%. This chapter presents a detailed analysis of the effect of different percentages of under and over-voltage unbalance on the temperature and performance of IE2, IE3, and IE4 class electric motors.

### 4.1. General Considerations

Voltage unbalance (VU) is a phenomenon that occurs in all electrical systems. A report by the American National Standards Institute [1], estimates that only 66% of electrical distribution systems in the United States have a VU of less than 1%. In addition, VU often occurs with voltage variations, resulting in variations in efficiency and power factor, as well as increased losses and consequently temperature of electric motors. Prolonged operation under these conditions can shorten the useful life of the motor [2, p. 1]. According to the National Electrical Manufacturers Association (NEMA)[3], unbalance exceeding 1% requires derating of the motor.

Voltage unbalance can occur in industry due to the uneven distribution and operation of single-phase loads, in distribution due to the operation of open delta transformer connections and uneven phase distribution throughout the electrical system, and in transmission systems due to the incomplete transposition of transmission lines [4], [5].

Considering the negative impact of VU on IMs and the new perspective that promotes the substitution of old and inefficient electric motors with high-efficiency motors, it is necessary to compare the performance of these new technologies in the presence of power system disturbances. Based on this, this chapter starts with the allowable limits related to this disturbance as well as a brief analysis of its impact on the IMs. Finally, through experimental tests, the temperature and power response of IE2, IE3, and IE4 classes of electric motors with 0.75 kW output power in the presence of different unbalanced voltages will be analyzed.

## 4.2. Voltage Unbalance Definitions

The nominal characteristics of electric motors are specified according to defined operating conditions, such as nominal voltage frequency, and operating altitude, among others. Limits have been defined for the correct operation of electric motors due to the wide range of voltages and frequencies, as well as the different disturbances present in electrical systems. Different standards have defined the maximum permissible limits of this phenomenon due to the numerous damages that VU represents in IMs. Currently, there are four definitions of voltage unbalance, defined by NEMA, IEEE, CIGRÉ, and IEC [3], [6], [7], each with different considerations. The NEMA definition is also known as the Line Voltage Unbalance Rate (LVUR) and is given by the equation (1):

$$LVUR (\%) = \frac{\Delta V_L^{Max}}{V_L^{Avg}} \quad (1)$$

where:

$$V_L^{Avg} = \frac{V_{ab} + V_{bc} + V_{ca}}{3}$$

$$\Delta V_L^{max} = \max \{ |V_{ab} - V_L^{avg}|, |V_{bc} - V_L^{avg}|, |V_{ca} - V_L^{avg}| \}$$

According to NEMA recommendations, to avoid overheating, the three-phase motor must be reduced depending on the degree of unbalance under such operating conditions. The value by which the power must be reduced is called the "power derating factor". The derating curve is shown in Figure 4-1. According to NEMA, continuous operation of the motor above 5% is not recommended.

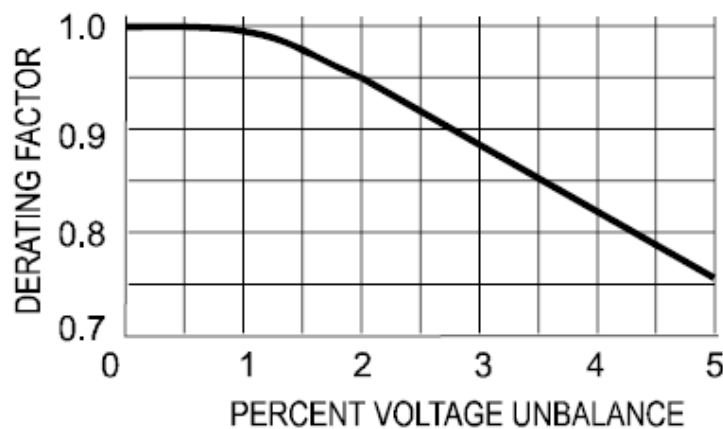


Figure 4-1 - Power derating curve for Induction Motors

In addition to the LVUR defined by NEMA, another method is the Voltage Unbalance Factor (VUF), also known as the IEC "true" definition, based on the relative magnitudes of the negative and positive sequences, shown in (2). The IEEE 1159 [6] definition of voltage unbalance is through the phase voltage unbalance rate (PVUR), as shown in (2), although the latest edition of this standard, also lists the VUF, the IEC.

$$VUF (\%) = k_v = \frac{|V_N|}{|V_P|} \quad (2)$$

where:

$$V_P = \frac{V_a + aV_b + a^2V_c}{3} \quad (2.1)$$

$$V_N = \frac{V_a + a^2V_b + aV_c}{3} \quad (2.2)$$

$$a = 1\angle 120^\circ \quad \& \quad a^2 = 1\angle 240^\circ$$

The IEEE definition is commonly referred to as the Phase Voltage Unbalance Rate (PVUR) and is described in terms of the line-to-ground voltages  $V_a$ ,  $V_b$ , and  $V_c$  as presented in (3):

$$PVUR (\%) = \frac{\Delta V_P^{Max}}{V_P^{Avg}} \quad (3)$$

where:

$$V_P^{Avg} = \frac{V_a + V_b + V_c}{3}$$

$$\Delta V_P^{max} = \max \{ |V_a - V_P^{avg}|, |V_b - V_P^{avg}|, |V_c - V_P^{avg}| \}$$

Since the LVUR definition of the NEMA standard is a simple method of obtaining the degree of unbalance in practice, it has been considered for this work.

#### 4.2.1. Complex Voltage Unbalance Factor (CVUF)

The Complex Voltage Unbalance Factor (CVUF) is an extension of the VUF, originally proposed by Wang [8], [9], and is similar to the VUF; the difference is that the angles are included in addition to the amplitudes of  $V_1$  and  $V_2$  or ( $V_n$  and  $V_p$ ), as shown in (4):

$$CVUF (\%) = k_v \angle \theta_v = \frac{|V_N| \angle \theta_n}{|V_P| \angle \theta_p} = VUF \angle (\theta_n - \theta_p) \quad (4)$$

where  $|V_N| \angle \theta_n$  and  $|V_P| \angle \theta_p$  are the magnitude and angle of the positive and negative sequence voltage and are calculated according to equations (2.1) and (2.2).

According to Wang [9], the use of both magnitude and angle must be considered to provide a global picture of the effect of voltage unbalance on motor operation. Many other studies, including [4], [10], [11], [12], have also considered the CVUF to analyze the effects of VU on electric motors. The current unbalanced factor can also be calculated in the same way as the VUF, as shown in equation (5).

$$CUF (\%) = k_c = \frac{|I_N|}{|I_P|} = \frac{V_N/Z_N}{V_P/Z_P} = \frac{Z_P}{Z_N} k_v \quad (5)$$

From equation (8) it can be concluded that the CUF is directly proportional to the VUF, in addition, it can be seen how the relationship between  $Z_P/Z_N$  is the sensitivity of the CUF concerning the VUF, according to the literature the current unbalance varies between 6-10 times the voltage unbalance, this is mainly because the positive sequence impedance of the induction motor is much greater than the negative sequence impedance. The complex current unbalance (CCUF) can be obtained through the equation (6), as follows:

$$CCUF (\%) = k_c = k_c \angle \theta_c = \frac{I_N}{I_P} = \frac{Z_P}{Z_N} k_v \angle (\theta_v + \varphi_p - \varphi_n) \quad (6)$$

where  $(\theta_v + \varphi_p - \varphi_n)$  is the angle of the CCUF.



### 4.2.2. Complex Voltage Unbalance Factor (CVUF) Diagram

The NEMA standard LVUR is one of the most widely used because of the difficulty of calculating positive and negative sequence voltages in practice due to the inclusion of complex numbers. However, other alternatives can be used, such as the X-Y graph shown in Figure 4-2. The Y-axis is the relationship between the line voltages  $V_{ca}/V_{ab}$ , while the X-axis is the relationship between the line voltages  $V_{bc}/V_{ab}$ .

For instance, if a meter measurement shows:  $V_{ab} = 220V$ ,  $V_{bc} = 220V$  and  $V_{ca} = 231V$ , the voltage ratios can easily be obtained, as  $X = 1.0$  and  $Y = 1.05$ . It will be found quickly in Figure 4-2 that  $k_v$  is 3.45% and the angle equals  $210^\circ$ . Practically, if we only want the VUF and not the angle, we can eliminate the radial lines that represent the angle.

In the graph it also can be seen how for the same percentage of VUF we can have different magnitudes, for example for a  $k_v = 7\%$ , the voltages can vary from about 0.89 p.u. up to 1.13 p.u., which suggests that the value of  $\theta_v$  must also be considered to more accurately account for the unbalance [13].

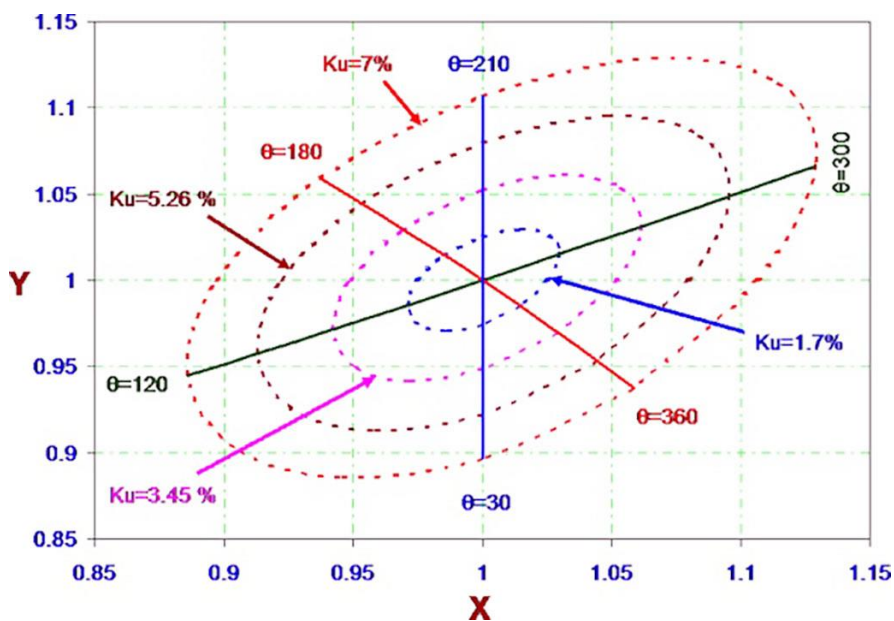


Figure 4-2 - The Complex Voltage Unbalance Factor Diagram [13].

### 4.3. Voltage Variation (VV) and Voltage Unbalance (VU) Basics

Two of the most frequent voltage disturbances in electrical systems are voltage variation and voltage unbalance. It can also exist voltage variations with over or under voltages, in addition to this problem, voltages in electrical systems are never balanced, although it is often small enough to have no impact negative on induction motors, in some cases, due to the configuration of the distribution systems and the unbalance of the single-phase loads within the industries, these percentages may be higher and a reduction in the power of the machine must be necessary to avoid affecting its useful life.

**Long-duration root-mean-square (rms) variation:** A variation of the rms value of the voltage or current from the nominal for a time greater than 1 min. The term is usually further described using a modifier indicating the magnitude of a voltage variation (e.g., undervoltage, overvoltage, voltage interruption). **Imbalance (voltage or current):** The ratio of the negative sequence component to the positive sequence component, usually expressed as a percentage. Syn: unbalance (voltage or current)

The life of electric motors can be shortened by the voltage variations and unbalance associated with a low maintenance program. In Figure 3-19a, an electric motor found in a coffee plant in Honduras, Central America, it is possible to observe how the dirt present in the environment prevents the transfer of heat from the internal components to the environment, resulting in higher temperatures inside the machine. Figure 3-19b also shows the voltage measurement at the machine, where the nominal line voltage of 240 V represents an unbalance of 4.11% according to the NEMA definition.

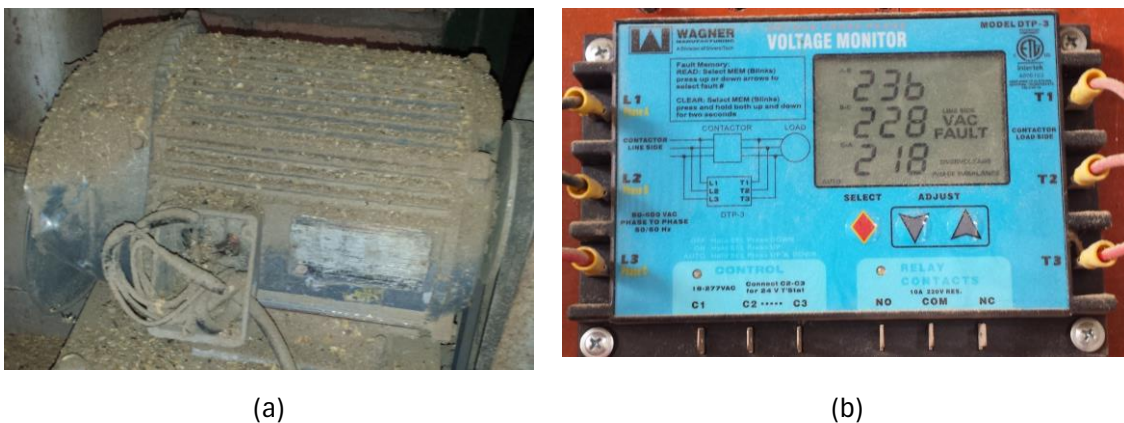


**Figure 4-3** - Induction motor subjected to voltage unbalance: (a) Induction motor with a low maintenance program, (b) Input voltage magnitudes in induction motor terminals.

### 4.3.1. Voltage Unbalance Analysis

Voltage unbalance in the motor supply has large negative effects depending on the degree of unbalance. To analyze this phenomenon, Figure 4-4 shows a graphical representation of the voltage unbalance with a supply of unbalanced voltages in the input of a motor with a delta connection. The presence of voltage unbalance results in three main components: positive, negative, and zero. Since most motors are connected in a delta or ungrounded wye, there is no path to the neutral for the zero-sequence components to flow. From there, the two resulting components (positive and negative) produce different effects, one contributing to the resulting torque, while the second produces opposite magnetic fields, resulting in greater oscillations, and speed reduction as a result of lower torque [14].

The presence of voltage unbalance (VU) also results in unbalanced currents in the stator windings, typically 6 to 10 times the unbalance of the voltages, which causes the winding to overheat [15], [16]. The positive sequence component also has a detrimental effect on the machine windings: Compared to nominal power conditions, a 5% increase in the positive sequence voltage causes an increase in motor temperature of approximately 12% above the reference value, as shown in [17].

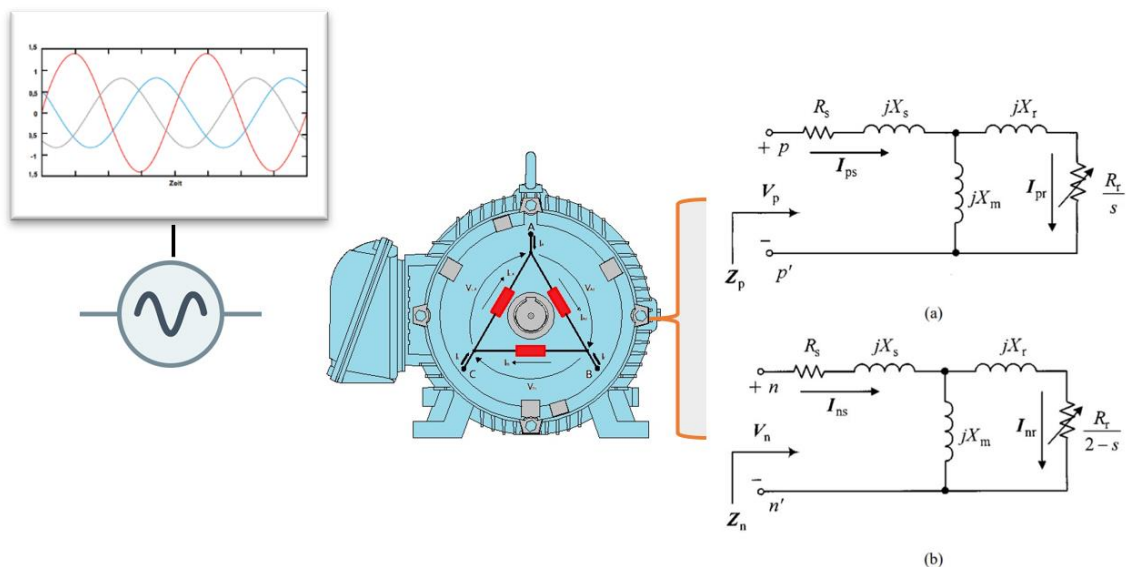


**Figure 4-4** - Voltage Unbalance supply on a delta-connected IM and the resulting positive (a) and negative (b) sequence components [9].

To better analyze this fact, we can see at Figure 4-5. The voltages at the input of the electric motor are given by:

$$\begin{aligned}\bar{V}_{AB} &= \bar{V}_{AN} - \bar{V}_{BN} \\ \bar{V}_{BC} &= \bar{V}_{BN} - \bar{V}_{CN} \\ \bar{V}_{CA} &= \bar{V}_{CN} - \bar{V}_{AN}\end{aligned}\tag{7}$$

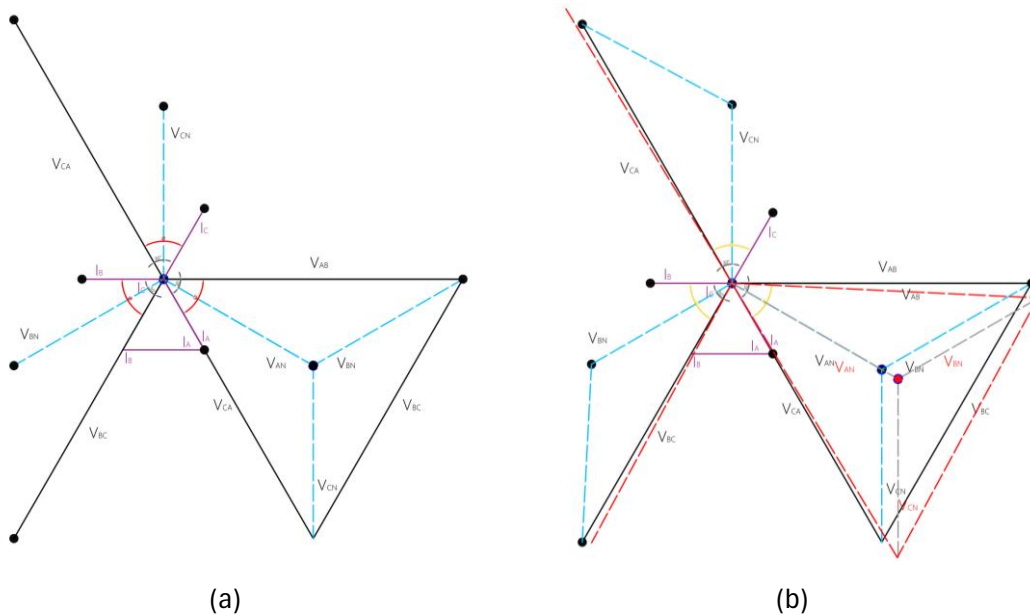


**Figure 4-5** - Induction motor voltages when subjected to voltage unbalance (a) Balanced voltage phasors; (b) Unbalanced voltage phasors.

The phase voltages, shown as blue lines, are 120° out of phase. The phase sum of the components gives the line voltages, as presented in (5). When added together, it is observed that the line voltages are  $\sqrt{3}$  times the phase voltages and are also 30° ahead. Within the same diagram, the currents are observed to be out of phase with the line voltages at a  $\phi$  angle corresponding to the power factor of the load, in this case assumed to be 60°.

In Figure 4-5a, where the sum of both voltages and currents is zero under equilibrium conditions, you can see the inverted triangle formed by the phasor sum of the phase and line voltages. As mentioned, voltage unbalance can be caused by several factors, including unbalanced phase voltages due to unevenly distributed phase loads. The unbalanced phase voltages in Figure 4-5b have been plotted to analyze this fact. It can be seen that the phase unbalance causes variations in both the magnitude and the angle of the line voltages. This results in a phase shift of the triangle, as shown by the red lines.

Figure 4-4 shows how the presence of the VUF results in two components of positive and negative sequence (ignoring the zero-sequence component due to the motor connection). To analyze this condition, the VUF concept is examined as follows. From equation (2) we have that:

$$VUF (\%) = k_v = \frac{V_N}{V_P}$$

The currents in the positive and negative sequences can be calculated using the Ohm's law between the voltages and impedances in the positive and negative sequences, as shown in (8.1-2).

$$I_P = \frac{V_P}{Z_P} \quad (8.1)$$

$$I_N = \frac{V_N}{Z_n} \quad (8.2)$$

As shown in (9), the line currents are the sum of the positive and negative sequence components:

$$\begin{aligned} \bar{I}_A &= \bar{I}_P + \bar{I}_N \\ \bar{I}_B &= a^2 \bar{I}_P + a \bar{I}_N \\ \bar{I}_C &= a \bar{I}_P + a^2 \bar{I}_N \end{aligned} \quad (9)$$

The stator currents are the respective sum of the positive and negative sequence components, as noted in (9). In addition, these parameters depend on the positive and negative sequence voltages and impedances, respectively, as observed in (8.1) and (8.2).

In a motor with balanced voltages, there is only one positive sequence component, so the presence of voltage unbalance is a condition in which the negative and zero sequence components affect the positive sequence component. In delta-connected motors, the main cause of the unbalance is the negative sequence component. It was also observed in (5) that the relationship  $Z_P/Z_N$  represents the variation of the current unbalance with respect to the voltage unbalance. In order to analyze the voltage unbalance and to compare it with the true definition, six conditions considering undervoltage and overvoltage were inserted in the IE2, IE3 and IE4 class motors. The phase voltages and the degree of unbalance according to the NEMA definition are shown in Table 4-1.

It is interesting to analyze the response of each technology to the different disturbances present in the power system, considering the evolution that electric motors have undergone in recent years in terms of materials and construction. In this sense, Table 4-2 to Table 4-4 show the variation of the positive-negative and zero-sequence voltages, currents and impedances for

the motors of the IE2, IE3 and IE4 classes analyzed in this study when they are subjected to the six VU conditions presented in Table 4-1.

**Table 4-1** Phase-voltage magnitudes IM with under and overvoltage.

Va (V)	Vb (V)	Vc (V)	NEMA VU%
127	127	127	0
117.6	107.48	127.98	1.29%
120.77	128.34	116.74	2.98%
121.62	126.50	123.96	4.33%
124.66	127	129.05	1.1%
129.90	139.30	127.10	2.95%
140.85	119.15	131.38	4%

As observed in Table 4-2 through Table 4-4, the positive sequence voltage varies with the magnitude of the voltage, i.e., it decreases with undervoltage and increases with overvoltage. The negative sequence component, on the other hand, increases with voltage unbalance, regardless of whether it is undervoltage or overvoltage. In addition to the motor supply voltages, the positive and negative sequence currents depend on the positive and negative sequence impedances generated within the motor. Although the negative current values under unbalanced conditions are not zero, the significance is minimal, so they are shown as such in the table, along with the impedance values. The positive-sequence impedance is much greater than the negative-sequence impedance, and it can be seen that with only 3% of the positive-sequence voltage, the negative-sequence voltage can produce up to 33% of the positive-sequence current in the negative-sequence current. This indicates the sensitivity of the motor to the negative sequence component. The current unbalance percentages (CUF) vary from 7 times the VU, up to 17 times for this output power analyzed (0.75 kW). It is also observed that the IE4 class LSPMM has higher current unbalances in case of undervoltage. This will be analyzed in detail throughout this chapter.

**Table 4-2** Voltage Unbalance Parameters for IE2 Class IM with under and overvoltage

V1 (V)	V2 (V)	I1 (A)	I2 (A)	Z1 ( $\Omega$ )	Z2 ( $\Omega$ )	VUF	CUF	NEMA
128	0.38	3	0	64	0	0.3%	0	0
125	1.80	3	0	41.67	0	1.44%	0	1.29%
123	3.73	3	1	41	3.73	3.03%	33.33%	2.98%
119	5.64	3	1	39.67	5.64	4.74%	33.33%	4.33%
128	1.43	3	0	42.67	0	1.12%	0	1.1%
133	4.03	3	1	44.33	4.03	3.03%	33.33%	2.95%
132	5.97	3	1	44	5.97	4.52%	33.33%	4%

**Table 4-3.** Voltage Unbalance Parameters for IE3 Class IM with under and overvoltage

V1 (V)	V2 (V)	I1 (A)	I2 (A)	Z1 (Ω)	Z2(Ω)	VUF	CUF	NEMA
128	0.38	2	0	64	0	0.3%	0	0
125	1.82	3	0	41.67	0	1.46%	0	1.29%
123	3.73	3	1	41	3.73	3.03%	33.33%	2.98%
119	5.69	3	1	39.67	5.69	4.78%	33.33%	4.33%
128	1.5	2.	0	64	0	1.17%	0	1.1%
133	3.99	2	1	66..5	3.99	3.00%	50%	2.95%
132	5.97	3	1	44	5.97	4.52%	33.33%	4%

**Table 4-4** Voltage Unbalance Parameters for IE4 Class LSPMM with under and overvoltage

V1 (V)	V2 (V)	I1 (A)	I2 (A)	Z1 (Ω)	Z2(Ω)	VUF	CUF	NEMA
128	0.41	2	0	64	0	0.3%	0	0
125	1.80	2	0	62.5	0	1.44%	0	1.29%
123	3.75	2	1	61.5	3.75	3.04%	50%	2.98%
119	5.69	2	1	59.5	5.69	4.78%	50%	4.33%
128	1.45	2.	0	64	0	1.13%	0	1.1%
133	4	3	1	44.3	4.00	3.00%	33.33%	2.95%
132	5.98	3	1	44	5.98	4.53%	33.33%	4%

From the values shown in Table 4-2 to Table 4-4, it can be seen that the NEMA definition maintains the same unbalance for each motor, while the IEC "true definition" based on positive and negative sequence voltages varies by IM, showing more sensitivity to different technologies. In this sense, Figure 4-6a and b show the variation of the positive and negative sequence impedance for the IE2, IE3 and IE4 class motors analyzed in this study. A greater variation of the positive sequence impedance is observed mainly for the IE3 and IE4 class motors. The negative sequence impedance, on the other hand, shows no variation between the technologies, except for the 1% VU with undervoltage for the IE4 class LSPMM, as shown in Figure 4-6b. The results show how the impedance of the LSPMM differs from the analyzed SCIMs due to the presence of permanent magnets in the rotor.

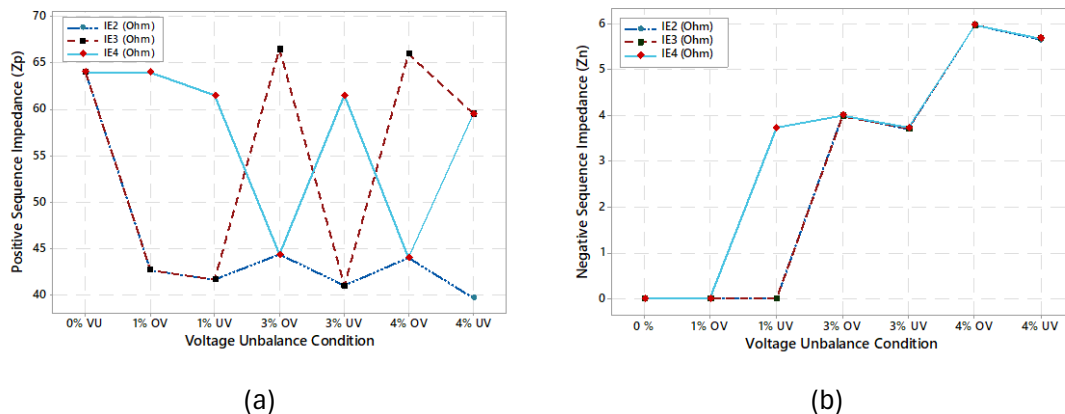


**Figure 4-6** – Positive and negative sequences for impedances (Ohms) for IE2 , IE3 and IE4 Class motors(a) Positive sequence and (b) Negative sequence.

#### 4.4. Assessing Voltage Unbalance Conditions in IE2, IE3 & IE4 classes IMs.

##### 4.4.1. Methodology

Figure 4-7 illustrates the methodology used to process the measured data and obtain the results. First, the six-voltage unbalance condition was applied to the supply voltage of each of the motors analyzed on the test bench, and then the measurements were taken with the power quality analyzer equipment and the images were taken with the infrared camera. The next step was to transfer the measurement data from the equipment to the analyzer (HIOKI) and camera (FLIR T620) software. After data analysis, they were converted into CSV format files compatible for reading in Minitab (Minitab 18) statistical software [18]. Minitab was used to analyze the data processed for plotting the results and statistical analysis of the study.

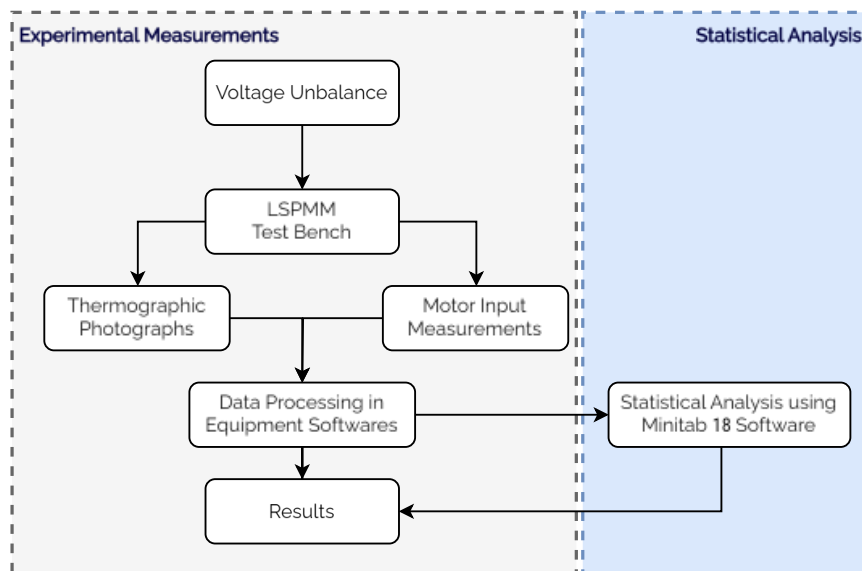


Figure 4-7 - Flowchart of methodology used to obtain the results from the measurements.

#### 4.5. Technical Analysis

##### 4.5.1. Current Behaviour

Voltage unbalance in the supply voltage results in greater unbalance in the line current, and the magnetization current also varies proportionally with the magnitude of the voltage. However, in the LSPMM, the induced voltage also depends on the magnetization current generated due to the MMF created in the permanent magnets [19], so the induced voltage varies less with the variation of the supply voltage.



In this way, the average current varies with the magnitude of the supply voltage for the LSPMM. Figure 4-8 shows the phase current variation for the IE4 class motor in the six VU conditions, and Figure 3-3 shows the average current variation for the IE2, IE3 and IE4 class motors. Unbalance with under and over voltage results in unbalanced currents of up to 10 times the existing VU for the analyzed conditions. Some conclusions are related to the observed currents: VU with under voltage results in higher phase currents in relation to over voltage in the IE2 and IE3 SCIM's, and the average current with both under voltage and over voltage shows an increase in relation to the initial one.

For the LSPMM VU with under voltage results in decreases in phase currents and therefore the average current, while over voltage produces an increase like in the SCIM 's. Although the LSPMM presents lower average currents, compared to the IE2 and IE3 class SCIM, it also presents the highest current unbalances in 5 of the 6 VU analyzed conditions, while the IE2 class SCIM presents the lowest current unbalances in 4 of the 6 VU analyzed conditions.

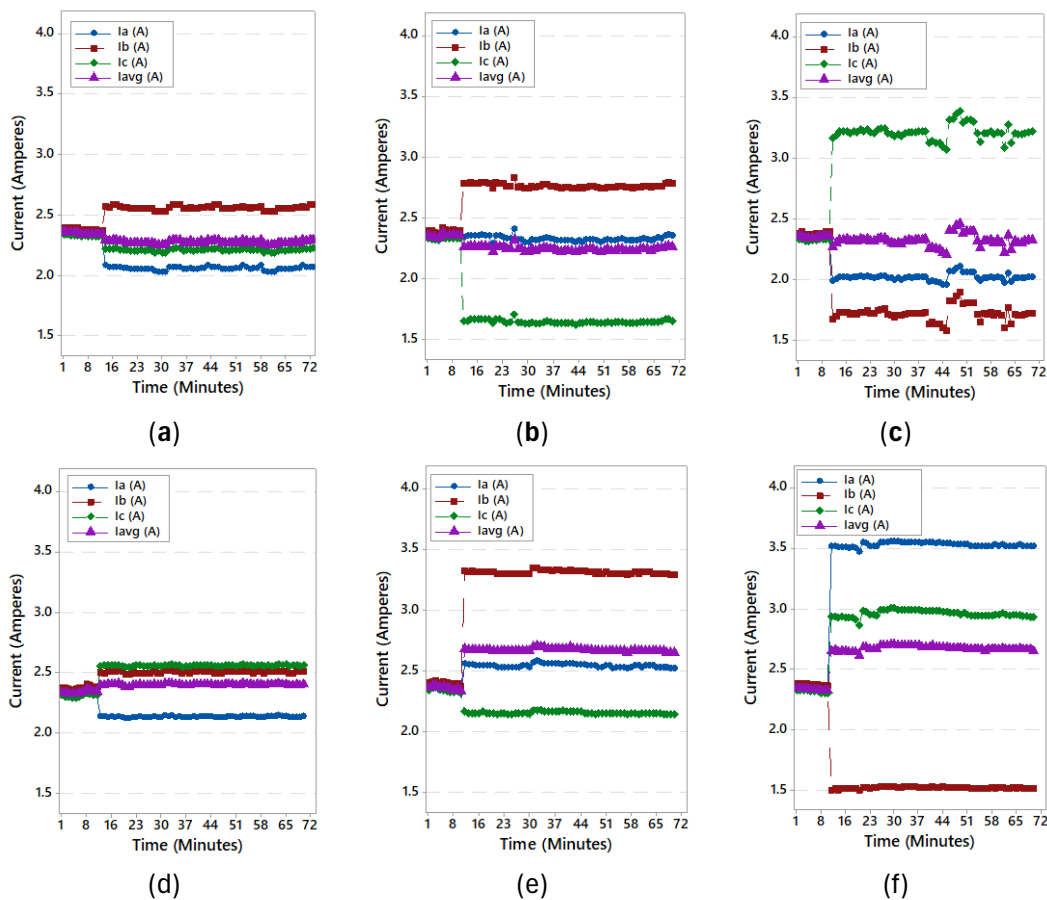


**Figure 4-8** - Line and average current for VU in IE4 LSPMM with: (a) 1% Under Voltage; (b) 3% Under Voltage; (c) 4% Under Voltage; (d) 1% Over Voltage; (e) 3% Over Voltage; (f) 4% Over Voltage.

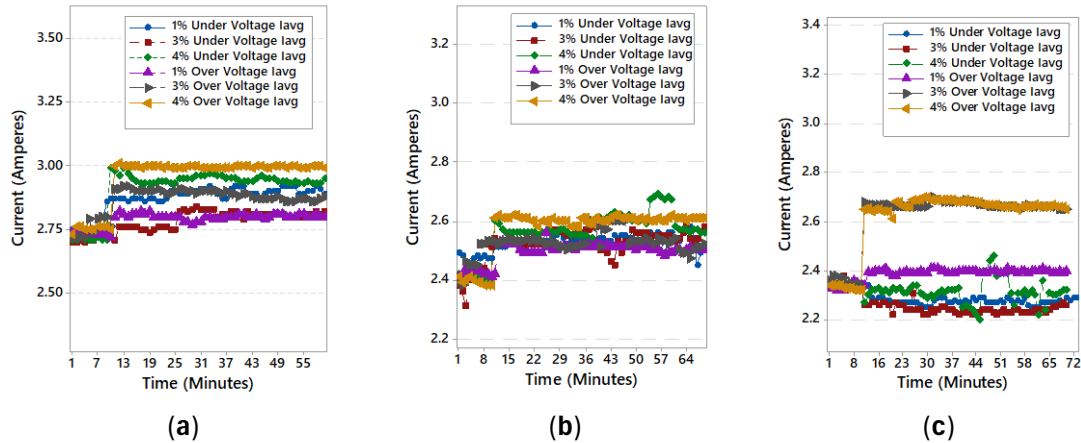


**Figure 4-9** - Average Current for under and over voltage unbalance conditions for: (a) IE2 SCIM; (B) IE3 SCIM; (c) IE4 LSPMM

#### 4.5.2. Power Factor

The power factor is inversely proportional to the positive sequence component, and it is increased with the presence of VU under voltage, while the VU with over voltage results in large decreases in this value according to the VU percentage [20]. Figure 4-10 shows the variation of this parameter with VU and the inverse relation with positive sequence phase voltage in the IE2, IE3 and IE4 Class motors.

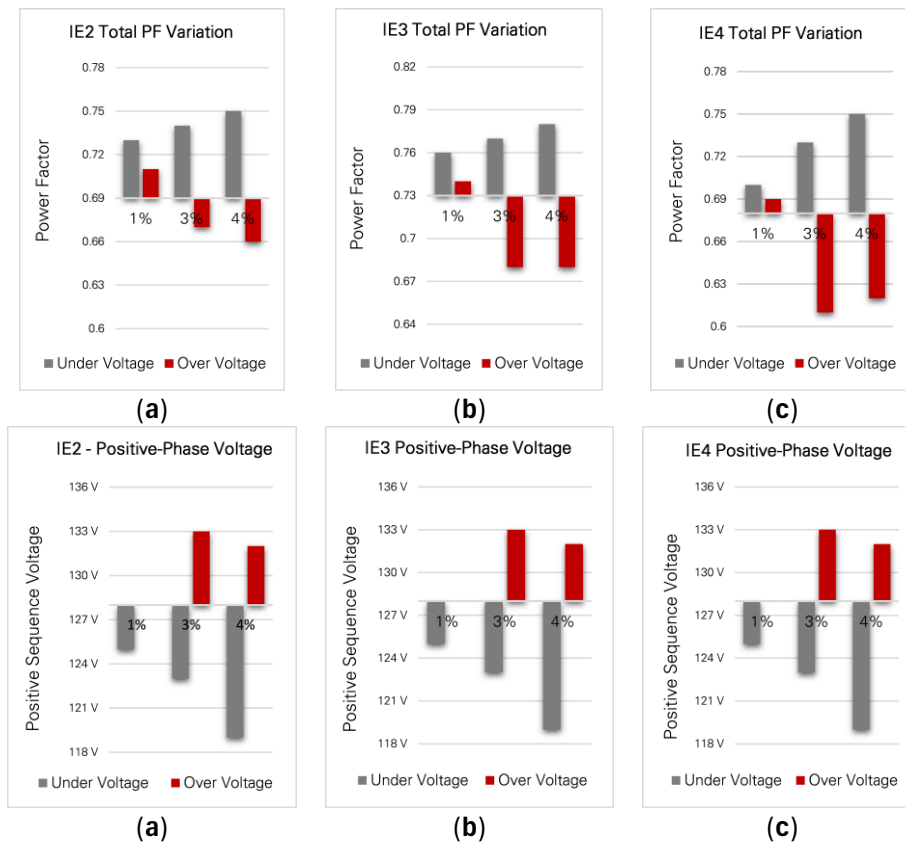


**Figure 4-10** - Power Factor (a-c) and Positive-Phase sequence voltage variation (d-e) with Under and Over Voltage Unbalance for IE2 Class SCIM, IE3 Class SCIM and IE4 Class LSPMM.

### 4.5.3. Total Power

For voltage unbalance conditions, the total power absorbed by IM's is the sum of the total power of positive and negative sequences [4]. In general, unbalances with under and over voltage result in increases in the total power consumed for SCIM Classes IE2 and IE3, as presented in Figure 4-11, while for the LSPMM VU with under voltage results in decrease in consumption for the same load percentage.

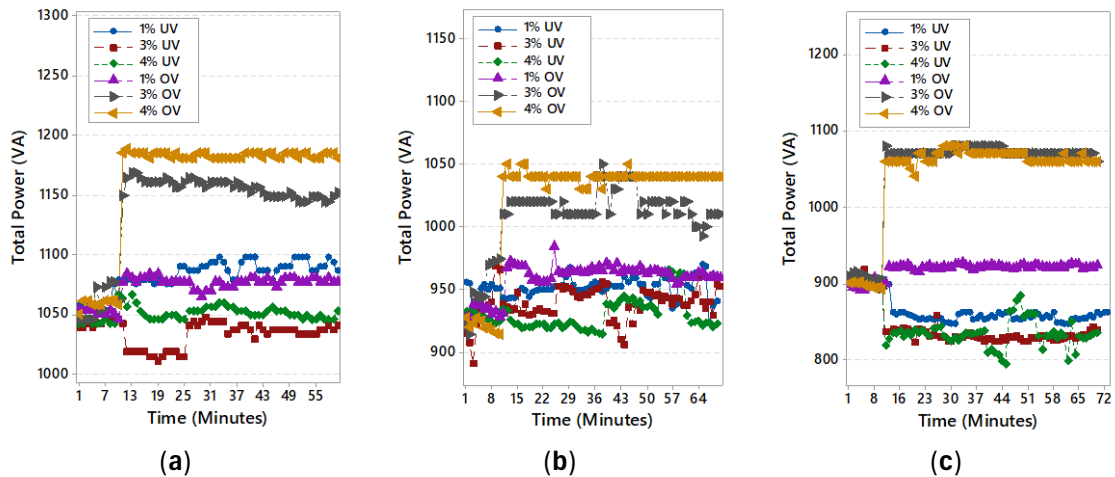


**Figure 4-11** - Total power variation with Under and Over Voltage Unbalance for: (a) IE2 Class SCIM; (b) IE3 Class SCIM; (c) IE4 Class LSPMM.

### 4.5.4. Current Total Harmonic Distortion

The presence of permanent magnets in the LSPMM resulted in a THDI up to 4 times that of SCIM classes IE2 and IE3, and this condition is aggravated when an unbalance in the supply voltage is added. Figure 4-12a-c presents the variation of this parameter with under and over voltage unbalanced conditions. Initially the IE2 and IE3 class motors present THDI less than 6% while the IE4 class motor exceeds 8% distortion, then in unbalanced conditions this parameter varies according to the percentage of unbalance as well as the current technology, being worst case scenarios with 4% under and over voltage, reaching values up to 12% and 15% respectively for IE2 and IE3 class motors. The hybrid motor, on the other hand, presents higher increases for this disturbance, reaching values up to 25%, and 20% for under and over voltage, respectively.

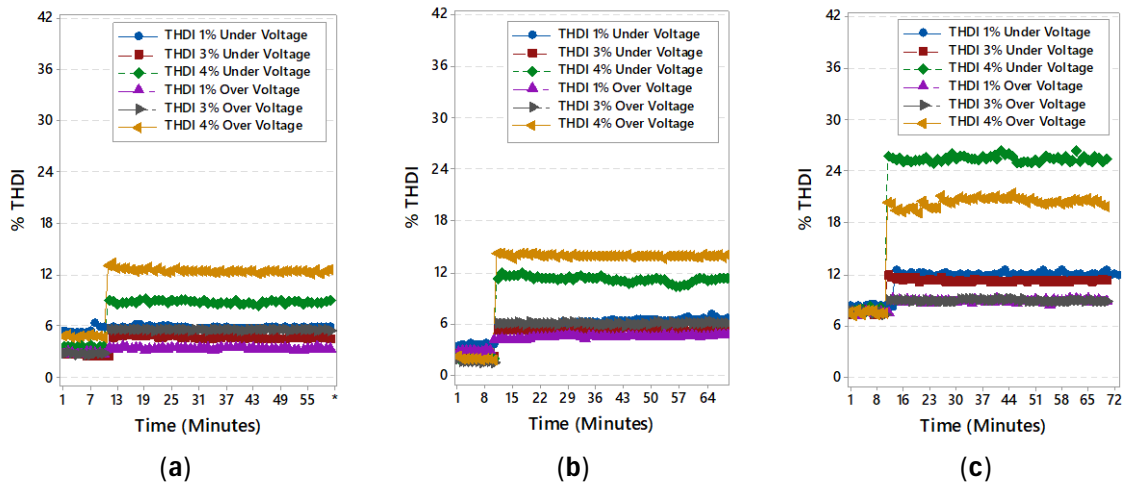


**Figure 4-12 -** Current Total Harmonic Distortion for under and over voltage unbalance conditions for: (a) IE2 SCIM; (b) IE3 SCIM; (c) IE4 LSPMM.

#### 4.5.5. Temperature Variation due to Voltage Unbalance

The improvements implemented in the LSPMM result in lower operational temperatures in relation to IE2 and IE3 class motors in ideal supply conditions. In VU conditions, large current unbalances are created, which increases the losses in the motor and therefore the inner and outer temperatures.

To analyze the VU impact with under and over voltage on the motor temperature, thermographic images representing the increase of this parameter in the motor end shield were captured, the results for each VU condition for the LSPMM are presented in Figure 4.13 and Figure 4.14. The photographs show how 1% of VU with under and over voltage does not result in visible increases in the LSPMM temperature, which justifies that it is not necessary to derate motor output power for this VU condition according to NEMA [3]. The worst visible scenarios correspond to unbalances of 3% and 4% with over voltage (Figure 4.14 d-f) turning out to be more damaging to the temperature of this motor than the VU with under voltage.

In addition to the current unbalance created by the voltage unbalance, the negative sequence component causes vibration and a decrease in the resulting torque due to the opposing torque generated. This contributes to the increase in temperature, a scenario that is worst for overvoltage due to the higher negative sequence impedance.

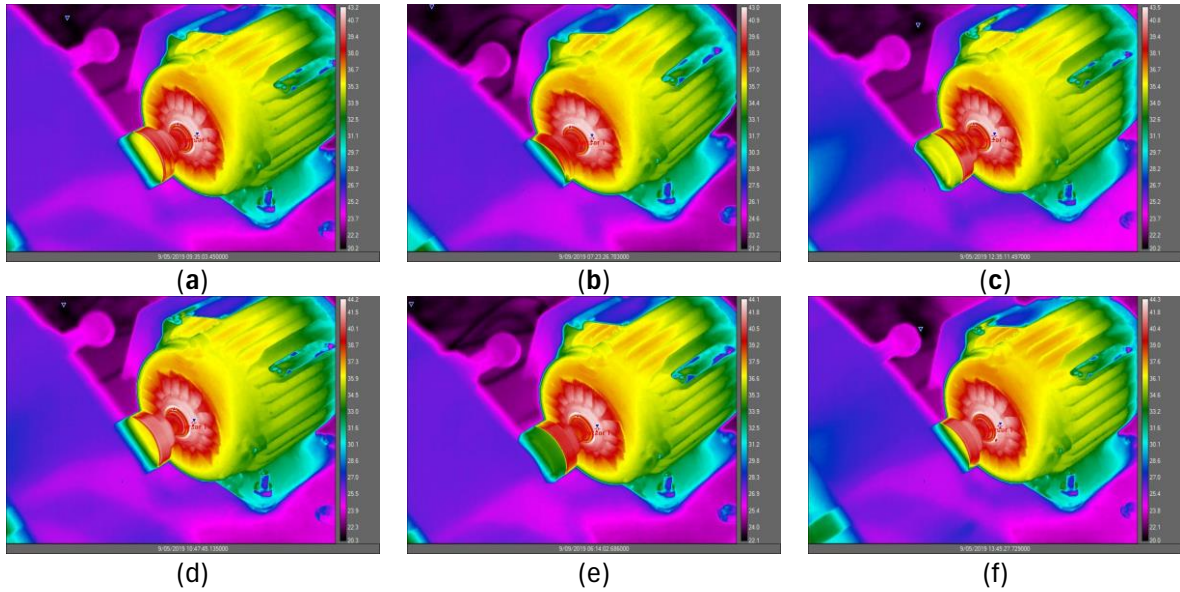


**Figure 4-13** - Frame Temperature with 1% under voltage (a & b); 3% under voltage (c & d); 4% under voltage.

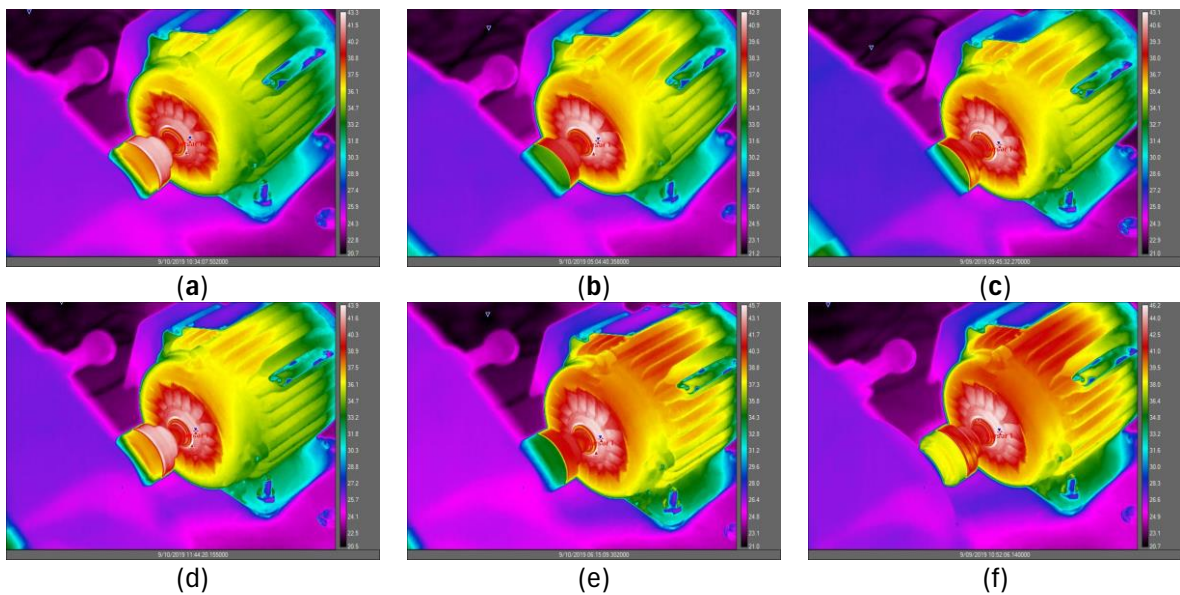


**Figure 4-14** - Frame Temperature with 1% over voltage (a & b); 3% over voltage (c & d); 4% over voltage (e & f).

Temperature variation for the three IMs in the six conditions analyzed are presented in Figure 4.18. Within the three technologies, the IE2 class motor has insulation class B (maximum temperature of 130 °C), while the IE3 and IE4 class motors have insulation class F (maximum temperature of 155 °C), which means that higher tolerance for temperature increases is expected. However, the results show that the IE4 and IE2 class motors have the lowest operating temperatures, below the IE3 class motor.

In the case of the IE4 class motor, it can be seen in Figure 4-15(a, b and c) that the VU with under voltage does not result in considerable increases in its operating temperature. This comes from the fact that in this case the current average magnitude did not increase, resulting in small temperature variations. This scenario changes with unbalance with over voltage, in which the LSPMM presents the highest temperature increases, mainly for cases of 3% and 4% of unbalance over voltage. In relation to the IE2 and IE3 class motors, similar increases for the conditions with unbalance with under and over voltage, the VU with over voltage resulted as being more damaging.

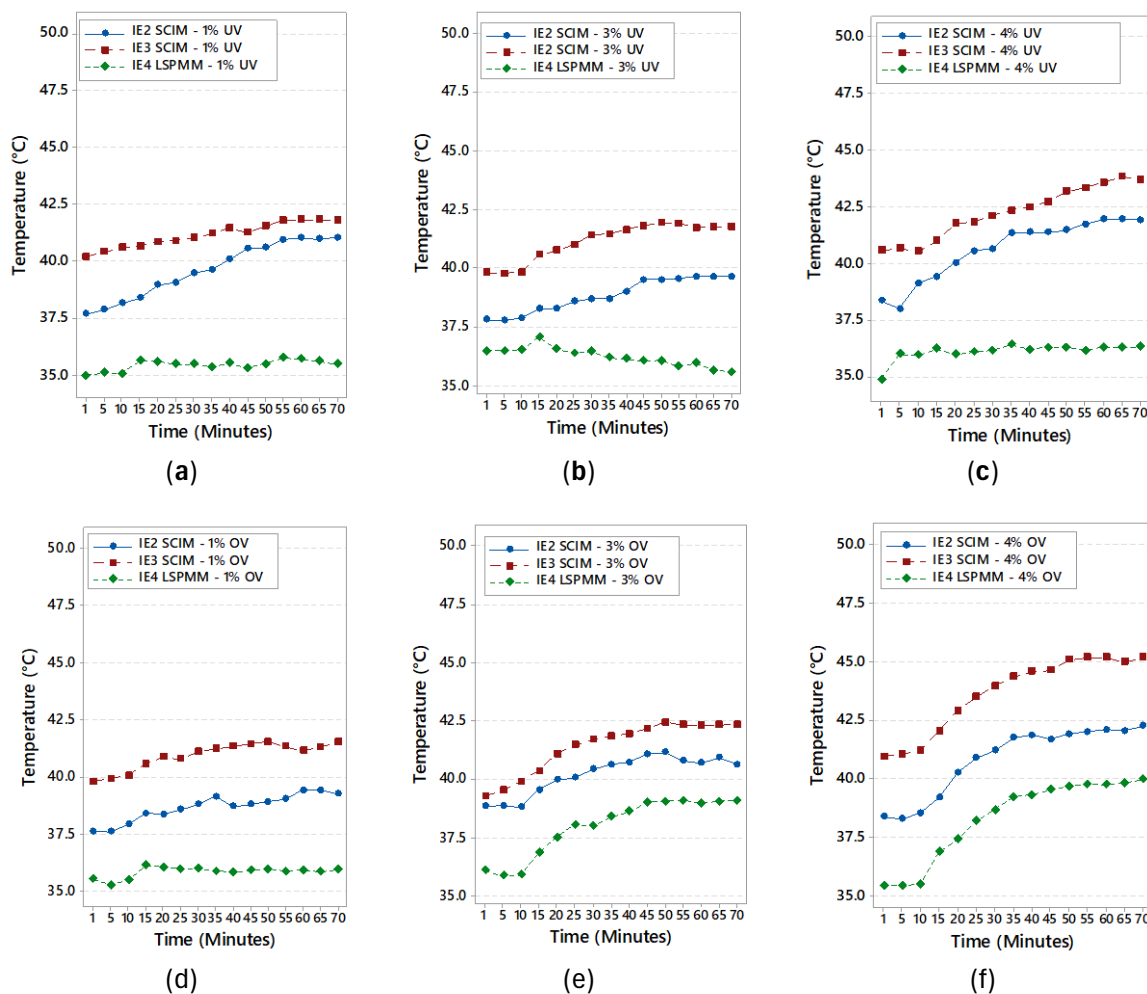


**Figure 4-15** - Temperature increase in IE2, IE3 and IE4 class IM’s with: (a) 1% under voltage; (b) 3% under voltage; (c) 4% under voltage; (d) 1% over voltage; (e) 3% over voltage; (f) 4% over voltage.

## 4.6. Statistic Assessment

### 4.6.1. Correlation Matrix for harmonic content

Aiming to analyze the VU influence in the current total harmonic distortion (THDI), a correlation analysis was developed in Minitab 18 [18], considering the THDI, the positive and negative sequence voltages (V +), (V-), the percentage of voltage and current unbalance (% VU), (% IU), total power (S), average current (Iavg), and active power (P). Figure 4.16 and Figure 4.17 present the correlations matrix.

In general, correlation analysis results in a number between -1 and +1, called the correlation coefficient. The higher the coefficient, the closer the relationship between the variables. For this case and after finding a nonlinear relationship between some variables, Spearman ´s correlation method was used [21]. In the correlation matrix the upper cell shows the Spearman coefficient while the lower cell shows the p-value, useful for rejecting the null hypothesis when compared to the significance level (0.05 assumed).

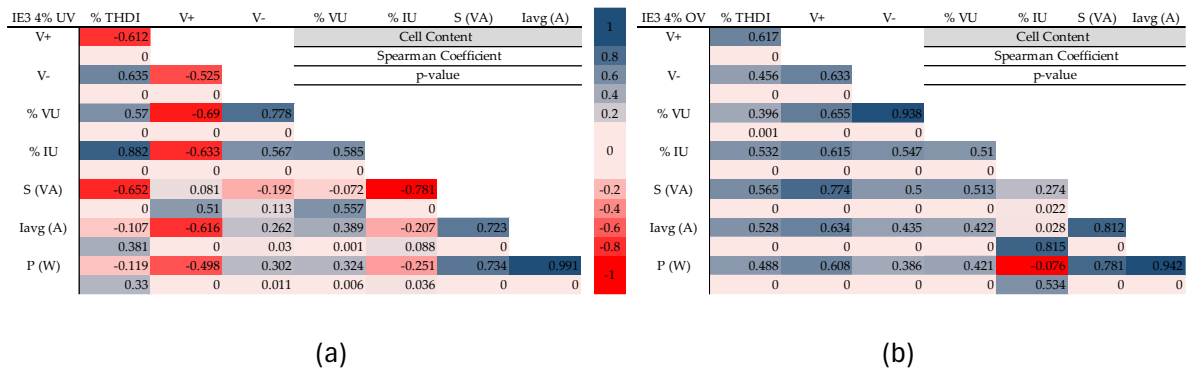


Figure 4-16 - Correlation matrix for IE3 Class SCIM motor parameters in the presence of VU with: (a) 4% Under voltage; (b) 4% Over voltage.

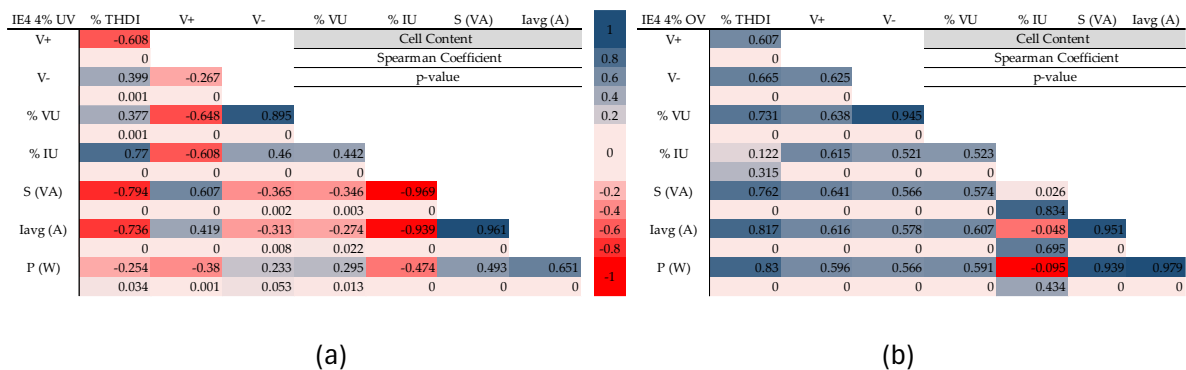


Figure 4-17 - Correlation matrix for IE4 Class LSPMM motor parameters in the presence of VU with: (a) 4% Under voltage; (b) 4% Over voltage.

It is observed that the parameters have inversely proportional relationships with respect to THDI in the case of under voltage unbalance, and directly proportional in the case of over voltage unbalance. For under voltage unbalance, the THDI is inversely proportional to positive sequence voltage (V+) and directly proportional to negative sequence voltage (V-). The percentage of current unbalance (% IU) also shows directly proportional relationships with respect to the THDI except for the case of over voltage in the LSPMM.

For the VU with over voltage, it is observed that the THDI varies proportionally with the positive sequence (V+) and negative sequence (V-) voltages, the percentages of voltage and current unbalance also show this behavior. The THDI also varies inversely proportional to the consumption in VA in the case of VU with under voltage, and directly proportional with the VU with over voltage. It is also observed how THDI presents higher correlations with the average current of the IE4 class hybrid motor, different to the IE3 class motor.

#### 4.6.2. Temperature models for VU in IE2, IE3 and IE4 class motors

As it was observed, VU resulted in increases in the operating temperature according to the unbalance percentage. In the graphs presented in Figure 4-15 it is observed how the temperature exhibits a certain increase pattern until reaching the thermal equilibrium with the new unbalance percentage. To analyze the influence of this disturbance on the temperature of each technology, a regression model was used for each percentage of VU using the Minitab 18 statistical software. Equation 5 presents the temperature change in (°C) over time until the thermal equilibrium is again reached for the IE4 Class hybrid motor when subjected to 4% VU with over voltage.

$$Temp (^{\circ}C) = 35.54 + 0.178 t - 0.001485 t^2 \quad (10)$$

where  $t$  is the time in minutes.

For the model presented in (10), an adjusted R2 = 0.9841 is obtained, also with a p-value less than 0.05. Figure 4-18a present the IE4 LSPMM prediction curve for the 4% over voltage unbalance, where the red fitted line shows the predicted temperature for 4% VU unbalance with over voltage and the blue dashed lines show the 95% prediction interval. It is noted that the initial measured temperature values are not quite well fitted by the regression model, presenting larger temperature residuals between values of measured temperature ( $T_{measured}$ ) and predicted



temperature ( $T_{fitted}$ ). This is due to the fact that these measured temperature points correspond to the first 10 minutes after starting to bring the motors to a thermal equilibrium condition, before applying the unbalance voltage supply. This condition is illustrated in Figure 4-18 (b) for IE2, IE3, and IE4 classes motors.

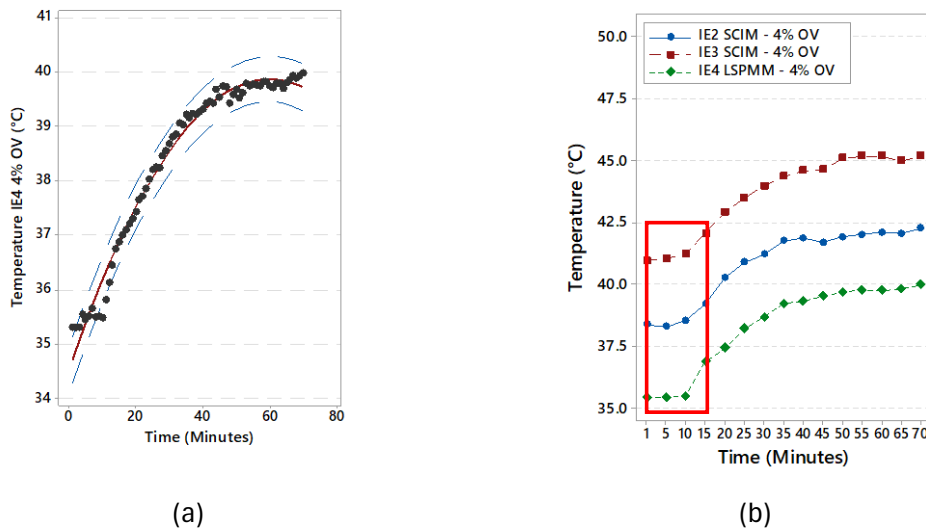


**Figure 4-18** - Temperature for the IE4 Class LSPMM: (a) Prediction plot for Temperature model with 95% of prediction interval; (b) Highlighting initial motors temperature measurements before applying unbalanced voltage supply.

To assess the proposed model accuracy, temperature residuals are plotted in Figure 4-19. Positive value for the residual (on the vertical axis) means the predicted temperature was lower than the measured temperature, and negative value means it was higher, zero means the prediction was correct [22]. It is observed that residuals are mostly clustered around zero, not exceeding temperature mismatches of  $\pm 1$  degree. Also, for this case, the calculated  $R^2$  value was 98.41%.

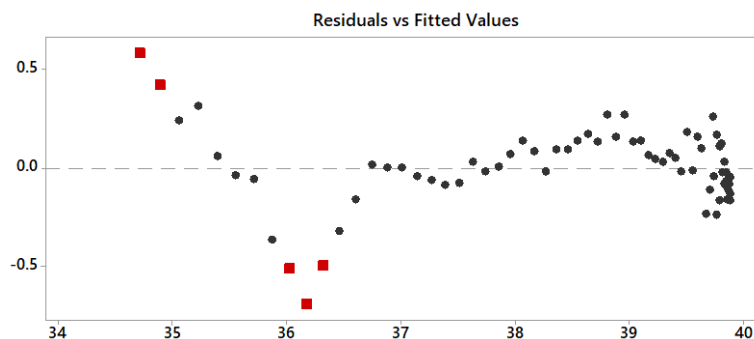


**Figure 4-19** - Residuals versus fitted or predicted temperature values.

This analysis was performed for the creation of temperature versus time models for each VU analyzed. Figure 4-20 presents the adjusted R<sup>2</sup> values for each created model, and Table 4.7 presents the results corresponding to the created models. SCIM classes IE2 and IE3 presented greater temperature increases in the six VU conditions analyzed, also presenting a similar increase pattern, due to which the models created present good approximation of the temperature variation over time until the thermal equilibrium is reached. A different scenario was observed for the LSPMM, which presented considerable increases only for the 3% and 4% unbalances with over voltage, this is reflected in the adjusted R<sup>2</sup> value, where the models best represent this variation, with values above 97 %.

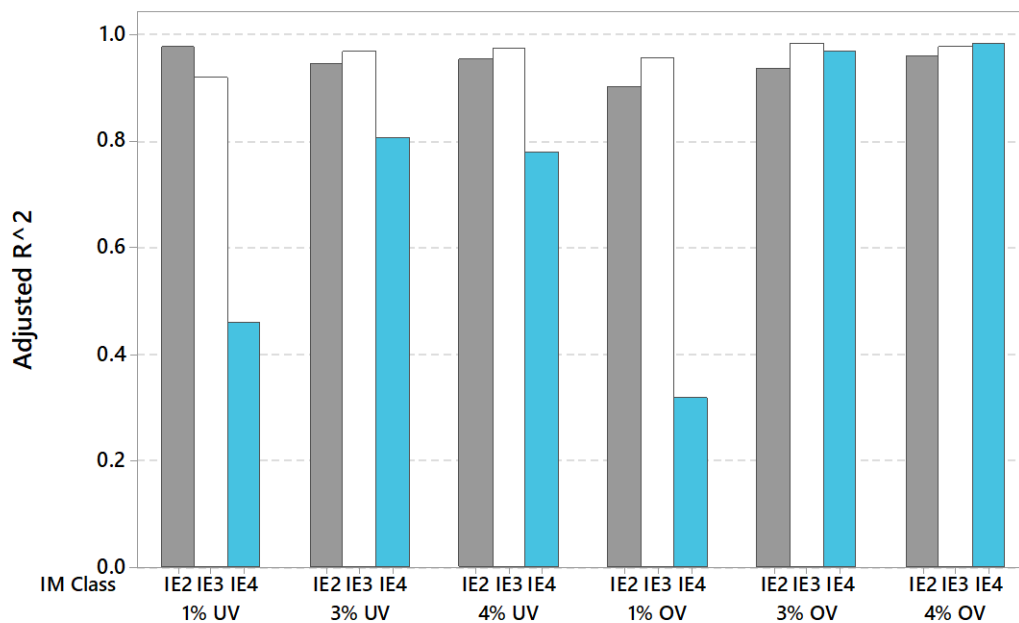


**Figure 4-20** - Adjusted coefficient (Adjusted R<sup>2</sup>) for generated models presented in Table 7

The Table 4-5 shows each of the temperature models for each unbalance condition, for each motor analyzed. In general, it is observed that almost all models have a quadratic term, useful for modeling the temperature curvature, until the thermal equilibrium is reached again. In these equations, the first coefficient corresponds to the motor’s initial temperature, after reaching thermal equilibrium with balanced voltages; the second term determines the rate of temperature increase over time. The third negative sign coefficient is useful to flatten the curve, until the thermal equilibrium is reached.

**Table 4-5** Summary of temperature models for voltage unbalance in IM 's classes IE2, IE3 and IE4.

% VU	IM Class	Equation Model	Adjusted R <sup>2</sup>
1% UV	IE2	$T (^{\circ}C) = 37.40 + 0.07935 t - 0.000348 t^2$	97.98%
	IE3	$T (^{\circ}C) = 40.10 + 0.04367 t - 0.000304 t^2$	92.20%
	IE4	$T (^{\circ}C) = 35.10 + 0.01631 t - 0.000141 t^2$	45.94%
3% UV	IE2	$T (^{\circ}C) = 37.49 + 0.05009 t - 0.000239 t^2$	94.65%
	IE3	$T (^{\circ}C) = 39.37 + 0.08460 t - 0.000722 t^2$	96.94%
	IE4	$T (^{\circ}C) = 36.64 - 0.002836 t - 0.000188 t^2$	80.84%
4% UV	IE2	$T (^{\circ}C) = 37.59 + 0.14810 t - 0.001310 t^2$	95.58%
	IE3	$T (^{\circ}C) = 40.15 + 0.07319 t - 0.000284 t^2$	97.44%
	IE4	$T (^{\circ}C) = 35.94 + 0.007334 t$	78.00%
1% OV	IE2	$T (^{\circ}C) = 37.63 + 0.03913 t - 0.000208 t^2$	90.46%
	IE3	$T (^{\circ}C) = 39.68 + 0.06225 t - 0.000551 t^2$	95.83%
	IE4	$T (^{\circ}C) = 35.53 + 0.02125 t - 0.000259 t^2$	31.79%
3% OV	IE2	$T (^{\circ}C) = 38.28 + 0.10270 t - 0.000983 t^2$	93.85%
	IE3	$T (^{\circ}C) = 38.94 + 0.12250 t - 0.001094 t^2$	98.42%
	IE4	$T (^{\circ}C) = 35.22 + 0.13000 t - 0.001079 t^2$	97.12%
4% OV	IE2	$T (^{\circ}C) = 37.52 + 0.15880 t - 0.001360 t^2$	96.24%
	IE3	$T (^{\circ}C) = 38.94 + 0.12250 t - 0.001094 t^2$	97.77%
	IE4	$T (^{\circ}C) = 35.54 + 0.17810 t - 0.001485 t^2$	98.41%

\* Where  $t$  represent the time in minutes for every VU condition.

#### 4.7. Final Considerations

Considering the future substitution between technologies as well as the growth in demand for electric motors, this chapter analyzed the response of the low power IE2, IE3 and IE4 IM classes under voltage unbalanced operating conditions.

The results indicated that undervoltage and overvoltage have different effects, mainly due to the variation of the positive and negative sequences. It was also observed how each class of technology presented different values for the impedance of the positive and negative sequences, with a high sensitivity for the impedance of the negative sequence. The current unbalance percentages (CUF) vary from 7 times the VU up to 17 times. It is also observed that the IE4 class LSPMM has higher current unbalances in case of undervoltage.

It was observed that undervoltage benefits the power factor, while overvoltage results in higher power consumption. In terms of power quality impact, the LSPMM had the highest percentage of distortion. It was observed how the THDI increases with the presence of unbalanced voltages.

Finally, an analysis of the temperature in electric motors with the presence of VU was also presented, with the creation of temperature models for each motor and for each VU condition, obtaining good approximations for the models created.

Considering the effect of voltage unbalance and harmonics on more efficient motors, the next chapter discusses the gain in efficiency versus the loss in power quality of more efficient motors when subjected to non-ideal power conditions. .

#### 4.8. Chapter Bibliography

- [1] ANSI C84.1, “ANSI C84.1 ELECTRIC POWER SYSTEMS AND EQUIPMENT - VOLTAGE RANGES.” Accessed: Apr. 04, 2020. [Online]. Available: <http://www.powerqualityworld.com/2011/04/ansi-c84-1-voltage-ratings-60-hertz.html>
- [2] V. Sousa Santos, P. Viego Felipe, and J. Gómez Sarduy, “Bacterial foraging algorithm application for induction motor field efficiency estimation under unbalanced voltages,” *Measurement*, vol. 46, no. 7, pp. 2232–2237, Aug. 2013, doi: 10.1016/j.measurement.2013.03.019.
- [3] NEMA MG1-2016, “Motors and Generators.” Accessed: Aug. 15, 2019. [Online]. Available: <https://www.nema.org/Standards/Pages/Motors-and-Generators.aspx>
- [4] E. Quispe, “Efectos del desequilibrio de tensiones sobre la operación del motor de inducción trifásico. Énfasis en la caracterización del desequilibrio de tensiones y el efecto sobre la potencia nominal,” 2012. doi: 10.13140/RG.2.1.3406.7287.
- [5] M. Al-Badri, P. Pillay, and P. Angers, “A Novel In Situ Efficiency Estimation Algorithm for Three-Phase Induction Motors Operating With Distorted Unbalanced Voltages,” *IEEE Transactions on Industry Applications*, vol. 53, no. 6, pp. 5338–5347, Nov. 2017, doi: 10.1109/TIA.2017.2728786.
- [6] “IEEE Recommended Practice for Monitoring Electric Power Quality,” *IEEE Std 1159-2019 (Revision of IEEE Std 1159-2009)*, pp. 1–98, Aug. 2019, doi: 10.1109/IEEESTD.2019.8796486.
- [7] “Power Quality Indices and Objectives,” e-cigre. Accessed: Apr. 04, 2020. [Online]. Available: <https://e-cigre.org/publication/261-power-quality-indices-and-objectives>
- [8] Yaw-Juen Wang, “An analytical study on steady-state performance of an induction motor connected to unbalanced three-phase voltage,” in *2000 IEEE Power Engineering Society Winter Meeting. Conference Proceedings (Cat. No.00CH37077)*, Jan. 2000, pp. 159–164 vol.1. doi: 10.1109/PESW.2000.849947.
- [9] Yaw-Juen Wang, “Analysis of effects of three-phase voltage unbalance on induction motors with emphasis on the angle of the complex voltage unbalance factor,” *IEEE Transactions on Energy Conversion*, vol. 16, no. 3, pp. 270–275, Sep. 2001, doi: 10.1109/60.937207.
- [10] J. Faiz, H. Ebrahimpour, and P. Pillay, “Influence of unbalanced voltage on the steady-state performance of a three-phase squirrel-cage induction motor,” *IEEE Transactions on Energy Conversion*, vol. 19, no. 4, pp. 657–662, Dec. 2004, doi: 10.1109/TEC.2004.837283.
- [11] P. Gnaciński, “Effect of unbalanced voltage on windings temperature, operational life and load carrying capacity of induction machine,” *Energy Conversion and Management*, vol. 49, pp. 761–770, Apr. 2008, doi: 10.1016/j.enconman.2007.07.033.
- [12] S. Singh and A. Singh, “Precise Assessment of Performance of Induction Motor under Supply Imbalance Through Impedance Unbalance Factor,” *Journal of Electrical Engineering*, vol. 64, pp. 31–37, Mar. 2013, doi: 10.2478/jee-2013-0004.
- [13] E. El-Kharashi, M. El-Dessouki, J. G. Massoud, A. W. Farid, and M. A. Al-Ahmar, “The use of the current complex factor to determine the precise output energy of the induction motor,” *Electric Power Systems Research*, vol. 154, pp. 23–36, Jan. 2018, doi: 10.1016/j.epsr.2017.08.008.
- [14] A. von Jouanne and B. Banerjee, “Assessment of voltage unbalance,” *IEEE Transactions on Power Delivery*, vol. 16, no. 4, pp. 782–790, Oct. 2001, doi: 10.1109/61.956770.
- [15] F. J. T. E. Ferreira, G. Baoming, and A. T. de Almeida, “Reliability and Operation of High-Efficiency Induction Motors,” *IEEE Transactions on Industry Applications*, vol. 52, no. 6, pp. 4628–4637, Nov. 2016, doi: 10.1109/TIA.2016.2600677.
- [16] M. Kostic, “Effects of Voltage Quality on Induction Motors’ Efficient Energy Usage,” *Induction Motors - Modelling and Control*, Nov. 2012, doi: 10.5772/51223.
- [17] A. M. S. Mendes, E. C. Quispe, X. M. López Fernández, and A. J. Marques Cardoso, “Influence of the positive sequence voltage on the temperature of three-phase induction motors,” in *The XIX International Conference on Electrical Machines - ICEM 2010*, Sep. 2010, pp. 1–6. doi: 10.1109/ICELMACH.2010.5608011.

- [18] “Minitab 18 Statistical Software (2010). [Computer software]. State College, PA: Minitab, Inc. (www.minitab.com).” Accessed: Aug. 15, 2019. [Online]. Available: <https://www.minitab.com/es-mx/>
- [19] C. Debruyne, S. Derammelaere, J. Desmet, and L. Vandeveldel, “Comparative study of the influence of harmonic voltage distortion on the efficiency of induction machines versus line start permanent magnet machines,” in *2012 IEEE 15th International Conference on Harmonics and Quality of Power*, Hong Kong, China: IEEE, Jun. 2012, pp. 342–349. doi: 10.1109/ICHQP.2012.6381217.
- [20] fatma zohra Dekhandji, L. Refoufi, and H. Bentarzi, “Quantitative assessment of three phase supply voltage unbalance effects on induction motors,” *International Journal of System Assurance Engineering and Management*, vol. 8, Nov. 2015, doi: 10.1007/s13198-015-0401-3.
- [21] Minitab, 2018, “A comparison of the Pearson and Spearman correlation methods,” Minitab 18, Support. [Online]. Available: <https://support.minitab.com/en-us/minitab/18/help-and-how-to/statistics/basic-statistics/supporting-topics/correlation-and-covariance/a-comparison-of-the-pearson-and-spearman-correlation-methods/#comparison-of-pearson-and-spearman-coefficients>
- [22] “Interpreting residual plots to improve your regression | Statwing Documentation.” Accessed: May 25, 2020. [Online]. Available: [http://docs.statwing.com/interpreting-residual-plots-to-improve-your-regression/#the\\_top](http://docs.statwing.com/interpreting-residual-plots-to-improve-your-regression/#the_top)

## Chapter 5

# Assessing Energy Efficiency and Power Quality Impacts in High-Efficiency Motors

The search for more competitive equipment in the global market has led to the implementation of new materials and technologies in the search for greater energy efficiency. This is certainly a guideline followed by the electric motor industry that has introduced new technologies in rotating machines, such as the permanent magnet motor, evolving into increasingly efficient motor classes. This Chapter presents a comparison between energy efficiency gain and the corresponding power quality degradation through a detailed harmonic analysis of the effects of voltage harmonics and voltage unbalance in electric motor classes: IE2, IE3, and IE4. The results achieved are interesting but rigorously reflect only the tested motor sample and cannot be generalized to all motors, in other power ranges, of the respective motor classes tested.

### 5.1. Introduction

#### 5.1.1. General Considerations

Over the years, the interest in implementing energy efficiency actions has been adopted by many countries, in search of a green and sustainable future. Different national and international programs have implemented actions promoting the search for greater operational efficiencies [1], [2], [3]. Actions include energy performance certificates, minimum energy performance requirements, mandatory energy audits, and financing for energy efficiency investments [4], [5], [6], among others. Technological advances have also allowed new loads (devices, electric motors, etc.) to be more efficient, through improvements in materials, and manufacturing processes, as well as the introduction of new technologies.

From the end user's point of view, the main benefits of energy efficiency actions in equipment must be seen from the economic point of view through the reduction of the energy bill, as well as more reliability and tolerance than less efficient technologies. This justifies the fact that the new equipment is built based on efficiency, measured through experimental tests in certified laboratories, and through which different efficiency categories are defined.

Regarding electric motors, the reference parameter is efficiency, first classified by IEC 60034-30-1 [7] in 2008. Currently, four efficiency classes are defined by the standard, i.e., IE1-IE4, and it

is expected that the next edition defines the IE5 efficiency class. From this classification, manufacturers have presented different proposals to achieve ever greater efficiencies in IMs. Studies comparing different technologies have been presented in [8], [9], [10], [11], [12], synchronous reluctance motors, permanent magnet motors (PMM,0 and copper rotor motors are the main alternatives to achieve higher efficiencies [13]. These new technologies present constructive variations concerning their predecessors, as well as new components, such as PM, which respond differently to the disturbances present in electrical systems.

### **5.1.2. Chapter Motivation and Contribution**

Although the impacts of voltage harmonics (VH) and/or voltage unbalances (VU) on IMs have already been extensively investigated, the focus is mainly on performance and temperature analysis, and few works address the impacts of these phenomena without a rigorous analysis of its own impacts on power quality. In addition, new scenarios arise with the introduction of new technologies as future substitutes for the conventional induction motor, such as the permanent magnet motor, which changes the paradigm of the conventional induction motor and its operating characteristics.

The introduction of new technologies translates into lower consumption and greater savings, making the substitution between technologies attractive. Given this scenario, studies on the performance of new technologies such as the line-start permanent magnet motor must be carried out to evaluate the advantages and points to consider in large-scale uses. In this sense, this work presents a comparison between energy efficiency gain and power quality degradation related to electric motors. To that end, laboratory experimental tests on three 0.75-kW induction motors belonging to classes IE2, IE3, and IE4 were analyzed under ideal operating conditions, as well as in the presence of voltage harmonics and voltage unbalance with under- and overvoltage, with special focus on the harmonics generated by each disturbance. The results revealed that, for the motors sample analyzed in this work, the more efficient motors are more sensitive to disturbances in the electrical systems, also behaving as sources of amplification of existing harmonics in the presence of these disturbances, with which the doubt arises: Are the most efficient motors less efficient in power quality terms?



## 5.2. Theoretical Foundation

### 5.2.1. Energy Efficiency Policies in Induction Motors

Minimum Energy Performance Standards (MEPS) defines the minimum efficiency class to be manufactured and marketed based on national and energy targets. In Brazil, the minimum efficiency level for electric motors from August 2019 is the IE3 class. Despite commercially existing proposals in the world to achieve higher efficiency classes, there is a global consensus that the IE3 class is the appropriate efficiency class at this time. The main actions used to encourage the more efficient motors in new installations as well as the replacement of old/non-efficient motors are listed below and depicted in Figure 5-1.

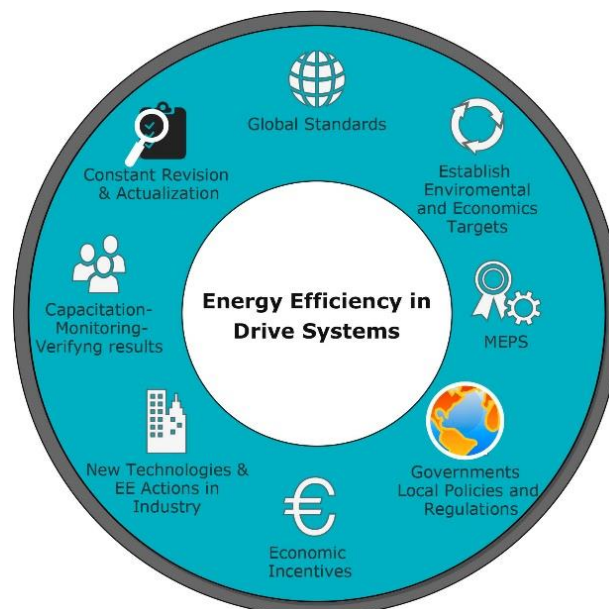


**Figure 5-1** - Steps toward the implementation of energy efficiency actions on induction motor policies.

The key steps for implementing energy efficiency initiatives are detailed below:

- The creation of global standards such as IEC 60034-30-1 and NEMA [14] to globally classify the efficiency classes in IMs and define the minimum efficiency levels to be within the classification [1], [7].
- The establishment of economic and environmental objectives to be met in defined periods for the correct implementation of minimum efficiency requirements for electric motors in accordance with national emission and energy reduction targets.
- The establishment of local regulations and policies by governments that define the minimum efficiency requirements as well as their classifications through departments destined for that purpose [1], [5], [15].

- The allocation of funds for the granting of incentives, through bonus to reduce the initial value of new motors, for the replacement of old/non-efficient motors or the purchase of new electric motors, as well as for research projects and development for the improvement of materials as well as the study of new technologies [6], [16], [17].
- Industry plays a key role in obtaining results. It must be the focus of regulations, motivating this sector to implement new more efficient technologies, as well as energy efficiency actions.
- The implementation of training and technical advice on the best paths to greater efficiencies as well as constant monitoring and verification.
- The constant verification and updating considering the results obtained, the definition of new routes toward greater efficiencies, considering the new technologies present in the market and updating the standards according to the indicators.

### **5.2.2. Process toward More Efficient Motors**

Modernization of industrial processes has also required more efficient drive systems. Different manufacturers offered higher efficiencies for the same nominal power, due to the materials and processes used in the construction of these rotative machines. However, it was not until 2008 that the IEC defined three efficiency classes, namely, IE1, IE2, and IE3.

The motors that did not reach the efficiency class IE1 were classified as IE0 and called unregulated motors, which by the year 2000 represented 80% of global electricity consumption by electric motors. With the implementation of policies and regulations that promoted the substitution between technologies, as well as the end of their useful life, this percentage went to be 30% of energy consumption in 2017. However, in this year, consumption by electric motors seems to be twice that of the year 2000 with which the IE0 class motors consumption in 2017 was two-thirds of those that existed in the year 2000, and there are still many opportunities for substitution. In 2014 the efficiency class IE4 was defined, with which efficiencies greater than 96% can be obtained with IMs. When these classifications were defined, the manufacturers understood that they would have to go beyond conventional induction motors to get higher efficiencies, and in this way new technologies were explored and perfected, coming up with proposals such as a copper rotor motor, the synchronous reluctance motor, and the permanent magnet motor, the latter present in this study.

### 5.3. Energy Efficiency and Power Quality Assessment

#### 5.3.1. Methodology

Measurements were performed in the Amazon Energy Efficiency Center (CEAMAZON) located at the Federal University of Pará (UFPA) in Belem City, Brazil, to analyze the influence of voltage unbalance with under- and overvoltage and voltage harmonics on the power supply of the three induction motors classes, i.e., IE2, IE3, and IE4. Figure 1.5 shows the general test setup. The balanced and pure sinewaves as well as the voltage unbalances and harmonics were generated using a three-phase AC source model FCATHQ™ (1), capable of generating a pure sine voltage waveform as well as voltage unbalances, sags, swells, and harmonics (up to the 50th order) with different distortion magnitudes. The IM's input parameters were measured using the class “A” quality analyzer HIOKI™ (2) model PW3198-90. The electric load used in this work then consists of an electromagnetic brake or Foucault brake (3). For the study, a torque of 3.8 Nm was applied to the Foucault brake, representing 92–95% of the IE2 class motor nominal torque. (4). Table 5-1 presents the nominal data of each motor.

**Table 5-1.** Induction Motors parameters

IM Class	IE2	IE3	IE4
Technology	SCIM,	SCIM	LSPMM
Power	0.75 kW	0.75 kW	0.75 kW
Voltage	220/380 V	220/380 V	220/380 V
Speed (rpm)	1730	1725	1800
Torque (Nm)	4.12	4.13	3.96
Current (A)	2.98/1.73	2.91/1.68	3.08/1.78
Efficiency (%)	82.6	82.6	87.4
Power Factor	0.80	0.82	0.73

At first, the induction motors were subjected to a 220-V perfect three-phase sine voltage for 1 h and 10 min so that they reached their thermal equilibrium. In a second moment, the value of each voltage harmonic (2nd, 3rd, 5th, and 7th) was increased by 2% every 10 min, until it reached 25%. In relation to voltage unbalance, after reaching the thermal equilibrium, voltage unbalances with 1%, 3%, and 4% according to NEMA definition with under- and overvoltages were inserted separately in each of the motors for a period of an hour until the thermal equilibrium was reached again. It should be noted that only voltage magnitudes were varied; the phase angles remained constant. Table 5-2 presents voltage magnitudes for each voltage unbalance.

**Table 5-2.** Voltage Unbalance magnitudes

% NEMA Voltage Unbalance	Vab	Vbc	Vca
1% Undervoltage	217.34 V	219.67 V	214.03 V
3% Undervoltage	217.72 V	214.46 V	206.8 V
4% Undervoltage	197.15 V	206.69 V	214.35 V
1% Overvoltage	220.40 V	224.54 V	221.2 V
3% Overvoltage	235.85V	233.57V	224.28V
4% Overvoltage	227.91 V	219.89 V	237.57V

Regarding the methodology used for the treatment of measurement data and obtaining the results, Figure 5-2 presents the steps performed in the present work. At first, the tests with VH and VU were performed separately on the test bench for each of the motors analyzed, and then the measurements were made using the Power Quality analyzer equipment. The next step was to transfer the measurement data from the equipment to the analyzer (HIOKI) software. After data analysis, they were converted to CSV format files, compatible for reading in Minitab (Minitab 18) statistical software. In Minitab, the data were processed for plotting the results related to harmonic analysis.

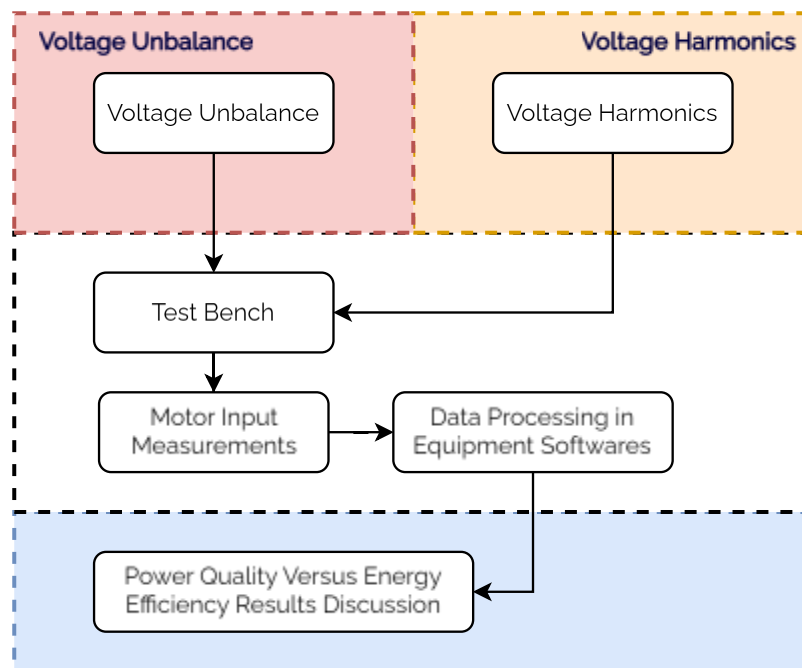


**Figure 5-2 – Methodology flowchart.**

## 5.4. Results and Discussion

### 5.4.1. Voltage Harmonics Impacts on Power Quality

The presence of voltage harmonics results in the decrease of the rotation speed for the electric motors analyzed. Figure 5-3 shows the speed variations in the presence of 2nd, and combined 2nd, 3rd, 5th and 7th voltage harmonics for the three IMs classes. It is observed that the second negative sequence harmonic results in greater decreases for the IE2 Class SCIM, falling from 1752 rpm to speed values of 1738 rpm, while the IE3 class motor decreases from 1753 rpm to 1744 rpm with 25% distortion. Then the combination of all the harmonics results in the greatest decreases in speed, the IE2 Class SCIM again being the most affected. For the LSPMM once the synchronism is reached, the presence of these disturbances does not result in any variation of speed in the presence of Voltage Harmonics. This highlights the benefits of LSPMM synchronism against various disturbances, especially in fixed speed applications.

Figure 5-4 presents the impact of the 5<sup>th</sup> and 7<sup>th</sup> voltage harmonics of positive and negative sequence, respectively. It is observed how result in decreases in the speed of SCIM, being the 5<sup>th</sup> harmonic most damaging, it should be noted that despite the 7<sup>th</sup> harmonic being of positive sequence (produces a positive torque) also results in a decrease in speed.

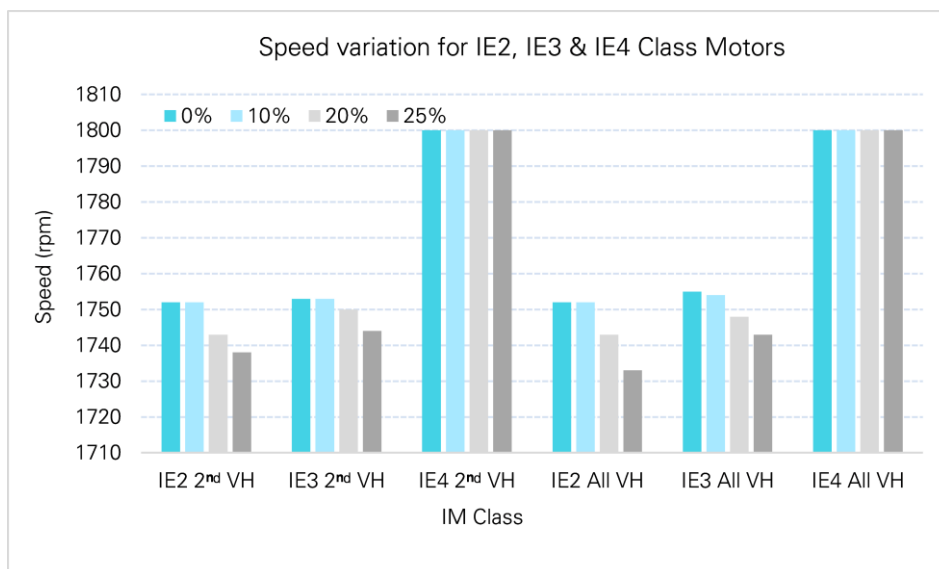


**Figure 5-3** - Speed variation for IE2, IE3 & IE4 Class motors in presence of 2nd, and combined 2nd, 3rd, 5th and 7th voltage harmonics.

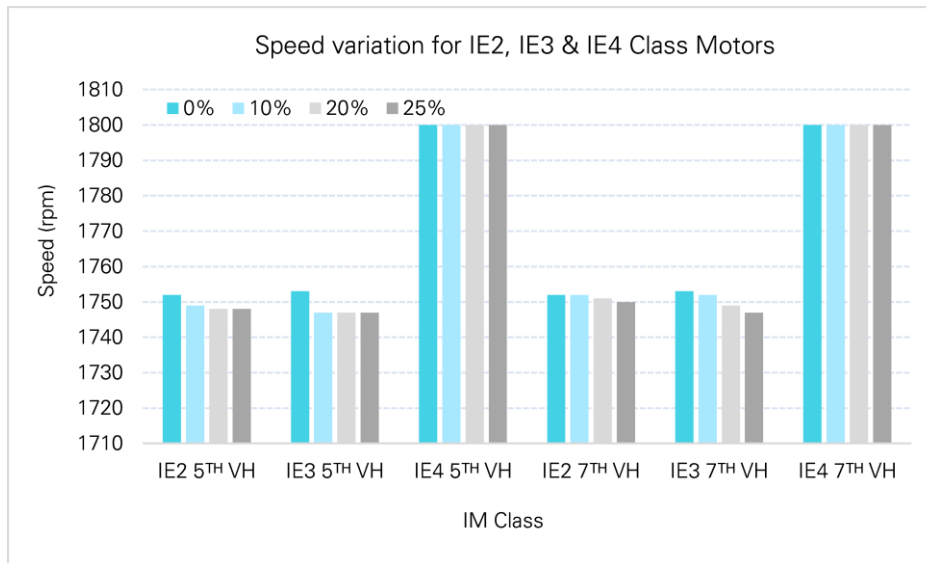


**Figure 5-4** - Speed variation for IE2, IE3 & IE4 Class motors in presence of 5th and 7th voltage harmonics.

To explain this phenomenon, an analysis considering the harmonics present in the waveform was developed for the three IM’s analyzed and is presented in Figure 5-5, it was observed that when the voltage distortion percentage of 7th order harmonic was increased, a 5th order current harmonic component appeared, and increased mainly for distortions greater than 8%, as it is a negative sequence harmonic, it can result in contrary torques, which reduces the speed in the motor shaft.

This situation was also observed for the 2<sup>nd</sup> and 5<sup>th</sup> negative sequence harmonic, when the 5<sup>th</sup> harmonic of negative sequence is present, a 7<sup>th</sup> current harmonic component appears, while when the 2<sup>nd</sup> harmonic is present, 4<sup>th</sup> and 5<sup>th</sup> order current harmonics components arise. The 4<sup>th</sup> order also appeared in the presence of all the harmonics analyzed. Despite the fact that these harmonics appear in the three analyzed all motors, the percentages found were higher for the 0.75 kW, line start permanent magnet motor class IE4, however, without impacting its rotation speed.

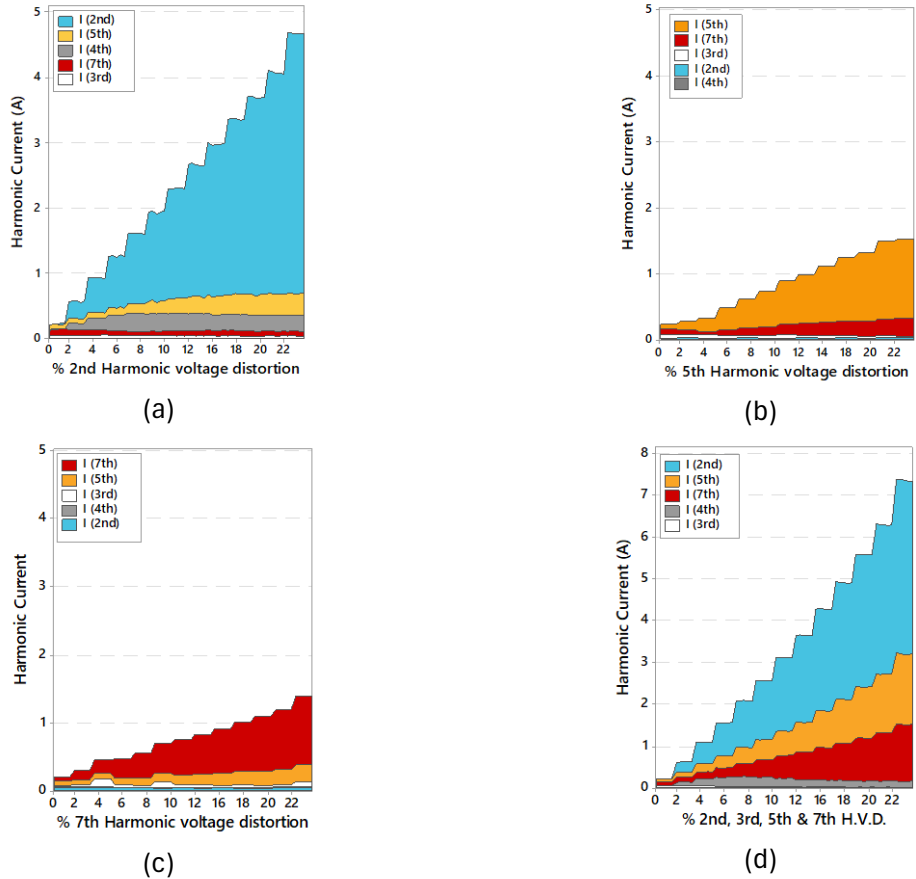


**Figure 5-5** - Harmonic currents present in IM's with harmonic voltage distortion of (a) 2nd harmonic order; (b) 5th harmonic order; (c) 7th harmonic order (d) 2nd, 3rd, 5th and 7th harmonic order combined.

### 5.4.2. Voltage Unbalance Impacts on Power Quality

Despite many studies have analyzing the impact that VU has on IM’s operation, the impact that this disturbance has on voltage and current harmonics in electric motors has not been deeply analyzed. In this way and aiming to analyze the impact of this disturbance on the power quality, this section analyzes the relationship that exists between the voltage unbalance and the harmonics present and those that arise with the presence of this disturbance in the electric motors presented in this study.

The presence of unbalanced voltages also results in decreases in the speed of electric motors according to the type of technology, as well as the loading percentage. Speed variation in the presence of six VU conditions with under and overvoltage is presented in Figure 5-6. In general, it is observed that the unbalance with undervoltage (UV) results in greater decreases in speed when compared to the unbalance with overvoltage (OV).

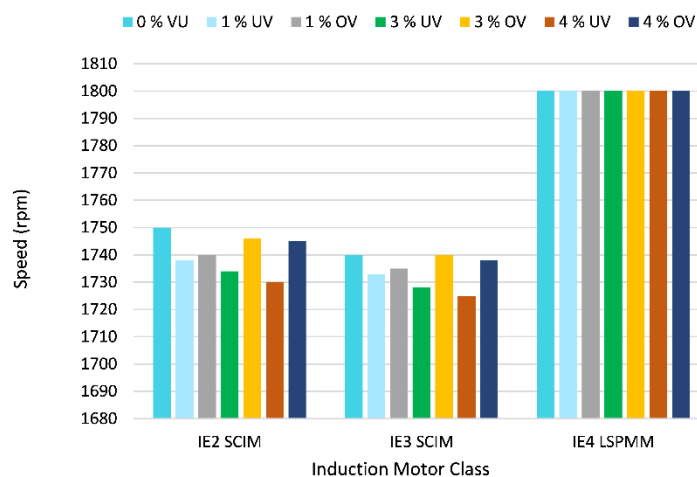


**Figure 5-6** - Speed variation for IE2, IE3 & IE4 Class motors in presence of 0%-4% Voltage Unbalance Conditions with under and over voltages;

In addition to the current unbalances, voltage unbalance also results in increases in the harmonics currents according to the voltage magnitude, the VU degree as well as the IM technology. Figure 5-7 and Figure 5-8 show the variation of the 5th order harmonic currents percentage for the IE3 and IE4 motors respectively for 1% and 4% VU with under and over voltage, the class IE2 motor presented percentages like those of the IE3 class motor.



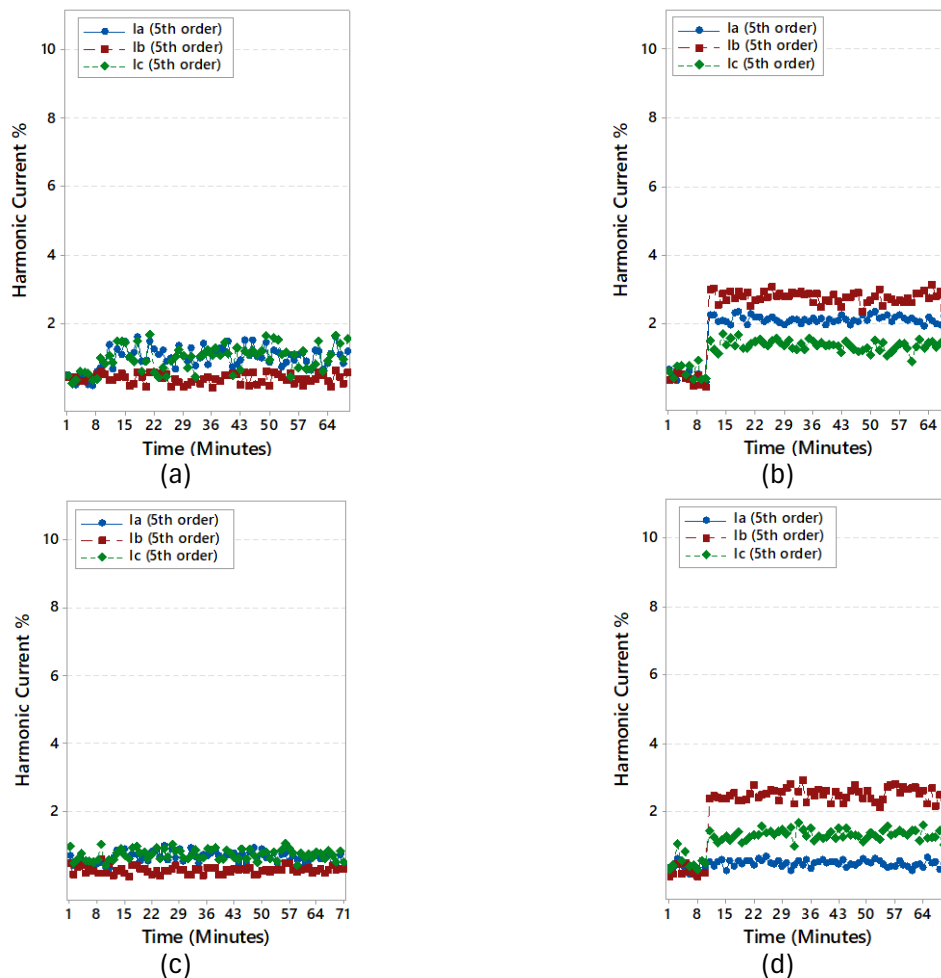


**Figure 5-7** - - Fifth harmonic currents variations for phases a-b-c for the IE3 Class motor for (a) 1% VU with Under Voltage; (b) 4% VU with Under Voltage; (c) 1% VU with Over Voltage; (d) 4% VU with Over Voltage

Initially, the oscillation that exists in each of the phase's currents for the 5th order harmonic can be observed for both technologies, and that is greater for the LSPMM (Figure 5-8) at the analyzed power (0.75kW). It was also observed how the fifth current harmonic follows a growth pattern opposite to that of the input line currents when subjected to VU for the three efficiency classes analyzed, with the lowest phase current presenting the highest 5th order harmonic current. It can also be observed that for IE2 and IE3 class motors the VU with under and over voltage result in similar distortion degrees, while for the LSPMM the VU with under voltage results in distortion degrees of up to twice that found in the condition with overvoltage, as shown in Figure 5-8. Despite the increase in this negative sequence harmonic, it does not impact on the motor synchronous operating speed, for the unbalance degrees analyzed, as presented in Figure 5-6, showing more tolerant to this type of disturbance in terms of operation.

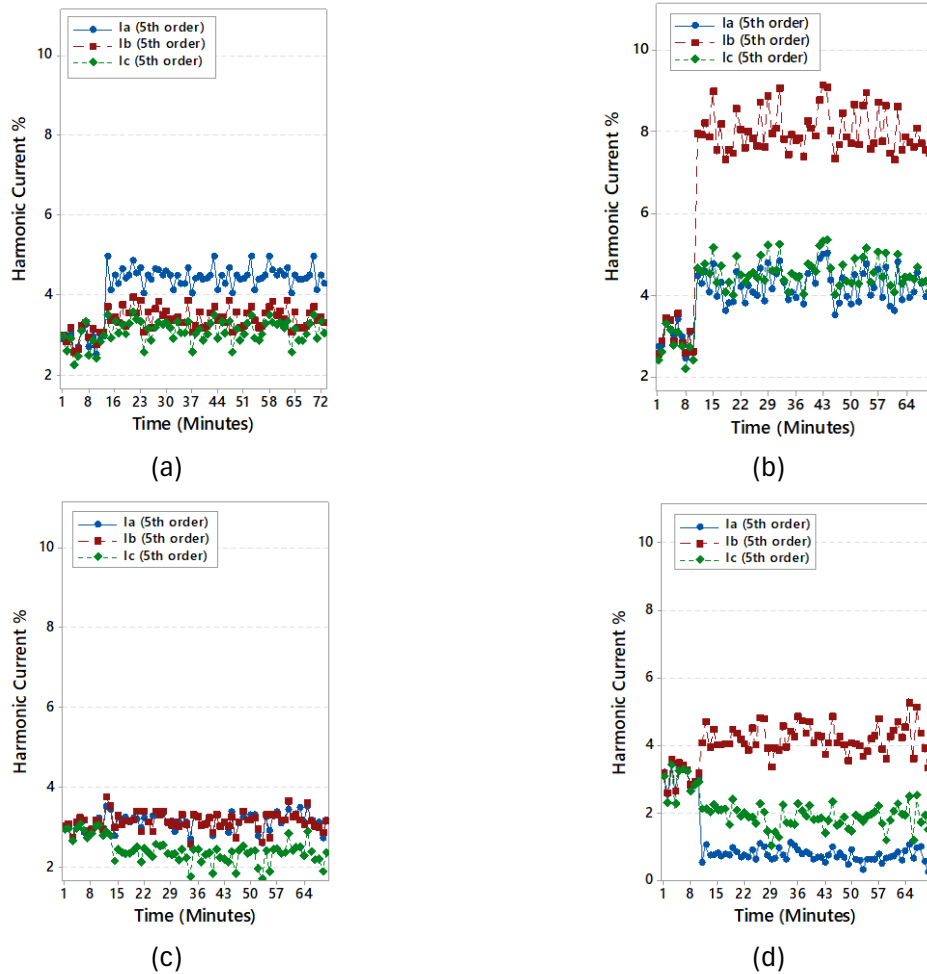


**Figure 5-8** – Fifth harmonic currents variations for phases a-b-c for the IE4 Class motor for (a) 1% VU with Under Voltage; (b) 4% VU with Under Voltage; (c) 1% VU with Over Voltage; (d) 4% VU with Over Voltage

The variation of the 7th positive sequence harmonic current was also analyzed for the three electric motors and is presented in Figure 5-9. Lower percentages when compared to the 5th negative sequence harmonic current are observed, also this harmonic did not follow the 5th harmonic growth pattern, undergoing random variations. For the IE2 and IE3 class motors, the increase in VU results in a decrease in the harmonic percentage, both for the under and over voltage unbalance conditions.

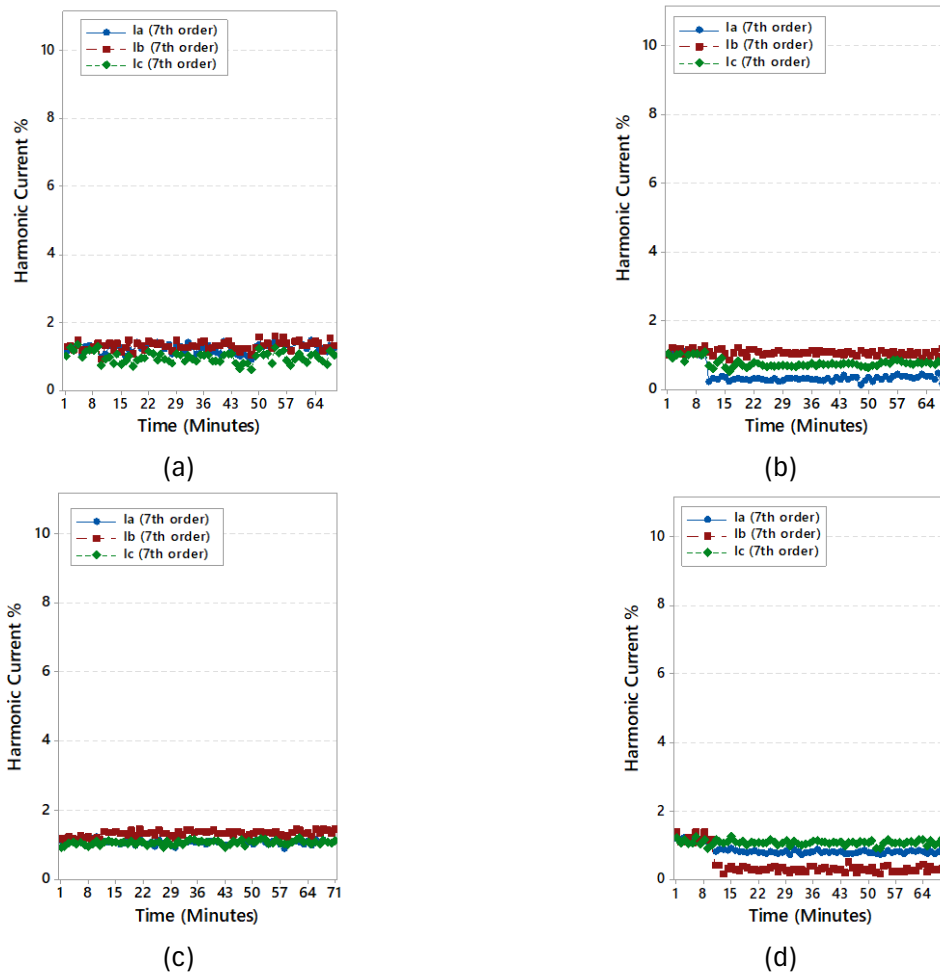


**Figure 5-9** - Seventh harmonic currents variations for phases a-b-c for the IE3 Class motor for (a) 1% VU with Under Voltage; (b) 4% VU with Under Voltage; (c) 1% VU with Over Voltage; (d) 4% VU with Over Voltage

Regarding the LSPMM, presented in Figure 5-10, voltage unbalance resulted in a variation of the 7th order harmonic currents. It is observed that in the case of VU with undervoltage, increases in one of the phases are observed for 1% and 4%, respectively. VU with overvoltage resulted in an increase in two of the phases for 1% while for 4% it resulted in a decrease. It is further observed that like the 5th negative sequence harmonic, the 7th positive sequence harmonic presents oscillations in these voltage unbalance conditions.

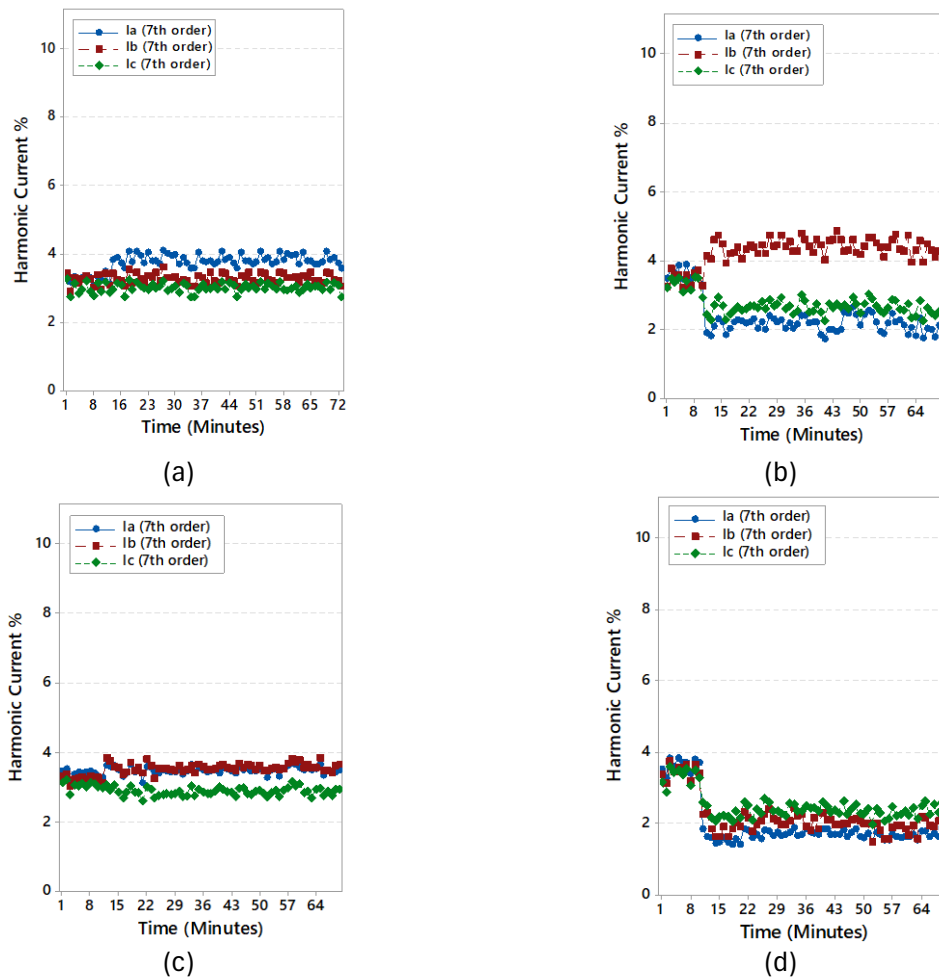


**Figure 5-10** - Seventh harmonic currents variations for phases a-b-c for the IE4 Class motor for (a) 1% VU with Under Voltage; (b) 4% VU with Under Voltage; (c) 1% VU with Over Voltage; (d) 4% VU with Over Voltage

In addition to the variation provoked in harmonic content present in the current waveform, VU also results in the creation of new harmonics, primarily for high unbalance percentages in the analyzed output powers. Figure 5-11 and Figure 5-12 presents the main current harmonics found for the IE3 and IE4 class motors for 4% unbalance with undervoltage and overvoltage, respectively.

The presence of permanent magnets results in a higher harmonic content for the 0.75 kW LSPMM mainly with higher order harmonics. In Figure 5-11b it is shown how 19th and 23rd order harmonics are present in the waveform before the motor is subjected to VU. Then with the presence of 4% VU with under voltage the 7th harmonic order component suffers a decrease, while the 5th, 19th and 23rd order components undergo increases, in addition it can be seen how a 21st order component arises with the presence of voltage unbalance. Then, Figure 5-12b shows how with the VU with overvoltage the present harmonics in the LSPMM tend to decrease,

except for the 21st order harmonic that appears with this VU condition at this motor output power.

This scenario occurs only for the LSPMM, while the IE2 and IE3 class motors show only 5th and 7th current harmonic variations, as shown in Figure 5-11a and Figure 5-12a, but the three analyzed motors presented greater oscillations for these harmonic orders.

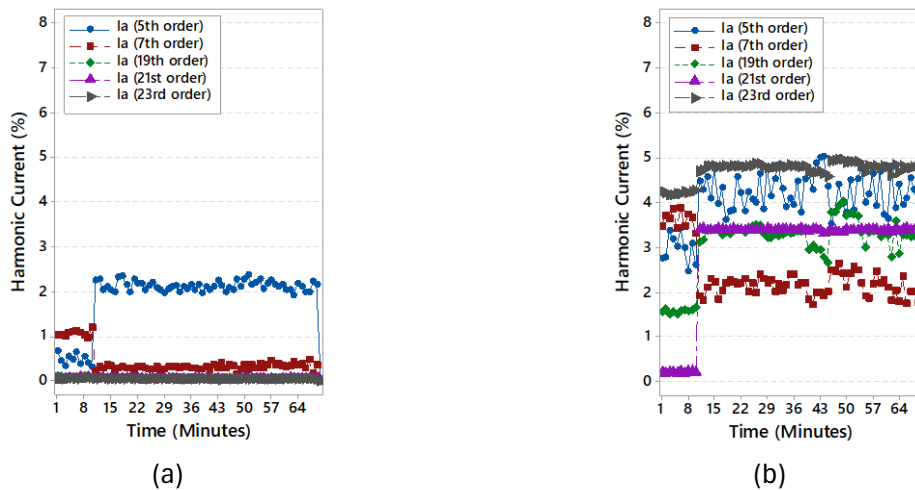


**Figure 5-11** - Phase “a” harmonic current variation for 4% Voltage unbalance with undervoltage for (a) IE3 and (b) IE4 Class motors

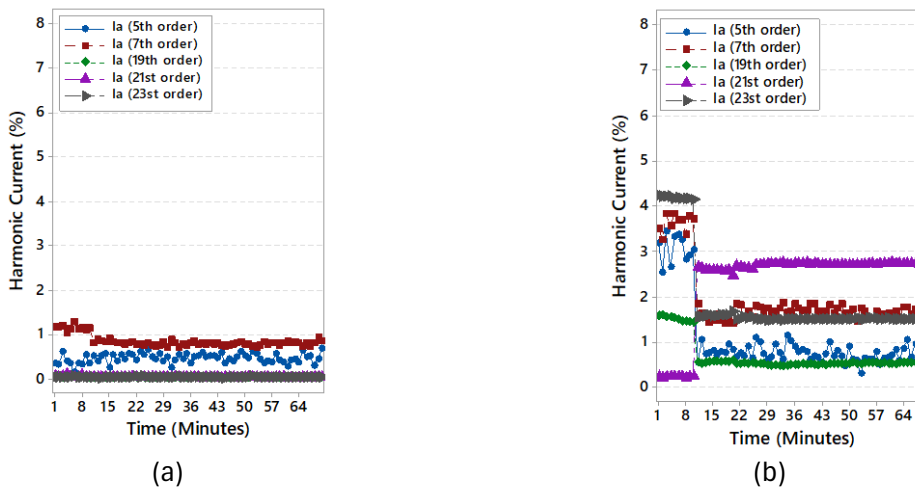


**Figure 5-12** - Phase “a” harmonic current variation for 4% Voltage unbalance with overvoltage for IE3 (a) and IE4 (b) Class motors

As a consequence of the current harmonic variation resulting from the voltage unbalance, the total current harmonic distortion also undergoes variations in relation to ideal power conditions as was presented before with the THDI of each motor for each analyzed unbalance condition.

## 5.5. Final Considerations

The results showed that the presence of voltage harmonics may result in amplification of current harmonics in electric motors for distortion percentages greater than 8% as well as in significant variations of other harmonic currents in the analyzed electric motors including negative and positive sequence harmonics, which ends up increasing the total harmonic distortion rate of the network. It was also observed how these new harmonics presented higher percentages for the higher efficiency motor analyzed (line-start permanent magnet motor).

This chapter also presented how the voltage unbalance results in an increase in the current total harmonic distortion for the three technologies, with higher percentages for the LSPMM. Finally, from the results presented, it is possible to establish some general guidelines that may be considered as recommendations:

- Replacing old/non-efficient electric motors with higher efficiency motors results in better economic benefits for the end user.
- New technologies can represent a challenge for electric utilities mainly in terms of power quality and large-scale uses.
- The study also recommends that consideration be given to oversized motors, given their prevalence in industry and the impact of oversizing on motor efficiency.
- Regulatory institutions must also observe the power quality impacts of higher efficient motors, so that manufacturers implement solutions to the challenges that the implementation of new technologies in induction motors can bring to the electric power systems.

Despite the observed impacts of voltage unbalance and voltage harmonics on power quality, the analyzed sample (three electric motors) only allows us to conclude in relation to this output power (0.75 kW). In this way, it is important to analyze the effects observed in this work with a larger sample of motors of different powers in accordance with IEC 60034-30-1 to make more general conclusions.

The next chapter discusses the effects of voltage variation on efficient motors at different voltage levels, with undervoltage and overvoltage.

## 5.6. Chapter Bibliography

- [1] “US Department - Energy Police Act 1992 (EPAAct), Public Law 102-486 - Oct. 24, 1992.” Accessed: Jul. 26, 2020. [Online]. Available: <https://afdc.energy.gov/files/pdfs/2527.pdf>
- [2] OFFICIAL DIARY OF THE UNION, “INTERMINISTERIAL ORDINANCE N° 1, OF 29 JUNE 2017 - National Press.” Accessed: Mar. 08, 2020. [Online]. Available: <http://www.in.gov.br/materia>
- [3] A. Anibal, B. Rob, B. Conrad U., D. Martin, and H. William, “Motor MEPS Guide, 1st Edition Zurich Switzerland, February.” 1st Edition Zurich Switzerland, Feb. 2009. Accessed: May 27, 2020. [Online]. Available: [https://www.motorsystems.org/files/otherfiles/0000/0100/meps\\_guide\\_feb2009.pdf](https://www.motorsystems.org/files/otherfiles/0000/0100/meps_guide_feb2009.pdf)
- [4] A. Fytrou-Moschopoulou, “European Commission: Good practice in energy efficiency,” Build Up. Accessed: Jul. 19, 2020. [Online]. Available: <https://www.buildup.eu/en/practices/publications/european-commission-good-practice-energy-efficiency-0>
- [5] “Minimum Energy Performance Standards (MEPS) – Policies,” IEA. Accessed: Jul. 26, 2020. [Online]. Available: <https://www.iea.org/policies/333-minimum-energy-performance-standards-meps>
- [6] ANEEL, “CALL N°. 002/2015 PRIORITY ENERGY EFFICIENCY PROJECT: ‘ENCOURAGING THE REPLACEMENT OF ELECTRIC MOTORS: PROMOTING ENERGY EFFICIENCY IN THE DRIVING POWER SEGMENT.’” Accessed: Mar. 08, 2020. [Online]. Available: [https://www.aneel.gov.br/sala-de-imprensa-exibicao/-/asset\\_publisher/XGPXSqdMFHrE/content/chamada-de-projeto-para-incentivar-substituicao-de-motores-eletricos-e-prorrogada/656877?inheritRedirect=false](https://www.aneel.gov.br/sala-de-imprensa-exibicao/-/asset_publisher/XGPXSqdMFHrE/content/chamada-de-projeto-para-incentivar-substituicao-de-motores-eletricos-e-prorrogada/656877?inheritRedirect=false)
- [7] IEC 60034-30-1:2014, “Rotating electrical machines - Part 30-1: Efficiency classes of line operated AC motors (IE code).” Accessed: Aug. 15, 2019. [Online]. Available: <https://webstore.iec.ch/publication/136>
- [8] H. Kärkkäinen, L. Aarniovuori, M. Niemelä, J. Pyrhönen, and J. Kolehmainen, “Technology comparison of induction motor and synchronous reluctance motor,” in *IECON 2017 - 43rd Annual Conference of the IEEE Industrial Electronics Society*, Oct. 2017, pp. 2207–2212. doi: 10.1109/IECON.2017.8216371.
- [9] R. M. Pindoriya, B. S. Rajpurohit, R. Kumar, and K. N. Srivastava, “Comparative analysis of permanent magnet motors and switched reluctance motors capabilities for electric and hybrid electric vehicles,” in *2018 IEEMA Engineer Infinite Conference (eTechNXT)*, Mar. 2018, pp. 1–5. doi: 10.1109/ETECHNXT.2018.8385282.
- [10] A. Castagnini, T. Käsäkangas, J. Kolehmainen, and P. S. Termini, “Analysis of the starting transient of a synchronous reluctance motor for direct-on-line applications,” in *2015 IEEE International Electric Machines Drives Conference (IEMDC)*, May 2015, pp. 121–126. doi: 10.1109/IEMDC.2015.7409047.
- [11] A. Tintelecan, A. C.- Dobra, and C. Martiş, “Life Cycle Assessment Comparison of Synchronous Motor and Permanent Magnet Synchronous Motor,” in *2020 International Conference and Exposition on Electrical And Power Engineering (EPE)*, Oct. 2020, pp. 205–210. doi: 10.1109/EPE50722.2020.9305636.
- [12] C. Li, D. Xu, and G. Wang, “High efficiency remanufacturing of induction motors with interior permanent-magnet rotors and synchronous-reluctance rotors,” in *2017 IEEE Transportation Electrification Conference and Expo, Asia-Pacific (ITEC Asia-Pacific)*, Aug. 2017, pp. 1–6. doi: 10.1109/ITEC-AP.2017.8080993.
- [13] U.S. Department of Energy, Energy Efficiency & Renewable Energy, “Premium Efficiency Motor Selection and Application Guide – A Handbook for Industry,” Energy.gov. Accessed: Aug. 15, 2019. [Online]. Available: <https://www.energy.gov/eere/amo/downloads/premium-efficiency-motor-selection-and-application-guide-handbook-industry>
- [14] NEMA MG1-2016, “Motors and Generators.” Accessed: Aug. 15, 2019. [Online]. Available: <https://www.nema.org/Standards/Pages/Motors-and-Generators.aspx>

- [15] user\_administrator, “National action plans and annual progress reports,” Energy - European Commission. Accessed: Jul. 26, 2020. [Online]. Available: [https://ec.europa.eu/energy/topics/energy-efficiency/targets-directive-and-rules/national-energy-efficiency-action-plans\\_en](https://ec.europa.eu/energy/topics/energy-efficiency/targets-directive-and-rules/national-energy-efficiency-action-plans_en)
- [16] “Database of State Incentives for Renewables & Efficiency®,” DSIRE. Accessed: Jul. 26, 2020. [Online]. Available: <https://www.dsireusa.org/>
- [17] “NEXT GENERATION ELECTRIC MACHINES – Project Descriptions,” Energy.gov. Accessed: Jul. 26, 2020. [Online]. Available: <https://www.energy.gov/eere/amo/next-generation-electric-machines-project-descriptions>



## Chapter 6

# Voltage Magnitude Variation Impacts on Efficient Electric Motors

Globally, the operating voltage may differ from the nominal voltage of the IM nameplate, according to the IEC 60038-2009. Therefore, the performance of new technologies under conditions of voltage variations (VVs) must also be assessed. This chapter presents a comprehensive analysis of a 0.75 kW line-start permanent-magnet motor (LSPMM) under different VV magnitudes while considering different load conditions. The study incorporates technical, economic, statistical, and thermal analyses to obtain important indicators related to power consumption, efficiency, power factor, and temperature.

### 6.1. General Considerations

The forthcoming global minimum energy performance standard (MEPS) regulations for electric motors will incorporate the IE4 efficiency class and cover a wider range of power outputs in rotating machines. To meet the efficiency requirements set by the IEC 60034-30-1 [1] for new efficiency classes, manufacturers have implemented new technologies such as permanent magnets and reluctance motors. These advancements have led to important benefits in terms of energy consumption, power factor, temperature, and noise reduction [2], [3]. These benefits have allowed motors to achieve higher efficiencies, such as the IE4 class, which has become mandatory in Europe since July 2023 for motors with output powers between 75 and 200 kW [4].

Furthermore, only a limited number of users in these regions have adopted new technologies, such as the LSPMM. Manufacturer recommendations and the inclusion of LSPMM technologies in equipment used in industrial processes have primarily influenced these decisions. The introduction of these technologies in electric motors requires comprehensive performance evaluations under diverse operating conditions prevalent in global industries. Such evaluations aim to validate these emerging technologies as viable alternatives to the conventional squirrel-cage induction motors (SCIMs) that currently dominate the market.

## 6.2. Theoretical Foundation

### 6.2.1. Standard IEC 60038-2009

Table 1 of the IEC 60038-2009 standard [5, p. 2009] lists the voltage options for AC systems, as presented in Figure 6-1. For 60 Hz three-phase systems, more than seven voltage options, such as 208, 230, 240, 277, or 400–480 V, are available without considering the voltage drops within the consumer or the distribution system, which can further exacerbate this voltage-magnitude deviation. Internal changes in the industry, such as tap adjustments in transformers or low-load conditions in the electricity distribution system, can also cause VV. Thus, VV can be linked to the difference between the electrical system voltages in a particular country or region and the nominal manufacturing voltages of the motors (Figure 4-1). For example, an electric motor manufactured in Brazil with a nominal voltage of 220 V can operate in Central America at a voltage of 208 V (transformer secondary windings in Y) or 240 V (transformer secondary windings in a triangle).

**Table 1 – AC systems having a nominal voltage between 100 V and 1 000 V inclusive and related equipment**

Three-phase four-wire or three-wire systems		Single-phase three-wire systems
Nominal voltage V		Nominal voltage V
50 Hz	60 Hz	60 Hz
–	120/208	120/240 <sup>d</sup>
230 <sup>c</sup>	240 <sup>c</sup>	–
230/400 <sup>a</sup>	230/400 <sup>a</sup>	–
–	277/480	–
–	480	–
–	347/600	–
–	600	–
400/690 <sup>b</sup>	–	–
1 000	–	–

<sup>a</sup> The value of 230/400 V is the result of the evolution of 220/380 V and 240/415 V systems which has been completed in Europe and many other countries. However, 220/380 V and 240/415 V systems still exist.

<sup>b</sup> The value of 400/690 V is the result of the evolution of 380/660 V systems which has been completed in Europe and many other countries. However, 380/660 V systems still exist.

<sup>c</sup> The value of 200 V or 220 V is also used in some countries.

<sup>d</sup> The values of 100/200 V are also used in some countries on 50 Hz or 60 Hz systems.

**Figure 6-1** - Image of Table 1 of the IEC 60038-2009 standard in relation to allowable voltages in power systems worldwide [5, p. 2009].

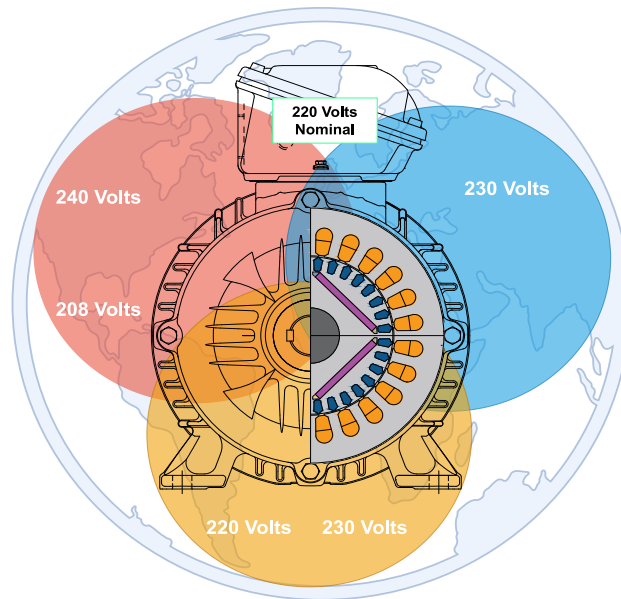


**Figure 6-2** - Three-phase nominal voltage by region for a nominal 220 V LSPMM in a delta connection.

Regarding electric motors, the NEMA MG1-2021 [6] standard stipulates that AC motors should operate successfully at a nominal load under voltage conditions of  $\pm 10\%$  of the nominal voltage. However, the performance of the motors under these conditions will differ from that under the nominal voltage. The evaluation of the LSPMM under VV conditions, including undervoltage and overvoltage, for the analyzed 0.75 kW motor will allow the evaluation of the response of this technology to such disturbances.

### 6.2.2. Permanent-Magnet Motors

The incorporation of permanent magnets into motors represents an important advancement in the pursuit of improved efficiency. The magnetic field provided by these magnets not only reduces magnetization and total current but also allows the synchronism speed. This yields a constant speed under load and different disturbances. In addition, it leads to a notable reduction in rotor losses and consequently lowers operating temperatures, therefore contributing to the durability of the motor and its components.

Among rare-earth materials, neodymium–iron–boron (NdFeB) magnetic materials are widely used in electric motors because of their superior magnetic properties (coercivity and remanent magnetization) over those of other rare elements [7]. Figure 3-19 shows the magnetic flux lines in the LSPM and its internal components.

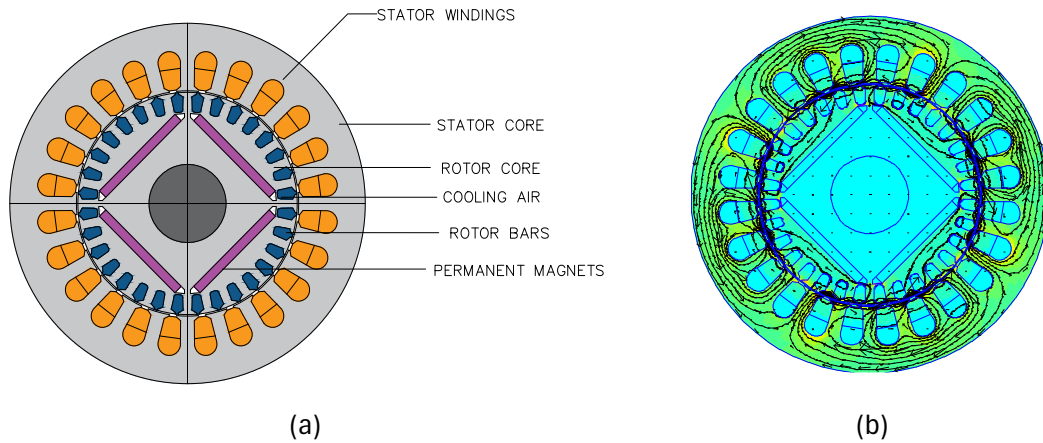


**Figure 6-3** - Line-start permanent magnet: (a) Component description in the first panel and (b) magnetic flux lines.

The presence of permanent magnets in the analyzed 0.75 kW IE4 Class motor (Figure 6-4a) results in a different current-versus-load curve compared with the SCIM (Figure 6-4b). The LSPMM has a squirrel cage, which provides self-starting capability and enables synchronous operation. In this state, no current flows through the rotor bars because the slip is zero, and there are no harmonic components in the airgap magnetomotive force. The LSPMM is a synchronous machine; however, because of the magnets inside the rotor, it produces magnetic fields without an external field current. Its no-load operation resembles that of a synchronous machine operating in an under-excited state. The current-versus-load curve of the LSPMM exhibits a V shape, particularly under low-load conditions; this curve demonstrates a small decrease in the case of the line current with the increasing load. From a 40% load, the current then increases with the load on the motor, as in the IE3 Class SCIM.

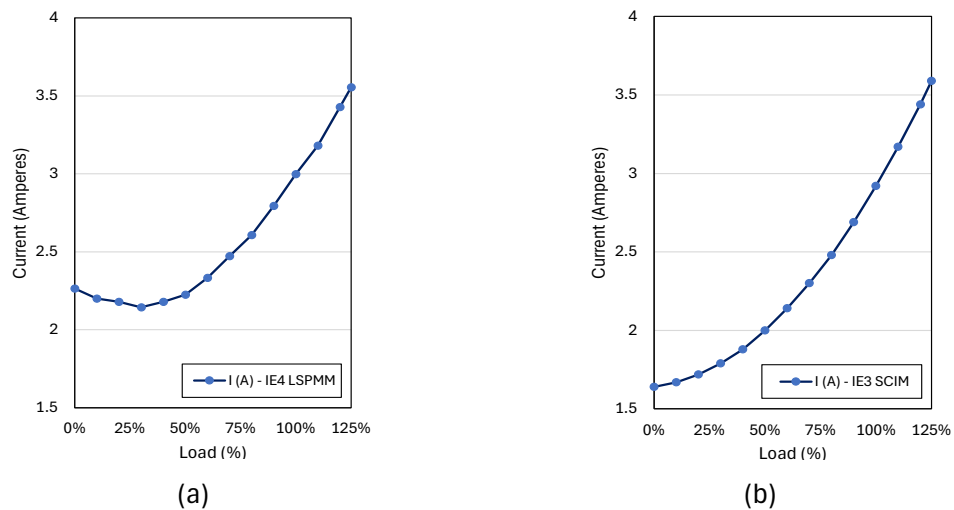


**Figure 6-4** - Experimental input current as a function of load for 0.75 kW: (a) IE4 Class LSPMM and (b) IE3 Class SCIM motor at nominal voltage and frequency conditions.

### 6.3. Assessing Voltage Magnitude Variation in IE2, IE3 & IE4 classes IMs.

#### 6.3.1. Standard IEC 60038-2009

The impacts of VV were evaluated using an experimental bench, as presented in Chapter 1. The bench comprises a three-phase alternating current (AC) programmable source (1), in which different voltages applied to the LSPMM (4) were configured. The LSPMM input parameters were measured using a class “A” power-quality analyzer (2), and an electromagnetic brake (3) was used as the electric load.

Figure 6-5 shows the methodology used. The LSPMM was supplied with a delta connection at 220 V, which served as the base voltage for defining the undervoltage and overvoltage values per unit (1 p.u. = 220V). Subsequently, the LSPMM was subjected to VV conditions of 0.90, 0.95, 1.0, 1.05, and 1.10 p.u. while considering loads ranging from 0% to 125%. The LSPMM was powered with VV from the programmable source, and the input data were recorded for further processing and analysis. Simultaneously, thermographic images were captured using a thermographic camera under the nominal-load conditions for each VV condition until thermal equilibrium was reached.

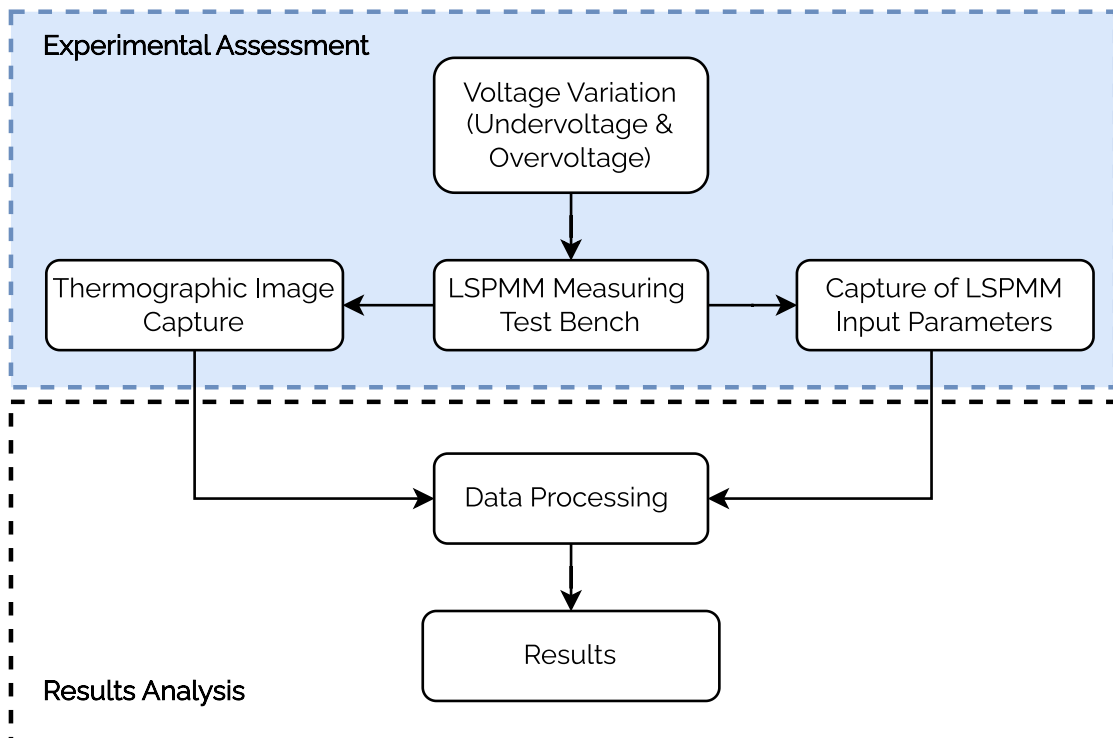


Figure 6-5 - Methodology flowchart.

## 6.4. Technical Assessment

### 6.4.1. Load Curve in VV Conditions

The voltage magnitude is related to the torque at motor start-up. It was noted specifically for this output power that the difficulty of reaching synchronism with nominal-load and nominal voltage conditions was analyzed. Therefore, experiments considering load were conducted after synchronism was achieved. However, in industrial applications with “quadratic torque” characteristics, such as centrifugal pumps and fans, the starting load torque is lower. Therefore, LSPMMs should be capable of starting and achieving synchronism even if the supply voltage is lower than the nominal voltage.

Under VV conditions, the analyzed motor exhibits an input current that varies with the voltage magnitude, particularly below the nominal condition (Figure 6-6). Notably, the same load on the motor shaft was configured for each voltage condition. The undervoltage results in lower input currents for the LSPM motor at loads below the nominal motor power output. Furthermore, for loads exceeding the nominal motor power output, all four analyzed non-nominal-voltage magnitude conditions result in higher currents than that of the nominal-voltage condition, with the VV conditions of 1.05 and 1.10 p.u. with the highest input currents. The deviation in voltages causes a proportional variation in the reactive consumption of the motor, mainly owing to the induced VV in the parallel impedance of the LSPMM. This causes the reactive losses due to the leakage reactance to be greater than those under the nominal-voltage condition.

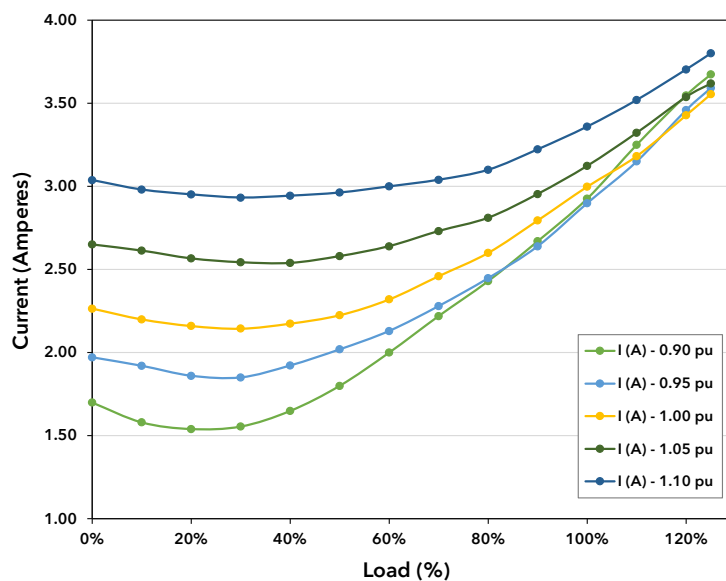


Figure 6-6 - Experimental input current as a function of load at different voltage magnitudes.

### 6.4.2. Active Power and Current Total Harmonic Distortion

Voltage variation inevitably increases Joule and core losses (Figure 6-6), wherein an increase in current can be observed. This is further demonstrated by the active power shown in Figure 6-7a wherein greater differences are observed for smaller loads, which decrease with the increasing motor load. The decrease in voltage magnitude weakens the main flux because of the lower induced voltage. Consequently, the current harmonic content of the LSPMM increases because of the magnets’ constant magnetic fields inside the rotor during the interaction with the stator magnetic fields to produce mechanical power (Figure 6-7b).

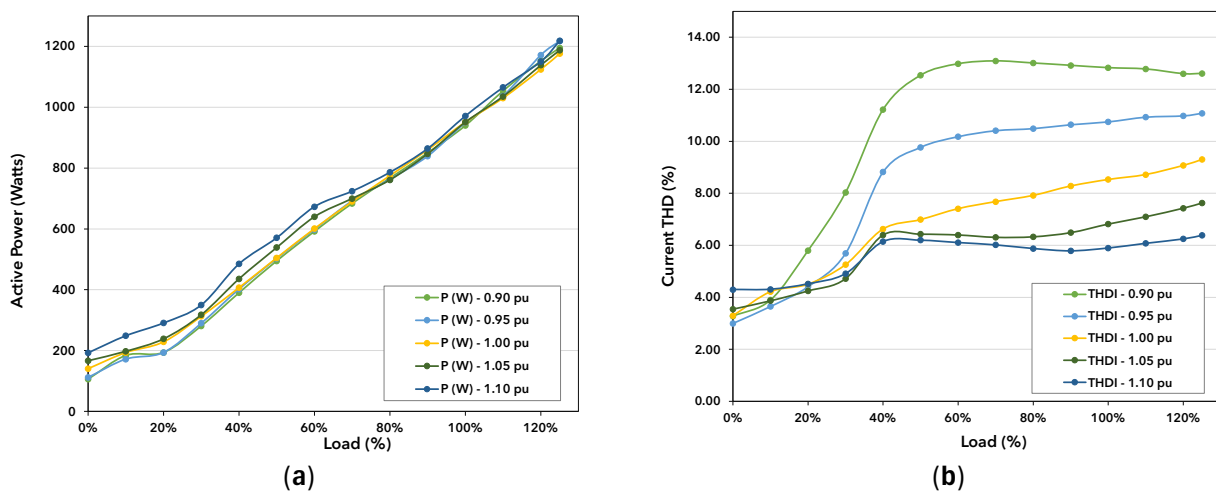
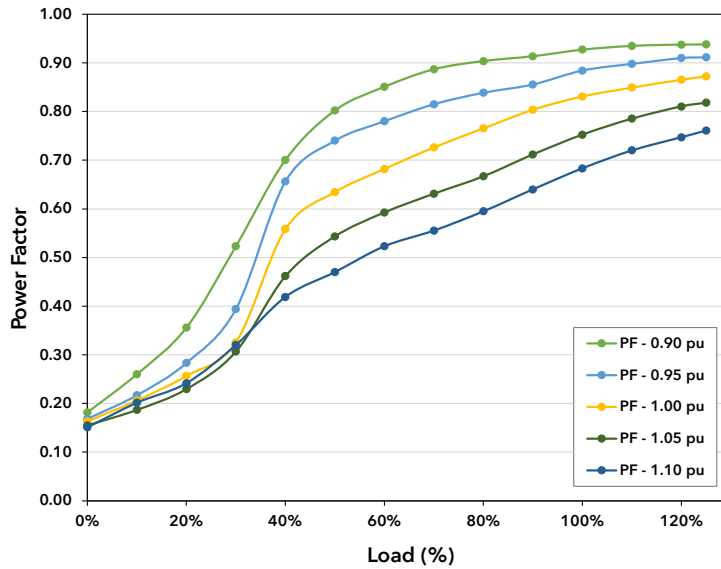


Figure 6-7 - LSPMM under VV conditions. (a) Active power and (b) current total harmonic distortion.

### 6.4.3. Power Factor

The low active power demand on the shaft, combined with the higher reactive power demand, particularly at low loads, results in a considerably low power factor under light-load conditions. Therefore, it is not recommended that this motor operate with loads below 50% to avoid a low power factor. Figure 6-8 illustrates the inversely proportional variation of the power factor with the voltage magnitude below the nominal condition. For instance, the power factor under the 1.10 p.u. condition at the nominal load (100%) is lower than that under the 0.90 p.u. condition at 40% load. This highlights the benefits of undervoltage for the operation of this LSPMM technology under variable load conditions.



**Figure 6-8** - Experimental power factor as a function of load under VV conditions.

Ridgeline plots were plotted for the power factor at each voltage condition based on the measurements shown in Figure 6-8 to better visualize the power factor variation across the load spectrum. Ridgeline plots can be used to visualize data distribution through density plots. In this context, Figure 6-9 presents the power factor point values shown in Figure 6-8. The y-axis represents the five voltage magnitudes assessed in this study, and the x-axis represents the power factor values obtained for different load conditions.

The undervoltage condition mostly represents power factors between 0.60 and 1.0 for most of the motor load curve, while the overvoltage condition represents power values between 0.40 and 0.80. Therefore, in situations where the choice is limited to the undervoltage or overvoltage, the undervoltage remains a more favorable choice in terms of the power factor.

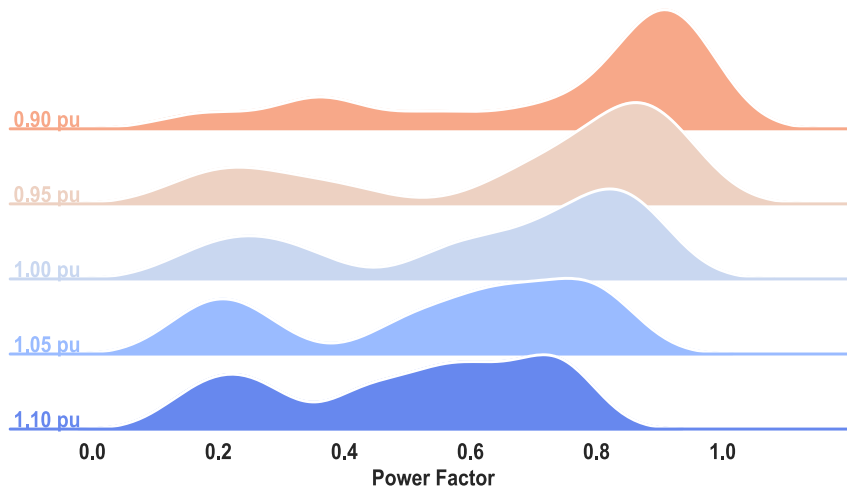


**Figure 6-9** - Ridgeline plot of power factor under VV conditions for the LSPMM.



Another important parameter of interest is active power, which is related to motor load and affects both industry consumption and demand. To present a comparison of the active power with the power factor under VV conditions, contour plots that depict the relationship between the two parameters for the 0.90, 1.0, and 1.10 p.u. conditions as a function of load are presented in Figure 4-8. The contour lines connect points with the same power factor response value, and the colored bands represent the measured power factor values. Figure 4-8a shows the undervoltage positively deviates from the nominal condition at 0.90 p.u in the behavior of the LSPMM, indicating that higher power factor values can be achieved at lower loads on the motor shaft, where lower active powers contribute to a reduction in consumption and demand for end users. Furthermore, Figure 4-8c shows how the overvoltage negatively deviates from the nominal condition (Figure 4-8b), indicating that lower power factors can be obtained along the motor load curve with higher active powers. Therefore, undervoltage is beneficial in this technology because consumption, demand, and power factor are the parameters of interest to specialists.

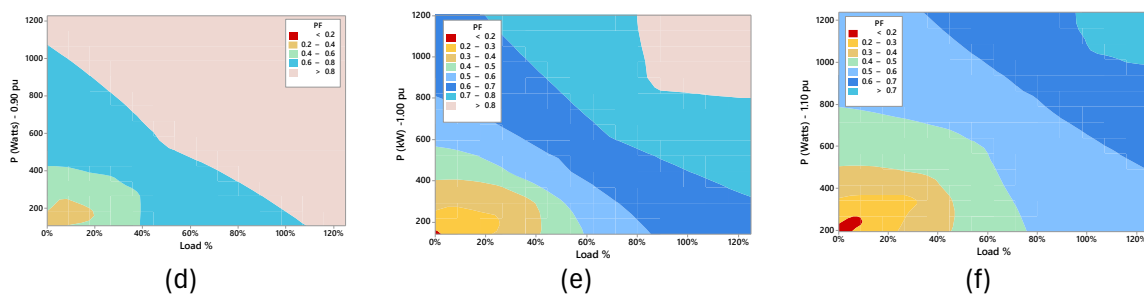


**Figure 6-10** - Contour plots for power factor variation with power and load for IE4 Class motor with (a) 0.90 p.u., (b) 1.00 p.u., and (c) 1.05 p.u.

#### 6.4.4. Efficiency

Synchronism contributes to high efficiency, particularly at low loads. In the case of the LSPMM (Figure 6-11), high efficiency values are obtained first at low loads. This is mainly attributed to the motor current curve (Figure 6-6), in which the current tends to decrease as the load increases up to approximately 30–40%. Consequently, the electrical power decreases, whereas the mechanical power increases, resulting in high efficiencies at these loads. The impact of VV on the LSPMM efficiency is most pronounced at low loads, and similar values are obtained for loads close to nominal loads.

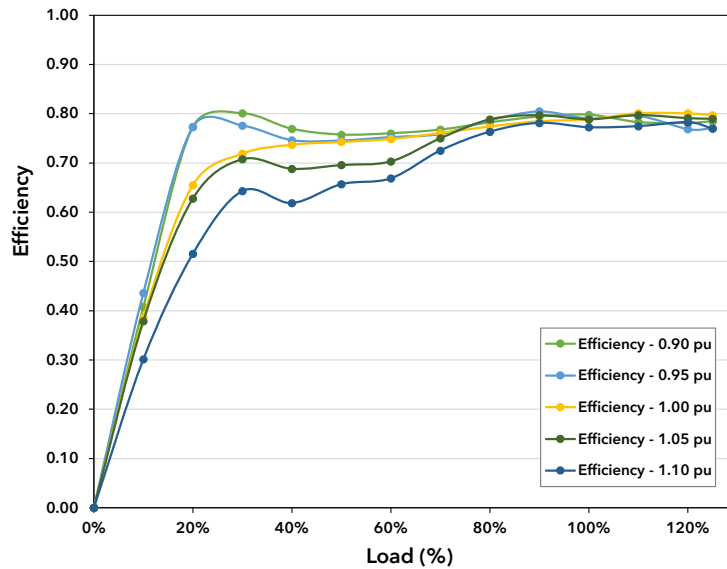


**Figure 6-11** - Experimental efficiency as a function of load under VV conditions.

#### 6.4.5. Temperature Assessment

Thermal load is an important indicator of the condition of an electric motor. To assess the impact of VV on temperature, thermographic images were captured every 2 min until thermal equilibrium was reached for each voltage-magnitude condition considering full load and capturing the lateral (stator) and front (rotor) angles of the motor. Figure 6-12 and Figure 6-13 show photographs of the LSPMM at thermal equilibrium under voltage conditions of 0.90, 1.0, and 1.10, with front and side views, respectively. Each condition results in temperature variations for the same connected load, which can affect the lifespan and maintenance period of electric motors operating under these conditions. The lateral view of the stator and the front view of the rotor reveals a temperature difference ranging from 5.5 °C to 8 °C between voltage magnitudes of 0.90 and 1.10 p.u.

Figure 6-14 illustrates the temperature curve data measured for each voltage magnitude obtained by analyzing the small triangle points in the images using the thermographic camera software version 5.13. The temperature values closely align between the nominal-voltage and overvoltage conditions at 1.10 p.u. This similarity is attributed to the comparable currents observed at the load percentages shown in Figure 6-6. These results indicate that the undervoltage and overvoltage conditions exhibit higher temperatures than the nominal condition, with temperature differences of up to 8 °C higher than the nominal condition.

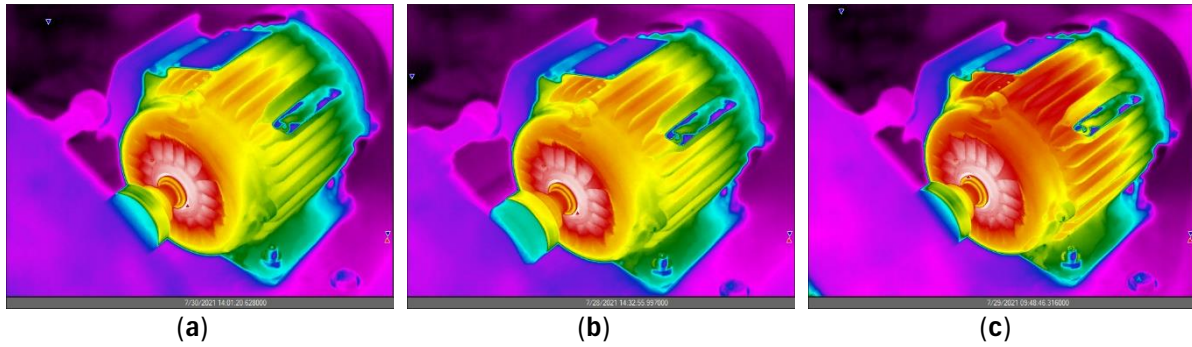


**Figure 6-12** - Frame temperature variation in the LSPMM under VV conditions. Frontal temperature with (a) 0.90 p.u., (b) 1.00 p.u., and (c) 1.10 p.u.

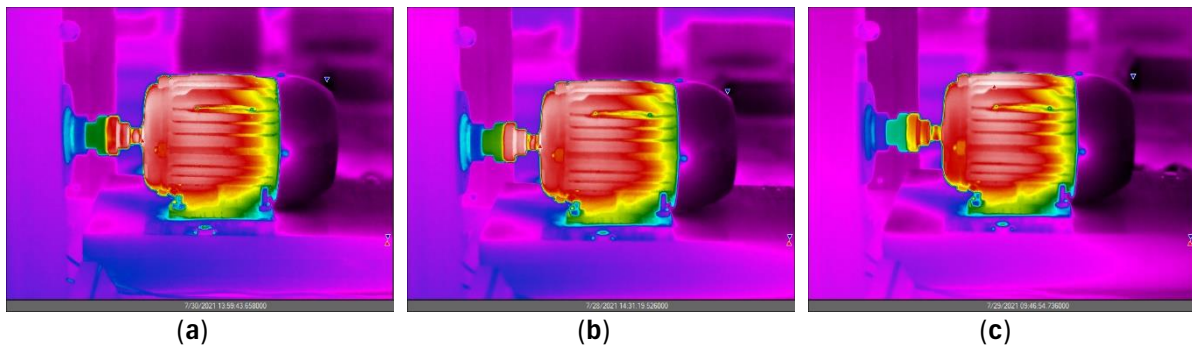


**Figure 6-13** - Frame temperature variation in the LSPMM under VV conditions. Lateral temperature with (a) 0.90 p.u., (b) 1.00 p.u., and (c) 1.10 p.u.

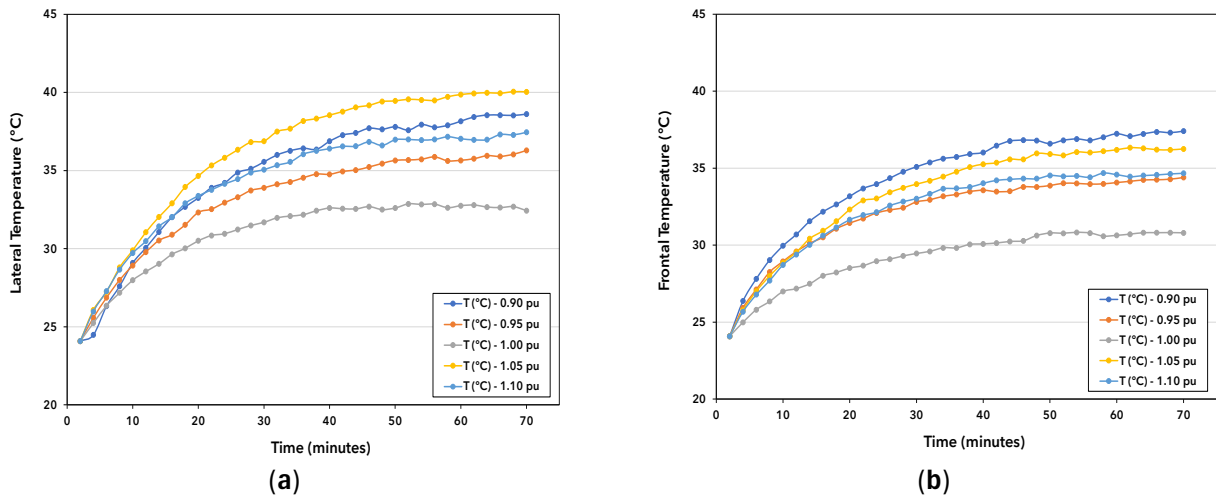


**Figure 6-14** - Measured absolute temperature under VV conditions: (a) lateral view; (b) frontal view.

Although the new efficiency classes have higher temperature tolerances (insulation letters), usually letter F (maximum temperature of 155 °C), the temperature increase continues to be detrimental to the lifespan of the motor by reducing the time between maintenance services. Furthermore, environments with high concentrations of airborne particles, combined with inadequate maintenance, contribute to the degradation of the motor’s internal components, thus reducing its lifespan.

## 6.5. Statistical Assessment

### 6.5.1. Correlation Matrix for Voltage Variation Conditions

To examine the impact of the voltage magnitude on the motor efficiency and power factor, an analysis based on Spearman's correlation was conducted using Minitab version 18 [8]. The analysis assessed the monotonic relationship between the voltage magnitude and various motor input parameters. Spearman's rank correlation coefficient, which is dependent on the ranks of values rather than the actual values themselves, is particularly suitable for ordinal and continuous variables. This method is valuable in situations where Pearson's correlation is unsuitable because of normality violations, nonlinear relationships, or the involvement of ordinal variables [9, p. 84], [10], [11]. Given the identification of a nonlinear relationship among certain variables in this specific case, Spearman's correlation method was selected [12]. The formulation for calculating the Spearman's rank correlation coefficient is presented in Equation (1).

$$r_s = 1 - \frac{6 \sum_{i=1}^n D_i^2}{n(n^2-1)}, \quad (1)$$

where  $n$  represents the number of value pairs and  $D_i = X_i - Y_i$  represents the difference between each corresponding  $X_i$  and  $Y_i$  value rank.

In general, the correlation coefficient resulting from the correlation analysis ranges from  $-1$  to  $+1$ . A higher coefficient indicates a stronger relationship between the variables.

To verify the influence of voltage magnitude variation on the efficiency and power factor, different load ranges were considered, and Spearman correlation coefficients were estimated for each range (Figure 6.15). The load ranges were divided into three blocks: the first block covers load percentages between 0% and 30% (Figure 6.15a), the second block includes loads between 40% and 70% (Figure 6.15b), and the last block comprises loads between 80% and 125% (Figure 6.15c). In these correlation matrices, the upper cell shows the Spearman coefficient, while the lower cell shows the p-value, which helps determine the rejection of the null hypothesis at the assumed significance level of 0.05.

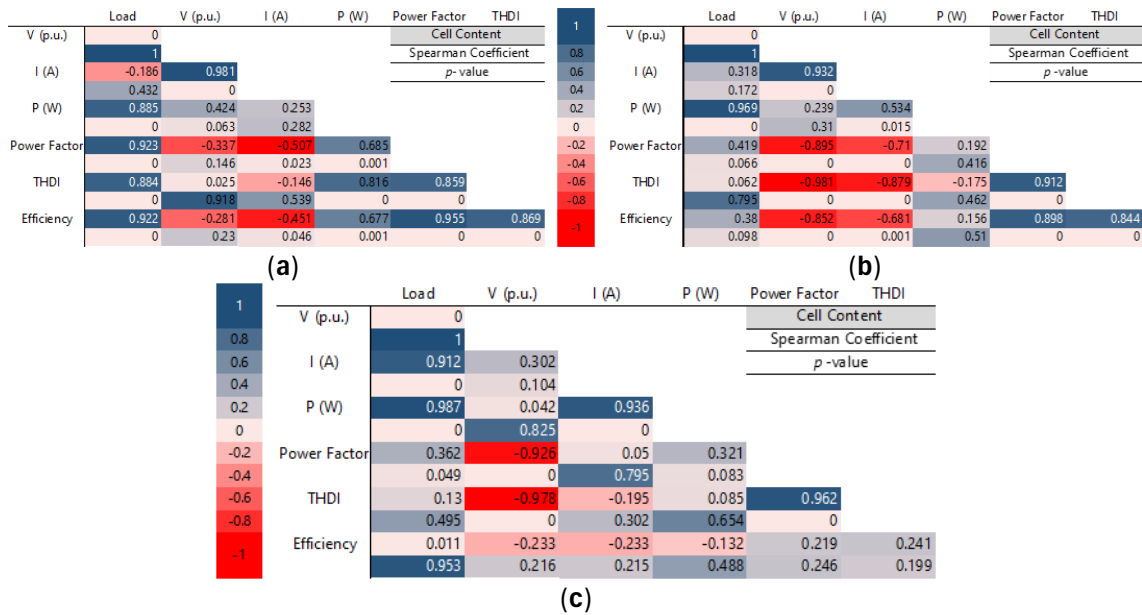


**Figure 6-15** - Correlation matrix between voltage magnitude and input parameters in the LSPMM for (a) output load between 0% and 30%, (b) output load between 40% and 70%, and (c) output load between 80% and 125%.

For the first load block (Figure 6.15 a) the results show that the input parameters, except for the voltage and current magnitudes, show high correlations with the load, indicating that the efficiency and power factor vary proportionally with the load. However, this relationship does not hold for the voltage magnitude, which exhibits low correlations and  $p$ -values of  $>0.05$ . In the second load block (Figure 6.15b), which includes loads between 40% and 80%, the efficiency and power factor vary inversely with the voltage magnitude because they have negative correlation coefficients. Thus, the efficiency and power factor increase with the decreasing voltage magnitude, confirming the results presented in the previous section and indicating that voltage magnitude exerts a greater influence on permanent-magnet motors operating within this load range.

For the higher loads in the range between 80% and 125%, (Figure 6.12c) shows that load exerts a greater influence on the current and active power than the efficiency and power factor. A similar scenario is observed for the voltage magnitude, indicating that for loads close to the nominal load, the voltage magnitude exerts less influence on the efficiency and power factor of the LSPMM analyzed in this study. The correlation matrices show that the voltage magnitude influences the efficiency of the LSPMM at certain load percentages, with lesser influence at lower loads (below 40%) and higher loads (above 80%) analyzed in this study.

## 6.6. Economic Analysis

Differences in currents, active power, efficiency, and power factor resulting from VV in the LSPMM were observed. To quantify these impacts, an economic analysis was conducted considering users in regions where the supply voltage magnitude for electric motors is determined according to the transformer's secondary connection. In this case, Honduras, located in Central America, was used as a reference, with three-phase nominal voltages of 208 and 240 V for star and delta connections, respectively.

For economic quantification with respect to each voltage level, the annual energy consumption for each load condition was estimated based on experimental power measurements and considering 6000 h of operation per year. Figure 6-16 shows the approximate energy consumption of the LSPMM under each voltage condition as a function of different voltage magnitudes and loads. Energy consumption increases with the increasing voltage magnitude.

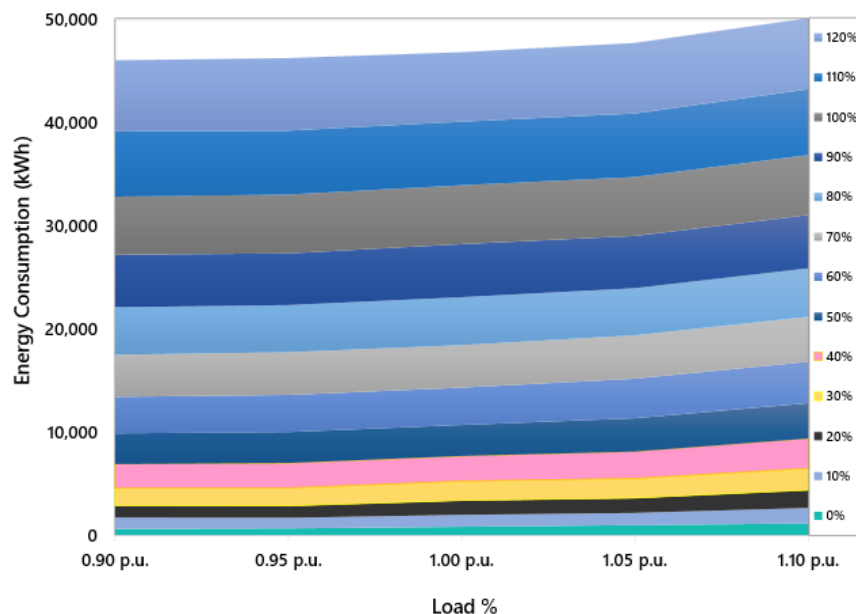


**Figure 6-16** - Consumption as a function of voltage magnitude under different load conditions.

Two scenarios were examined to evaluate the economic benefits of undervoltage. The scenarios involved time-of-use (TOU) pricing, where energy costs varied based on specific times of the day (Figure 6-17). The peak hours covered a 3-hour duration from 18:30 to 21:30, with the remaining hours classified as an off-peak period. During the peak period, a kilowatt-hour (kWh) cost equivalent to ten times (USD 0.8/kWh) that of the off-peak period (USD 0.08/kWh) was considered based on industry references.

In the first scenario, the TOU pricing structure was not considered. In this case, the economic costs and benefits associated with the variation in the voltage magnitude were obtained by multiplying the reduced consumption by a single tariff of USD 0.08/kWh. In the second scenario, two different energy charge rates are implemented: one for off-peak hours with a value of USD 0.08/kWh and the other for peak hours, corresponding to USD 0.8/kWh (Figure 14).

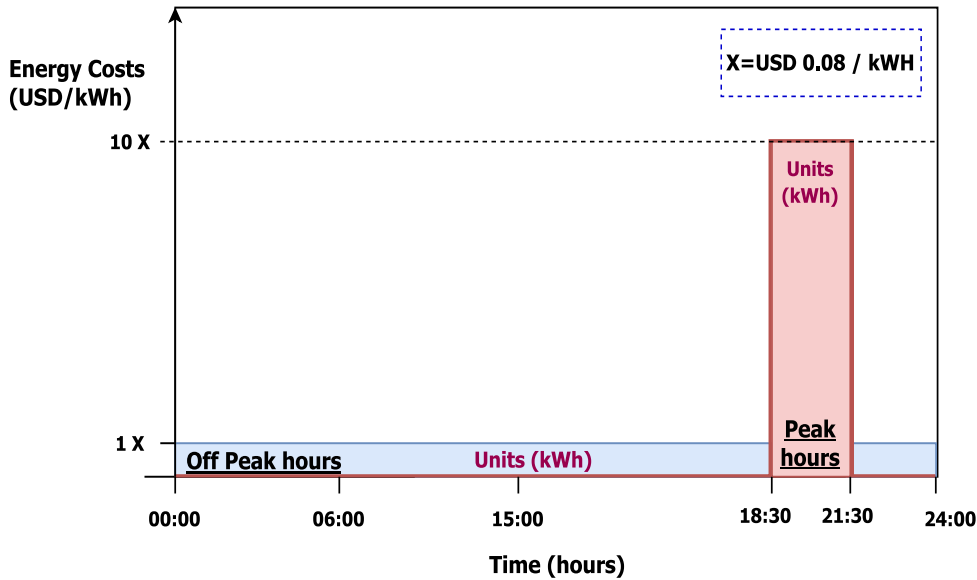


**Figure 6-17** - Representation of the time-of-use tariff pricing scheme considered in the economic analysis.

By comparing the operating costs of the motor under different voltage conditions, the cost difference was determined. This calculation assumes a change in the motor supply from a delta connection with 240 V to a star connection with 208 V for a motor with a nominal voltage of 220 V. This corresponds to a change from 1.10 to 0.95 p.u. at the motor supply voltage (Equation (2)). The energy savings during peak and off-peak periods are determined by multiplying the difference in the active power obtained from Equation (2) by the annual operating time. For this analysis, 5500 yearly operating hours during off-peak periods and 500 yearly operating hours during peak periods were considered.

Equation (5) is used to calculate the total cost savings in USD by taking the sum of the energy consumption multiplied by the cost per kWh in each period (Figure 13). The first scenario considers only the first term of the sum, whereas the second scenario, which incorporates TOU pricing, considers all terms of the equation.

$$P_{1.10 \text{ p.u.}} (\text{kW}) - P_{0.95 \text{ p.u.}} (\text{kW}) = P_{economy} (\text{kW}), \quad (2)$$

$$E_{off-peak} (\text{kWh}) = P_{economy} (\text{kW}) \times (\sum \text{Yearly hours}_{off-peak}), \quad (3)$$

$$E_{peak}(\text{kWh}) = P_{economy}(\text{kW}) \times \left( \sum \text{Yearly hours}_{peak} \right), \quad (4)$$

$$\text{Economy (USD)} = \left\{ E_{off-peak}(\text{kWh}) \times \left[ EC_{off-peak} \left( \frac{\text{USD}}{\text{kWh}} \right) \right] \right\} + \left\{ E_{peak}(\text{kWh}) \times \left[ EC_{peak} \left( \frac{\text{USD}}{\text{kWh}} \right) \right] \right\}, \quad (5)$$

where  $P_{1.10 \text{ p.u.}}$  (kW) and  $P_{0.95 \text{ p.u.}}$  (kW) represent the active powers measured for each load condition with 1.10 and 0.95 p.u. voltage magnitudes, respectively;  $\sum \text{Yearly hours}_{peak}$  and  $\sum \text{Yearly hours}_{off-peak}$  represent the sum of operation hours in the peak and off-peak periods, respectively;  $E_{peak}$  (kWh) and  $E_{off-peak}$  (kWh) represent the energy consumption in the peak and off-peak periods, respectively, and  $EC_{off-peak}$  and  $EC_{peak}$  represent the energy costs in  $\left( \frac{\text{USD}}{\text{kWh}} \right)$  for the off-peak and peak periods, respectively.

Equation (6) was used to estimate the payback period [13, p. 6]. The analysis was based on the initial cost of an IE3-efficiency class motor with the same power output to assess the impact of altering the motor supply voltages under each load condition. Figure 6-18 shows the results for the two analyzed scenarios. For the first scenario (Figure 6-18a), the estimations indicate that for loads below 60%, decreasing the voltage magnitude from 1.10 to 0.95 p.u. can result in cost advantages that would enable the purchase of a new motor with the savings generated over its lifetime. This highlights the benefits of this analysis. For the second scenario (Figure 6-18b), where a peak time and a ten-fold higher energy cost are considered, the payback period is reduced to less than 10 years for any load percentage and less than 5 years for loads below 60%. Given that this is a widely used tariff in the industry, the study can be valuable for specialists and engineers aiming to reduce energy consumption through energy efficiency measures. However, the load percentage and power output must be verified because this study was limited to a motor with an output power of 0.75 kW.

$$PBP \text{ (years)} = \frac{P}{\text{Economy (USD)}}, \quad (6)$$

where  $PBP$  represents the payback period in years,  $P$  represents the total project investment and  $\text{Economy (USD)}$  represents the annual cash flow in USD/year.



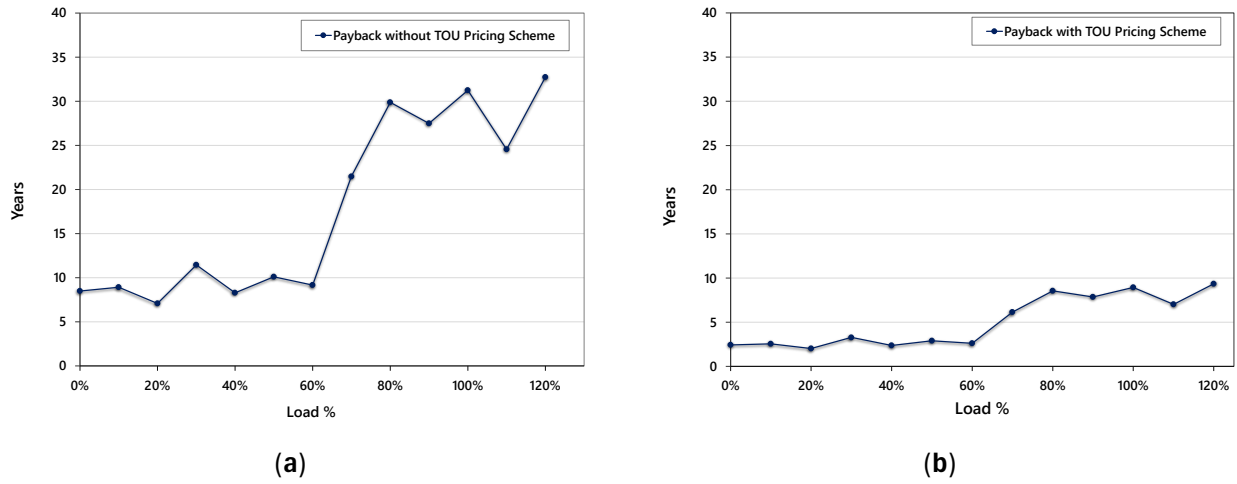


**Figure 6-18** - Payback for the initial cost of a new motor by changing the LSPMM voltage supply level: (a) without considering the TOU; (b) considering the TOU.

## 6.7. Final Considerations

Given that the LSPMM is a relatively new technology, an electrical assessment was conducted by considering the voltages found in different electrical systems as well as diverse load scenarios and analyzing the parameters of interest to end users. Findings indicate that operating a motor under undervoltage conditions (0.90 p.u.) results in higher efficiencies, an improved power factor, and lower operating temperatures. These outcomes translate into enhanced economic benefits and an extended motor lifespan. However, specialists should analyze the results presented to make optimal use of them according to the type and nature of the loads. The results show that the impact of voltage-magnitude variation is minimized under nominal-load and overload conditions. Undervoltage is not the best alternative under these conditions.

Considering the type of application, because the starting torque depends on the input voltage, undervoltage may limit the starting torque with heavy motor-shaft loads. Therefore, undervoltage is mainly recommended for loads with quadratic torque characteristics, such as centrifugal pumps and fans, where the starting load torque is lower when compared to other loads' torque characteristics. Results of the statistical analysis based on Spearman correlation matrices revealed that the voltage magnitude exerts a greater influence on the efficiency and power factor for loads ranging between 40% and 80% of the motor output power.

Temperature is a critical parameter because it is related to the performance, lifespan, and maintenance frequency of permanent magnets and electric motors. Therefore, the impacts of different voltage magnitudes on temperature are presented and discussed. The results of the electrical analysis align with those of the thermal analysis, demonstrating that overvoltage leads to operating temperatures up to 7°C higher than that in the case of undervoltage and 3°C higher than that in the case of the nominal condition. This temperature difference can affect the lifespan of the LSPMM.

As part of the contributions of this thesis and considering the impact that different disturbances can have on the useful life of electric motors, the following chapter proposes an indicator of the health of electric motors when subjected to different power quality disturbances. energy from a frequency domain approach and analysis.

## 6.8. Chapter Bibliography

- [1] “IEC 60034-2-1:2014 | IEC Webstore | energy efficiency, smart city.” Accessed: Jul. 27, 2022. [Online]. Available: <https://webstore.iec.ch/publication/121>
- [2] A. T. de Almeida, J. Fong, H. Falkner, and P. Bertoldi, “Policy options to promote energy efficient electric motors and drives in the EU,” *Renewable and Sustainable Energy Reviews*, vol. 74, pp. 1275–1286, Jul. 2017, doi: 10.1016/j.rser.2017.01.112.
- [3] A. De Almeida, J. Fong, C. U. Brunner, R. Werle, and M. Van Werkhoven, “New technology trends and policy needs in energy efficient motor systems - A major opportunity for energy and carbon savings,” *Renewable and Sustainable Energy Reviews*, vol. 115, p. 109384, Nov. 2019, doi: 10.1016/j.rser.2019.109384.
- [4] “Electric motors and variable speed drives,” European Commission - European Commission. Accessed: Nov. 25, 2022. [Online]. Available: [https://ec.europa.eu/info/energy-climate-change-environment/standards-tools-and-labels/products-labelling-rules-and-requirements/energy-label-and-ecodesign/energy-efficient-products/electric-motors\\_en](https://ec.europa.eu/info/energy-climate-change-environment/standards-tools-and-labels/products-labelling-rules-and-requirements/energy-label-and-ecodesign/energy-efficient-products/electric-motors_en)
- [5] “IEC 60038:2009 | IEC Webstore | rural electrification, LVDC.” Accessed: Nov. 28, 2022. [Online]. Available: <https://webstore.iec.ch/publication/153>
- [6] “Motors and Generators,” NEMA. Accessed: Jul. 04, 2022. [Online]. Available: <https://www.nema.org/standards/view/motors-and-generators>
- [7] J. Cui *et al.*, “Current progress and future challenges in rare-earth-free permanent magnets,” *Acta Materialia*, vol. 158, pp. 118–137, Oct. 2018, doi: 10.1016/j.actamat.2018.07.049.
- [8] “Minitab 18 Statistical Software (2010). [Computer software]. State College, PA: Minitab, Inc. ([www.minitab.com](http://www.minitab.com)).” Accessed: Aug. 15, 2019. [Online]. Available: <https://www.minitab.com/es-mx/>
- [9] C. Heumann and Shalabh, Michael Schomaker, *Introduction to Statistics and Data Analysis With Exercises, Solutions and Applications in R /*, 1st ed. Gewerbestrasse 11, 6330 Cham, Switzerland: Springer International Publishing AG, 2016. [Online]. Available: 10.1007/978-3-319-46162-5
- [10] G. G. de O. Costa, *Probabilidades e Estatísticas Inferencial: Teoria e Prática*, 2nd Edition. Brazil: EDITORA ATLAS S.A., 2018. Accessed: Jun. 16, 2020. [Online]. Available: <https://www.institutodeengenharia.org.br/site/2018/07/25/livro-curso-de-probabilidades-e-estatisticas-inferencial-teoria-e-pratica/>
- [11] “Spearman’s Rank-Order Correlation - A guide to when to use it, what it does and what the assumptions are.” Accessed: Jun. 16, 2020. [Online]. Available: <https://statistics.laerd.com/statistical-guides/spearmans-rank-order-correlation-statistical-guide.php>
- [12] Minitab, 2018, “A comparison of the Pearson and Spearman correlation methods,” Minitab 18, Support. [Online]. Available: <https://support.minitab.com/en-us/minitab/18/help-and-how-to/statistics/basic-statistics/supporting-topics/correlation-and-covariance/a-comparison-of-the-pearson-and-spearman-correlation-methods/#comparison-of-pearson-and-spearman-coefficients>
- [13] I. Dincer and A. Abu-Rayash, “Chapter 6 - Sustainability modeling,” in *Energy Sustainability*, I. Dincer and A. Abu-Rayash, Eds., Academic Press, 2020, pp. 119–164. doi: 10.1016/B978-0-12-819556-7.00006-1.

## Chapter 7

### Electric Motor Degradation Index (EMDI)

Electric motors remain the world's largest load and a critical piece in the industrial sector. Given its important role in industrial, commercial, and modern applications, significant efforts have been dedicated to predictive maintenance, aiming to enhance existing techniques with new proposals that increase their effectiveness in diagnosing the health of rotating machines. This Chapter proposes an Electric Motor Degradation Indicator (EMDI), which relies on signal processing techniques for the frequency spectrum analysis of electric motors' input current waveforms. The presented results strongly support the efficacy of the proposed approach in facilitating the implementation of predictive maintenance practices.

#### 7.1. Introduction

##### 7.1.1. General Considerations

Electric motor diagnosis remains a crucial aspect within industries, as it represents one of their key assets, given the economic costs associated with unplanned downtime. Consistently, higher-power induction motors are predominantly found in commercial and industrial applications. These motors serve as critical components in manufacturing processes, and any interruption in their operation can result in significant economic losses for businesses. Hence, online monitoring of these motors' performance to extract relevant parameters that can indicate imminent failures is crucial. Implementing predictive maintenance measures based on these indicators can prevent untimely process shutdowns and mitigate the accompanying economic and technical losses. Considering the prevailing trend of integrated production systems in today's world, which emphasizes technological advancements and quality across various sectors of the production chain, predictive maintenance techniques have gained significant importance in the pursuit of productivity in diverse industries.

The methodology proposed here is intended, at the level of maturity at which it will be presented, to be a general diagnostic tool for failures in electric motors, in this way the tool identifies that there is an abnormal operation in the motor, and from this the specialists must evaluate it aiming to guarantee the useful life of the motor from experience as well as from the other identification tools for specific failures.

### 7.1.2. Chapter Motivation and Contribution

In the search for innovative and complementary techniques, this study introduces a novel methodology based on the frequency-domain analysis of electric motor current waveforms. The approach utilizes spectral analysis of the motor's load current during online operation. To accomplish this, the Contact Degradation Indicator (CDI), originally developed for predictive diagnosis of failures in electric power substation bays [2], will be adapted to create the Electric Motor Degradation Indicator (EMDI). By utilizing a degradation coefficient, this methodology aims to provide a reliable reference for assessing the health state of electric motors.

The key feature of the diagnostic system presented here is its ability to generate online predictive indications of electric motor failure conditions. This enables proactive measures to be taken, preventing imminent motor failures and the resulting unavailability. To validate the proposed methodology, comprehensive bench testing will be conducted in a laboratory using induction motors of different efficiency classes. Based on the obtained results, a diagnostic system will be proposed, meeting the specific operational conditions of induction motors. It intends to become a valuable and contemporary tool for monitoring motor-driven systems and implementing predictive diagnoses. By presenting this new methodology, the study aims to contribute to the field of predictive maintenance for electric motors, offering a practical solution for identifying and addressing potential failures on time.

## 7.2. Theoretical Foundation

### 7.2.1. Time-domain and Frequency-domain Analysis

The presence of electric current harmonic distortions during the steady-state operation of electrical systems can be primarily attributed to the nonlinear characteristics of connected electrical loads. However, other factors such as imperfections in electrical connections and contacts, material aging, and insulation degradation also contribute to these distortions. The harmonic distortions typical of the electric loads' dynamics are usually of lower harmonic orders [3], while those from electrical contacts and connections imperfections, material aging, and loss of electric insulation, produce partial micro discharges of high frequencies in the spectrum of flowing electric currents [2].

Consequently, the frequency spectrum of the electric current can be divided into two distinct sections, separated by a cutoff frequency ( $F_c$ ). The low-frequency range ( $f < F_c$ ) primarily reflects

the behavior of the electric load, while the high-frequency range ( $f > F_c$ ) is predominantly associated with the degradation of materials.

Figure 6-1 provides a graphical representation of the proposed analysis methodology. Considering a typical driving load, for example, an electric motor, it is expected that throughout its continuous operation for longer periods, the high-frequency spectrum ( $f > F_c$ ) will become more significant representing the continued degradation of the equipment. That is, the equipment becomes less efficient, presenting larger losses, and following a trajectory that will fatally lead to a failure condition, due to mechanical and/or electrical nature. Then, a metric that calculates the relationship between the frequency spectrum power associated with harmonic distortions of the load (up to the frequency  $F_c$ ), and due to harmonic distortions above the frequency  $F_c$ , continuously during the operation of the electrical system, will be able to evaluate the motor's performance and issue a diagnosis on its degradation state, for predictive maintenance decision-making.

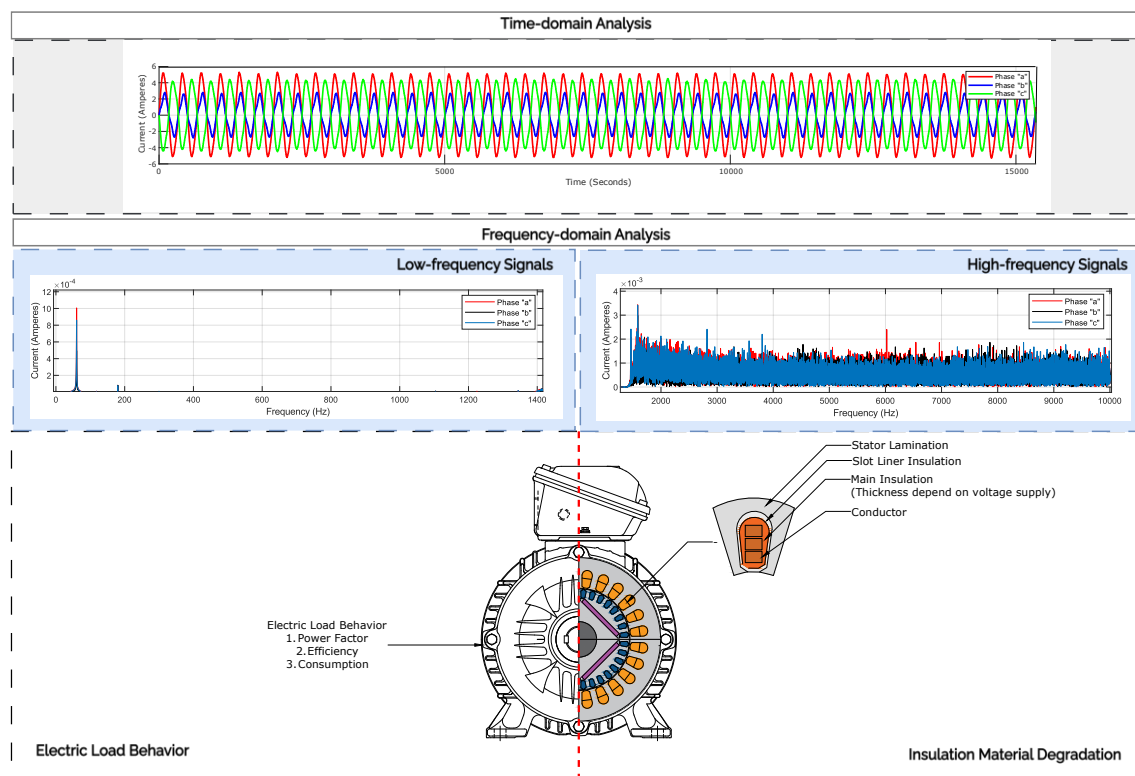


**Figure 7-1** - Graphical representation of the Electric Motor Degradation Index (EMDI) methodology.

The frequency spectrum is obtained by the Fourier transform of the motor's measured load current. The Fourier transform (FT) is used to map time aperiodic signals to the frequency domain, resulting in a continuous frequency spectrum. However, a wide range of engineering problems involves discrete time series, obtained from data acquisition systems such as oscillographs, and

energy quality meters, among others. In these cases, the Fourier Discrete Transform (FDT) version should be used, which is the numerical application of FT, as shown in its definition in equation (1).

$$F_n = \sum_{k=0}^{N-1} f(k) \cdot e^{-j\frac{2\pi}{N}n.k} \quad n = 0, \dots, (N - 1) \quad (1)$$

where:  $N$  – Number of samples by period,  $f(k)$  – Magnitude of each sample, and  $F_n$  the Complex values (module and phase) of the  $N$  sine waves obtained with FDT.

### 7.2.2. Metric for Electric Motor Degradation Measurement

The metric to be used for indicating the electric motor degradation, which is here called EMDI – Electric Motor Degradation Indicator, comes from the metric CDI - Contact Degradation Indicator, developed in [2] which is defined in dB, by similarity with the Signal to Noise relationship (SNR), that is widely used in the telecommunications area, and here is repeated as equation (2).

$$CDI_{dB} = 20 \log_{10} \left( \frac{\sqrt{\frac{1}{n} \sum_{k=1}^n S_k^2}}{\sqrt{\frac{1}{n} \sum_{k=1}^n R_k^2}} \right) \quad (2)$$

where:

$S_k$  — Load current frequency spectrum magnitudes obtained from the Fourier Discrete Transform, for the low-frequency region ( $f \leq F_c$ ) using a low pass filter.

$R_k$  — Load current frequency spectrum magnitudes obtained from the Fourier Discrete Transform, for the high-frequency region ( $f > F_c$ ) using a high pass filter.

The CDI developed in [2] was applied to load currents that flow in bays of high voltage substations, that is, corresponding to large equivalent loads, so that the frequency spectrum of individual loads that make up the equivalent are not relevant. For this condition, the IDC as defined in (2) consistently reflected the bay's electric components contacts degradation condition, since the equivalent load presents a harmonic profile with small variability throughout the online operation cycle, and therefore the term  $\sum_{k=1}^n S_k^2$  also presents little variability during the operation cycle. On the other hand, the term  $\sum_{k=1}^n R_k^2$ , which is associated with losses in the electric contacts, material aging, isolation degradation, and others, tend to increase with the continuous operation of the electrical system, resulting CDI's with decreasing lower gain values in dB, along the operation horizon as expected.

When evaluating the individual performance of electric motors, on the other hand, the CDI as originally conceived in [2], did not present a consistent behavior in all tested operating conditions. It is known that the best performance of electric motors when it presents lower losses, corresponds to the nominal operating condition. Any deviation from this nominal condition tends to increase electrical losses, with the appearance of more significant harmonics in the range ( $f < f_c$ ), essentially the harmonics of 5th, and 7th. orders. This causes an increase in the term,  $\sum_{k=1}^n S_k^2$ , which often may supplant the increase in the term,  $\sum_{k=1}^n R_k^2$ , in such a way that the CDI gain in dB increases, rather than decreasing, as expected. To correct this inconsistency, a change in the CDI definition is proposed here, such that the term  $\sum_{k=1}^n S_k^2$  includes only the frequency spectrum at the nominal frequency (60 Hz or 50 Hz), resulting in the definition of EMDI in dB, as expressed in (3).

$$EMDI_{dB} = 20 \log_{10} \left( \frac{\sqrt{S_{nf}^2}}{\sqrt{\frac{1}{n} \sum_{k=1}^n R_k^2}} \right) \quad (3)$$

The EMDI value calculated in dB for the operating condition under analysis can be used as input for a diagnostic system, which will qualify the analyzed operation condition with an indication of motor's imminent failure. To characterize how far the motor in operation is in relation to a critical condition that represents an imminent failure, a threshold value should be established for the EMDI, in dB, such that this value represents the fault condition that should be avoided. Thus, the simple comparison of the calculated value for EMDI with the adopted threshold value is already a predictive diagnosis of failure, which can be better qualified by an intelligent inference system, using Artificial Neural Networks, or Fuzzy Logic, for example, such that the smaller or greater approximation with the threshold characterizes the motor operation state as, for example, Secure, Alert, and Emergency. Other security qualifications may also be eligible.

### 7.3. Electric Motor Degradation Index

#### 7.3.1. Methodology

To measure the induction motors operation variables the class “A” quality analyzer HIOKI™ model PW3198-90 was used (2). The electric load used in this work consists of an electromagnetic brake or Foucault brake (3), which includes two load cells that are connected to the ends of the brake with which it is possible to measure the opposite force produced by eddy



currents which were varied with the load controller (5). The methodology and test bench for the electric motors' predictive fault diagnosis system proposed in this paper, is presented schematically in Figure 7-2.

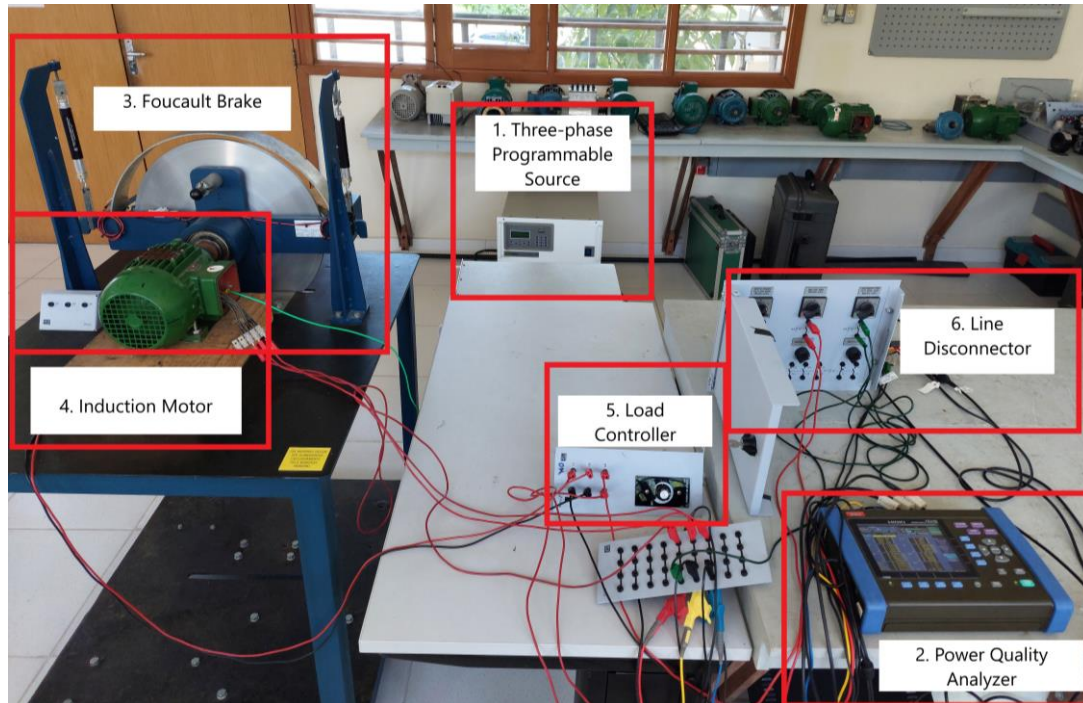


**Figure 7-2** – General test setup.

Sinusoidal three-phase voltages were generated using a three-phase AC programmable source (1). Initially, for the experimental tests on electric motors, the two 0.75 kW, IE2 and IE3 Class motors presented in Chapter 1 were considered, under different test conditions. Before performing the test procedures, the electric motors were submitted to bench tests, and it was verified that they are in perfect electrical and mechanical operation conditions, being checked their nameplate specifications, and presented no imminent indication of mechanical failures, such as audible noise, and vibration.

The initial test evaluated the motor in nominal voltage conditions and considered its load varying from 30% to 125% of nominal loading, according to the manufacturer's information. Off-nominal voltage conditions, like under and over voltages were also analyzed, as well as unbalanced voltage operation conditions were also tested. In each operating condition, the Electric Motor Degradation Indicator (EMDI) was calculated in dB, following the procedure outlined in Figure 7-3.

The IE2 and IE3 Class motors were supplied with a nominal voltage of 220 V and subjected to varying loads ranging from 30% to 125% of the rated load. In each operating condition, the Electric Motor Degradation Indicator (EMDI) was calculated in dB, following the procedure outlined in Figure 4.

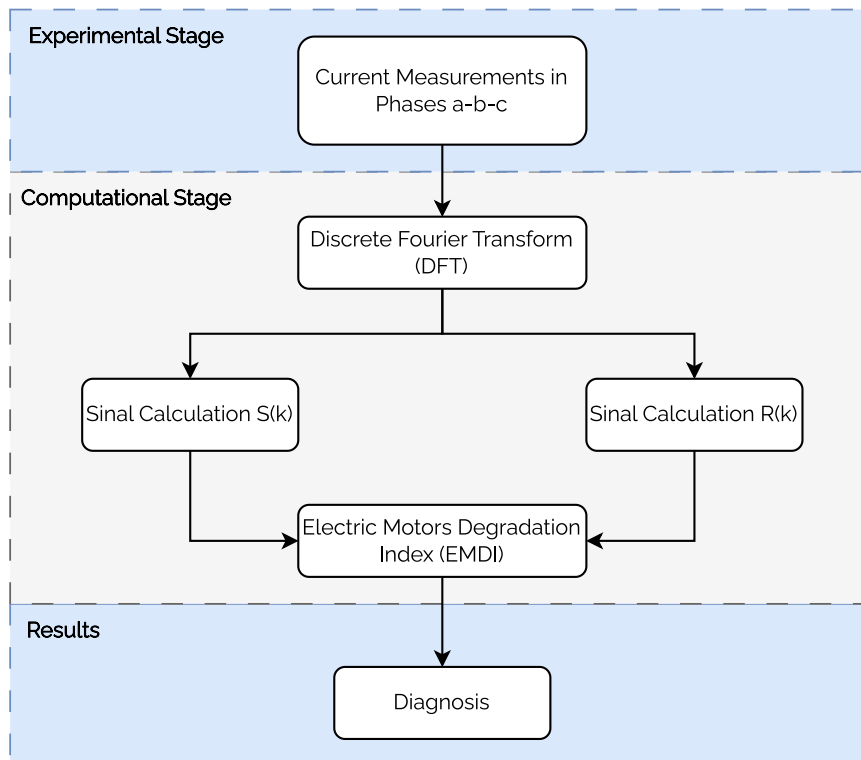


Figure 7-3 – Methodology Flowchart.

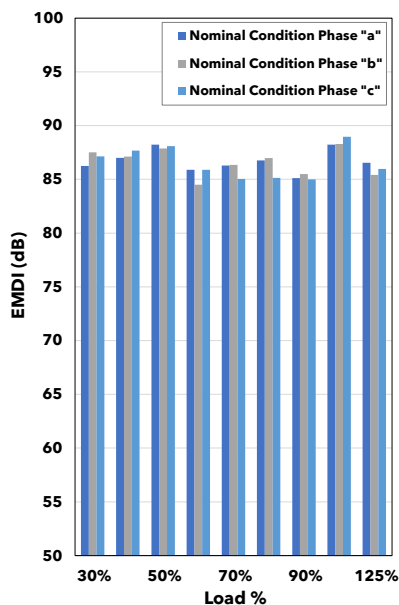
## 7.4. Results and Discussion

### 7.4.1. Nominal Condition

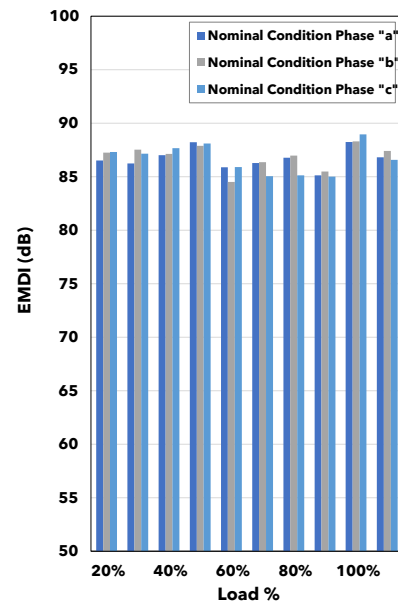
The IE2 and IE3 Class motors were supplied with a nominal voltage of 220 V and subjected to varying loads ranging from 30% to 125% of the rated load. The IE2 and IE3 induction motors have very similar operational parameters, and the calculated EMDI values for phases a, b, and c, for nominal voltage condition and varying loading from 30% to 125%, have resulted also very similar. So, the results presented in Table 7-1 and graphically illustrated in Figure 7-4 for the IE2 Class motor, also illustrate adequately the IE3 Class motor performance.

**Table 7-1.** Electric Motor Degradation Indicator in Nominal Conditions for IE2 Class motor.

Motor Loading	EMDI Phase a	EMDI Phase b	EMDI Phase c
30 %	86.2428	87.5236	87.1389
40 %	87.0015	87.1201	87.6690
50 %	88.2100	87.8751	88.0966
60 %	85.8797	84.5075	85.8934
70 %	86.2761	86.3544	85.0378
80 %	86.7646	86.9739	85.1271
90 %	85.1195	85.4872	85.0008
100 %	88.2357	88.2956	88.9620
125 %	86.5370	85.4181	85.9668



(a)



(b)

**Figure 7-4** – EMDI calculation in dB for the nominal voltage operation condition and loading varying from 30% to 125% of nominal for: (a) IE2 Class motor and (b) IE3 Class motor.

A first analysis of the presented results demonstrates that the suggested EMDI index in dB, in general, is able to reflect the motor performance for the various operating conditions, presenting the highest gain for the nominal condition, as expected. The other operating conditions, which are off-nominal ones, presented systematically lower gains, to a greater or lesser extent, as compared to the nominal one.

#### 7.4.2. Single Phasing

One undesirable scenario is the loss of one of the power supply phases in an electric motor. Despite the presence of protective equipment for such events, known as single phasing protection, the phenomenon of single phasing can lead to the degradation of the motor's internal insulation, depending on the connected load. To explore this scenario, bench tests were conducted using the IE3 Class electric motor. In the event of a phase loss, the current in the remaining phases increases, as illustrated in Figure 7-5. This rise in current, varying with the motor's load percentage, can lead to excessive heat, degradation of coil insulation, and, ultimately, internal coil short-circuits.

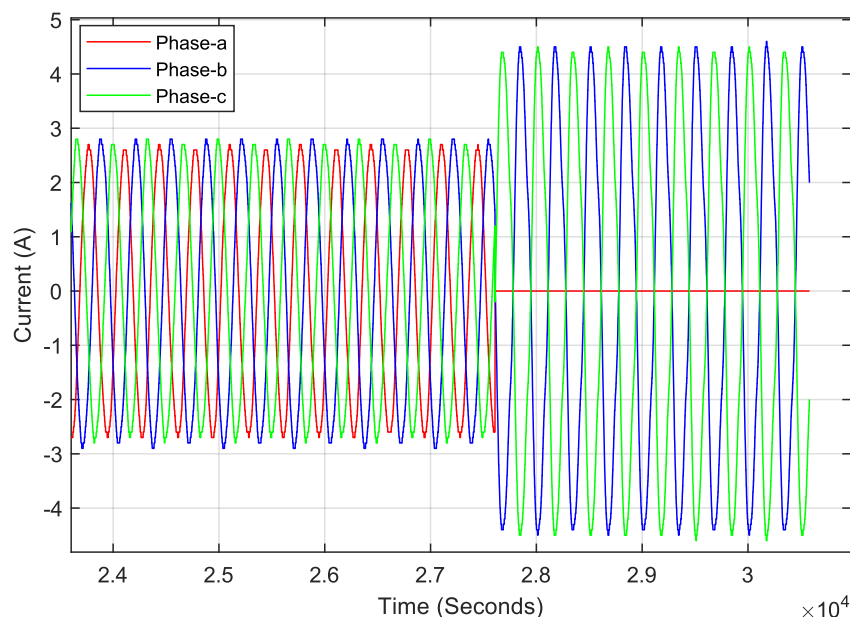


**Figure 7-5** – Single phasing triggered in IE3 Class motor to evaluate the EMDI.

In light of this situation, the Electric Motor Degradation Indicator (EMDI) was derived (Figure 7-6). By examining the graph and comparing the EMDI coefficients in both the nominal condition (external dodecagon) and the phase-loss condition (internal dodecagon), it becomes evident that a decrease in the EMDI values occurs, for each loading condition. This reduction should be regarded as an alert signal by the operator.

It is important to highlight that in the fault condition, phase "a" exhibits an EMDI value as a result of considering the oscillography depicted in Figure 7-5. During the fault, the two remaining phases recorded minimum values of 62.54 dB.

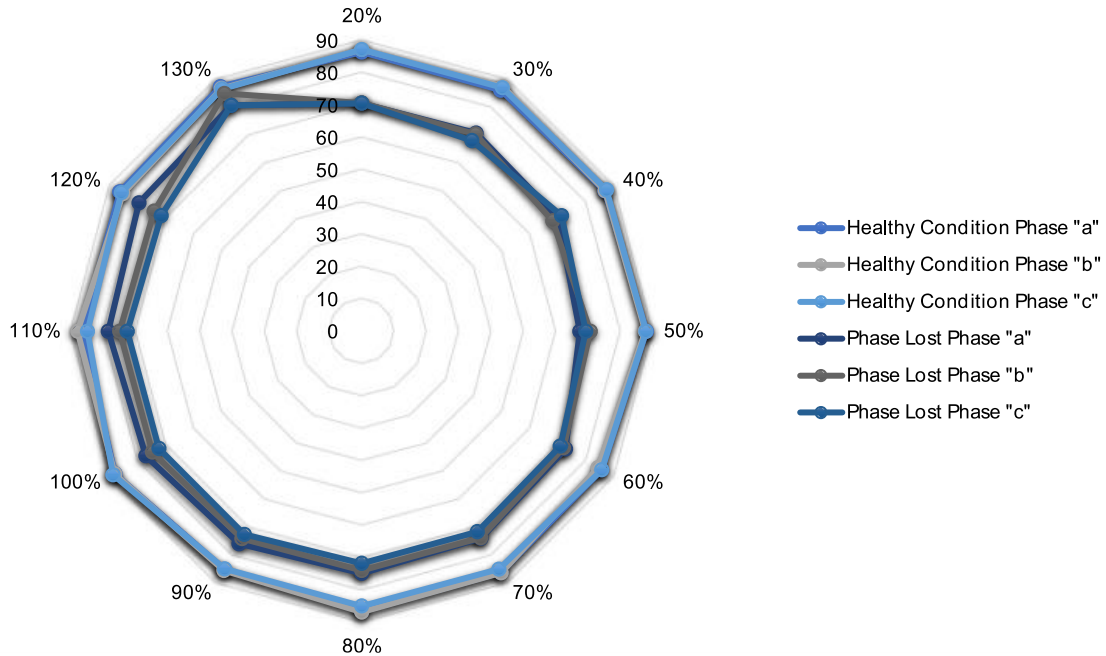


Figure 7-6 – EMDI calculation in dB for a single phase-loss in the IE3 Class motor.

### 7.4.3. Voltage Variation

According to the IEC 60038-2009 standard, electrical systems can operate at various voltage levels. As a result, electric motors can operate at voltages that differ from their rated values, thereby impacting their performance and lifespan. Figure 7-7 illustrates the current curve as a function of load for two voltage conditions: 1.0 p.u. and 1.10 p.u. It is evident that overvoltage leads to higher currents for the same connected load, which ultimately influences the losses and temperature of the electric motor. This, in turn, contributes to the degradation of its components and reduces its useful life.

To evaluate the EMDI performance under these operation conditions, experimental tests were performed, and are presented in Figure 7-8. Once again, it is observed how the coefficient varies in conditions other than the nominal ones, the voltage variation translates into a variation in the power supply currents, and with it, a decrease in the EMDI.

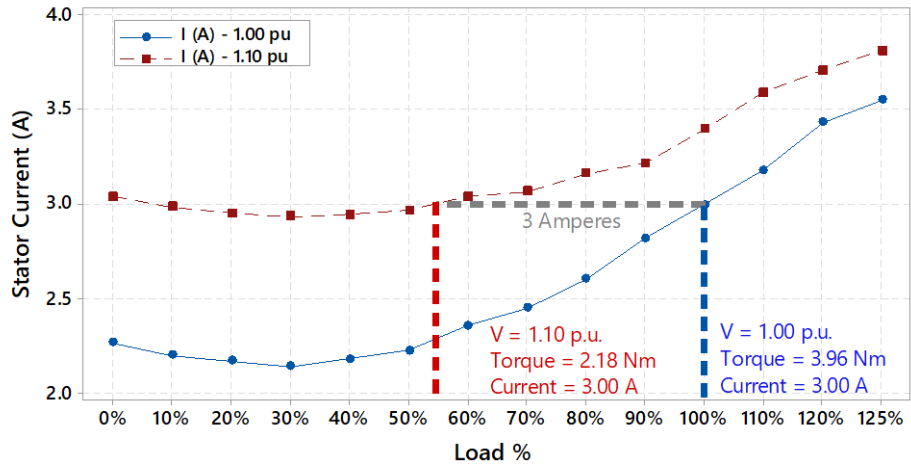


Figure 7-7 – Input current variation as a function of load in VV conditions.

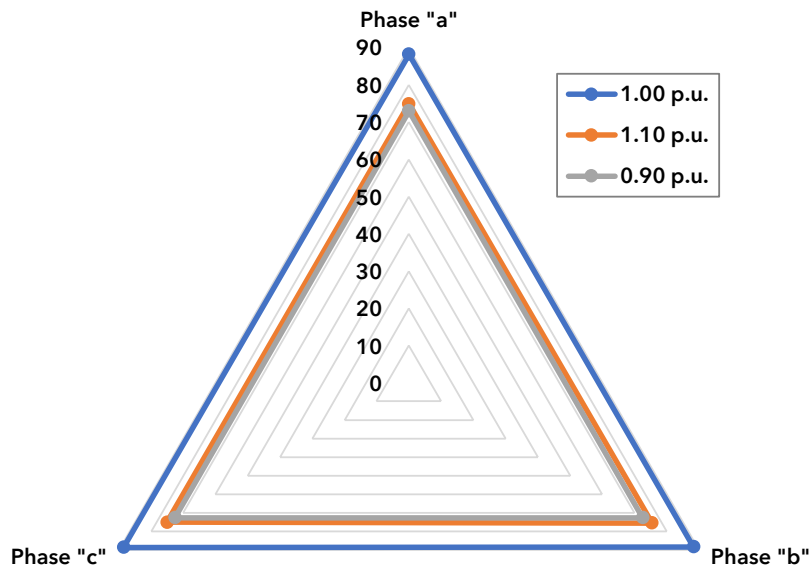


Figure 7-8 – EMDI calculation in VV conditions for nominal load condition.

## 7.5. On-site Validation

To validate the proposed methodology a 15-kW output power electric motor that is part of a water pumping system as presented in Figure 7-9. The nominal data of the motor are presented in Table 7-2. Both motors in the figure present the same power output and were classified as class IE1 according to IEC 60034-30-1 and had been recently rewound at the time of the measurements.



**Figure 7-9** – Pumping System at the Federal University of Pará: (a) 15 kW SCIM and (b) Power quality analyzer for electric motors consumption measurement.

**Table 7-2.** Squirrel Cage Induction Motor in Pump System parameters

Characteristics	IM Nameplate data
Output Power (kW)	14.92
Efficiency	0.902
Power Factor	0.82
Nominal Current (Amps - 380 V)	30.5
IEC Class	IE1

### 7.5.1. Measurement Campaigns

To verify the operation cycle and consumption of the analyzed systems, power quality analyzers were installed for each system, from the manufacturer HIOKI™ model PW3198. The measurements were made in a period of 11 days. Figure 7-9b presents the power quality analyzers installed in the electric motor panel.

In the analysis of the measurements, Figure 7-10 shows the motor, with a rated nameplate voltage of 380 V, operates with almost 420 Volts (1.10 p.u.), this value is the maximum allowed above the nominal (1.00 p.u.) by the NEMA and IEC standards in relation to voltage variation. In addition, currents higher than the nameplate nominal were recorded, and are presented in Figure

7-11, with values higher than the nominal current, which may be due to overloads on the shaft, as well as the influence of the overvoltage in the supply.

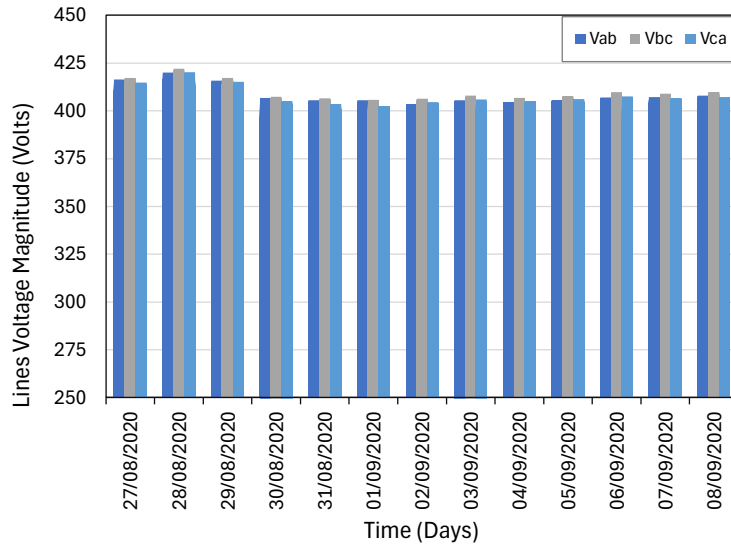


Figure 7-10 – Voltage magnitude variation for the electric motor input.

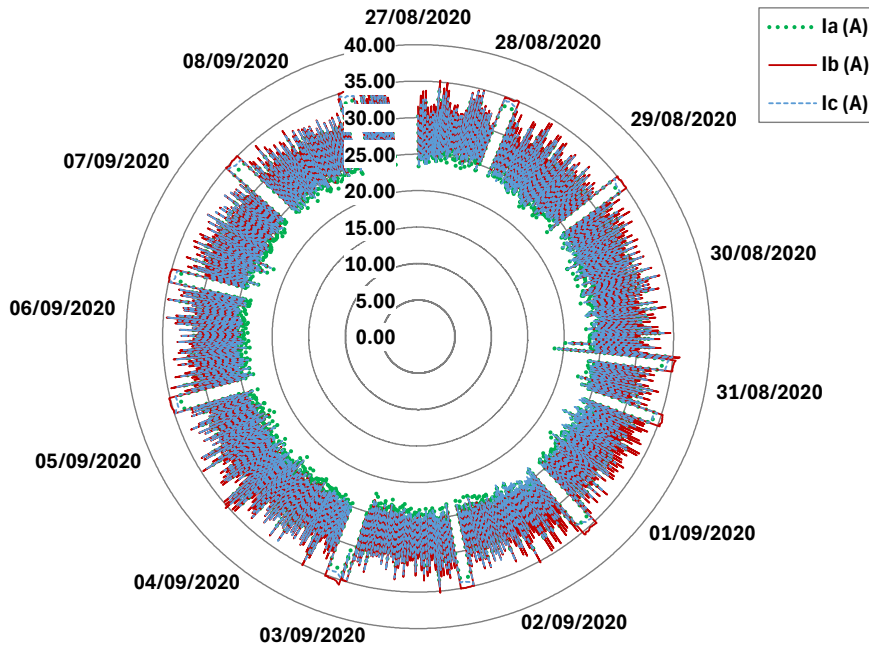


Figure 7-11 – Measured input line currents as a function of time.

To verify the influence of the overvoltage, a voltage of 1.10 p.u. was applied to the motor shown in Figure 7-2. under laboratory conditions, the results are shown in Figure 7-7, where the impact of the overvoltage on the supply current is clearly visible., this is because in the induction motors, the current in the magnetization branch is close to 50% of the nominal current, which in turn



depends on the induced voltage, which in turn depends on the supply voltage, thus varying with the voltage at the motor terminals.

To evaluate the proposed methodology, the oscillography of the presented measurements was used and the EMDI was estimated for the overvoltage condition with 1.10 p.u. The results are presented in Figure 7-12, and are compared with the indexes obtained for a 0.75 kW motor with nominal voltage (1.00 p.u.) and overvoltage (1.10 p.u.), and show how when compared with the nominal condition, the overvoltage produces a reduction in the proposed EMDI, then, the evaluation of the field measurements showed that the installed motor presents even lower coefficients, mainly due to the age of the motor, although it had been recently rewound. The field validation is consistent with the values collected and calculated in laboratory bench tests so that the proposed methodology is shown to be valid and effective. The observed degradation shows the effect of continued operation in low-power quality conditions, as well as the effect of motor rewinding.

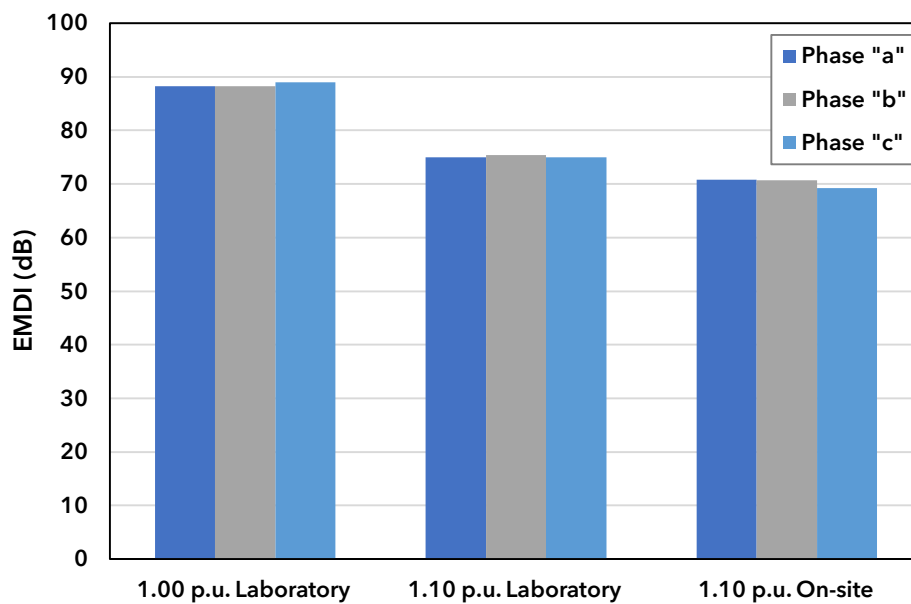


Figure 7-12 – Electric motor diagnosis indicator comparison in VV conditions.

## 7.6. Final Considerations

This Chapter proposed a new degradation indicator for electric motors defined as EMDI, based on the frequency-domain analysis of the current waveform of electric motors in the presence of voltage variation with undervoltage and overvoltage. The proposed methodology demonstrated that disturbances and deviations in the motor power supply result in a degradation of its components, as observed from the coefficients obtained.

The study also included a field validation based on measurements on a 15-kW motor fed with overvoltage, also confirming its efficiency. Although this study presented only an evaluation including voltage variation, the EMDI is presenting excellent approximations in other detrimental disturbances such as phase loss, unbalance, etc. The proposed indicator can be easily used to correlate it with maintenance frequency or with other indicators such as Mean Time Between Failures (MTBF), of widespread application in the industries.

As observed and initially indicated, the tool allows to identify deviations in the normal operation of a motor compared to the nominal conditions, thus proving to be a useful tool in the predictive diagnosis of electric motors and, in combination with more specific diagnostic tools, allows to identify the component or cause of such non-nominal operation, as well as its impact on the useful life.

In future work, further experiments will be carried out, including motor burnout, with the aim of identifying the minimum EMDI and from there estimating the time to motor failure.

The next chapter presents the main published and disseminated results obtained in this thesis.

## 7.7. Chapter Bibliography

- [1] “IEC 60034-30-1:2014 | IEC Webstore | pump, motor, water management, smart city, energy efficiency.” Accessed: Jun. 10, 2022. [Online]. Available: <https://webstore.iec.ch/publication/136>
- [2] F. V. V. Bezerra, G. P. S. Cavalcante, F. J. B. Barros, M. E. L. Tostes, and U. H. Bezerra, “Methodology for Predictive Assessment of Failures in Power Station Electric Bays Using the Load Current Frequency Spectrum,” *Energies*, vol. 13, no. 19, Art. no. 19, Jan. 2020, doi: 10.3390/en13195123.
- [3] J. Muñoz Tabora, M. E. de Lima Tostes, E. Ortiz de Matos, T. Mota Soares, and U. H. Bezerra, “Voltage Harmonic Impacts on Electric Motors: A Comparison between IE2, IE3 and IE4 Induction Motor Classes,” *Energies*, vol. 13, no. 13, Art. no. 13, Jan. 2020, doi: 10.3390/en13133333.

## Chapter 8

### Achievements during the Ph.D. Studies

This chapter summarizes the results obtained during the Ph.D. in terms of scientific dissemination, conferences, and international awards, as well as the application of the studies carried out for the implementation of minimum energy performance standards in Honduras.

#### 8.1. Journal Conferences Publications

##### 8.1.1. Papers published in International Journals with Qualis A1-A3 (Brazil) /Q1 (International)

1. J. Muñoz Tabora, M. E. de Lima Tostes, E. Ortiz de Matos, T. Mota Soares, e U. H. Bezerra, "Voltage Harmonic Impacts on Electric Motors: A Comparison between IE2, IE3 and IE4 Induction Motor Classes", *Energies*, vol. 13, no 13, Art. no 13, jan. 2020, doi: 10.3390/en13133333.
2. J. M. Tabora, M. E. De Lima Tostes, E. O. De Matos, U. H. Bezerra, T. M. Soares and B. S. De Albuquerque, "Assessing Voltage Unbalance Conditions in IE2, IE3 and IE4 Classes Induction Motors," in *IEEE Access*, vol. 8, pp. 186725-186739, 2020, doi: 10.1109/ACCESS.2020.3029794.
3. J. M. Tabora et al., "Assessing Energy Efficiency and Power Quality Impacts Due to High-Efficiency Motors Operating Under Nonideal Energy Supply," in *IEEE Access*, vol. 9, pp. 121871-121882, 2021, doi: 10.1109/ACCESS.2021.3109622.
4. Tabora, J.M.; Paixão Júnior, U.C.; Rodrigues, C.E.M.; Bezerra, U.H.; Tostes, M.E.d.L.; Albuquerque, B.S.d.; Matos, E.O.d.; Nascimento, A.A.d. Hybrid System Assessment in On-Grid and Off-Grid Conditions: A Technical and Economical Approach. *Energies* 2021, *14*, 5284. <https://doi.org/10.3390/en14175284>.
5. Tabora, J.M.; Tshoombe, B.K.; Fonseca, W.d.S.; Tostes, M.E.d.L.; Matos, E.O.d.; Bezerra, U.H.; Silva, M.d.O.e. Virtual Modeling and Experimental Validation of the Line-Start Permanent Magnet Motor in the Presence of Harmonics. *Energies* 2022, *15*, 8603. <https://doi.org/10.3390/en15228603>.
6. Tabora, J.M.; Correa dos Santos Júnior, L.; Ortiz de Matos, E.; Mota Soares, T.; Arrifano Manito, A.R.; de Lima Tostes, M.E.; Holanda Bezerra, U. Exploring the Effects of Voltage Variation and Load on the Electrical and Thermal Performance of Permanent-Magnet Synchronous Motors. *Energies* 2024, *17*, 8. <https://doi.org/10.3390/en17010008>
7. Juan C.H. Paye; João P. A. Vieira; **Jonathan M. Tabora**; André P. Leão; Murillo A.M. Cordeiro; Ghendy Cardoso Jr; Adriano P. de Moraes; Patrick E. Farias "High Impedance Fault Models for Overhead Distribution Networks: A Review and Comparison with MV Lab Experiments". *Energies* 2024.
8. dos Santos Junior, L.C.; **Tabora, J.M.**; Reis, J.; Andrade, V.; Carvalho, C.; Manito, A.; Tostes, M.; Matos, E.; Bezerra, U. Demand-Side Management Optimization Using Genetic Algorithms: A Case Study. *Energies* 2024, *17*, 1463. <https://doi.org/10.3390/en17061463>

### 8.1.2. Papers published in other Journals.

9. Jonathan M. Tabora, Thiago M. S., Edson Ortiz de Matos, M.E. de Lima Tostes, Juan C. Huaquisaca, “Efeitos de Harmônicos em Motores de Indução de Alto Rendimento,” in Revista Eletricidade Moderna – Brasil, ISSN: 0100-2104 (Qualis C -2013-2016)
10. Andreia Palheta, Jonathan M. Tabora, Maria Socorro, Ana Rosa Carriço de Lima, Maria Emília de Lima Tostes, Andreia Antogla do Nascimento, “Application of the Sustainable Development Goals in the Amazon: A Case at Federal University of Pará (UFPA), in Revista Lium Concilium, 2023;
11. Rozal Filho, E. O., Tabora, J. M., Tostes, M. E. de L., de Matos, E. O., Soares, T. M., Bezerra, U. H., & Manito, A. R. (2023). HARMONIC CLASSIFIER FOR EFFICIENCY INDUCTION MOTORS USING ANN. Revista Contemporânea, 3(10), 17660–17678. <https://doi.org/10.56083/RCV3N10-054>
12. Tabora, J. M., Andrade, V. B., Lima, C. M., da Silva, J. C. A., Carvalho, C. C. M. de M., Tostes, M. E. de L., de Matos, E. O., & Bezerra, U. H. (2023). Abordagem ex-ante de engenharia em edifícios com funcionamento em horário de ponta. Revista Caribeña De Ciencias Sociales, 12(8), 3598–3614. <https://doi.org/10.55905/rcssv12n8-011>

### 8.1.3. Scientific papers submitted/ready to be submitted to journals in 2024.

13. Work Title: “Energy Demand Prediction Model with Dynamic Bayesian Networks”. **To be submitted at the Journal Computers and Electrical Engineering, Qualis A2/Q1.**
14. Work Title: “On-Line Monitoring of Electric Motors Operation Aiming at Detecting Failure Indication by Using the Load Current Spectral Analysis”. **To be submitted to the journal IEEE Transactions on Energy Conversion or Industry Applications, Qualis A1/Q1**
15. Work Title: “High Impedance Fault Models for Overhead Distribution Networks”. **To be submitted to the journal Energies, Qualis A1/Q1**
16. Work Title: “Estimation of losses in electric motors from experimental tests of rotor inertia.”. **To be submitted to the journal IEEE Transactions on Instrumentations, Qualis A1/Q1**

## 8.2. International Conferences

### 8.2.1. Papers published in International Conferences

17. ANDRADE, VINICIUS ; MUÑOZ TABORA, JONATHAN ; CARVALHO PAIXÃO JÚNIOR, ULISSES ; TOSTES, MARIA ; SANTANA DE ALBUQUERQUE, BRUNO ; CARRICO DE LIMA MONTENEGRO DUARTE, ANA ROSA ; DO NASCIMENTO, ANDREIA ANTLOGA ; MORAES, WUANDA . Estimativa de impacto na fatura de energia em um prédio comercial utilizando sistemas fotovoltaicos e banco de baterias. In: ANAIS DA XIV CONFERÊNCIA BRASILEIRA SOBRE QUALIDADE DA ENERGIA ELÉTRICA, 2021, São Paulo. Anais da XIV Conferência Brasileira sobre Qualidade da Energia Elétrica, 2021
18. [MUÑOZ TABORA, JONATHAN](#); FONSECA DE SOUZA PRATA, MATHEUS ; ANDRADE, VINICIUS ; MATOS LIMA, CLEYDSON ; AZEVEDO DA SILVA, JAMILLY CRISTINA ; PINHEIRO DOS SANTOS, WELTON JOHN ; MOURA DE MOURA CARVALHO, CARMINDA CÉLIA ; ORTIZ DE MATOS, EDSON ; TOSTES, MARIA ; BEZERRA, UBIRATAN . Análise de Engenharia Ex-Ante aplicada a uma Edificação com Operação em Horário de Ponta. In: ANAIS DA XIV CONFERÊNCIA BRASILEIRA SOBRE QUALIDADE DA ENERGIA ELÉTRICA, 2021, São Paulo. Anais da XIV Conferência Brasileira sobre Qualidade da Energia Elétrica, 2021.
19. [MUÑOZ TABORA, JONATHAN](#); AZEVEDO DA SILVA, JAMILLY CRISTINA ; ANDRADE, VINICIUS ; FONSECA DE SOUZA PRATA, MATHEUS ; MATOS LIMA, CLEYDSON ; PINHEIRO DOS SANTOS, WELTON JOHN ; MOURA DE MOURA CARVALHO, CARMINDA CÉLIA ; TOSTES, MARIA ; ORTIZ DE MATOS, EDSON ; BEZERRA, UBIRATAN . Modelo Estatístico e Análise de Viabilidade Econômica Aplicados a Avaliação ex-ante de uma Edificação Pública. In: ANAIS DA XIV CONFERÊNCIA BRASILEIRA SOBRE QUALIDADE DA ENERGIA ELÉTRICA, 2021, São Paulo. Anais da XIV Conferência Brasileira sobre Qualidade da Energia Elétrica, 2021.
20. TSHOOMBE, BENDICT KATUKULA ; MUNOZ TABORA, JONATHAN ; DA SILVA FONSECA, WELLINGTON ; EMILIA LIMA TOSTES, MARIA ; DE MATOS, EDSON ORTIZ . Voltage Harmonic Impacts on Line Start permanent Magnet Motor. In: 2021. In 14th IEEE International Conference on Industry Applications (INDUSCON), 2021, São Paulo. 2021 14th IEEE International Conference on Industry Applications (INDUSCON), 2021. p. 962.
21. [TABORA, JONATHAN MUNOZ](#); ANDRADE, V.B. ; LIMA, CLEYDSON M. ; DE MOURA CARVALHO, C.C. M. ; PAIXAO, ULISSES J. ; DA SILVA, J.C.A. ; DE LIMA TOSTES, M.E. ; DE MATOS, EDSON ORTIZ ; BEZERRA, UBIRATAN HOLANDA . Induction Motors Assessment: A Substitution Case Analysis. In: 2021 14th IEEE International Conference on Industry Applications (INDUSCON), 2021, São Paulo. 2021 14th IEEE International Conference on Industry Applications (INDUSCON), 2021. p. 783.
22. [TABORA, JONATHAN MUNOZ](#); DE LIMA TOSTES, M. E. ; DE MATOS, EDSON ORTIZ ; BEZERRA, UBIRATAN HOLANDA . Voltage Unbalance & Variations Impacts on IE4 Class LSPMM. In: 2021 14th IEEE International Conference on Industry Applications (INDUSCON),

- 2021, São Paulo. 2021 14th IEEE International Conference on Industry Applications (INDUSCON), 2021. p. 940.
23. [MUÑOZ TABORA, JONATHAN](#); MOREIRA RODRIGUES, CARLOS EDUARDO ; MOTA SOARES, THIAGO ; DO NASCIMENTO, ANDREIA ANTLOGA ; CARVALHO PAIXÃO JÚNIOR, ULISSES ; TOSTES, MARIA ; BEZERRA, UBIRATAN ; ORTIZ DE MATOS, EDSON ; MOURA DE MOURA CARVALHO, CARMINDA CÉLIA . Power Quality Assessment in E-Bus Charging Cycle. In: ANAIS DA XIV CONFERÊNCIA BRASILEIRA SOBRE QUALIDADE DA ENERGIA ELÉTRICA, 2021, São Paulo. Anais da XIV Conferência Brasileira sobre Qualidade da Energia Elétrica, 2021.
  24. ANDRADE, V. B. ; PAIXAO JUNIOR, U. C. ; Jonathan M. Tabora ; NASCIMENTO, A. A. ; TOSTES, M. E. L. ; BEZERRA, U. H. ; MATOS, E. O. ; ALBUQUERQUE, B. S. ; RODRIGUES, C. E. ; TAKEDA, F. M. ; CARVALHO, C. C. M. M. . Modelagem e simulação de cenários da operabilidade de uma mini rede híbrida com geração fotovoltaico-diesel, armazenamento de energia conectada à rede elétrica. In: <https://www.xiicbpe.com.br/>, 2020, Foz de Iguaçu. Congresso Brasileiro de Planejamento Energético, 2020.
  25. M. TABORA, JONATHAN; O. DE MATOS, EDSON ; M. SOARES, THIAGO ; DE L. TOSTES, MARIA EMÍLIA . Voltage Unbalance Effect on the Behavior of IE2, IE3 And IE4 Induction Motor Classes. In: Simpósio Brasileiro de Sistemas Elétricos SBSE2020, 2020. Anais do Simpósio Brasileiro de Sistemas Elétricos 2020.
  26. BORGES ANDRADE, VINICIUS ; C. PAIXÃO JR., ULISSES ; E. MOREIRA, CARLOS ; M. SOARES, THIAGO ; [M. TABORA, JONATHAN](#) ; EMÍLIA DE L. TOSTES, MARIA ; H. BEZERRA, UBIRATAN ; S. ALBUQUERQUE, BRUNO ; DA S. GOUVEIA, LUCIANO . Modelagem de um sistema de distribuição real desbalanceado e análise do impacto da geração distribuída utilizando o software OpenDSS. In: Simpósio Brasileiro de Sistemas Elétricos SBSE2020, 2020. Anais do Simpósio Brasileiro de Sistemas Elétricos 2020.
  27. [Jonathan M. Tabora](#); MATOS, E. O. ; TOSTES, M. E. L. ; SOARES, T. M. ; ANDRADE, V. B. ; MORAIS, I. R. M. R. . Voltage Unbalance Impacts on Temperature of IE2, IE3 & IE4 Class Induction Motors. In: Congresso Brasileiro de Automática (CBA), 2020, Porto Alegre. Congresso Brasileiro de Automática (CBA), 2020.
  28. MORAIS, I. R. M. R. ; [Jonathan M. Tabora](#) ; SOARES, T. M. ; TOSTES, M. E. L. . Impactos do 2º, 3º e 5º Harmônicos na Temperatura e Corrente de Motores Elétricos Classes IE2, IE3 e IE4. In: Congresso Brasileiro de Automática (CBA), 2020, Porto Alegre. Congresso Brasileiro de Automática (CBA), 2020.
  29. MONTEIRO, D. W. M. ; Jonathan M. Tabora ; PAIXAO JUNIOR, U. C. ; LOBATO, E. P. S. ; SOUSA, A. R. M. ; CARVALHO, C. C. M. ; TOSTES, M. E. L. . Desenvolvimento de Aplicação Web para gerenciamento e Eficientização de Sistema de Iluminação. In: Congresso Brasileiro de Automática (CBA), 2020, Porto Alegre. Congresso Brasileiro de Automática (CBA), 2020.
  30. [Jonathan M. Tabora](#); SOARES, T. M. ; MATOS, E. O. ; TOSTES, M. E. L. ; RODRIGUES, C. E. . Impactos do 5º Harmônico na Temperatura de Motores Elétricos Classes IE2, IE3 e IE4. In:

- Conferência Brasileira sobre Qualidade da Energia Elétrica (CBQEE), 2019, São Paulo. Impactos do 5º Harmônico na Temperatura de Motores Elétricos Classes IE2, IE3 e IE4, 2019.
31. [Jonathan M. Tabora](#); SOARES, T. M. ; MATOS, E. O. ; TOSTES, M. E. L. ; PAYE, J. C. H. . Fifth & Seventh Harmonic Effects on the Performance of IE2, IE3 & IE4 Induction Motor Classes. In: 13th LATIN-AMERICAN CONGRESS ON ELECTRICITY GENERATION AND TRANSMISSION - CLAGTEE 2019, 2019, Santiago de Chile. Fifth & Seventh Harmonic Effects on the Performance of IE2, IE3 & IE4 Induction Motor Classes, 2019.
  32. IAGO R.M.R. Morais, IM. TABORA, JONATHAN; O. DE MATOS, EDSON ; M. SOARES, THIAGO ; DE L. TOSTES, MARIA EMÍLIA, UBIRATAN HOLANDA BEZERRA. AVALIAÇÃO DOS IMPACTOS DE HARMÔNICOS DE SEQUÊNCIA POSITIVA E ZERO EM MOTORES ELÉTRICOS CLASSES IE2, IE3 E IE4 COM LIGAÇÕES DELTA E ESTRELA. In: Simpósio Brasileiro de Sistemas Elétricos SBSE2020, 2020. Anais do Simpósio Brasileiro de Sistemas Elétricos 2022, São Paulo, Brazil
  33. Lauro C. dos Santos Jr., M. TABORA, JONATHAN; O. DE MATOS, EDSON ; M. SOARES, THIAGO ; DE L. TOSTES, MARIA EMÍLIA, UBIRATAN HOLANDA BEZERRA. VOLTAGE VARIATION IN HIGH EFFICIENCY MOTORS: A TECHNICAL AND COMPUTATIONAL APPROACH. In: Simpósio Brasileiro de Sistemas Elétricos SBSE2020, 2020. Anais do Simpósio Brasileiro de Sistemas Elétricos 2022, Brazil.
  34. M. TABORA, JONATHAN; M. SOARES, THIAGO; IAGO R.M.R. MORAIS, O. DE MATOS, EDSON ; M. SOARES, THIAGO ; DE L. TOSTES, MARIA EMÍLIA, UBIRATAN HOLANDA BEZERRA, SANALTO SILVA. Minimum Energy Performance Standards for Central América. International Conference on Energy Efficiency in Motor Driven Systems, Stuttgart, Germany, 2022
  35. IAGO R.M.R. MORAIS, M. TABORA, JONATHAN; M. SOARES, THIAGO; O. DE MATOS, EDSON ; M. SOARES, THIAGO ; DE L. TOSTES, MARIA EMÍLIA,. M, *“Impacts of 2nd , 3rd and 5th order harmonics on the thermal behavior of IE2-, IE3-and IE4-class electric motors in grounded star and triangle connections”*. In International Conference on Energy Efficiency in Motor Driven Systems, Stuttgart, Germany.
  36. M. TABORA, JONATHAN; CORREA dos SANTOS, LAURO., M. SOARES, THIAGO, O. DE MATOS, EDSON ; M. SOARES, MARIA EMÍLIA, UBIRATAN HOLANDA BEZERRA. “Voltage Variations Impacts on Electrical Motors: A Central America Study Case”. In International Conference on Energy Efficiency in Motor Driven Systems, Stuttgart, Germany, 2022
  37. Isaías Ferreira, Jonathan M. Tabora; Pedro Sampaio, Carminda C. M. de M. C., M. E. de L. Tostes, Edson Ortiz de Matos, Ubiratan H. Bezerra, Andreia Antloga do Nascimento. Charging strategies for electric vehicles from renewable hybrid systems. In: 14th LATIN-AMERICAN CONGRESS ON ELECTRICITY GENERATION AND TRANSMISSION - CLAGTEE 2022, 2022, Rio de Janeiro, Brazil.
  38. Edilberto O. R. F., Jonathan M. Tabora, M. E. de L. Tostes, Edson Ortiz de Matos, Allan Manito, Thiago Soares, Ubiratan H. Bezerra, Andreia Antloga do Nascimento. Charging strategies for electric vehicles from renewable hybrid systems. In: 14th LATIN-AMERICAN CONGRESS ON ELECTRICITY GENERATION AND TRANSMISSION - CLAGTEE 2022, 2022, Rio de Janeiro, Brazil.

39. Nuno Gomes, M. TABORA, JONATHAN; CORREA dos SANTOS, LAURO., M. SOARES, THIAGO, O. DE MATOS, EDSON ; M. SOARES, MARIA EMÍLIA, UBIRATAN HOLANDA BEZERRA. “Loading Prediction using Artificial Neural Networks”. In IEEE Kansas Power and Energy Conference, Manhattan, Kansas, 2023.
40. M. TABORA, JONATHAN; CORREA dos SANTOS, LAURO., M. SOARES, THIAGO, O. DE MATOS, EDSON; M. SOARES, MARIA EMÍLIA, UBIRATAN HOLANDA BEZERRA. “Efficient Electric Motors Performance Under Voltage Variation Conditions”. In IEEE Kansas Power and Energy Conference, Manhattan, Kansas, 2023.
41. Roberto Nascimento, Josivan Reis, Marcos Printes, Dante Barone, Jonathan Tabora, Maria Tostes. Augmented Reality Applications in Mathematics and Science: Exploring Pedagogical Viability in the Amazon Region, The 32nd Annual Conference of the European Association for Education in Electrical and Information Engineering (EAEEIE), June,2022, Netherlands.
42. I. Ferreira, Jonathan M. Tabora, et al., "Investigating the Effects of Load Conditions and Voltage Unbalance on Premium and Superpremium Motor Performance," 2023 15th IEEE International Conference on Industry Applications (INDUSCON), São Bernardo do Campo, Brazil, 2023, pp. 1111-1116, doi: 10.1109/INDUSCON58041.2023.10374999.
43. J. M. Tabora et al., "Synchronous Motor Operation in Voltage Imbalance Conditions," 2023 15th IEEE International Conference on Industry Applications (INDUSCON), São Bernardo do Campo, Brazil, 2023, pp. 1105-1110, doi: 10.1109/INDUSCON58041.2023.10374610.
44. I. R. Miranda Rodrigues Morais, Jonathan M. Tabora et al., "Evaluation of Electromagnetic Behavior in an Induction Motor Under Voltage Variation," 2023 15th IEEE International Conference on Industry Applications (INDUSCON), São Bernardo do Campo, Brazil, 2023, pp. 1078-1083, doi: 10.1109/INDUSCON58041.2023.10374741.
45. J. M. Tabora et al., "An Assessment of Power Factor Correction Strategies from Billing and Measurement Systems: A Case Study in Medium Voltage Consumers," 2023 15th IEEE International Conference on Industry Applications (INDUSCON), São Bernardo do Campo, Brazil, 2023, pp. 1451-1455, doi: 10.1109/INDUSCON58041.2023.10374990.
46. J. M. Tabora, F. V. Vieira Bezerra, T. M. Soares, E. Ortiz de Matos, M. E. de Lima Tostes and U. Holanda Bezerra, "Electric Motor Degradation Indicator in Non-Ideal Supply Conditions," 2023 IEEE Workshop on Power Electronics and Power Quality Applications (PEPQA), Cali, Colombia, 2023, pp. 1-5, doi: 10.1109/PEPQA59611.2023.10325777.
47. Gabriel Matusanga, M. TABORA, JONATHAN; Edson Ortiz de Matos., Thiago M. SOARES, Carminda Célia Moura, MARIA EMÍLIA, UBIRATAN HOLANDA BEZERRA. “Demand Side Management Strategies for the Introduction of Electric Vehicles: A Case Study”. In: IEEE Colombian Caribbean Conference (C3), Colombia 2023.
48. Ayrton Lucas Lisboa Do Nascimento, Bruno Santana de Albuquerque, Miguel Gomes Brilhante, Luiza da Rocha Marum Jorge, Edilberto Oliveira Rozal Filho, Jonathan Munoz Tabora Danielly Priscila Ribeiro Carrera, Carminda Célia Moura de Moura Carvalho, Maria Emília de Lima Tostes, Erik Kauã Costa Monteiro, and Andréia Antloga Do Nascimento. “Battery Energy Storage Systems Operation in a Hybrid Renewable System”. In: IEEE Colombian Caribbean Conference (C3), Colombia 2023.



49. Ayrton Lucas Lisboa Do Nascimento, Danielly Priscila Ribeiro Carrera, Jonathan Munoz Tabora, Bruno Santana de Albuquerque, Marcos Vinicius Pereira Braga, Josivan Rodrigues dos Reis, Edson Ortiz de Matos, Allan Rodrigo Arrifano Manito, Carminda Célia Moura de Moura Carvalho and Maria Emília de Tostes Lima “Assessing Accuracy in Capacitors Bank Estimations: A Case Study”. In: IEEE Colombian Caribbean Conference (C3), Colombia 2023.

### 8.2.2. Scientific papers submitted/ready to be submitted to journals in 2024.

50. Work Title: “The Harmonic Voltage Impact on the 1 hp LSPMM Efficiency under Different Load Conditions”. **Abstract accepted at EEMODS 2024**
51. Work Title: “Active Power Demand Prediction using Neural Networks and the Sarimax Method” **Submitted to IEEE Conference ANDESCON 2024.**
52. Work Title: “Use of Ancillary Services and Renewable Energy in Electric Vehicles: An Integrative Literature Review for Application in Brazil”. **To be submitted at an IEEE Conference.**
53. Work Title: “Integration of Microgrids into Real Distribution Networks: A Case Study Using Demand Response through Storage Systems”. **To be submitted at an IEEE Conference.**

### 8.3. Publications in Book Chapters

54. Capítulo 13: Modelo estatístico em avaliação ex-ante de uma edificação pública. Libro: Engenharia no Século XXI, Editora Poisson, Volume 23. ISBN: 978-65-5866-147-4 DOI: 10.36229/978-65-5866-147-4

#### **8.4. Participation as a speaker at international events**

1. High-efficiency electric motors. Department of Electrical Engineering. National Autonomous University of Honduras (UNAH), 2019.
2. Harmonic voltage effects on the performance of IE3, IE3 & IE4 class induction motors. Renewable Energy and Resources Webinar. France, 2020.
3. Power Quality. Opera Learning Week. UNAH, 2021.
4. Electric Vehicles. International Engineering Week (SII, 2021). Technological University of Central America (UNITEC), 2021.
5. Electric Mobility and the Interface with Smart Cities. Fair of Electric Vehicles, Mobility and Innovation of the Northeast, Brazil, 2021.
6. Minimum Energy Performance Standards for Central America in Semana Internacional de Ciencia y Tecnología. Buenos Aires, 2022.
7. Renewable Hybrid Systems - Iberoamerican Congress of Engineering and Technology, CIBITEC23, Madrid, Spain, April 2023.
8. Sustainable Electric Mobility: A case study for its implementation in cities. Conference given for the Central American Integration System (SICA) and the Energy Secretariat in Honduras SEN, October, 2023.

#### **8.5. Application of Standards and Regulations for electric induction motors in Honduras**

The studies presented in this thesis will serve as a basis for the implementation of minimum energy performance standards in Honduras, for which the Technical Regulation Committee is currently being formed. Its objective is to elaborate the Honduran Technical Regulation on Energy Efficiency for three-phase alternating current induction squirrel-cage motors with a rated power from 0.746 to 373 kW, limits, test methods and labeling.

## Chapter 9

## Final Considerations

This chapter summarizes the final considerations and contributions of this doctoral thesis.

### 9.1. General Considerations

The main goal of this thesis was to technically and economically evaluate the impact of disturbances such as voltage harmonics, voltage unbalance, and voltage magnitude variation on IE2, IE3, and IE4 class electric motors, the latter being a permanent magnet synchronous motor. The study also included discussions on the relationship between energy efficiency and power quality in these new technologies in the presence of low power quality conditions. Finally, this work presents preliminary results of a new indicator of motor component degradation due to operation in low power quality conditions from a frequency domain analysis, validated by field measurements. The results of this approach may be of great significance to the industry in terms of the impact that various disturbances may have on electric motors, including new technologies. By providing information on the benefits in terms of energy and economic efficiency of electric motors, the thesis also shows applicability for countries that intend to adopt and implement labeling of induction electric motors.

### 9.2. Comparison of Motor Efficiency Classes in Good Power Quality Conditions

The experimental tests provided a technical comparison of the feasibility of substitution between technologies, and based on the results, some aspects should be considered when substituting older, oversized, and/or inefficient motors with higher efficiency motors:

- More efficient motors can lead to greater energy and economic savings, especially in systems with good power quality;
- An analysis of the power quality at the installation site must be performed before replacement, as well as an analysis of the other elements of the drive system before replacement (e.g. leaks in the compressed air system). Poor power quality reduces the efficiency of the electric motor. In the case of the 0.75 kW LSPMM analyzed, although it has a lower current, reactive power, and operating temperature under ideal operating conditions, it has the worst performance of the three motors analyzed due to the presence of harmonics in the supply voltage.

- Another factor to consider is the distortion presented by the LSPMM, which initially presents values already superior to those of the other technologies analyzed, and with the presence of harmonics, due to the presence of permanent magnets, higher percentages of THDI are found for this technology. For this reason, in large applications, studies must be carried out on the quality of the power supply before and after installation.
- The type of application must also be considered for this technology. The LSPMM has been observed to have difficulty starting with load at startup, which can be critical, especially in applications with frequent start/stop cycles, and is recommended for fixed-speed applications.

### 9.3. Impacts of Voltage Harmonics on IE2, IE3 and IE4 Class motors

In this work, the main harmonics present in electrical systems and their effects on electric motors have been evaluated. Based on the experimental tests, the following conclusions have been drawn:

- The analyzed negative sequence harmonics (2nd and 5th) are individually more harmful than the analyzed positive sequence harmonic of 7th order. However, the three harmonics analyzed have an impact on the consumption, efficiency, and power factor of electric motors. The analyzed negative sequence harmonics (2nd and 5th) are individually more harmful than the analyzed positive sequence harmonic of 7th order. However, the three harmonics analyzed (2nd, 5th, and 7th) have an impact on the consumption, efficiency decrease, and power factor of electric motors;
- The third zero-sequence harmonic did not produce significant variations in electric motors, where the parameters showed variations around their initial values. The combination of all the harmonics proved to be more harmful than any single harmonic analyzed, of which the second harmonic had the largest contribution.

The correlation between consumption, temperature, and power factor with voltage harmonics was evaluated from correlation matrices. The results confirmed the effects of harmonics and temperature, which are higher the lower the harmonic order present, as well as the negative sequence. Statistical analyses were performed to create temperature models from the present harmonics, good approximations were found for the analyzed output power in the

three efficiency classes and can be used to estimate the external temperature from the present harmonic in the input voltage.

The simulations in the FEMM software also allowed a better evaluation of the magnetic losses in the presence of voltage harmonics. From the magnetic flux paths changes in the presence of harmonics that produce additional temperatures in the motor, observed in the experimental measures and validated from the model built based on the motor geometry, and can be certainly useful to determine the main effects of these disturbances on components such as motor bearings or insulation degradation, aiming to program predictive maintenance with adequate frequencies to the disturbances present in the motor. The creation and validation of the LSPMM model allow evaluating the state of the motors from the experimental data using numerical methods that will certainly give a clearer scenario of the thermal-magnetic behavior of the motor, which can be easily extended to a predictive maintenance product with wide application in the industry and in electric mobility in general.

#### **9.4. Impacts of Voltage Unbalance on IE2, IE3, and IE4 Class motors**

The presence of voltage unbalance with undervoltage and overvoltage also showed negative effects on the technologies analyzed. Voltage unbalance leads to higher current unbalance and harmonics for the IMs, resulting in uneven losses and increased temperatures. The power factor also varies inversely with the positive sequence voltage, with an increase for undervoltage unbalanced conditions and a decrease for overvoltage unbalanced conditions. In terms of consumption, for SCIM classes IE2 and IE3, unbalance with undervoltage and overvoltage causes an increase in total power consumption, while for the LSPMM VU with undervoltage causes a decrease in consumption for the same load.

Through the Spearman correlation matrices, it was also observed that the THDI is inversely proportional to the positive sequence voltage component and directly proportional to the negative sequence voltage component for the undervoltage unbalanced condition. While for the overvoltage unbalance condition it was found to be directly proportional to both positive and negative sequence components.

### **9.5. Impacts of Voltage Magnitude Variation on IE2, IE3 and IE4 Class motors**

The findings indicate that operating the motor under undervoltage conditions (0.90 p.u.) results in higher efficiencies, improved power factor, and lower operating temperatures. These outcomes translate into enhanced economic benefits and an extended motor useful life. However, specialists should analyze the results presented to make the best use of the results according to the type and nature of the loads. The results show that the impact of the variation in the magnitude of the voltages is minimized in nominal load and overload conditions. Moreover, undervoltage is not shown as the best option in these conditions. Concerning the type of application, since the starting torque depends on the input voltage, undervoltage may be limited starting with heavy motor shaft loads. Therefore, undervoltage is mainly recommended in loads with quadratic torque characteristics, such as centrifugal pumps and fans, where the starting load torque is lower.

Temperature is a critical parameter as it is related to the performance, useful life, and frequency of maintenance in permanent magnets and electric motors. Therefore, the impacts of each voltage magnitude on temperature are presented and discussed. The results of the electrical analysis align with the thermal analysis, showing that overvoltage leads to operating temperatures up to 7°C higher compared to undervoltage and 3°C higher compared to the nominal condition. This temperature difference has the potential to affect the useful life of the LSPMM.

It is worth noting that a significant portion of motors operate at loads below their nominal capacity. An economic evaluation was conducted to assess the economic implications of VV in the LSPMM. In the analysis, consumers with a simple energy tariff and end users with a TOU pricing scheme were considered. The evaluation quantifies both the benefits and drawbacks of VV, particularly emphasizing how undervoltage can generate cost savings. These savings might be significant enough to cover the expenses of acquiring a new motor within the lifespan of the one under analysis, especially for loads below 60%. Moreover, the payback period is further reduced when there is tariff cost differentiation.

### **9.6. Electric Motor Degradation Indicator**

The diagnosis of electric motors stands out as one of the most critical areas of interest for the industry and other fields, especially with the emergence of new categories such as electric

vehicles. As a result, monitoring and diagnosis have become essential elements for users. To explore innovative and complementary techniques, this work presents a novel methodology based on frequency domain analysis of electric motor current waveforms.

The study included both steady state and transient disturbances such as phase loss and voltage variation with undervoltage and overvoltage. Considering that the developed methodology will become an important indicator of the health status of electric motors, experimental tests with extreme overvoltage and undervoltage conditions are developed to identify a minimum threshold close to motor failure to anticipate future unexpected failures in industrial, commercial, and transportation sectors. The proposed indicator has been successfully validated under different disturbances commonly found in electrical systems that motors may encounter in real operating conditions.

Finally, and with a view to its application in real conditions, an evaluation of the health status of 15 kW electric motors in a water pumping system was presented, in which EMDI revealed the effects of continued operation under overvoltage conditions on the degradation of motor components. In conclusion, the results strongly suggest that the EMDI (Electric Motor Degradation Index) is a valuable and timely tool for monitoring motor-driven systems and implementing predictive diagnostics. Thus, it contributes significantly to the field of predictive maintenance of electric motors.

### **9.7. Final Considerations and Future Works**

Finally, it can be concluded from the contributions of this work that the commitment to new technologies in the search for higher efficiencies will bring important benefits for the energy transition of the industrial and automotive sectors globally. Electric motors will continue to represent the largest end-use of energy worldwide, and given this, an important aspect in increasing efficiency is that the implementations are environmentally friendly from the origin of the materials used, as well as with a reduced impact on power quality, which could also be an efficiency derating factor of electric motors. Incentives to replace or upgrade old, oversized, and inefficient motors should be monitored to ensure their success. The adoption of minimum energy performance standards, such as the IE4 class for Brazil, already adopted in Europe, could bring important benefits to the country and the region, considering that Brazil is a major importer of electric motors.

The results presented highlight the importance of considering the effects of such disturbances on electric motors, so that experiments can be carried out on more significant samples with different power ratings. This will allow a more general conclusion to be drawn from a statistical point of view about the effects observed on the sample analyzed in this work.

A valuable contribution of this thesis is the fact that the methodologies, experimental tests, and results in the different operating conditions evaluated will be an important reference for the implementation of labels for electric motors in Honduras. The author is part of the commission for the revision and approval of the regulation in this country.

Given the contributions of this thesis, as well as the topics on which continuity can be given, the following are suggestions for future work:

- Evaluate the effects of unbalanced harmonics in IE2, IE3 and IE4 class electric motors;
- Computational simulation using finite elements of the variation of losses and efficiency with validation of the results from experimental measurements;
- Digital twins for electric motors in the presence of different power quality disturbances;
- Electric motor degradation index for other disturbances with tool/product installed on the motor for predictive fault diagnosis;
- Studies on the effects of analyzed disturbances in the presence of frequency converters in electric motors.



## Appendix

This chapter summarizes the final considerations and contributions of this doctoral thesis.

### IE2 Class Motor

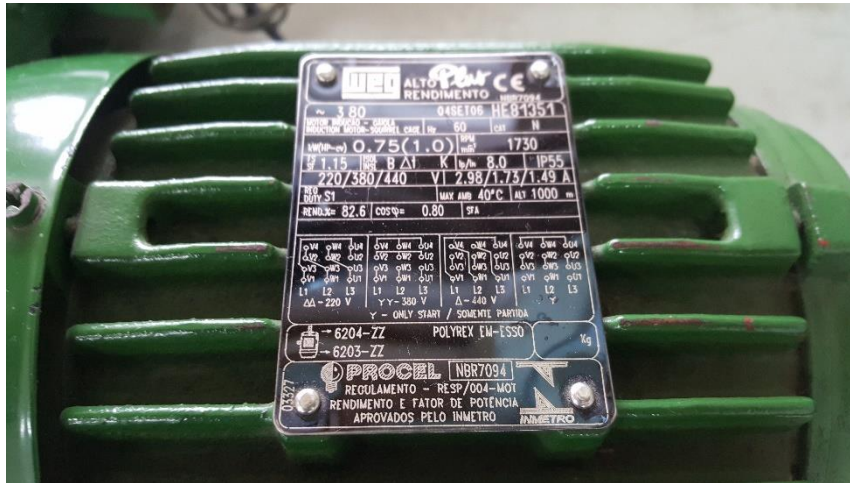


Figure 0-1 - IE2 Class induction motor nameplate.


FOLHA DE DADOS			
Motor Trifásico de Indução - Rotor de Gaiola			
Cliente	:		
Linha do produto	: W22		
Carcaça : 80 Potência : 0.75 kW (1 HP-cv) Número de polos : 4 Frequência : 60 Hz Tensão nominal : 220/380/440 V Corrente nominal : 3.02/1.75/1.51 A Corrente de partida : 19.9/11.5/9.97 A Ip/In : 6.6 Corrente a vazio : 1.85/1.07/0.925 A Rotação nominal : 1730 rpm Escorregamento : 3.89 % Conjugado nominal : 0.422 kgfm Conjugado de partida : 210 % Conjugado mínimo : 175 % Conjugado máximo : 260 % Classe de isolamento : F Fator de serviço : 1.15 Momento de inércia (J) : 0.0032 kgm <sup>2</sup>	Tempo de rotor bloqueado : 13 s (quente) 23 s (frio) Elevação de temperatura : 80 K Regime de serviço : S1 Temperatura ambiente : -20 °C a +40 °C Altitude : 1000 m Grau de proteção : IP55 Método de refrigeração : IC411 - TFVE Forma construtiva : B3D Sentido de rotação <sup>1</sup> : Ambos Nível de ruído <sup>2</sup> : 48.0 dB(A) Classe de vibração : A Método de partida : Partida direta Acoplamento : Direto Massa aproximada <sup>3</sup> : 15.4 kg Plano de pintura : 207A Cor : RAL 5009 Categoria : N		
Potência : 50%    75%    100% Rendimento (%) : 77.5    80.0    80.5 Cos Φ : 0.57    0.71    0.81	Tipo de carga acionada : - Conjugado da carga : - Momento de inércia : -		
Tipo de mancal : Dianteiro    Traseiro Intervalo de lubrificação : -    - Quantidade de lubrificante : -    - Tipo de lubrificante : MOBIL POLYREX EM	Esforços na fundação : Tração máxima : 27.4 kgf Compressão máxima : 42.8 kgf		

Figure 0-2 - IE2 Class induction motor parameters.

IE3 Class Motor



Figure 0-3 – IE3 Class induction motor nameplate.


FOLHA DE DADOS			
Motor Trifásico de Indução - Rotor de Gaiola			
Cliente	:		
Linha do produto	: W22 - Premium Efficiency	Código do produto	: 11417378
Carcaça	: 80	Tempo de rotor bloqueado	: 16 s (quente) 29 s (frio)
Potência	: 0.75 kW (1 HP-cv)	Elevação de temperatura	: 80 K
Número de polos	: 4	Regime de serviço	: S1
Frequência	: 60 Hz	Temperatura ambiente	: -20 °C a +40 °C
Tensão nominal	: 220/380 V	Altitude	: 1000 m
Corrente nominal	: 2.89/1.67 A	Grau de proteção	: IP55
Corrente de partida	: 21.1/12.2 A	Método de refrigeração	: IC411 - TFVE
Ip/In	: 7.3	Forma construtiva	: B3D
Corrente a vazio	: 1.65/0.955 A	Sentido de rotação <sup>1</sup>	: Ambos
Rotação nominal	: 1715 rpm	Nível de ruído <sup>2</sup>	: 48.0 dB(A)
Escorregamento	: 4.72 %	Classe de vibração	: A
Conjugado nominal	: 0.426 kgfm	Método de partida	: Partida direta
Conjugado de partida	: 300 %	Acoplamento	: Direto
Conjugado mínimo	: 255 %	Massa aproximada <sup>3</sup>	: 15.0 kg
Conjugado máximo	: 300 %	Plano de pintura	: 207A
Classe de isolamento	: F	Cor	: RAL 5009
Fator de serviço	: 1.25	Categoria	: N
Momento de inércia (J)	: 0.0029 kgm <sup>2</sup>		
Potência	50%      75%      100%	Tipo de carga acionada	: -
Rendimento (%)	82.3      83.0      83.0	Conjugado da carga	: -
Cos Φ	0.63      0.74      0.82	Momento de inércia	: -
Tipo de mancal	Dianteiro      Traseiro	Esforços na fundação	
Intervalo de lubrificação	6204-ZZ      6203-ZZ	Tração máxima	: 33.4 kgf
Quantidade de lubrificante	-      -	Compressão máxima	: 48.4 kgf
Tipo de lubrificante	MOBIL POLYREX EM		

Figure 0-4 - IE2 Class induction motor parameters.

IE4 Class LSPMM



Figure 0-5 – IE4 Class line-start permanent magnet motor nameplate.